Development of novel bioconjugation methods for the regio- and chemoselective modification of native proteins

Ilias Koutsopetras

Université de Strasbourg

UNIVERSITÉ DE STRASBOURG

EDSC École Doctorale des Sciences Chimiques

ÉCOLE DOCTORALE DES SCIENCES CHIMIQUES

Laboratoire de Conception et Application de Molécules Bioactives

THÈSE présentée par :

Ilias KOUTSOPETRAS

soutenue le : **07 décembre 2023**

pour obtenir le grade de : **Docteur de l'Université de Strasbourg**

Discipline/ Spécialité : Chimie Biologique et Thérapeutique

Développement de nouvelles méthodes de conjugaison régiosélectives et chimiosélectives pour la modification de protéines natives

THÈSE dirigée par :

M CHAUBET Guilhem	Chargé de recherche, UMR 7199, Université de Strasbourg
M WAGNER Alain	Directeur de recherche, UMR 7199, Université de Strasbourg

RAPPORTEURS :

Mme HARTRAMPF Nina	Professeur, Université de Zurich
M GOIS M. P. Pedro	Professeur, Université de Lisbon

EXAMINATORS :

Mme CIANFERANI Sarah	Directrice de recherche, UMR 7178, Université de Strasbourg
M WASER Jérôme	Professeur, École Polytechnique Fédérale de Lausanne

“Η ταπεινή γνώση του εαυτού μας πρέπει να τιμάται περισσότερο από το ύψος όλων των επιστημών.”

Άγιος Νικόδημος ο Αγιορείτης

"The humble knowledge of ourselves should be honored above the height of all sciences."

St. Nicodemus the Athonite

ACKNOWLEDGEMENTS

Writing this chapter of the thesis I realized how many people were involved in many different ways during these last 3 challenging years of my life helping me to reach at this stage, just a few months before my PhD defense.

I will begin by thanking Guilhem; Dr Guilhem Chaubet, who initially gave me the opportunity to join his new established team in the BFC lab under a Marie Skłodowska Curie scholarship in order to prove myself to him and all our partners. Of course, we had our moments, especially at the beginning since I was coming from an industrial environment and adjusting to academia was a bit of challenge, but in the end, Guilhem and I made it along, that along that I will stay for 6 to 12 more months for a postdoc in his lab. So, Guilhem although I have thanked you many times in person, I will also try to list here all the things that you did for me since as Latins say "*verba volant – scripta manent".* Thank you for the beautiful brainstorming conversations that we had these years, your constructive comments on my reports / publication drafts / presentations, your eye for detail that (un)fortunately I inherited at some point, the amazing time that we had during our trips at the consortium meetings, the thesis corrections (which I am sure should be such a pleasure for you to correct ☺), the help that you offered me with the French bureaucracy, for sending me to conferences / secondments and everywhere by just saying yes Ilias you are free to go with no further discussion, and finally for the understanding and your trust!

Next, I would like to thank Dr Alain Wagner for accepting me to his lab (BFC) after our interview in May 2020. Although we did not collaborate during my thesis, it was so nice discussing with you all these nice topics about cycling and hiking. Finally, I would like to thank you for introducing me to the postdoc opportunity that I have happily accepted and will spend the following months together.

Now is the time to thank all people who vouched for me as referees to Alain and Guilhem in order to join this role. Hence, I would like to thank Dr Alexander Grisin and Dr Daniel To from Manchester Organics Ltd, Pr Steven Bull from the University of Bath and last Dr Andrew Edmunds for telling all these amazing words for me and thus allowing me to pursue this PhD.

Pr Vijay Chudasama and Léa Rochet from University College of London (UCL) in the UK and Dr Christophe Salome and Loic Herter from Spirochem, AG in Switzerland are the next people that I would like to include in this chapter. I thank them for welcoming me to their teams and trusting me with their projects and for the amazing discussions and knowledge that they offered to me during these 4-month secondments at each of these places. It was a great pleasure to meet you all and more importantly that all four of you will remain my friends. It was also amazing that in just 3 - 4 months we managed to collaborate so effectively that we ended

up with 2 publications. Apart from the science part, though, it was so nice to meet two F1 fans; Vijay and Loic, who although are not Ferrari supporters, they were two amazing guys to talk about the F1 races alongside some nice pints.

Being in these two labs, I have met some wonderful people who very quickly made me a member of their company, by inviting me to play football, poker, target darts and axes, go-carts and so many other activities. From these people, I will never forget the invaluable input of Dr Alina Chrzastek from UCL, who taught me how to produce the perfect Fabs, how to use their Agilent LC-MS and how to make SDS-PAGE gels and of course the great collaboration with Dr Calise Bahou for sharing all the small tricks for the synthesis and purification of pyridazinedione molecules.

During my thesis, I had the unique opportunity to collaborate with many researchers (early and senior ones) as part of the plenty collaborative projects that I had been involved in. First, I would like to thank Dr Sarah Cianferani, Dr Oscar Hernandez, Ms Hélène Diemer and Rania Benazza from the Laboratoire de Spectrométrie de Masse BioOrganique (LSMBO) at the Université de Strasbourg for the amazing collaboration that we had all these years and all the analysis that they conducted for my projects. Next, is the turn of Pr Skerra, Carmen Longo and Yağmur Ersoy from the Technische Universität München (TUM), whose fruitful collaboration and contribution, by providing various Anticalins proteins to test our bioconjugation methods, proved vital for the better understanding of our approach. Finally, I would like to thank Pr Jérôme Waser, Dr Stefano Nicolai and Dr Abhaya Mishra from École Polytechnique Fédérale de Lausanne (EPFL) for trusting me and Guilhem to unveil all the hidden properties of their new established molecule.

These 3 years, I was lucky enough to meet many good scientists and amazing people that a few of them ended up becoming my friends! Initially I would like to thank my new Italian fratello, Lorenzo Turelli, who during those tough Covid and PhD years was the only person here in Strasbourg that supported me and was always there for me. A thank you is not enough but you know how high I have you in my appreciation! Next, I would like to thank some people from the BFC lab for some nice moments that we had together and especially for their translation skills in French. Dr Enes Dursun, Dr Tony Rady, Robin Dufossez, Dr Héloise Cahuzak, Safae Mouftakhir, Indréalie Lantus Penn, Louis Moreira De Silva, Dr Julien Most, Michel Mosser, Fanny Bousson and of course Ketty Pernod thank you so much. It was such a great pleasure to meet each one of you.

At this point, I would also like to thank the rest ESRs and their supervisors from the Marie Curie consortium for the unique time that we had together during the 6 meetings across Europe where the knowledge exchange alongside the constructive feedback and our nights

out were something that I will never forget. Thus, a huge thanks to Pr Christopher Scott, Bianka Jackowska and Ana Carvalho from QUB, to Dr. Bauke Albada and Irene Shajan from WUR to Dr. Torsten Hechler and Alessandra Totti from Heidelberg Pharma & to our project manager Dorothée Fraleux.

Last but not least, I would like to thank from the depth of my heart my family; Petros (father), Stella (mother), Eleni (sister) and Apostolos (brother), my cousin Theodoros who without him I would not be here now, as well as my best friends; Asteris, Giannis, Angelos and Andy (i.e., Dr Andrew Edmunds) and of course our new petite amie Chiara who recently joined our “gang”, for their unequivocal love and their implicit support during these very tough for me years.

PREFACE

This thesis was a part of a general project named TACT (Targeted Anticancer Therapies), an Innovative Training Network (ITN) funded by the European Union under the Marie Skłodowska Curie actions, *via* the Horizon 2020 Research and Innovation Program under the Action Grant Agreement No 859458.This training program enrolled 11 early-stage researchers (ESRs) from 9 different institutes (both from academia and industry) located in five different European countries.

ITN promotes communication, collaboration, and extensive exchange of knowledge among the several parties, to maximize benefits of the partnerships. During this three-year PhD-period, multiple networking activities were organized and held in various cities among the host institutions of the beneficiaries to enhance the competency of the ESRs *via* conferences, workshops, monthly reports, and regular meetings to present and discuss each researcher's results. Moreover, during these three years, we, the ESRs, had to perform one or two secondments, enabling us to pursue research in another institution of the consortium. By doing so, we were able to acquire complementary knowledge outside our area of expertise; an invaluable asset for our training and our future career.

The main objective of TACT project was the design of next generation treatments against cancer based on antibody-drug conjugates (ADCs), a fast-growing class of oncology therapeutics. ADCs are composed of a monoclonal antibody (mAb), on which cytotoxic drugs are attached – *conjugated* – in a covalent manner *via* small chemical linkers. The mAb is thus used as a carrier protein to deliver the antitumor agent directly into the cancer cell *via* the blood stream. As soon as they reach their target, the ADC binds to its targeted antigen (Ag) before the ADC-Ag complex gets internalized and hydrolyzed into the lysosome, resulting in the release of the cytotoxic drug intracellularly and the cell's apoptosis (**Figure 1**). All these three components exhibit different properties that can affect the ADC in various ways.

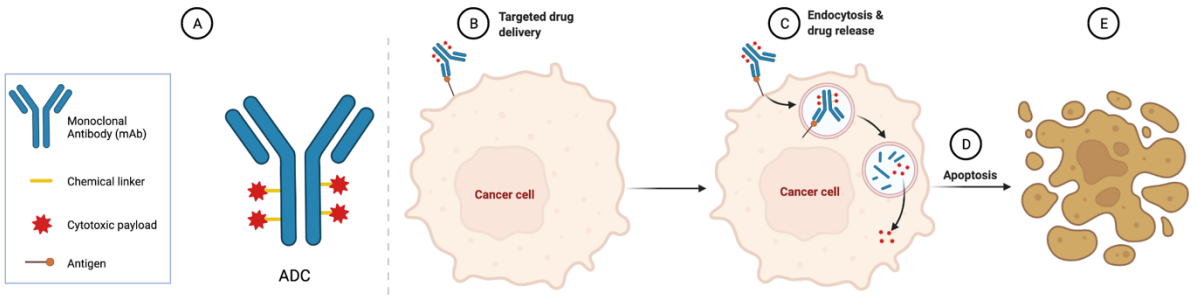

Figure 1. A) Antibody Drug Conjugate (ADC) components, B, C, D, E) ADCs mode of action.

To achieve the primary goal and based on these properties, the TACT consortium was divided in 5 major disciplines – the elaboration of novel carrier proteins, the design of novel linkers,

the synthesis of novel drug-payloads, the development of new bioconjugation methods connecting the protein with the linker attached with the drug payload and the development of novel analytical methods for the characterization of the new protein conjugates. Thus, 11 different projects among the fields of biology, chemistry, chemical biology and proteomics were carefully designed to ensure the most optimal outcome.

I was recruited at the University of Strasbourg in the group of Dr Guilhem Chaubet and Dr Alain Wagner in order to develop novel bioconjugation methods for the selective labelling of native proteins, such as mAbs. On this aspect, I have been involved in the study of site-selective conjugation of lysine residues and the efficient rebridging of solvent accessible disulfide bonds on mAbs. A **heterobifunctional hypervalent iodine(III) molecule** was first evaluated for the rebridging of cystine residues in different protein formats. Next, based on multicomponent reactions (MCR), we envisioned to target two spatially close amino acids (lysine and aspartate or glutamate) simultaneously *via* an **Ugi MCR** in order to reduce the number of modification sites. These projects were conducted in close collaboration with other ITN members, such as with the group of Dr Sarah Cianferani at the University of Strasbourg and the group of Pr Skerra at the TUM, along with other research groups, such as the group of Pr Jérôme Waser at EPFL.

In addition to my two main projects, I also participated in the design and syntheses of various **pyridazinedione** derivatives to evaluate their conjugation – deconjugation properties with cysteine residues during my first secondment (15/01/2022 – 17/04/2023) at UCL in the group of Pr Vijay Chudasama.

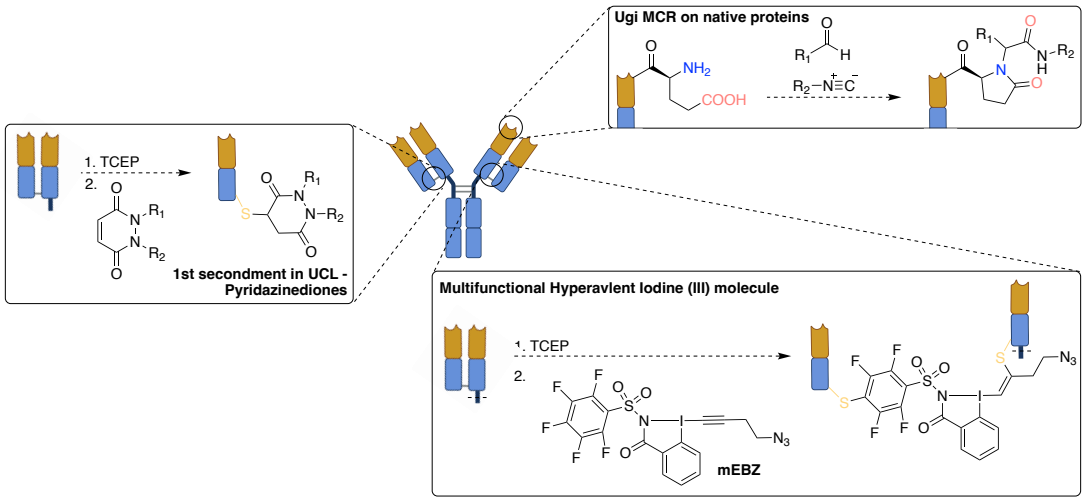

Figure 2. Thesis main objectives.

Finally, the 4th project that I have been involved in, took place during my 2nd secondment (18/4/2023 – 31/07/2023) at Spirochem, AG in Basel, Switzerland and was related with the synthesis of novel bicyclo[2.1.1]hexanes molecules under the supervision of Dr Christophe

Salome. Briefly, we developed two efficient and modular approaches allowing us to access new 1,2-disubstituted bicyclo[2.1.1]hexane modules, which are emerging bicyclic hydrocarbon bioisosteres for ortho- and meta-substituted benzenes, in good yields. Our strategy was based on the use of photochemistry to access new building blocks via [2+2] cycloaddition, in order to perform various derivatization reactions, opening the gate to sp^3-rich new chemical spaces (**Figure 3**). My desire to join Spirochem, AG was based on my will to further develop my synthetic organic skills and to experience working in a competitive and high demanding industrial environment. Although this work led to a publication,[1] a big part of my work there still remains confidential. Hence, in the interest of concision and clarity, since the subject of my PhD is mostly focused on the development of bioconjugation methods, this work will not be discussed in this manuscript.

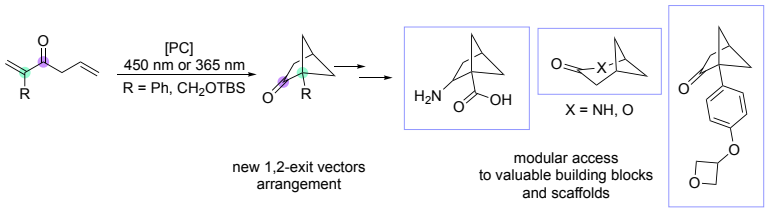

Figure 3. 2nd secondment in Spirochem, AG - synthesis of novel bicyclo[2.1.1]hexanes molecules

ABBREVIATIONS

AA	Amino acid
ADC	Antibody Drug Conjugate
BBS	Borate Buffer Saline
BCN	Bicyclononyne
BSA	Bovine serum albumin
cHex	Cyclohex(ane)yl
Cy5	Sulfo-Cyanine5
DAR	Drug to Antibody ratio
DBCO	Dibenzocyclooctyne
DBM	Dibromo-Maleimide
diBrPD	Dibromo-Pyridazinedione
DM1	Mertansine
DoC	Degree of Conjugation
dSEC-MS	Denaturating Size Exclusion Chromatography coupled with Mass Spectrometry
DTT	Dithiothreitol
EBX	Ethynyl benziodoxolones
EBZ	Ethynyl benziodazolone
EDG	Electron-donating group
EDTA	Ethylenediaminetetraacetic acid
EMA	European Medicines Agency
equiv.	Equivalents
EtOAc	Ethyl acetate
EWD	Electron-withdrawing group
Fab	Fragment Antigen binding
Fc region	Fragment crystallizable region
FITC	Fluorescein isothiocyanate
GFP	Green fluorescent protein
GSH	Glutathione
h	Hour(s)
HC	Heavy chain
HER2	Human epidermal growth factor receptor 2
HPLC	High performance liquid chromatography
HRMS	High resolution mass spectrometry

HSA	Human serum albumin
Hz	Hertz, s^{-1}
IC_{50}	Half maximal (50%) inhibitory concentration
IEDDA	Inverse electron demand Diels-Alder
IgG	Immunoglobulin G
IR	Infrared
kDa	Kilo Dalton
LC	Light chain
m/z	Mass-to-charge ratio
mAb	Monoclonal antibody
MCR	Multicomponent reaction
min	Minute(s)
MW	Molecular weight
nAA	Natural amino acid
NCL	Native chemical ligation
NGM	Next Generation Maleimide
NHS	N-hydroxysuccimide
nm	Nanometer
nM	Nanomolar
NMR	Nuclear Magnetic Resonance
nMS	Native Mass Spectometry
OEG	Oligoethylene glycol
PB	Phosphate Buffer
PBS	Phosphate Buffer Saline
PD	Pyridazinedione
PEG	Polyethylene glycol
***p*fp**	*Para*-fluorophenyl
PIPES	Piperazine-N,N′-bis(2-ethanesulfonic acid)
POI	Protein of interest
ppm	Parts per million
SDS-PAGE	Sodium dodecyl-sulfate polyacrylamide gel electrophoresis
Sec	Selenocysteine
SMCC	Succinimidyl4-(N-maleimidomethyl) cyclohexane-1-carboxylate
S_NAr	Nucleophilic aromatic substitution
SPAAC	Strain-promoted azide – alkyne click chemistry

***t*-Bu**	*tert*-butyl
T-DM1	Trastuzumab emtansine
TAMRA	Tetramethylrhodamine
TCEP	Tris(2-carboxyethyl)phosphine
TLC	Thin Layer Chromatography
TNBS	Trinitrobenzenesulfonate
Tris	Tris(hydroxymethyl)aminomethane
U-4C-3CR	Ugi four-component three-centre reaction
UAA	Unnatural amino acid
VBZ	Vinylbenziodazolone

TABLE OF CONTENTS

1. INTRODUCTION

Bioconjugation can be defined as the formation of a chemical bond between two molecules, one of which at least is a biomolecule. The resulting bioconjugates can display either the combined properties of its separate constituents or a new set of properties that cannot be explained by simply considering the two conjugated entities separately. Although based on empirical observations without a clear understanding of the molecular processes taking place, the chemical modification of proteins had long been present and used for practical purposes before becoming a topic of interest in chemical biology. The first successful applications of bioconjugation dates back to the mid-nineteenth century in the tanning industry, when chromium(III) salts and/or aldehydes were used to conjugate collagen from animal hides to form rot-resistant and waterproof leather products, although at the time the term bioconjugation has not been introduced yet.[2]

Back in 1920s, vaccines for bacterial infections were developed in the form of "toxoids" – *viz.* chemically inactivated bacterial toxins –, helping to prevent critical diseases, such as tetanus or diphtheria.[3] Recently, it was found that the inactivation mechanism was attributed to the initial conjugation of formaldehyde **I3** with primary amine groups, derived from lysine residues **I1** ,forming methylol adducts **I4** that were partially dehydrated yielding labile Schiff bases **I5**. The latter ones generate intramolecular cross-links with accessible, reactive amino acid residues, including arginine, asparagine, glutamine, histidine, tryptophan, or tyrosine **I2**, thus leading to inactive toxins (i.e., toxoids) most probably due to the permanent alteration of critical domains in the protein, for example, the catalytic site (NAD^+-binding cavity) and the receptor-binding site (**Scheme 1**).[4] Next, when the immune system receives a vaccine containing a harmless toxoid, it produces antibodies that opsonize the bacterial toxins without resulting in toxin-induced illness, thus learning how to fight off the natural toxin and neutralize its deleterious effects.

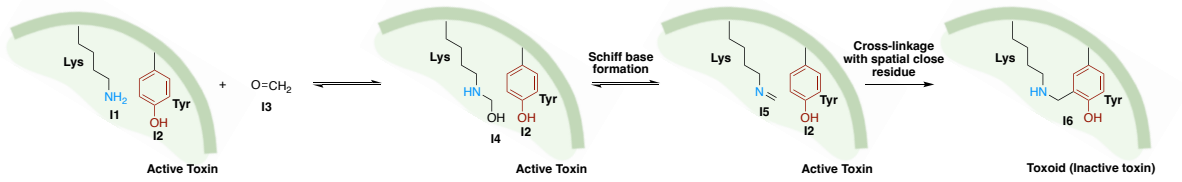

Scheme 1. Representative example of formaldehyde **I3** conjugation with an amino acid's amine; such as lysine, of an active toxin, followed by Schiff base formation due to partial methylol adduct's dehydration, that led to cross linkage with a spatially close residue, such as Tyrosine, resulting to the toxoid (inactive toxin) formation.

An explosion of interest in this field, in mid to late 1990s, emerged the desire/curiosity of better understanding proteins' properties. Proteins are composed of multiple copies of about twenty proteinogenic *α*-amino acids (AAs), and the lack of accurate analytical methods that would

determine the exact amount of each AA was an obstacle toward this goal. Crystallography and ion-exchange chromatography, best epitomized by the Durrum D-500 Amino Acid Analyzer, were two of the most abundantly used analytical techniques at the time, but none could provide quantification data, thus making protein characterization elusive. At that time, to decipher this puzzle, the focus was oriented on the so-called "group-selective" modifications, which describe the modification of a single type of amino acid (e.g., only lysines).[5,6] This was done by applying known *chemo-selective* organic reactions to target specific functional groups, such as the Van Slyke's procedure for example.[7] In this case, quantification of amine groups in intact proteins became possible by measuring the amount of gaseous dinitrogen released from proteins hydrolysates when reacted with nitrous acid. Inspired by this procedure, trinitrobenzenesulfonate (TNBS) **I10** or 5,5'-dithiobis-(2-nitrobenzoic acid) (DTNB) **I9** were used for the determination of amino and thiol groups, respectively, as shown in **Scheme 2**, by measuring the absorbance of their adducts; **I12** and **I14**, at 420 and 412 nm, respectively in a spectrophotometer.[8–11] Similarly, Barman & Koshland proposed a chemo-selective labeling of tryptophan residues with 2-hydroxyl-5-nitrobenzyl bromide (HNB-Br) **I11**, forming UV-active complexes **I13**, whose absorbance at 410 nm was an indirect measure of the number of indoles present in the protein. However, in the latter case, this procedure could only be performed in the absence of free thiols, while the measurement should preferentially take place at alkaline pH (>10) to maintain the chemoselectivity of the method.[12]

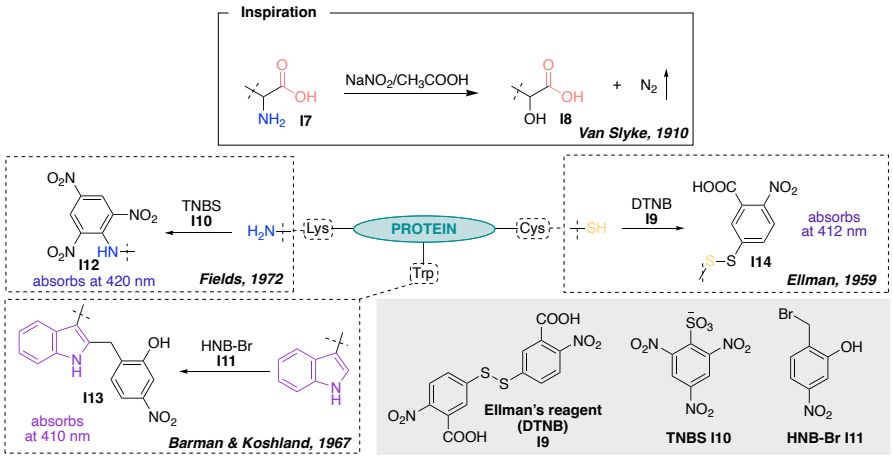

Scheme 2. Overview of quantification methods in proteins, using "*group selective*" reagents for the modification of specific functional groups.

Although limited, these early-stage bioconjugation methods proved to be invaluable tools for the characterization of proteins and were a decisive milestone toward a better understanding of the role and functions of proteins. Following a virtuous circle, the evolution of science, and more particularly in the therapeutic area, created breeding ground for the development of modern bioconjugation strategies that would enhance the selectivity and preserve the integrity

of the biomolecule. This would result in the discovery of new families of reagents and reactions that could be employed under *bioorthogonal* conditions – *viz.* chemical reactions that take place in living systems without interfering with its constituents – as they have been described by Nobel Prize-winner C. Bertozzi in 2003.[13,14]

Based on these early strategies, the identification of all amino acids composing proteins was achieved ending up with a rough overview of their abundance in them as listed in **Table 1**.[15]

Table 1. List of 20 proteinogenic amino acids abundance.[15]

Amino acid	Symbols	Structure	Abundance	Amino acid	Symbols	Structure	Abundance
Alanine	Ala, A		8.8%	**Leucine**	Leu, L	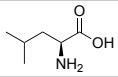	9.7%
Arginine	Arg, R	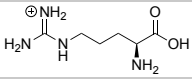	5.8%	**Lysine**	Lys, K	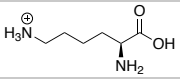	5.2%
Asparagine	Asn, N	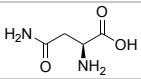	3.9%	**Methionine**	Met, M	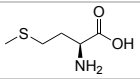	2.3%
Aspartate	Asp, D	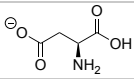	5.5%	**Phenylalanine**	Phe, F	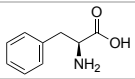	3.9%
Cysteine	Cys, C	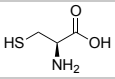	1.4%	**Proline**	Pro, P	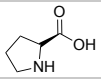	5.0%
Glutamine	Gln, Q	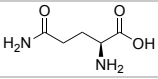	3.9%	**Serine**	Ser, S	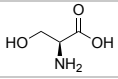	7.1%
Glutamate	Glu, E	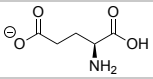	6.3%	**Threonine**	Thr, T	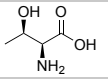	5.5%
Glycine	Gly, G		7.0%	**Tryptophan**	Trp, W	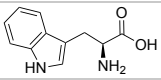	1.3%
Histidine	His, H	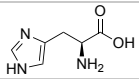	2.3%	**Tyrosine**	Tyr, Y	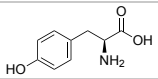	2.9%
Isoleucine	Ile, I	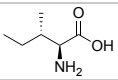	5.5%	**Valine**	Val, V	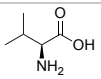	6.7%

This practically means that a small protein of about 300 AAs (with an approximate MW of 45 kDa) has for example 19 glutamates, 17 arginines, 16 lysines, 16 aspartates, 9 tyrosines, 4 cysteines, etc. Taking into consideration that the majority of AAs have nucleophilic side chains to some extent, the limited use of organic solvents, the narrow range of applicable temperatures and the restriction in using strong oxidizing/reducing agents, bases or acids makes the chemical conjugation of proteins challenging on many aspects. However, unlocking the door of this challenge would unveil many opportunities in proteins modification, thus synthetic chemists took up the gauntlet and by playing with proteins' physico-chemical properties created space for the development of new chemical tools. In this regard, chemoselectivity ("group selective") – targeting selectively only one family of amino acid residues; and site/regio-selectivity – targeting a single copy of a precise amino acid –

represent the central issues to be addressed, in order to develop techniques that would be reproducible and lead to homogeneous, well-defined protein conjugates.

Our group has recently reported a comprehensive review[16] on the field of chemical conjugation of native proteins. In the following sections, a subset of all strategies described in the aforementioned review shall be presented, insisting on the most known strategies for lysine, cysteine and *N*-terminal modification, with a focus on the most recently published studies that were not discussed in the original report.

1.1. CHEMO-SELECTIVE APPROACHES

1.1.1. Chemo-selective conjugation of natural AAs

Chemo-selective approaches, as defined before, concern only single type of functional group modification. Due to their nucleophilicity, abundance, and solvent accessibility, lysines and cysteines have been the subject of intense scrutiny by bioconjugation scientists, explaining their prevalence in the following examples.

1.1.1.1. Amine labelling

Among the 20 canonical proteinogenic *α*-amino acids, lysines represent approximately 5.2% of all residues in human proteins.[15,17] Alongside with histidines, arginines and *N*-terminal *α*-amines, lysines contribute to the net positive charge of proteins, and, due to their polar character, are solvent exposed thus are usually found on their outer surface, readily available for chemical derivatization. In comparison with the *N*-terminus *α*-amino group, the *ε*-amine of lysine possesses a slightly higher ionization point (*p*Ka of *ε*-amine is comprised between 9.3 and 9.5, while *α*-amine between 7.6 and 8.0), thus favoring the formation of positively charged ammonium groups at physiological pH. Hence, lysines modification tends to work best at alkaline pH (i.e., between 8.0 and 9.0) and a large variety of different electrophilic reagents have been reported for this purpose. However, three families dominate the field: *i*) carbonyls, *ii*) activated esters, and *iii*) iso(thio)cyanates.

As mentioned before, the use of carbonyl reagents for the formation of imines is one of the oldest examples of amine functionalization, and is at the heart of essential processes, such as the Maillard reaction. Although not widely used alone due to the poor stability of the resulting adducts, imine **I16** formation is often found as a preliminary step in several strategies, which use a companion nucleophile to trap these reactive intermediates. For example, reductive amination with various hydride sources, such as sodium cyanoborohydride **I17**, to form stable secondary amines **I18** have been reported (**Scheme 3**),[18,19] but many more exist and will be discussed in the following chapters.

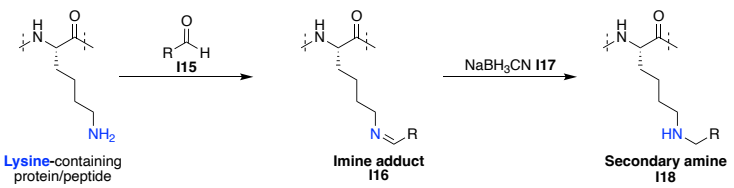

Scheme 3. Labelling of lysines *via* reductive amination.

Another strategy that has been also widely exploited in amine modification was the use of isocyanates and isothiocyanates, leading to urea and thiourea adducts, respectively. As

isocyanates are very susceptible to hydrolysis, they are not often used in bioconjugation. On the contrary, isothiocyanates are much more resistant, making them a more common reagent for the labelling of biomolecules, as best epitomized by fluorescein isothiocyanate (FITC) **I19**, a frequently used reagent for the fluorescent labelling of proteins (**Scheme 4**).[20,21] Finally, a lack of chemoselectivity has been documented in some cases, with reports showing that arginines' guanidines could also react with these electrophiles.[22,23]

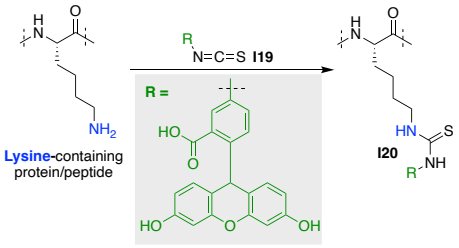

Scheme 4. Representative example of lysines labelling with FITC **I19**.

However, the most studied and most preferred strategy for amine modification remains acylation reaction with activated esters, leading to exceedingly stable amide bonds in just one step. In this domain, the most famous reagents are undoubtedly *N*-hydroxysuccinimidyl (NHS) esters **I21** and their more polar derivatives sulfo-NHS **I22** (**Scheme 5**), due to their convenient preparation and mild reaction conditions associated with their use (e.g., room temperature, fast kinetics, tolerant to various buffers and pH).[24] Despite their broad applications, issues in chemoselectivity have been reported, notably following a thorough study conducted by Kalkhof & Sinz in 2008 that demonstrated side reactivity with cysteines, serines, tyrosines, and threonines.[25] This could be sustained by "playing" on the pH of the reaction medium: under slightly acidic conditions (pH 6.0), NHS esters react preferentially with *N*-terminal *α*-amines and tyrosine's phenol groups, while lysine's *ε*-amine selectivity is the most pronounced at alkaline pH, even though this is accompanied with increased hydrolysis of the reagent.[26,27]

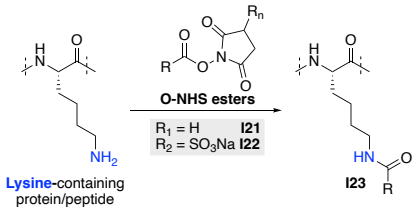

Scheme 5. Lysines labelling with NHS esters.

Amine conjugation has been extensively studied but due to amine's group high abundance, this strategy is accompanied by elevated degrees of heterogeneity, which is problematic for pharmaceutical applications for example. For this reason, people turned to other residues, still highly nucleophilic, but less abundant.

1.1.1.2. Cysteines labelling

In comparison to lysines, the low abundance (1.4%) and enhanced nucleophilicity of cysteines, with their thiolate side-chain group at alkaline pH (thiol's *p*Ka 8.0 – 8.3), make them an ideal target for labelling.[28,29] However, being usually found in native proteins in the form of oxidized cystine dimers, linked through a disulfide bond, a preliminary reductive step is often needed to reveal the hidden thiols, usually conducted with tris(2-carboxyethyl)phosphine (TCEP) or dithiothreitol (DTT).[30] Cysteine conjugation can take on several forms, but most of these correspond to alkylation or arylation. Alkyl halides have been used – and still are – for decades, before being supplanted by maleimide and organometallic reagents.

Alkylation *via* nucleophilic substitution (S_N2) and arylation via aromatic nucleophilic substitution (S_NAr), with the employment of *α*-halocarbonyls or aryl halides, respectively, represent two traditional methods for cysteine modification. Due to their high reactivity and fast kinetics, they were reported to lead to side reactions with other amino acids and functional groups (i.e., histidine, methionine, lysine, *N*-terminal residues),[31] an obstacle that could be overcome by either varying the halide source or "playing" with reaction conditions. A representative example of such application is iodoacetamide derivatives **I24** (**Scheme 6**), which, when used in stoichiometric amounts under slightly alkaline conditions for a few min., lead to excellent degrees of thiol chemoselectivity.[32]

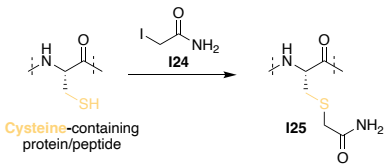

Scheme 6. Incorporation of iodoacetamide **I24** for the labelling of cysteine residues.

Among the traditional methods used for cysteine labelling, vinylpyridine **I26** and acrylamide **I28** derivatives, are two other well-known types of reagents that react *via* thio-Michael addition to yield thio-alkyl conjugates **I27** and **I29**, respectively (**Scheme 7**). These reagents have subsequently opened the way for development of modern strategies that will be thoroughly discussed in the following paragraphs and chapters.[33–35]

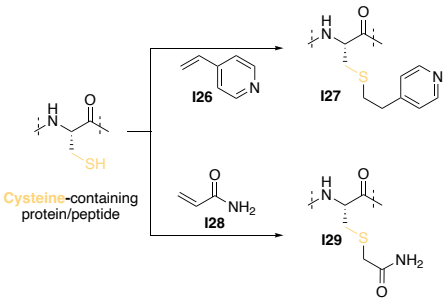

Scheme 7. Incorporation of vinylpyridine **I26** and acrylamide **I28** for the labelling of cysteine residues.

First introduced by Friedman in 1949 as cysteine selective reagents, maleimides **I31** are, to this day, the most prominent and widely used reagents for this type of conjugation, due to their exceptionally fast kinetics and significantly high selectivity.[36,37] A major setback to this strategy was the hydrolysis of maleimide reagent **I31** leading to ring opening adduct **I30** which was found to be unreactive to cysteine residues, thus extensive research has been conducted, by many groups, in an effort to better understand the mechanism hidden behind it. These studies unveiled that pH had an enormous impact on the efficacy of the conjugation strategy, with near-neutral values (i.e., 6.5 ≤ pH ≤ 7.5) offering the best compromise between selectivity and stability. At slightly higher pH (i.e., ≥ 8.0) it has been observed that a competitive Michael addition of amines could occur, leading to loss of chemoselectivity. Furthermore, to this observation, a retro-Michael addition of thiol-adduct **I32** was regularly spotted, leading to complete 'deconjugation' of the protein or cause a significant change in the properties of the conjugate. Finally, especially at pH > 9, maleimide ring opening by adjacent amine may yield to undesired cross-linked products (**Scheme 8**). However, it is also worth mentioning that post-conjugation hydrolysis of thiol-adduct **I32** leading to **I33** increased the stability of thiol-maleimide conjugates since it was found to prevent the retro-Michael addition due to the irreversibility of this step.[38,39]

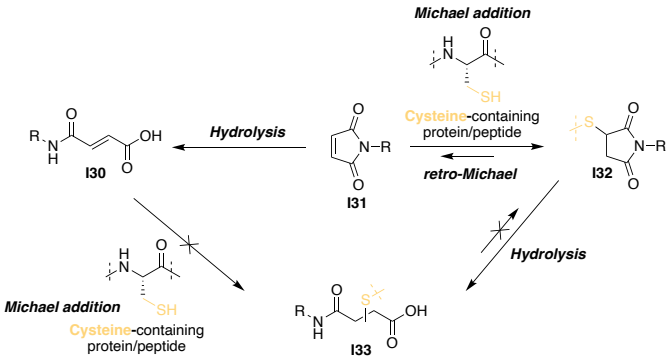

Scheme 8. General hydrolytic pathways of maleimides and thiosuccinimides.

The instability of maleimide-thiol moiety **I32** led to an in-depth evaluation of the *N*-substituent, in an effort to better understand its influence on the hydrolysis rate of imide moiety **I33**. *N*-Aryl,[40] or other substituents containing positively charged groups, such as amines,[41] demonstrated rapid hydrolysis, as shown in **Figure 4**. The presence of electron-withdrawing groups (EWG), other than amides, also yielded hydrolytically labile thiosuccinimides,[42] while the presence of carboxylate on the alkyl chain of **I36**, which introduced a more pronounced resistance towards hydrolysis, proved to be a notable exception to this trend, most likely because it is ionized at physiological pH. On the other hand, thiol adducts of *N*-alkyl maleimides showed exceptional stability, highlighting the importance of stereoelectronic effects on the stability of the imide electrophile and offering additional perspectives into the thiosuccinimides hydrolysis mechanism.[41,42] Hence, it can be concluded that *N*-substituents with electron-donating groups (EDGs), such as alkyl ones, decelerates the hydrolysis of thiosuccinimides while the opposite effect is taking place in the case of EWGs. This theory was further supported by the Wagner group who showed that maleimide **I38** containing a succinimidyl 4-(*N*-maleimidomethyl)cyclohexane-1-carboxylate (SMCC) linker resisted to hydrolysis in comparison with its 1,3-dioxan analogue **I39**.[43] However, the latter adduct did not suffer from *retro*-Michael elimination when incubated in human plasma for 120 h at 37 °C.[43] Efforts to further control the maleimides' ring hydrolysis or to tame the thiol deconjugation were pursued by introducing next-generation maleimides[38] and pyridazinedione scaffolds[44,45] that will be extensively discussed in the following chapters.

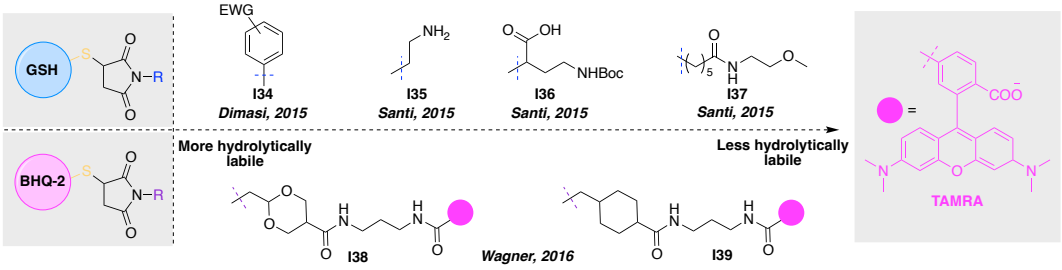

Figure 4. Maleimides stability based on the nature of the *N*-substituent.

Inspired by Rieghetti and coworkers who incorporated vinyl pyridines to selectively alkylate cysteines for quantitative proteomics in 2003,[46] Spring group engaged in an in-depth investigation of vinyl heteroarenes motifs to produce stable cysteine bioconjugates. After extensive research, they found that vinylpyrimidine derivatives, such as **I40**,could selectively conjugate cysteines yielding alkylated cysteine adducts **I41,** in both human serum albumin (HSA) and monoclonal antibody (mAb) Trastuzumab – used for the treatment of HER2-positive breast cancers –, necessitated 2 and 4 h, respectively, at 37 °C in Tris buffer at pH 8 (**Scheme 9**). At this point, it is noteworthy to mention that both albumin and antibody conjugates exhibited significant stability to deconjugation of the payload after 7 days of

incubation at 37 °C in various media (i.e. phosphate buffer saline (PBS), cell lysates, plasma).[47]

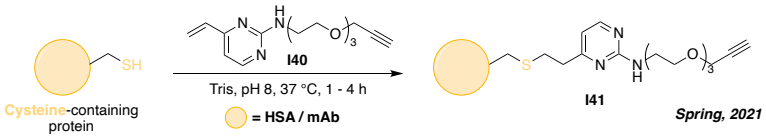

Scheme 9. Cysteine labelling of proteins with vinylpyrimidine derivative **I40**.

On a different note, Wang & Goldberg have recently reported the rapid electrophilic arylation of cysteines on medium molecular-weight proteins (~30 – 65 kDa) with almost stoichiometric amount of water-soluble *N*-alkyl-*o*-fluoropyridinium salt derivative **I42** in just 1 h in pH 7 piperazine-N,N′-bis(2-ethanesulfonic acid) (PIPES) buffer, as illustrated on **Scheme 10**. Interestingly, preliminary stability studies of glutathione (GSH) – conjugates revealed enhanced stability in deuterated water at 25 °C as their half-life was found to be greater than 300 h. However, it would be worth to see a future study demonstrating the stability results of larger protein conjugates in aqueous media.[48]

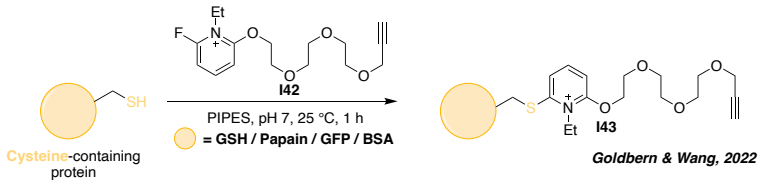

Scheme 10. Cysteine labelling of proteins with N-alkyl-o-fluoropyridinium salt derivative **I42**.

Elaborating a phosphorus(V)-based platform, Hackenberger and co-workers described the use of ethynylphosphonamidates **I44** and vinylphosphonothiolates **I46** for the labelling of cysteines. Both reagents showed excellent chemoselectivity at pH 8.5 and were employed on a large variety of proteins, whose resulting conjugates exhibited outstanding stability in different media (i.e., PBS, cell lysates, serum). While powerful, this new family of reagents yet exhibited slow kinetics (i.e., 3 to 24 h to reach full conversion depending on proteins size) and needed to be used in huge excess to offer full conversion (i.e., 1000 equiv. of DDT and 10 to 20 equiv. per thiol of either **I44** or **I46**), as shown in **Scheme 11**.[49,50]

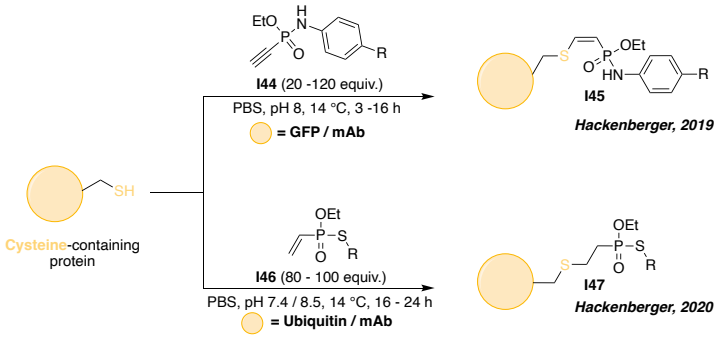

Scheme 11. Cysteine labelling of proteins with ethynylphosphonamidates **I44** and vinylphosphonothiolates **I46**.

In a similar vein, Waser and co-workers proposed the use of hypervalent iodine(III) derivatives for the modification of cysteines.[51,52] In 2020, they introduced ethynylbenziodoxolones (EBX) reagents, demonstrating that these highly reactive molecules necessitated just 5 min to reach full protein conjugation at 25 °C in PBS at pH 8.5. Azide-bearing EBX reagent **I48** was used for the introduction of bioorthogonal groups into proteins in the form of conjugate **I49**. Unexpectedly, a different reactivity was observed with trimethylsilyl derivative **I50**, where an alkynyl group was transferred on the cysteine's sulfhydryl one,[53] following a mechanism that will be extensively explained on chapter 2.3.1.2 on *page 43*. (**Scheme 12**)

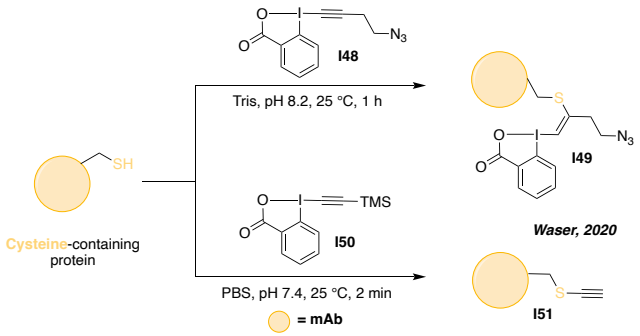

Scheme 12. Cysteine labelling of proteins with hypervalent iodine (III) EBX reagents.

Last but not least, palladium-catalyzed carbon-sulfur (C-S) bond formation has been well studied by several groups, leading to biocompatible conditions for the modification of several proteins. For example, Pentelute and Buchwald groups developed a platform for the incorporation of carborane groups on antibodies and sub formats thereof by palladium-mediated cross-coupling chemistry, as shown in **Scheme 13**.[54] Similarly, the Frost group synthesized a wide range of cyclopalladated Pd(II) complexes **I52** in situ, based on *N,N*-dimethylbenzylamine and acetanilide scaffolds, capable to selectively tag BSA's cysteine residue in just 1 h in PBS at 37 °C with over 90% conversion.[55]

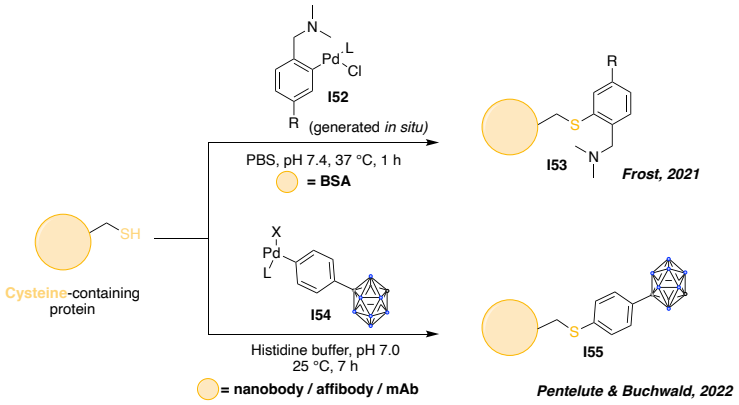

Scheme 13. Chemo-selective cysteines conjugation strategies employing organometallic reagents.

The number of methods for the chemo-selective labelling of cysteines is not limited to the previously mentioned reagents. Additional reagents were described over the years, especially for the re-bridging of disulfide bonds, and will be described in more details in the second part of this introduction.

The development of all these bioconjugation strategies led to the generation of myriad protein conjugates with numerous applications, such as the incorporation of fluorophores that helped with the understanding of cellular mechanisms by analyzing the trafficking of labelled proteins,[56] or introduction of polyethylene glycol (PEG) chains on bioactive molecules (PEGylation) to yield less-immunogenic and more plasma-stable proteins,[57,58] or the conjugation of cytotoxic drugs on a carrier protein aiming to diminish the systemic toxicity and facilitate their targeted delivery to malignant cells.[59,60]

Taking as an example the latter case and especially for antibody-drug conjugates (ADCs), the conjugation method was found to be one of the pivotal parameters for the efficacy of the resulting conjugates.[59,61] Although chemo-selective strategies led to highly potent therapeutics, such as ADCs Mylotarg®, Kadcyla® and Besponsa®, whose cytotoxic payloads were attached on the corresponding mAbs *via* lysine conjugation, they have also generated complex and highly heterogeneous regioisomeric mixtures. Composed of thousands of species with various degrees of conjugation, all of which possess different properties, chemo-selective strategies proved to be not the ideal strategy to ensure batch-to-batch reproducibility and consistency of immunoconjugates production. This is a direct consequence of the large size of antibodies (approx. 150 kDa) thus leading to an enhanced number of potential conjugation sites. The Heck group has effectively demonstrated this complication, by identifying that 69 out of 88 possible reactive amine groups (84 lysines and 4 *N*-termini) on immunoglobulins G1 (IgG1) could be labelled with NHS esters.[62] Based on this reactivity profile, this means that an IgG conjugated with six payloads would actually correspond to a mixture of approximately 120 million regio-isomers!

Hence, in order to address the heterogeneity issues that chemo-selective bioconjugation methods triggered, regio-selective (i.e. site-selective) – conjugation of one precise residue among its many copies – methods and reagents were developed. This was notably achieved by biochemical engineering, with the generation of artificial proteins containing specific amino acids or sequences that are naturally absent from the protein, allowing a site-selective modification. A simpler approach to achieve regio-selective conjugation would be to use native proteins and develop chemical strategies with the incorporation of small molecules and tuned conditions. These two different strategies will then be discussed in the following pages.

1.2. REGIO-SELECTIVE APPROACHES

1.2.1. Site-specific labelling of engineered proteins

1.2.1.1. Insertion of natural *α*-amino acids

Genetic engineering of proteins allows the controlled introduction of chemical handles at designated sites. Of great importance is the choice of the mutation site and the chemical nature of the natural *α*-amino acid (nAA) incorporated, in order to not only be readily accessible and reactive towards the conjugation reagents, but also to retain the protein's structure and function.

Based on their numerous advantages discussed beforehand, the incorporation of cysteines has been a method of choice, allowing the rapid and selective labelling of the mutant proteins with a plethora of reagents, as discussed previously and in recent reviews.[63] One of the most famous examples of such approach is the Thiomab® technology, initially developed by Genentech and now widely used in the industry for the manufacture of regio-selectively conjugated ADC. The selection of cysteine residues was based on their absence in free form as they are mostly present as disulfides to stabilize proteins' tertiary structure. On top of that, the exact site of mutation should be carefully planned as the antibody's binding site should remain unaffected in order to maintain its initial properties. Thus, after extensive studies,[64] two key residues of an IgG1 were identified as the ideal ones for this purpose and were replaced with cysteines (i.e., light chain's V110C and heavy chain's A114C in Trastuzumab), creating two amenable sites for conjugation with maleimide-containing cytotoxic payloads **I56**. However, the introduced cysteines formed undesirable disulfides with cysteines (Cys) or glutathione (GSH), presumably formed during the fermentation process, thus an extra reduction/re-oxidation step was required before their conjugation as demonstrated on **Scheme 14**. [65,66]

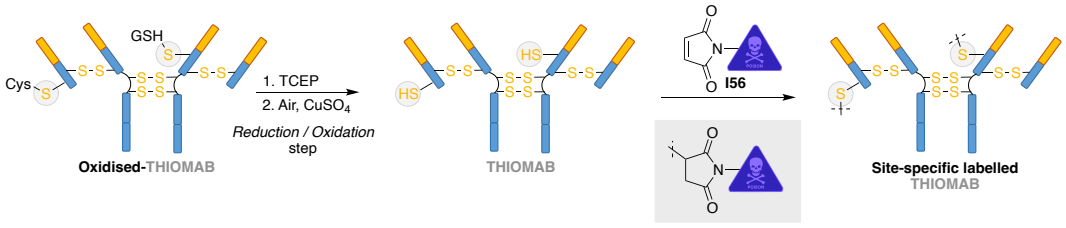

Scheme 14. Labelling of monoclonal antibodies with Thiomab® technology.

A well-known alternative to the insertion of cysteines is the incorporation of selenocysteine (Sec) residues;[67,68] the so-called 21st proteinogenic amino acid,[69] chalcogen analogues of cysteines, bearing a selenium atom instead of a sulfur. Selenocysteines are far less abundant

than cysteines in nature, as only 25 discrete selenoproteins have been identified in humans so far.[70] The selenol group has a pK_a of 5.2, making it more easily deprotonated and, all things being equal, more nucleophilic than its sulfhydryl counterpart (pK_a 8.3). Similar to Thiomab's technology, Selenomab was introduced by Hofer *et al.* in 2008 for the manufacture of ADCs, with the insertion of one or two Sec residues on the *C*-termini of various mAbs, which were subsequently readily available for conjugation with maleimide- or iodoacetamide-containing payloads **I57** and **I58**, respectively (**Scheme 15**), for instance. In comparison with cysteines, selenocysteines demonstrated faster kinetics due to their enhanced reactivity, avoidance of the extra reformation step of disulfide bridges in comparison to Thiomab technology, while the produced ADCs exhibited excellent stability in diverse *in-vitro* and *in-vivo* models.[67,68,71]

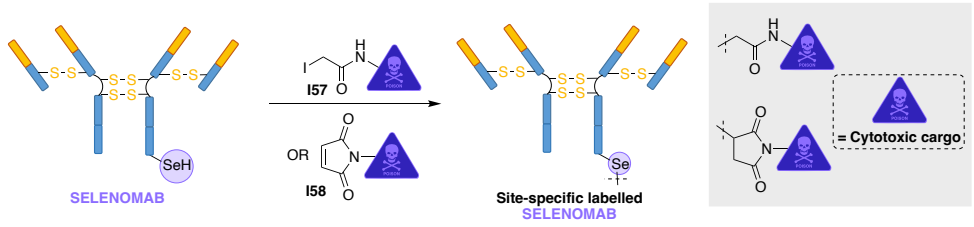

Scheme 15. Labelling of monoclonal antibodies with Selenomab® technology.

Other low-abundant amino acids have also been engineered on proteins, such as tryptophans, tyrosines, methionines and histidines. However, contrary to cysteines which are usually in the form of disulfides or to selenocysteines that are rarely found in proteins, thus not readily available for modification, these AAs exist in their free forms, hence addition of one of those could reveal regio-selectivity issues. Finally, due to the lower reactivity of these four side chains in comparison to more nucleophilic ones – such as cysteines, selenocysteines or lysines – more extreme conditions – such as prolonged incubation times, high temperature, use of oxidizing agents – with the simultaneous use of catalysts were necessitated to overcome this limitation.[72–75]

1.2.1.2. Insertion of unnatural *α*-amino acids

Employment of unnatural *α*-amino acids (UAAs) for protein engineering represents another reliable method to achieve site-selective protein modification. This approach was based on a "plug and play" platform where a large variety of functional groups could be inserted into proteins *via* genetic code expansion offering the possibility to facile bioorthogonal modifications (*v. supra)*. The well-known click chemistry strategy that takes place between alkyne- and azide- containing molecules to generate cycloaddition products,[76] represents a nice example of such type of chemical modifications. Among these "plug and play" approaches that could take place under bioorthogonal conditions, the Staudinger ligation, the inverse electron demand Diels-Alder reaction (IEDDA) or the oxime ligation are only some of the most famous and representative examples. For this reason, azide, alkyne, alkene, tetrazine or carbonyl-containing amino acids were designed and incorporated into proteins offering the possibility to use bespoke reagents to modify these exogenous, unnatural moieties selectively without interfering with any natural functional groups.

Schultz & Kazane in 2014 reported one of the first examples of an engineered protein featuring an UAA and used to manufacture a homogeneous ADC. Alanine (A122) of the heavy chain (HC) of an anti-CXCR4 antibody was genetically replaced by *p*-acetyl-L-phenylalanine (*p*AcF) **I59** and was further modified *via* oxime ligation with a *O*-alkoxyamine derivative of the cytotoxic drug **I60** (**Scheme 16A**).[77] However, acidic pH and prolonged incubation times were required for such reactions usually lead to protein denaturation, thus alternative solutions were emerging.

Around the same period, Sato and coworkers have incorporated another phenylalanine-based UAA, this time featuring an azide group and coined *p*-azidomethylphenylalanine (pAMF) **I65**, which could undergo rapid strain-promoted azide – alkyne click chemistry (SPAAC) reaction under physiological conditions. In more details, *p*AMF **I65** was incorporated into Trastuzumab's HC in lieu of serine S136 and was further conjugated at 25 °C for 12 h with dibenzocyclooctyne (DBCO)-containing cytotoxic payload **I66** to form stable ADC **I67** (**Scheme 16B**).[78] Switching to another family of UAA, several groups have incorporated azido-lysine (AzK) **I71** in various IgG isotypes (**Scheme 16C**); enabling the subsequent generation of genetically modified ADCs with various cycloalkyne-containing payloads *via* SPAAC.[79–81]

Parallel to the development of SPAAC for the labelling of proteins, IEDDA also emerged as a new promising tool. Reacting electron-poor dienes with tetrazine dienophiles led to exceedingly fast bioorthogonal reactions. A representative example of such approach was described by Chin and co-workers who reported the incorporation of a cyclopropene derivative of lysine (CypK) **I62** into Trastuzumab that could subsequently undergo a rapid (3 h) and

efficient inverse-electron demand Diels–Alder (IEDDA) reaction with tetrazine-containing payloads **I65** (**Scheme 16D**).[82] Similarly, both Christie and Marellis groups have replaced Trastuzumab's HC lysine K274 with cyclopentadiene-containing UAA spiro[2.4]hepta- 4,6-diene-lysine (SCpHK) **I68** that underwent irreversible Diels–Alder cycloadditions with maleimide-modified drugs **I69** (**Scheme 16E**).[81,83]

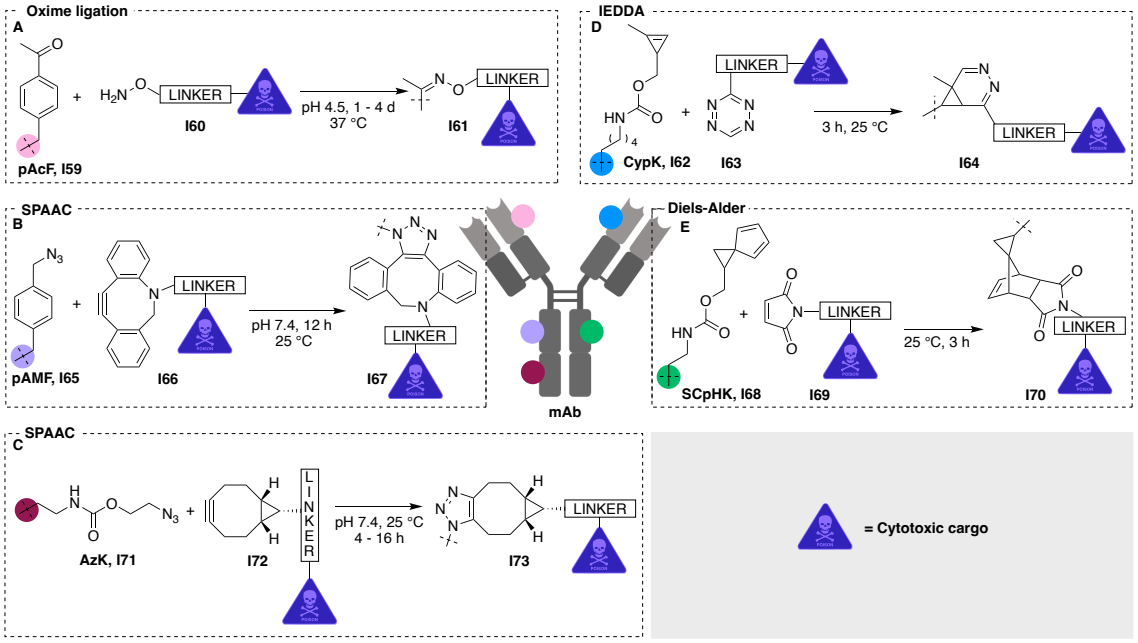

Scheme 16. Overview of chemical ligation strategies on engineered monoclonal antibodies with the introduction of UAAs. A) Oxime ligation between ***p*AcF** with alkoxyamine-modified drug **I60**. B) SPAAC reaction between ***p*AMF** and DBCO-modified drug **I66**. C) SPAAC reaction between **AzK** and BCN-modified drug **I72**. D) IEDDA reaction between **CypK** and tetrazine-modified drug **I63**. E) Diels-Alder reaction between **SCpHK** and maleimide-modified drug **I69**.

Up to the present time, several UAAs have been effectively employed into proteins in order to be selectively modified with bespoke reagents in a bioorthogonal manner. Dehydration or cycloaddition strategies, as the ones described beforehand, are only some of the most facile and widely used reactions, while a large variety of other methods for such type of modification has been also described (e.g., incorporation of aryl/alkenyl halide-containing UAAs for cross coupling reactions, insertion of alkenes prone to Michael additions or cross metathesis reactions).[84–91] Besides single-residue incorporation, though, the insertion of peptide and protein tags offers a complementary and valuable alternative as they open the door to site-selective conjugation of artificial proteins.

1.2.1.3. Insertion of protein/peptide tags

Complementary to the site-selective labelling of UAA-containing macromolecules, researchers have also investigated the genetic engineering of fusion proteins, *viz.* a chimeric artificial protein resulting from the combination of two or more proteins or fragments thereof. Taking advantage of the exceptional selectivity that enzymes offer, small protein domains or peptides, derived by them, would be incorporated into the protein of interest (POI) in order to be covalently and selectively labelled by desirable small molecule, thus offering site-selective bioconjugation.

Human O^6-alkylguanine-DNA alkyltransferase (hAGT) is a DNA repair protein that acts as a scavenger of O^6-alkylated guanine nucleobase by transferring the alkyl group to one of its reactive cysteine residues. Inspired by this transformation, O^6-benzylguanine derivatives **I75** were synthesized, targeting selectively and rapidly engineered proteins of interest (POI) fused with hAGT, a platform named SNAP-Tag **I74**. Relatedly, the CLIP-tag **I77** technology, which uses *O*-benzylcytosine derivatives **I78** to label a reactive cysteine residue, was later introduced. Surprisingly, despite similar structural features, SNAP-tag **I74** and CLIP-tag **I77** were shown to be orthogonal to one another, allowing simultaneous and selective labelling of two different fusion proteins.[92–94]

Other famous examples of fusion proteins are HALO-tag **I80** and PYP-tag **I83**, based on *Rhodococcus*'s haloalkane dehalogenase (DhaA), using alkyl chlorides **I81** as substrates for carboxylate alkylation, and on the photoactive yellow protein (PYP), derived from bacterial enzymes and functionalized by thioester coumarin derivatives **I84**, respectively (**Scheme 17**).[95–97]

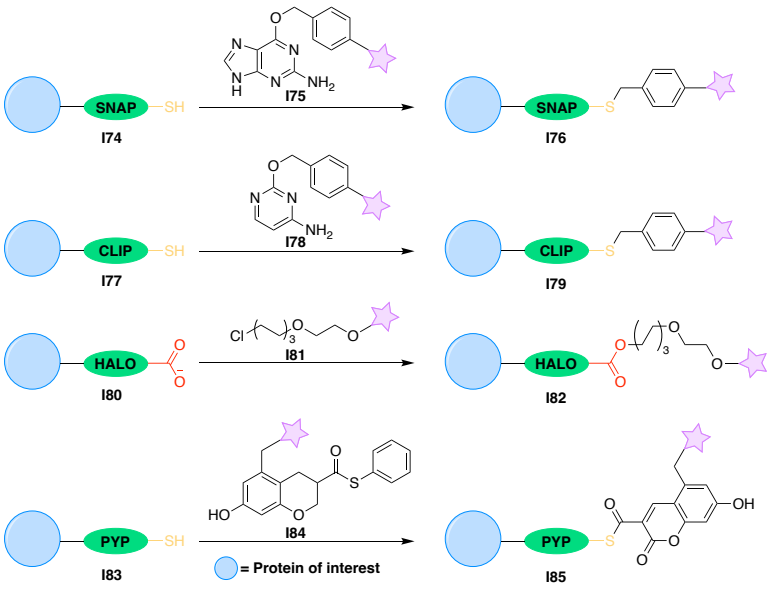

Scheme 17. Site-selective protein labelling with the incorporation of protein tags.

Although a powerful method, protein fusion on larger proteins, such as mAbs, could be challenging, as the resulted molecular weight of these chimeric assemblies would alter some key properties of the POI (e.g., structure, function, dynamics, localization). In addition, the fusion site is of major importance, as it could disturb key properties of the protein (e.g., binding affinity, signaling, aggregation due to potential differences in proteins' ionization points). Thus, more 'tolerable' motifs were introduced, like small peptide sequences comprising few AAs and were mainly genetically incorporated either on the *N*- or the *C*-terminus of the POI. Finally, in mAbs' case, modifications at the *N*-terminus should be carefully monitored to ensure that conjugation does not hinder antigen's binding affinity; a topic that will be thoroughly discussed at the third chapter.

A representative example of this approach was reported by the Pentelute group who installed a tetrapeptide motif (FCPF) **I86** coined π-clamp, whose hydrophobic and phenyl-rich micro-environment helped to site-selectively label the tag's unique cysteine with perfluoro-aromatic reagents **I87**, even in the presence of other competing cysteine residues. The π-clamp sequence was initially appended to the *C*-termini of Trastuzumab's heavy chains, followed by its selective conjugation with a drug-containing perfluoro aromatic probe via an S_NAr reaction under mild conditions yielding *para*-substituted analogues **I88**.[98] Two years later, the same group, after extensive screening of various cysteine-containing heptapeptides with random amino acid flanking the Cys residue (such as XCXXXXX, where X represents any natural amino acid except Cys, Arg, Ile, Asn, and Gln), identified a particularly reactive heptapeptide tag (LCYPWVY) **I89** that was introduced at the *C*-terminus of Trastuzumab, enabling highly regio-selective cysteine modification *via* a DBCO-containing payload **I90** (**Scheme 18**).[99]

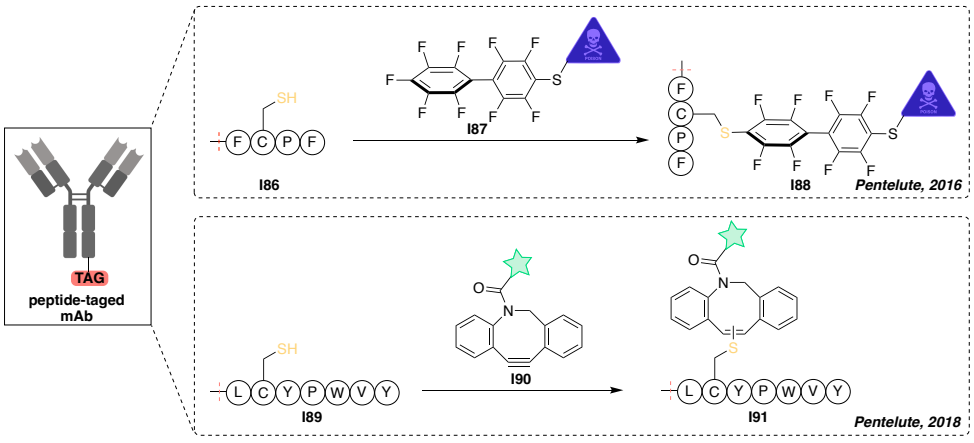

Scheme 18. Installation of small peptide tags on the *C*-terminus of a POI followed by selective labelling with bespoke probes.

Site-selective chemical conjugation of artificial proteins thus offered prominent results thanks to the incorporation of nAAs or UAAs, either as single residues or as part of peptide and protein tags. Although the high degree of site-selectivity and good conversion these methods offered, they also proved to be tedious and costly, while some of these conjugates even led to immunogenic response or aggregation arising from changes in their amino acids sequence, thus rendering their application challenging. A cheaper and quicker alternative to this technology was thus to investigate the development of chemical, regio-selective approaches employing native proteins.[100]

1.2.1.4. Site-selective labelling of native proteins

1.2.1.4.1. Single lysine residue labelling

As previously mentioned, lysines are high value targets but their high abundance in proteins make their site-selective conjugation daunting, attracting notable attention from various chemistry groups to pick up this challenge.

A first approach consisted in starting from known chemo-selective reagents and strategies and trying to enhance their selectivity, notably by playing on kinetic parameters. This was best epitomized by the work of Weil and co-workers in 2012, who site-selectively conjugated K1 on two proteins (RNase A and lysozyme C) *via* a kinetically controlled labelling by adding 0.01 equiv. of NHS-ester **I92** over 100 min (totaling 0.5 equiv.) (**Scheme 19**). This selectivity was attributed to stereoelectronic effects after careful examination of the two proteins' crystal structures: K1's best solvent accessibility in the case of RNase A, and hydrogen bond between K1 side-chain's ammonium and E7's neighbouring carboxylate group, increasing K1's nucleophilic character in the case of lysozyme C. As expected from the conjugation conditions, site-selectivity occurred to the detriment of partial conversion and limited yield, even though this could be overcome by affinity purification on avidin column isolating the desired monoconjugates.[101]

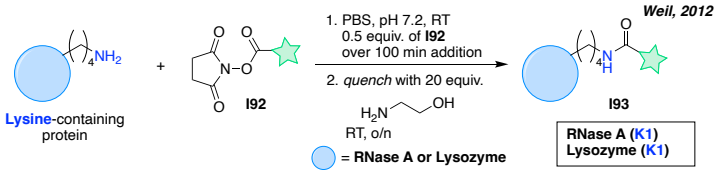

Scheme 19. Lysine site-selective conjugation of both RNase A and Lysozyme C *via* kinetically controlled addition of NHS-ester derivatives.

Remaining on the same concept but "playing" with another parameter, Cellitti, Geierstanger and co-workers demonstrated in 2018 how temperature can have a pivotal role in site-selectivity. Utilising pentafluorophenyl esters **I94** and the Fab fragment of Trastuzumab, they showed that by lowering the temperature to 4 °C in combination with flow chemistry could reach nearly quantitative labelling of K188 residue. Interestingly, they demonstrated that this selectivity was certainly due to the micro-environment surrounding the labelled residue, as mutation of either one of the spatially close histidine H189 and aspartic acid D151 to Ala led from little to no conjugation of the resulting mutants under the exact same conditions (**Scheme 20**).[102]

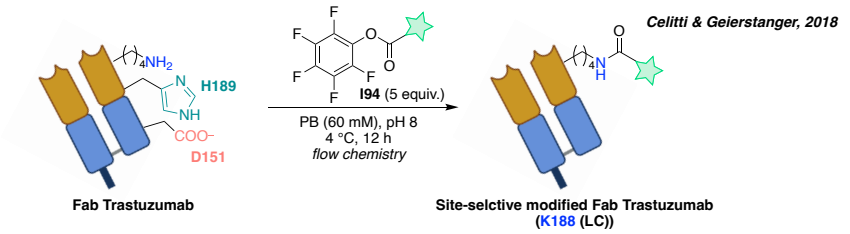

Scheme 20. Lysine site-selective labelling of Fab-Trastuzumab with pentafluorophenyl esters **I94** *via* flow chemistry at low temperature.

On the same year, Bernardes and co-workers reported another – computer-assisted – site-selective strategy exploiting lysines' microenvironments. Their research led to the identification of lysine residues in a pool of native proteins with enhanced nucleophilicity, presumably caused by the surrounding hydrophobic environment. By proceeding through a low energy, H−bond assisted chair-like addition transition state, the addition-elimination of the *ε*-amine of the most reactive lysine to the sulfonyl group of the sulfonyl acrylate reagent **I95** led to N−C bond formation and spontaneous elimination of methanesulfinic acid. Modification with the sulfonyl acrylate was highly efficient (>95% conversion) on all proteins evaluated and proceeded under mild conditions with stoichiometric quantities of reagent **I95** required, since excess ones were leading to loss of selectivity (**Scheme 21**).[103]

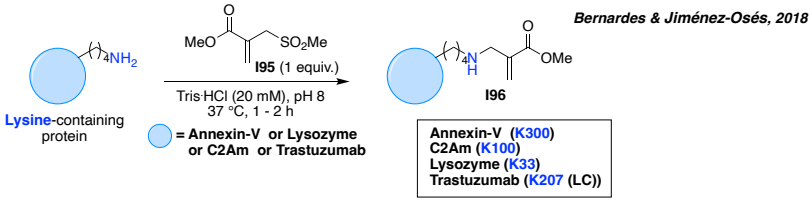

Scheme 21. Lysine site-selective labelling of native proteins with stoichiometric quantities of sulfonyl acrylate reagent **I95** *via* computer assisted exploration of lysines' microenvironment.

Extensive work on site-selective conjugation of lysines has been exploited by the Rai group, who demonstrated in the past 6 years, that a different type of approach than the thermodynamically / kinetically controlled reactions or computer assisted ones by incorporating multicomponent reactions (MCRs). Their initial efforts started in 2017 when they employed a copper-catalyzed multicomponent reaction by reacting formaldehyde **I3** and terminal alkyne **I97** to achieve site-selective conjugation of lysine residues on various proteins.[104] Although the large excess of equiv. accompanied with prolonged incubation times (3 days!) and multiple cycles of EDTA washes to remove copper residues, this MCR approach delivered medium to good conversion rates – protein dependent (**Scheme 22**) – with admirable site-selectivity.

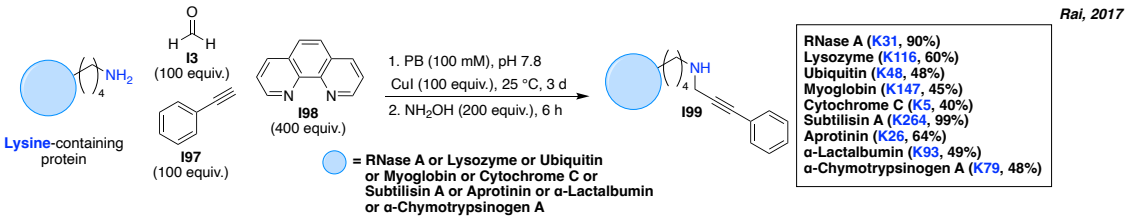

Scheme 22. Lysine site-selective labelling of native proteins *via* catalytic MCR.

One year later, in 2018, the Rai group reported another metal free multicomponent approach, by employing a phospha-Mannich, Michaelis-Arbuzov-like reaction to target a single lysine residue of numerous small proteins with benzaldehyde **I100**, forming an imine as an *in-situ* electrophile. The resulted imine was substituted irreversibly by nucleophilic alkylphosphites, generating stable and site-selective conjugates. By using a similar aldehyde motif (**I103**) but keeping the conditions intact, they formed a Trastuzumab conjugate by selectively modifying K183 of the light chain (LC) (**Scheme 23**).[105]

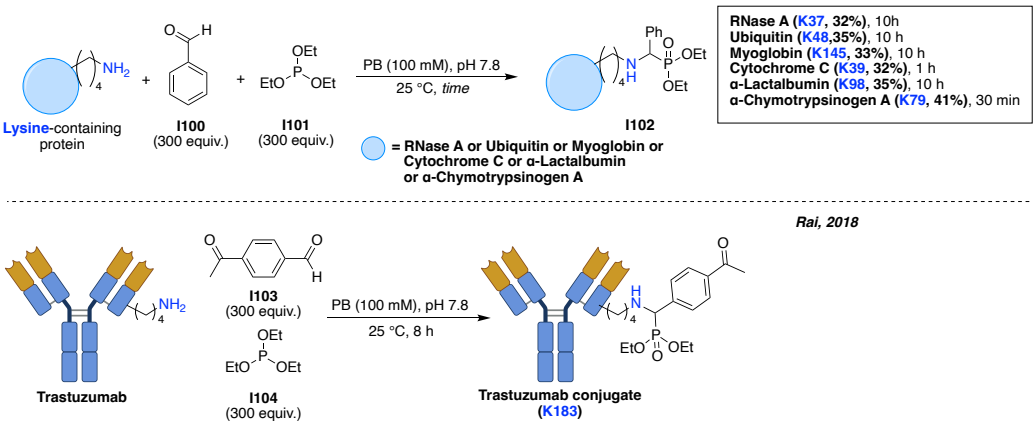

Scheme 23. Lysine site-selective labelling of native proteins *via* phospha-Mannich type MCR.

Drifting from MCRs which tend to be promptly affected by the spatial close residues of the targeted lysine, another strategy that follows a similar pattern will be introduced. By incorporating covalent tethers, an initial, often reversible, reaction on a temporary binding site can bring another reactive moiety in closer proximity to the desirable site of modification. An example of covalent tethering is native chemical ligation (NCL), which is commonly used for site-selective protein modification, utilising a thioester-mediated chemo-selective reaction.[106] More precisely, NCL relies on a rate-determining reversible transthioesterification between a *C*-terminal thioester and a *N*-terminal cysteine, before a spontaneous *S*- to *N*- acyl transfer *via* a 5-membered ring intermediate leads to an irreversible amide bond formation. Such application has been nicely described by Chudasama's & Baker groups who utilized **I105** for the site-selective modification of lysine K136 residue of Fab-Trastuzumab, achieving 80% conversion (**Scheme 24**).[107]

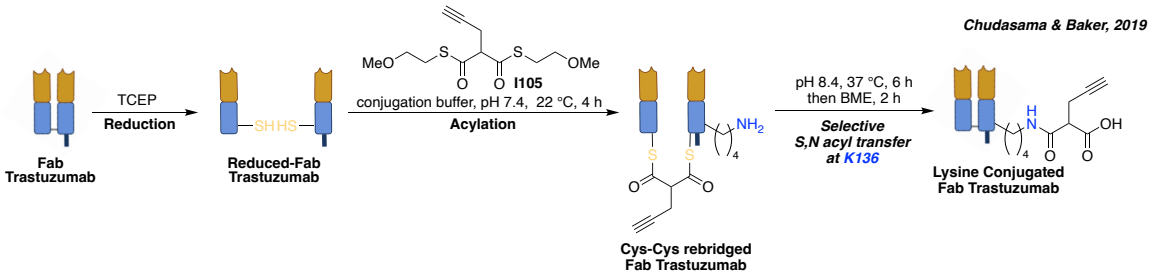

Scheme 24. Lysine site-selective labelling of Fab-Trastuzumab *via* NCL.

Rai and co-workers developed a variation of NCL for the site-selective labelling of lysines, named linchpin strategy.[108] To achieve their objectives, reagents like **I106** with two reactive handles separated by spacers of different sizes and structures were designed. On the one side of these reagents, an aromatic aldehyde would form Schiff bases **I107** with two spatial close lysines *via* a fast and reversible reaction. This would consequently direct the approach of the activated carbonyl group, located on the other side of molecule, towards a proximal lysine to form *N*-alkylated adducts (**I108**) *via* a slow and irreversible manner. A lot of examples of site-selective conjugation in various proteins (**Scheme 25**) *via* this method were described. Although high degree of selectivity was achieved, the conversion rates were low with noticeable differences from protein to protein, perhaps attributed to the different microenvironment of lysines, a phenomenon that has been previously seen in other lysine-modification strategies. The huge range of incubation times (2 – 16 h) could indicate that the reaction was kinetically controlled, while it was also found to be depended on the length of the spacer. The final irreversible step tends to direct the reaction; a feature that it is also seen on the Ugi MCR last step, where a Mumm rearrangement takes place, and is essential for the formation of the desirable adduct (*v. infra)*.

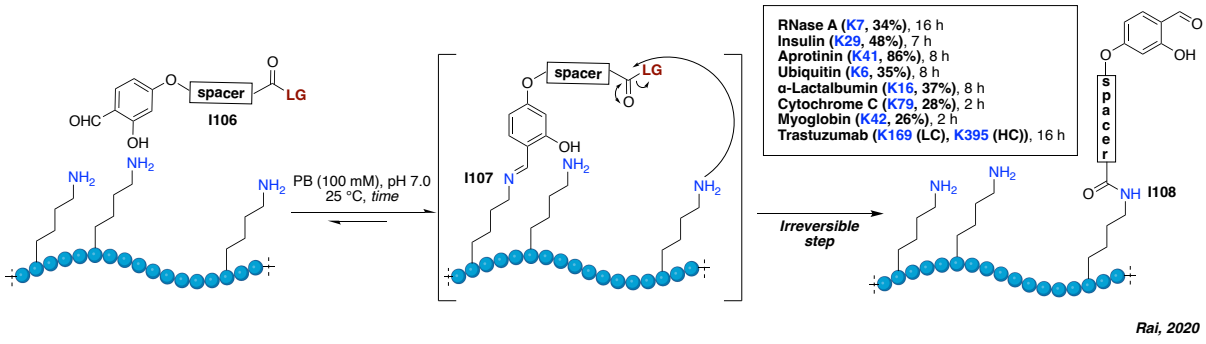

Scheme 25. Lysine site-selective labbeling of native proteins *via* Rai group's Linchpin strategy.

A completely different strategy was employed by the company Ajinomoto Bio-Pharma, that exploited a technology under the brand name AJICAP® for the regio-selective conjugation of K248[109] on the Fc region of IgG1. Derived from Protein A – a protein that recognizes and selectively binds on the Fc region of this type of isotype IgGs – Yamada and co-workers

designed the Fc-affinity tag **I109** – containing at the one end the recognition peptide that directs the conjugation to K248 and an activated ester on the other end that allows its ε-amine's alkylation – to selective introduce a thiol group on K248, after a consecutive red-ox step, readily available for functionalization with desirable payloads as illustrated on **Scheme 26**.[110] However, this red-ox treatment can lead to disulfide bond scrambling or aggregates production; risks that have been previously detected on THIOMAB® technology.[111] Thus, a 2nd generation, red-ox-free AJICAP® reagent **I110** based on a thioester motif was introduced, which allowed access to the desirable sulfhydryl group in a single step, after hydroxylamine treatment.[112]

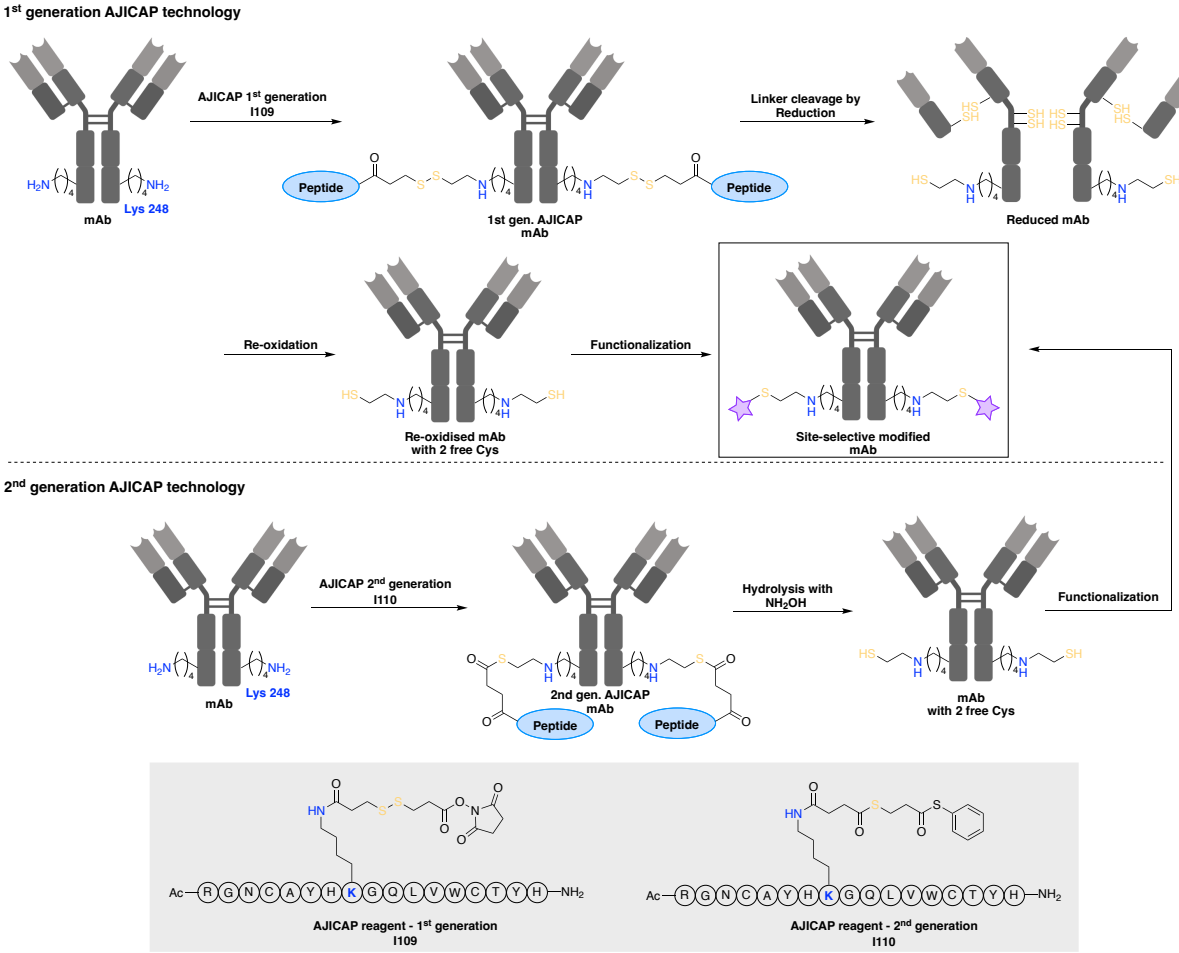

Scheme 26. Lysine site-selective labeling of IgG1 isotype of mAb *via* AJICAP technology.

Taking into careful consideration these studies, it can be concluded that lysines' microenvironment and the chemical structure of the electrophile are both equally important, while the slightest variation in either of these parameters can drastically alter the site-selectivity of a given strategy. Focusing instead on cysteines conjugation, which are less abundant than lysine residues – 8 solvent accessible cysteines *versus* 88 lysines in an IgG1 – could enhance our chances to develop a site-selective method with higher conversion rates by simply conjugating all 8 residues.

1.2.1.4.2. Rebridging of cystine residues

As stated before, cysteines mostly exist in the form of disulfide bonds in proteins. Taking advantage of this close proximity between two cysteines, a strategy named ‘disulfide rebridging’ was introduced. Disulfide rebridging consists in the reduction of disulfide bonds followed by reaction with a cysteine-selective bifunctional reagent, bearing two reactive sites per scaffold. By reconnecting cysteine residues in a covalent manner, the stabilising effect of disulfide bonds is maintained and a controlled loading of one rebridging molecule per disulfide can be achieved. Depending on the number of payloads attached to each reagent, highly modular average degree of conversion (avDoC) can be obtained – e.g., values of 4 for an IgG1 isotype containing 4 solvent accessible disulfide bonds; i.e., 8 cysteines.[117] Here, I will mainly focus this short review on the latest developments of the field after introducing some of the most established disulfide-rebridging strategies.

Bissulfone-containing reagents were the first to be reported for disulfide rebridging in 1990, with an application to the generation of antibody conjugates.[113,114] Formally, the rebridging occurs following two consecutive thio-Michael addition-elimination reactions, resulting in three-carbon rebridging bond. Recently, bissulfones have been applied to the synthesis of ADCs, in the form of a bissulfone linker technology licensed by Abzena to various pharmaceutical companies under the tradename ThioBridge® **I112**.[115] Typical reaction conditions are very mild and involve incubation of reduced IgG1 with 5 – 6 equiv. of bissulfone **I111** at pH 7.5 for 16 h at 22 °C, yielding highly homogeneous conjugates with DoC 4 – indicating the site-selective conjugation of all 8 cysteines – and conversion rates ranging from 70 – 95% (**Scheme 27**). However, as in most cases with cystines rebridging of IgG1 isotypes, the final product consists in a mixture of two isomeric species; one being the “natively rebridged” species, with all polypeptide chains rebridged in an interchain manner, and the second corresponding to ‘‘half-antibody’’ species, where disulfide scrambling led to intrachain rebridging in the hinge region.[115]

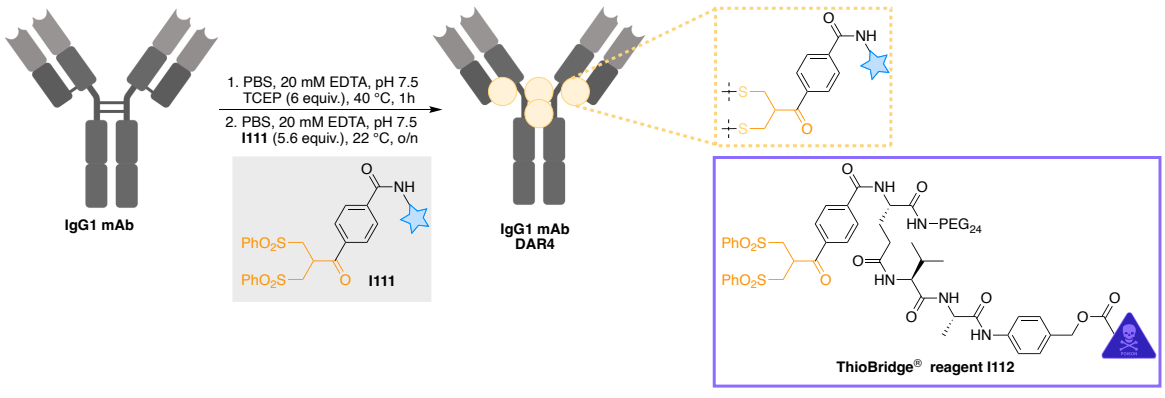

Scheme 27. Cysteine – Cysteine rebridging of an IgG1 mAb *via* bissulfone-containing reagents.

In a seminal report in 2010, Caddick & Baker first reported next-generation maleimides (NGMs) **I113**, a class of maleimide reagents modified to contain two halide or thiophenol leaving groups amenable to disulfide rebridging. Following a similar mechanism as bissulfones, these reagents could efficiently rebridge reduced disulfide bonds under mild conditions, inserting a two-carbon bridge between the two cysteine residues. However, NGMs suffer from the same instability toward hydrolysis in basic pH as their parent maleimide, a limitation that could yet be overcome by using either diiodomaleimides,[116] "hybrid" thiobromomaleimides,[117] or an *in-situ* protocol[118] in which reducing agent and dithiophenolmaleimide reagent are added simultaneously**.** These methods have demonstrated excellent yields and conversion values when used for mAb conjugates with DoC 4 being the sole species detected in certain cases, albeit coexisting generation of half-antibody isoforms could systematically be observed. According, though, to my personal experience the *in-situ* protocol with NGMs leads to poor rebridging and rapid hydrolysis; a matter that will be further discussed at the second chapter of this manuscript (i.e., *page 59)*.

In 2011, the Caddick group[119] reported the conjugation of proteins and the bridging of cyclic peptides with dibromopyridazinedione (diBrPD) analogues, like **I114**. While being structurally related to NGM, diBrPDs possess the advantage of presenting one extra point of attachment *via* the two pyridazine nitrogens, grafted with different bioorthogonal tags allowing the dual labelling of the POI.[120–122] To date, a great variety of diBrPD reagents have been synthesized, mainly by the groups of Chudasama, Baker & Caddick, offering exciting applications such as the formation of well-defined homogeneous ADCs with diverse DAR species ranging from 2 to 8 (or 4+4). However, after careful examination of their exhaustive work on the development of these reagents, huge fluctuations in reaction conditions can be seen, which can either be attributed to the inner reactivity and sensitivity of the PD, or to the variability introduced by different experimenters (e.g., time ranges from 1.5 to 16 h; temperature from 4 to 37 °C; diBrPDs' equiv. from 5 to 20; EDTA concentration from 0.5 to 2 mM; TCEP equiv. from 8 to 80).[123–126]

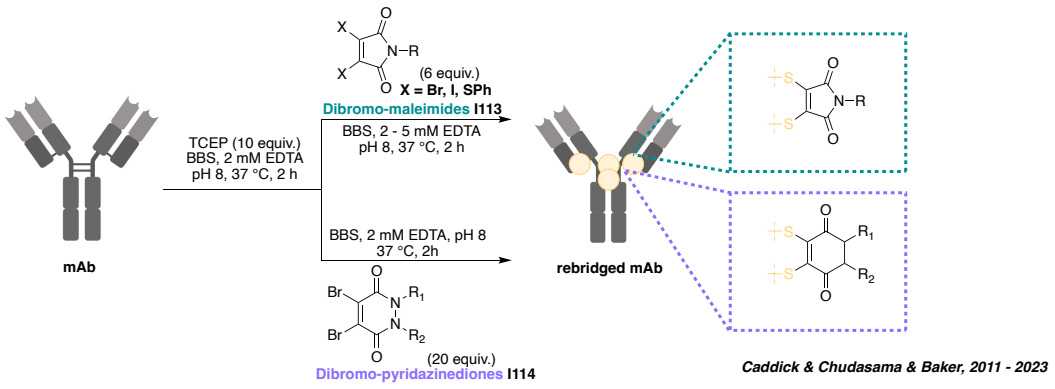

Scheme 28. Cysteine-Cysteine rebridging of IgG1 mAb *via* NGM **I113** or diBrPD **I114** derivatives.

Applications of diBrPD are plentiful. A few years ago, Chudasama and Scott groups employed the diBrPD-containing reagent **I115** to re-bridge antibody fragments for the modular formation of oriented antibody–nanoparticle conjugates.[127] More recently, Thoreau *et al.* synthesized diBrPD linkers **I116** and **I117** where alongside with **I115** generated mono- and bispecific synthetic antibodies constructs with combinations as shown in **Figure 5** – usually accessed through protein engineering – containing two paratopes capable of binding two distinct epitopes on target molecules and thus able to perform complex biological functions.[128]

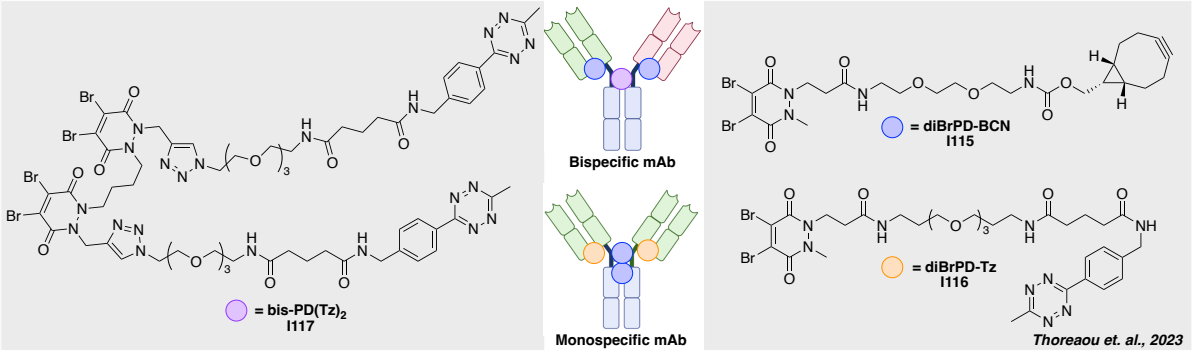

Figure 5. Construction of mono- and bi-specific antibodies with the incorporation of diBrPD analogues.

Shifting from pyridazinedione scaffolds to aromatic rings, Spring group described an alternative to diBrPD molecules by introducing two new reagents - divinyl triazine (DVT) and divinyl pyrimidine (DVP) – for the rebridging of full antibodies aiming to generate homogeneous D4 (i.e., DoC4) formats. Although both reagents were producing stable conjugates, disulfide scrambling was systematically observed, as evidenced by the formation of half-antibodies in all cases.[129,130] In an effort to minimize this regio-selectivity issue, they recently demonstrated that tetra-divinylpyrimidine (**tetra-DVP**) analogues could react simultaneously with all eight cysteine residues, thereby affecting the all-in-one rebridging of all four interchain disulfides of an IgG1 antibody with a single linker molecule (**Scheme 29**). By "playing" with the number *n* of central core unit – a propargylamine-modified glycine –, conjugates with DoC1, 2, 3, or 4 (**Scheme 29**) with >95% conversion could be easily accessed, with only traces of half-antibody species, in just 4 h at 37 °C.[131] Further functionalization with the azide-containing Alexa Fluor 488 *via* a CuAAC reaction proceeded smoothly with almost quantitative yield. However, when an MMAE-containing payload for the construction of an ADC was incorporated, mediocre conversion values due to incomplete click reaction were obtained, thus leading to avDAR values ranging from 0.5 to 2.4. This limitation could potentially be overcome by adjusting the linker length and/or flexibility of the current tetra-DVP's design, a fact indicating that there is still space for development.

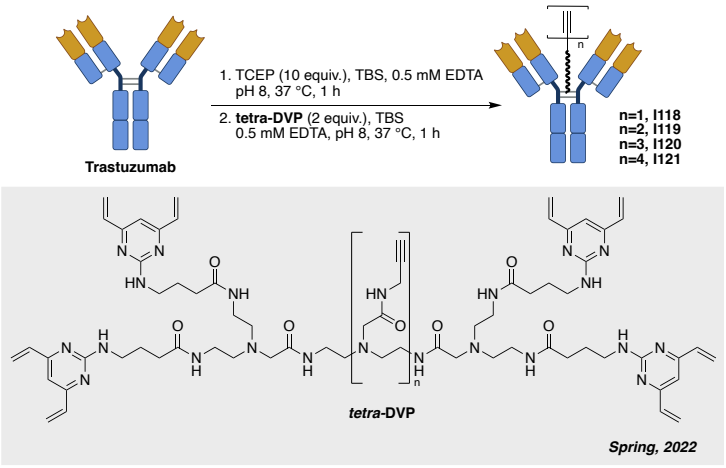

Scheme 29. Cysteine-Cysteine rebridging *via* tetra-divinylpyrimidine (**tetra-DVP**) derivatives.

Another interesting approach was recently described by Chudasama and Baker groups with the introduction of dual reactivity disulfide bridging reagents. By inserting one stable linkage (i.e., a thioether), and one labile linkage (i.e., a thioester), these reagents could afford a robust attachment to the protein on one end of the bridge whilst offering the second end a reactive site for subsequent ligation. Initial introduction of "dual reactivity reagent" **I122** on a reduced Fab-Trastuzumab allowed the sequential addition of two different payloads *via* a NCL with *N*-terminal cysteine peptide **I123** followed by a *de novo* rebridging of the new disulfide bond with a fluorophore-containing diBrPD **I124** to afford the dual-functionalized Fab **I126**. Alternatively, the use of hydrazine as the ligating nucleophile enabled a separate cargo to be attached to each cysteine residue, which could be exploited to insert variably cleavable linkers, such as a disulfide **I125,**and an acetohydrazide (**Scheme 30**). Although both methods exhibited novelty and good site-selectivity, many synthetic/conjugation steps and a great excess of reagents equiv. were required; a setback that in the former case could be potentially overcome by simply using a doubly substituted diBrPD with the fluorophore attached on the first nitrogen and the desirable peptide on the second, thus achieving the same thing but in two steps instead of five.[132]

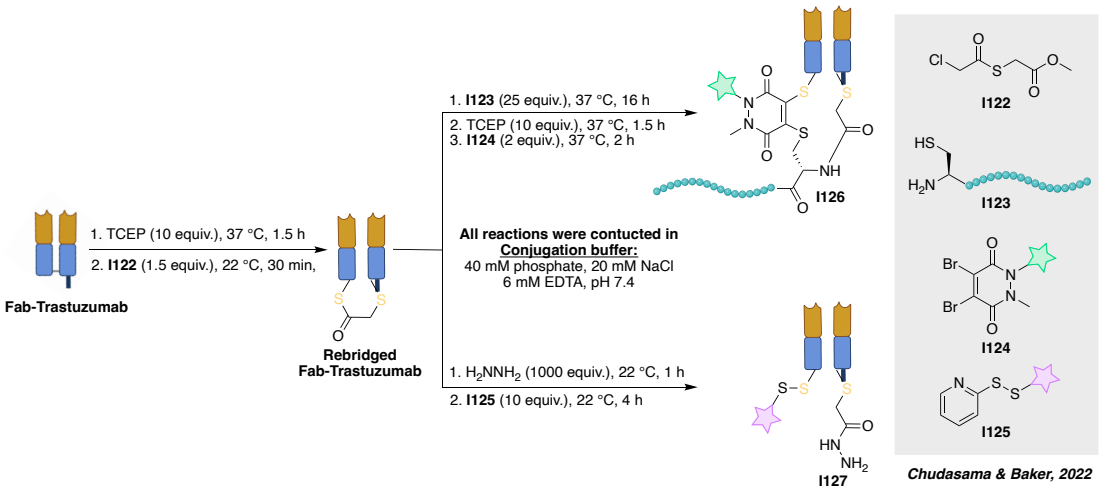

Scheme 30. Site-selective conjugation of cysteines *via* dual reactivity disulfide bridging reagents.

To sum up, cysteine rebridging offers an innovative and safe chemical approach for the regio-selective labelling of native proteins, while a handful of such strategies have been described. In this case, chemo- and regio-selectivity cannot be clearly distinguished as they seem to be the two faces of the same coin, since not only cysteine residues are selectively targeted but also precise amino acids are modified (*v. supra)*. Although positioned in the chemo-selective chapter, maleimides can lead to regio-selective conjugation of mAbs offering D8 species while NGMs D4 ones. Their hydrolysis issues, though, led to the design of the more stable reagents like diBrPDs with similar scaffold to that of NGMs but with an extra nitrogen thus offering dual functionalization possibilities, with the generation of rebridged mAbs with up to 8 payloads. Similarly, tetraDVP derivatives can furnish D1 to D4 species, by simply “playing” with the reagents’ length. Comparing these 4 different types of reagents one can conclude that all of those offers regio-selective cysteine labelling producing stable conjugates. Depending though on the desirable payload number – ranging from D1 to D8 – and their nature, one can select the most optimal reagent to his/her needs. Finally, it would be interesting to see in the near future a study among these reagents comparing the generation of half mAb species in a quantitative manner, since so far, we can only spot them both on the SDS-PAGE and the LC-MS but we cannot quantify them, thus we cannot conclude which of these reagent are more prone to half-mAb species formation.

Focusing now on the *N*-terminal conjugation, which exists in a less abundant manner than cysteine residues – 4 *N*-terminal residues *versus* 8 solvent accessible cysteines in an IgG1 for instance – could be prominent for the development of another site-selective method that would deliver D4 conjugates.

1.2.1.4.3. *N*-Terminal residues conjugation

As mentioned in the beginning of this chapter, *N*-terminal *α*-amines offer an appealing target for the site-selective labelling of proteins. Their increased reactivity in combination with their intrinsically low abundancy inspired several research groups to develop methods for such purpose.

Francis group was the first to report the use of pyridine carboxaldehydes for the selective oxidation of the *N*-terminal residues (**Scheme 31**). Using pyridoxal-5-phosphate (PLP) **I128**, they converted *N*-terminal *α*-amino acid residues to pyruvamides **I130** which were prone for derivatization to yield oxime-containing payloads. *N*-terminal residues (i.e., valine, glycine, lysine, methionine, aspartate) of several native proteins were successfully modified, with conversions up to 67%, while other residues were deemed not optimal for this approach due to possible oxazolidine/thiazolidine ring formation (i.e., serine and threonine/cysteine, respectively), competing Pictet–Spengler cyclization (i.e., tyrosine), or to a lack of reactivity (i.e., proline).[133]

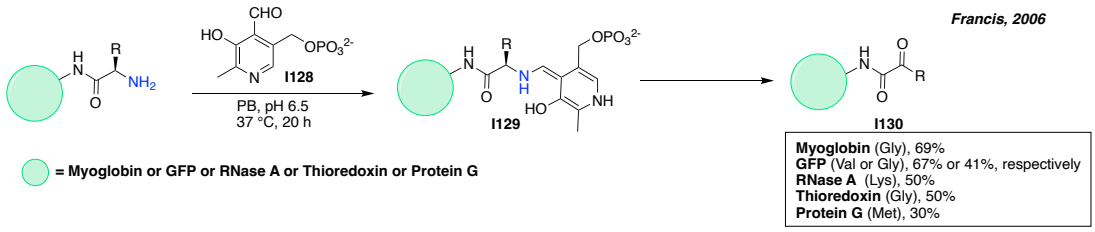

Scheme 31. Site-selective conjugation of *N*-terminal of various proteins with PLP **I128** reagent.

N-terminal transamination is another strategy employed to modify antibodies in a site-selective manner *via* conversion of *N*-terminal's *α*-amine to an aldehyde. *N*-Methylpyridinium-4-carboxaldehyde benzenesulfonate salt **I131**, known as the Rapoport's salt, was used to transaminate Trastuzumab's heavy chain *N*-terminal glutamate residue (67% conversion) and install a pyruvamide functional handle readily available for labelling with either oxime or hydrazone linkages (**Scheme 32**). Interestingly, no modification of the light chain's *N*-terminal aspartate was observed, as according to the authors it was attributed to the steric environment of the folded protein that suspected to suppress the accessibility of the less-reactive aspartate substrate.[134]

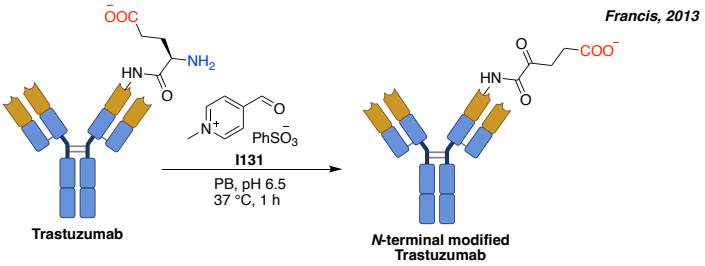

Scheme 32. Site selective conjugation of Trastuzumab's E1 *N*-terminal with Rapoport's salt **I131**.

As the scope of *N*-terminal selective modification was found to be limited with these reagents, 2-pyridinecarboxyaldehyde (2-PCA) **I132** was later reported as a more broadly applicable strategy for the site-selective conjugation of peptides and proteins, regardless of the *N*-terminus' nature.[135] Proceeding *via* another mechanism, this reagent led to the formation of imidazolidinones **I134**, with the imine **I133** formed in a first step undergoing intramolecular addition of the *n* + 1 *α*-amino group in a second step; a feature explaining why proteins with proline as the *n* + 1 residue failed to be conjugated *via* this strategy. While this conjugation proved to be partially reversible at 37 °C in the presence of cysteine residues (i.e., GSH), it benefitted from a large protein scope, with good conversions being observed in most cases. Even though *N*-terminal serine-containing proteins were listed as potential limitations with PLP **I128** reagent (*vide supra*), thioredoxin was still successfully labelled with 2-PCA furnishing 63% conversion (**Scheme 33**).

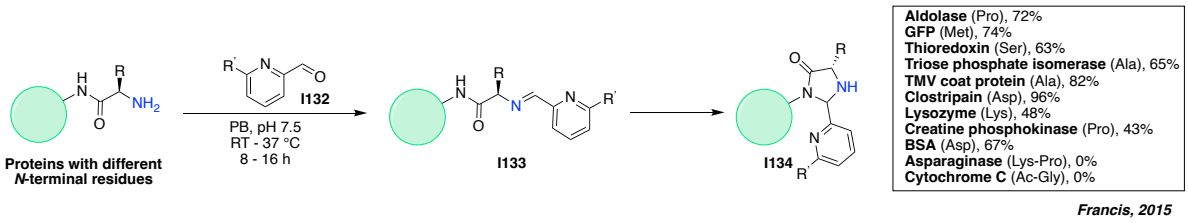

Scheme 33. Site-selective conjugation of various proteins containing different *N*-terminal residues with 2-PCA **I132**.

In conclusion, *N*-terminal conjugation offers another possibility for site-selective modification of various proteins by furnishing stable conjugates in a large range of conversions, attributed to the different nature of the modified residues or the variable microenvironment. One potential limitation of this approach is the possibility of blocking the protein's binding site, especially in the case of IgG isotypes whose *N*-terminus are located on the fragment-antigen binding (Fab) region. Another restraint is the formation of pyroglutamic acid (PyroGlu or PyroE) at the *N*-termini of proteins, including antibodies. However, according to the reported procedures, neither of these potential obstacles found to be problematic for the conjugated proteins.

1.3. CONCLUSION

In conclusion, the most effective way to construct homogeneous protein-conjugates is *via* site-selective labelling. The selective modification of desirable residues in large proteins is, though, a challenging process since they consist in multiple copies of 20 AAs. Thus, construction of recombinants proteins *via* genetic manipulation for the introduction of UAAs and peptide tags has proved to be a promising approach. Yet, this is an expensive process, while changes in the AA sequence often leads to the formation of aggregates, hence limiting their application.

Incorporating a small molecule to achieve site-selective conjugation is a cost and time-efficient alternative, thus lately improving at a fast rate. Dozens of reagents have been designed by targeting various AAs and are commonly used both in academia and industry for the manufacture of stable bioconjugates. Currently, the simplest way to do so is by targeting reduced cysteine residues, due to their poor abundance and high reactivity. Achieving regio-selectivity on other AAs is yet a challenging task but can be achieved either by sacrificing conversion rates or by thoroughly examining the microenvironment of the desirable residues. Hence, limitations in this field still exist, but undoubtedly this triggers the scientific desire for innovation for the development of novel strategies in the upcoming years. Stoichiometric amount of reagents, high kinetics, complete conversion and easy *de novo* functionalization with desirable payloads are only some of the features that are expecting to be seen at the next generation regio-selective reagents.

2. DEVELOPMENT OF NOVEL REAGENTS FOR CYSTEINE SELECTIVE CONJUGATION

2.1. INTRODUCTION

As already stated in the beginning of chapter 1, among the 20 proteinogenic *α*-amino acids, cysteine is an appealing target for site-selective protein modification because of its low abundance and the enhanced nucleophilicity of the sulfhydryl group. Plethora of strategies and reagents have already been described and discussed for the selective labelling of cysteine residues in proteins, such as the well-known maleimide reagent and its derivates, as well as divinylpyrimidines or dibromopyradizinediones. Despite the large number of existing methods, the development of new chemo-selective reagents, especially if presenting uncommon properties such as the possibility to partake in a controlled de-conjugation process, is still attractive. This chapter will be dedicated to this topic, and will feature to underexplored scaffolds: pyridazinediones and hypervalent iodine(III) compounds.

2.2. PYRIDAZINEDIONES

2.2.1. Introduction – Pyridazinediones in bioconjugation

Substantial efforts have been made towards the development of methods for the selective and irreversible (i.e., blood stable) modification of cysteine(s) on various proteins to enable diverse applications in medicine, e.g., antibody-drug conjugates (ADCs), imaging agents, radioimmunoconjugates.[121,124,136–138] However, recent reports of reversible cysteine modification found a breeding ground in a variety of fields, such as selective enzymatic inhibition or the controlled release of cargo from a material or a protein.[121,139,140] A characteristic example is demonstrated by hydrogel-drug conjugates, which showed that among various strategies, covalent approaches for the attachment and release of a drug are preferred, since they provide better spatial and temporal control.[141] In this context, the drug release is mostly dependent on ester bond hydrolysis, disulfide bond exchange and/or a *β*-elimination mechanism,[142–145] while similar approaches have also been applied to the release of a drug from a peptide or protein.[146,147]

While these examples led to fruitful applications, the most notorious and investigated approach undoubtedly relies on the thiol-succinimide linkage, which is known to undergo a *retro*-thio-Michael reaction.[148,149] However, the rapid kinetics of maleimide–thiol conjugation makes any released maleimide highly susceptible to off-target thiol modification by other biomolecules (e.g., human serum albumin; HSA),[150] thus limiting its use. Moreover, such thiol-succinimide

adducts can undergo a competitive ring hydrolysis **R2**, which prevents a further *retro*-thio-Michael pathway, rendering the conjugation irreversible (**Figure 6A**).[38] Therefore, there is a clear demand for the development of novel platforms to reversibly modify cysteines in a highly selective manner.

Motivated by the plethora of applications that could be exploited, the Chudasama group has previously showed, in a single example, that a non-brominated pyridazinedione (PD) **R4** displayed attractive features as a novel reversible covalent cysteine modifier with expected tolerance to ring hydrolysis (**Figure 6B**).[151] Nonetheless, that work was limited by: *i)* the use of a single PD analogue (bearing ethyl groups on both nitrogens), *ii)* the lack of PDs bearing reactive handles for functionalization, *iii)* the lack of kinetics data. To fill these gaps and unveil the hidden properties of PDs, I was tasked with generating a small library of PDs bearing various *N*-substituents by Pr Chudasama in collaboration with the ESR Ms Lea Rochet during my three-month stay at UCL. Together, we developed synthetic routes to access novel functionalisable pyridazinedione derivatives and tested their conjugation/deconjugation kinetics.

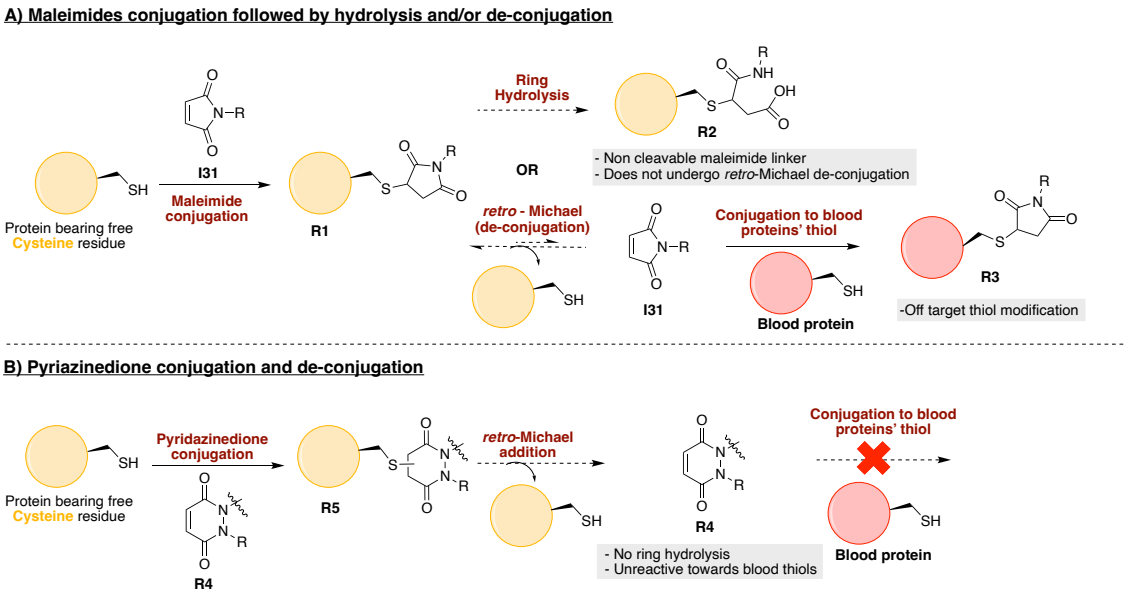

Figure 6. A) Representation of maleimides reactivity in cysteine conjugation. B) Representation of the desirable pyridazinedione reactivity.

2.2.2. Synthesis of non-brominated pyridazinedione analogues

It was initially hypothesized that modifying at least one of the nitrogen atoms on the PD scaffold (R group in **Figure 6B**) with an aromatic π-system could have a significant effect on the PD ring core that would influence its electrophilicity, as well as potentially influence the acidity of the *α*-proton in the resultant thiol-PD conjugate **R5**, thus leading to faster *retro*-Michael addition rates. To appraise this theory, as well as to investigate whether the nature of the aryl group had any effect on reactivity, a small library of various PDs bearing different aromatic groups (e.g., electron-poor, electron-rich and electron-neutral) on one of the nitrogen atoms and an ethyl group on the other nitrogen were synthesized by the ESR Ms Lea Rochet, while kinetic assays of these molecules using UV-Vis followed, confirming the initial hypothesis. In view of these results, we focused on the preparation of PD scaffolds containing one reactive handle and displaying different release rates. Thus, we planned to synthesize *N*-methyl and *N*-phenyl PD derivatives bearing *N'*-alkyl-bicyclononyne (BCN) groups expecting slow and fast thiol-release, respectively.

Preparation of *N*-Me-*N*'-alkyl-BCN PD **R18** as accomplished *via* a 5-step synthetic procedure. Starting from *N*-Boc-protected methylhydrazine **R6**, *N,N'*-di-Boc-protected methylhydrazine **R7** was obtained by treating the former with di-*tert*-butyl dicarbonate, and was then refluxed with *tert*-butyl acrylate **R10** under basic conditions to furnish the *β*-hydrazino ester **R11** in excellent yield. Carboxylic acid **R13** was next obtained after refluxing **R11** with furan-2,5-dione in acetic acid for 3 consecutive days. Finally, **R13** was coupled with *N*-hydroxysuccinimide (NHS-OH) to yield its NHS derivative **R15** in average yield, which was further coupled with BCN-amine **R17** to deliver the expected *N*-Me-*N*'-alkyl-BCN PD **R18** in good yield (**Scheme 34**).

Preparation of the *N*-phenyl PD analogue **R19** was achieved *via* a slightly altered but similar route. Staring from phenyl hydrazine **R8, R9** was obtained after reacting the former with 4.2 equiv. of di-*tert*-butyl dicarbonate for 4 h at 60 °C in the presence of a catalytic amount of DMAP, followed by treatment with magnesium perchlorate for additional 10 min. The rest of the synthetic sequence was identical to that previously described and allowed the facile synthesis and isolation of **R19** in four subsequent steps, as illustrated in **Scheme 34**.

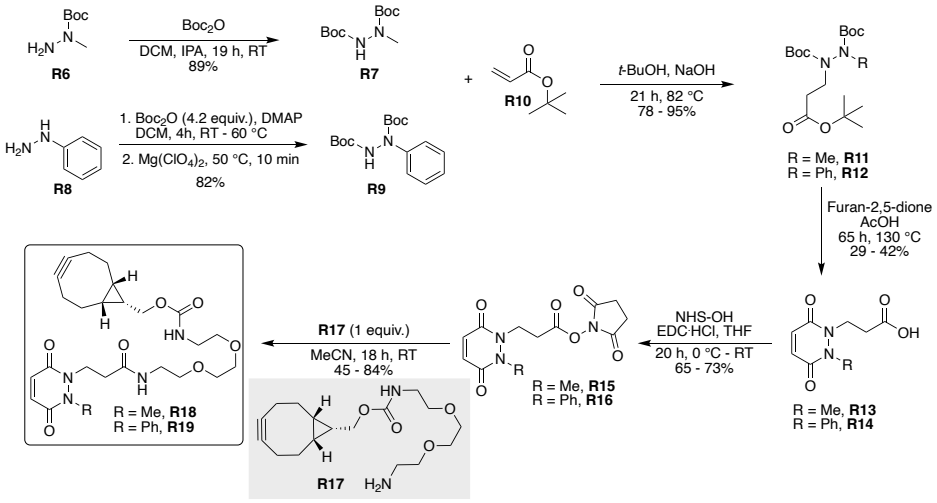

Scheme 34. Synthetic path for the preparation of non-Brominated PDs **R18** & **R19.**

The last part of my synthetic work in the group of Pr Chudasama included the synthesis of diPh-PD **R23**, as its release rate comparison with the *N*-methyl-*N'*-phenyl PD, from Lea's library, would give us important information to further support, or not, our initial hypothesis. PD **R23** would then be reacted with a small cysteine-containing peptide **R24** and would then be given to Lea Rochet to test its de-conjugation rate and evaluate its kinetics profile. Monophenyl PD **R21** was accessed by refluxing *N*-phenyl hydrazine **R8** with 2,5-dihydrofuran **R20** in acetic acid, followed by recrystallisation of the crude product in ethanol. Installation of the second *N*-phenyl substituent was performed through a Chan-Lam coupling between monophenyl PD **R21** and phenylboronic acid **R22**, giving **R23** in excellent purity despite its mediocre yield. This novel PD was further reacted with a model cysteine-containing dipeptide **R24** to afford the desired peptide **R25** (**Scheme 35**), in order to assess its kinetics *via* UV-Vis. In comparison with the other di-substituted PDs, **R23** showed enhanced *retro*-thio-Michael addition rates, as expected, but unexpectedly though, it also demonstrated hydrolysis issues, upon conjugation to a protein, potentially attributed to its electron poor nature.

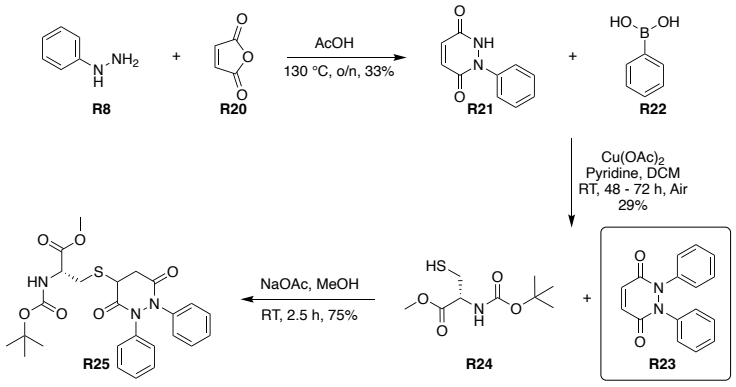

Scheme 35. Synthetic route to access *N,N'*-diPh PD **R23** and conjugation with cysteine-containing peptide **R24** to afford the PD conjugated peptide **R25**.

2.2.3. Bioconjugation of non-brominated pyridazinedione analogues **R18** & **R19**

To evaluate the conjugation profile of PDs **R18** & **R19**, Fab-Trastuzumab was selected as our model protein. Trastuzumab is an EMA-approved mAb used to treat HER2-positive breast cancers (*v. supra)*.[151,152] With a molecular weight of around 150 kDa, it belongs to the IgG1 class of antibodies and is composed of two HCs and two LCs connected via four disulfide bonds. Each LC is connected to a HC *via* one disulfide bond, forming half of a monoclonal antibody (½ mAb). The Y shape of the whole mAb comes from the connection of two ½ mAbs through two additional disulfide bonds between the two HC, in what is called the hinge region. Thus, the reduction of IgG1 gives access to eight free, solvent-accessible thiols poised for modification (**Figure 7**). Maintaining the affinity of a whole mAb but with a smaller size, Fab conjugates are attractive due to their enhanced tissue penetration.[153] Structurally speaking, they consist of a LC covalently connected through a single interchain disulfide bond to a Fd chain – the digested remnant of the mAb's HC – whose reduction leads to two free thiols and a more homogenous conjugation profile. The desirable Fab-Trastuzumab was easily obtained after two consecutive pepsin- and papain-mediated digestion steps (see experimental section for procedure, *pages 113 – 114*).[154]

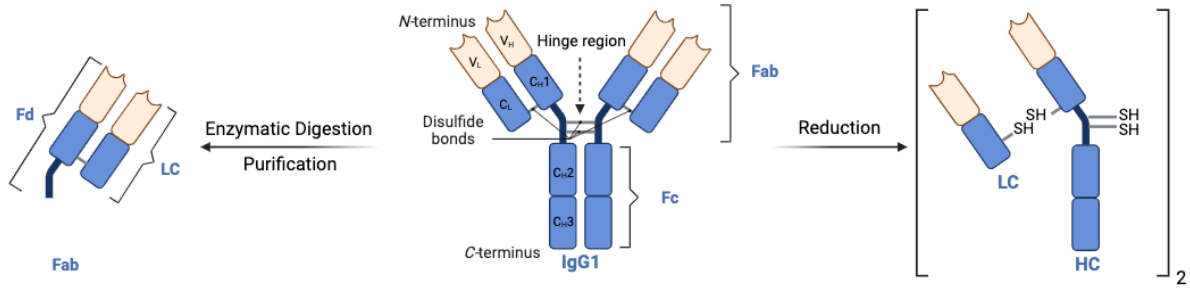

Figure 7. IgG1 structure explanation and representation of its fragments after digestion (left) and reduction (right).

After the successful synthesis of PDs **R18** & **R19**, both were evaluated for their de-conjugation properties on the Fab fragment of Trastuzumab. Each of these compounds was initially reacted with amide-PEG_2-N_3 **R26** – thus yielding **R27** & **R28,** respectively – to mimic the attachment of cargo while still displaying the same kinetic rates (**Figure 8A**), before they were conjugated to reduced Fab-Trastuzumab to form conjugates **R29** and **R30**. These conjugates were subsequently left to incubate at 37 °C (after removing any excess PD from the solution *via* two consecutive gel filtration chromatography purifications), at a concentration of 35 µM in PBS buffer at pH 7.4 (**Figure 8B**). In this case, no EDTA was added, in order to facilitate the re-oxidation of the Fab disulfide after the deconjugation step, acting as a trap to remove free thiols from the mixture and prevent the formation of an equilibrium. The deconjugation of functionalised PDs from the LC and Fd chains of the Fab, was assessed *via* LC-MS (see the

representative spectra in the experimental section on *pages 152 - 158*) and SDS-PAGE by analysing aliquots sampled after 2.5 h, 6.5 h, 24 h, 48 h and 72 h. As expected, after 48 h almost full deconjugation was observed for *N*-phenyl functionalised PD **R19** whilst a significant amount of the *N*-methyl derivative **R18** was still conjugated, as observed using both SDS-PAGE and LC-MS (**Figure 8C** and **8D**, respectively). This serves to further emphasise that we can exert control over the rate of deconjugation from a protein by simply changing the substituent on one of the nitrogen atoms of a PD.

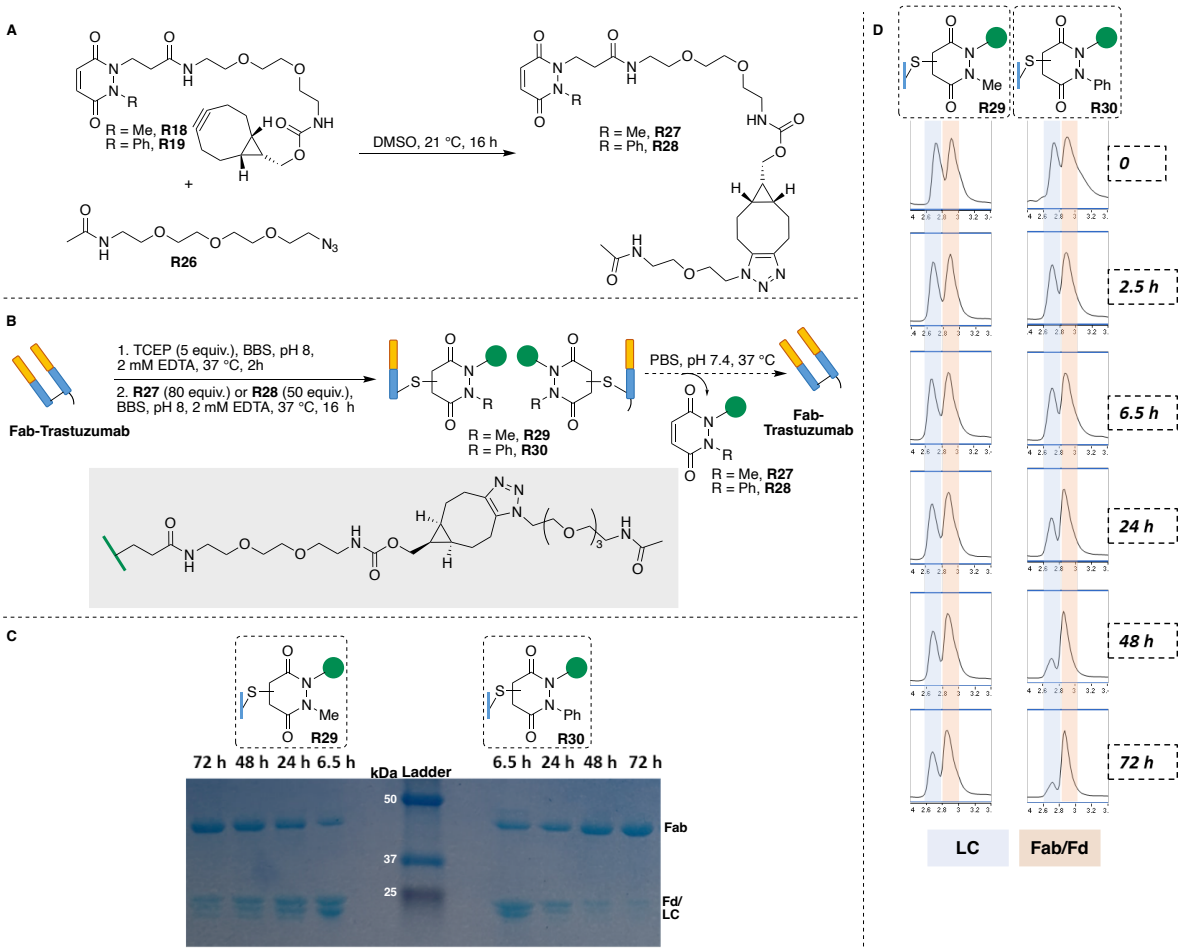

Figure 8. A) In-situ click reaction of *N*-Methyl PD derivative **R18** & *N*-Phenyl PD derivative **R19** with amide-PEG_2-N_3 **R26**. B) Conjugation & de-conjugation reaction of functionalized PDs **R27** & **R28** with Fab-Trastuzumab. C) SDS-PAGE of **R29** & **R30** conjugates demonstrating their de-conjugation profile over time. D) UV-Vis, derived by LC-MS, chromatogram illustrating the de-conjugation of **R27** & **R28** from Fab-Trastuzumab over time.

2.2.4. Conclusion

In this work, the potential of pyridazinediones as novel reversible and tunable cysteine covalent modifiers was demonstrated. The development of novel strategies to access diPhPD and functionalisable PD derivatives allowed to better understand the de-conjugation properties of these molecules as a function of their *N*- substituents. In the case of *N*-alkyl-BCN PDs, it was found that the *N'*-phenyl bearing analogue was fully deconjugated from Fab-Trastuzumab after 48 h in contrast with the *N'*-methyl one that still showed a significant amount of conjugated species, even after 72 h. This demonstrated the versatility of non-brominated PDs and the importance of the *N*-substituent that can either enhance or diminish the de-conjugation rate. Finally, this project could be the groundwork for potential applications in various areas with exemplification of this chemistry on clinically relevant cysteine or disulfide conjugated proteins, such as for the temporal display of integrin binding peptides or as a refillable drug depot,[155–157] by showing different rates of deconjugation with readily functionalized "clickable" PDs on all systems.

2.3. HYPERVALENT IODINE(III) MOLECULES

2.3.1. Introduction - Hypervalent iodine(III) molecules in bioconjugation

Hypervalent iodine molecules have recently emerged as powerful reagents in bioconjugation for the functionalization of both peptides and proteins. These highly reactive compounds have surprisingly showed high functional group tolerance and outstanding stability in biocompatible media,[158] leading to the development of a variety of such reagents over the last decade. While many of them are known for their oxidizing character, others have been used as electrophilic group transfer reagents in umpolung reactions. Thanks to these unique properties, it is thus not surprising to see that these reagents have contributed to the development of novel bioconjugation methods.

2.3.1.1. Fluoroalkylation of cysteine residues

The groups of Togni & Beier were some of the pioneers in the domain of hypervalent iodine reagents for bioconjugation, where they used molecules like **R38** for the introduction of fluorinated groups in biomolecules and, in particular, of trifluoromethyl ones with the utilization of reagents such as **R31** or **R39**.[159–161] This reaction was proved to be chemo-selective toward cysteines, since other nucleophilic residues – containing amino or carboxylic groups – stayed intact in the presence of this type of reagents.[162] From a mechanistic point of view, and according to computational studies initiated by the Togni group, the reaction starts with protonation – by either the thiol or the solvent – of hypervalent iodine molecule **R31**, with the simultaneous I−S bond formation (intermediate **R33**), thus yielding **R34**. After homolytic cleavage, the generation and recombination of CF_3 **R36** and thiyl **R37** radicals yields the desired compound **R32**, as illustrated in **Scheme 36**.[163]

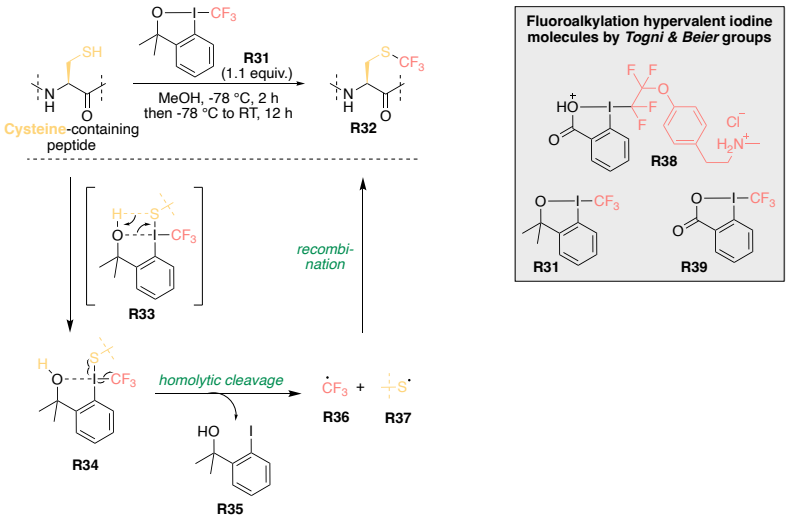

Scheme 36. Labeling of cysteine residues with trifluoromethyl benziodoxol(on)e **R31** followed by mechanistic explanation. In the grey frame, various fluoroalkylation hypervalent iodine (III) reagents developed by Togni & Beier groups are represented.

This type of reagents used in stoichiometric amounts, were found to be compatible with aqueous buffers and proceeded rapidly under mild conditions during their reaction with cysteine-containing peptides, thus establishing a promising strategy for the effective fluorination of biomolecules. Furthermore, the incorporation of fluorinated groups allowed the use of ^{19}F NMR spectroscopy for reaction monitoring and the precise determination of the modified peptides.[161,164] However, these reagents were limited to small peptides and their application to larger biomolecules, such as proteins, is yet to be documented.

2.3.1.2. Alkynylation & vinylation of cysteine residues

In 2013, the group of Pr Waser applied the commercially available hypervalent iodine reagent 1-[(triisopropylsilyl)ethynyl]-1,2-benziodoxol-3(1*H*)-one (TIPS-EBX, **R40**) for the alkynylation of cysteine residues (**Scheme 37**). Under mild conditions, various thioalkynes **R41** were rapidly produced (< 5 min) in excellent yields and great chemoselectivity.[165] Based on these promising results, the same group next synthesized a small library of EBX compounds, bearing alkyne substituents of various lengths and substitution patterns,[166] in order to investigate the mechanism guiding this modification.

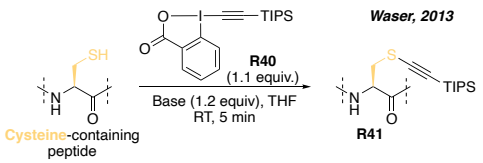

Scheme 37. TIPS-EBX **R40** conjugation with cysteine residues.

Computational and experimental studies suggested that the initiation step was triggered by the formation of thiolate **R43**, since in the absence of a base, only traces of the thioalkyne product **R50** were observed. The reaction was next proceeded with the electrostatic interaction of **R43** with the Lewis-acidic iodine of reagent **R42** (see transition state **R44**) following either of two possible reaction pathways. In the case of path A, computational studies revealed that the low energy transition state intermediate **R45** was formed after the addition of the sulfhydryl group on the *α*-carbon of EBX reagent **R42** followed by a concerted *α*-addition/elimination to subsequently yield the thioalkyne product **R50**. Path B proceeded through a nucleophilic attack of thiolate **R43** on the *β*-carbon of EBX's alkyne **R42** *via* the transition state **R46**, leading to *β*-addition and formation of the vinyl anion **R47**. The latter would then undergo an *α*-elimination to form **R49**, which, after a 1,2-shift, would yield the final thioalkyne **R50**. However, intermediate **R47** could also be intercepted by protic solvents, thus leading to vinylbenziodoxolone (**VBX**) products **R48** (**Scheme 38**).[167,168]

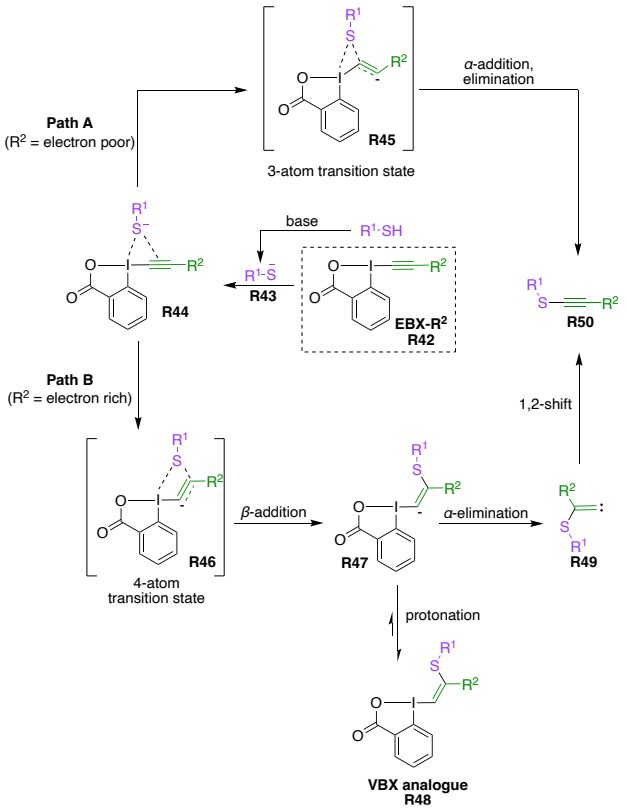

Scheme 38. Proposed mechanistic pathways for thioalkynylation using **EBX-R²** reagents. R^2 = OMe, Me, $SiMe_3$, Si*i*Pr_3, Ph, CO_2Me. Adapted from: Allouche, E. M. D.; Grinhagena, E.; Waser, J. Hypervalent Iodine-Mediated Late-Stage Peptide and Protein Functionalization. *Angewandte Chemie International Edition* 2022, *61* (7), e202112287. https://doi.org/10.1002/anie.202112287.

The free energy values of the transition states of different hypervalent iodine reagents revealed that the alkyne's R^2 group has a strong influence on the reaction's pathway. More specifically, when R^2 is an electron-withdrawing group (EWG), the route going through an *α*-

addition is the lowest energy pathway, since the partial negative charge is stabilized. On the contrary, when R^2 is an electron-donating group (EDG), such as an alkyl substituent, the favored pathway is the *β*-addition. For aryl and silyl substituents, both pathways are possible, since the energy difference is small.[167,168]

Two examples that followed these paths were demonstrated by the reaction of cysteine-containing proteins with EBX-alkyl azide **I48** and EBX-TMS **I50** reagents. Although in small proteins the transfer of the alkyl chain bearing an azide from EBX-alkyl azide **I48** to a free cysteine successfully occurred following path B,[52] degradation of the payload and chemoselectivity issues were observed when it was reacted with reduced Trastuzumab. For the latter reagent **I50**, the optimal conditions to yield unique thioalkyne adduct **I51** in 60% conversion – following either path A or B – were found to be the incorporation of 8 equiv. of this hypervalents iodine (III) reagent in PBS at pH 7.5 incubated for 2 min at 25 °C. The obtained bioconjugate was further functionalised with tetramethylrhodamine (TAMRA) azide, in a chemo-selective manner and with an average degree of conjugation (avDoC) of 1.2 after a CuAAC (**Scheme 39**). The efficiency of this reaction was proved to be dependent on many parameters (i.e., temperature, time, equiv., buffer, and pH) with avDoC values ranging from 0.1 to 4.4.[53]

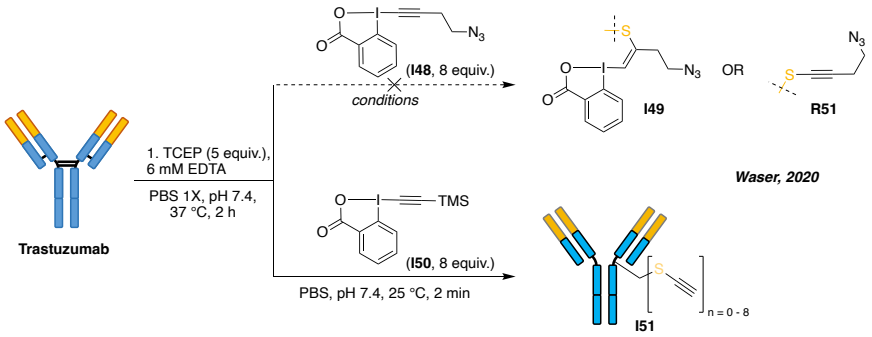

Scheme 39. Alkynylation attempts of Trastuzumab with EBX-alkyl azide **I48** and EBX-TMS **I50** reagents.

In 2020, another application of these reagents was proposed by the same group, further demonstrating their versatility. More specifically, they incorporated bis-hypervalent iodine reagent **R52** for the cysteine-cysteine cross linking of small peptides **R53** in quantitative yields. In addition, they showed that reagent **R54** allowed the cysteine-lysine stapling **R55** in quantitative yields in just 30 min at 37 °C (**Scheme 40**).[169] Although both methods showed promising results in organic solvents, their application to larger biomolecules in aqueous buffers was not investigated.

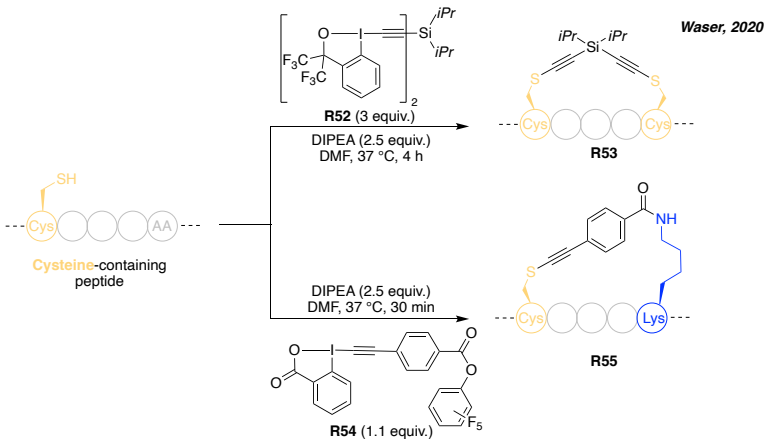

Scheme 40. Cys-Cys & Cys-Lys cross-linking of small peptides with homo- and hetero-bifunctional hypervalent iodine reagent **R52** & **R54**, respectively.

Application of reagent **I48** was also extended from hyperreactive Cys (**Scheme 39**) to less acidic and surface-exposed Cys (**Scheme 41**). **I48** was applied to small peptide sequences, derived from native proteins containing a single cysteine residue. In this case, a basic buffer (pH 8.2) was used to convert these less-reactive Cys residues, generating exclusively VBX products, like **R56,** as expected from the reaction conditions and the mechanism proposed in path B (see **Scheme 38**).[52]

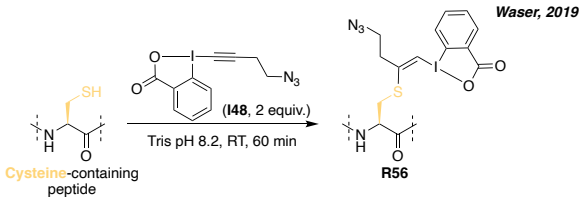

Scheme 41. Vinylation of cysteine residue with EBX-alkyl azide **I48** following path B of the mechanism detailed in Scheme 38.

2.3.1.3. Application of hypervalent iodine molecules to other residues

Recently, Novál & Beier groups reported fluoroalkylation reagents **R57**, **R58**, **R59** and **R60** for the selective modification of tryptophan residues in peptides and small proteins containing cysteines.[170,171] Being a radical process, sodium ascorbate or visible light were mandatory for the reaction to proceed and deliver **R61** in good yields (**Scheme 42.1**). Similarly, Waser[172,173] and Hoeg-Jensen[174] groups combined TIPS-EBX **R40** with catalytic amount of gold(I) catalysts and applied it to the selective alkynylation of tryptophan residues in small peptides and low molecular weight proteins to obtain tryptophan-alkyne analogues, like **R62** (**Scheme 42.2**).

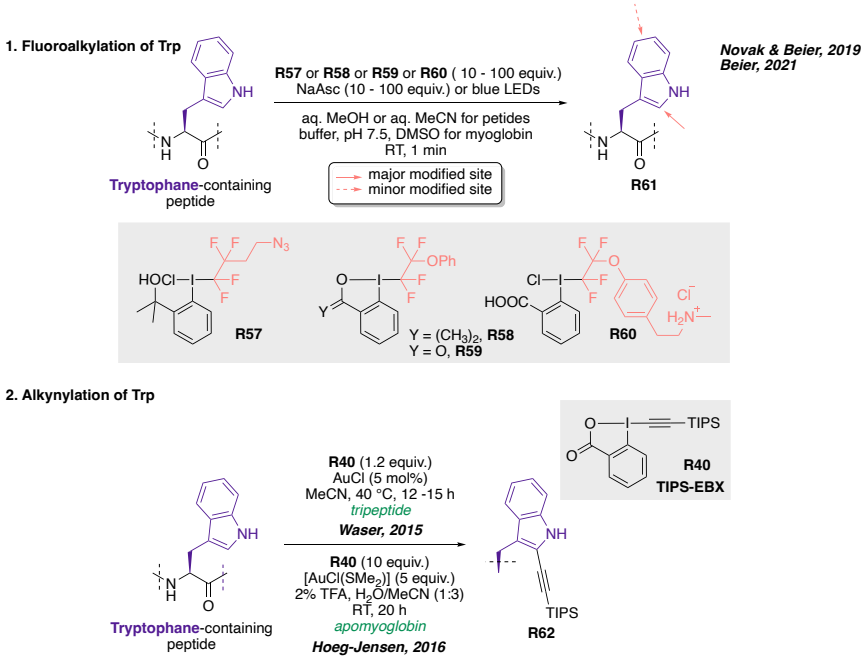

Scheme 42. 1) Fluoroalkylation of tryptophan residues with either of the hypervalent iodine reagents **R57**, **R58**, **R59** and **R60**. 2) Alkynylation of tryptophan residues with TIPS-EBX **R40** in the presence of gold catalysts.

In a similar manner, the Fang group reported the successful modification of tyrosine residues in cysteine-free oligopeptides with (diacetoxyiodo)benzene (PIDA **R63**).[175] This reagent led to the oxidation of the phenol ring to form a reactive 4-hydroxycyclohexadienone intermediate **R64**, which, after treatment with functionalized hydrazines, generated the desired tyrosine-modified peptide **R65** through a dehydrative re-aromatisation process (**Scheme 43**).

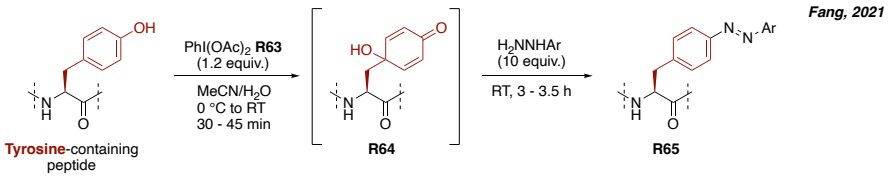

Scheme 43. Oxidation of tyrosine residues with PIDA **R63** followed by functionalization with hydrazine derivatives.

Photoredox-catalyzed decarboxylation is another application of hypervalent iodine reagents, this time used for the functionalization of the peptides *C*-terminus. As this position is easier to decarboxylate than side-chain carboxylates under oxidative conditions,[176,177] the rapid generation of reactive species under mild reaction conditions allowed a high degree of regio-selectivity. In 2015, the Waser group developed a similar approach where they reacted EBX-CN **R66** in the presence of an iridium catalyst under blue-light LEDs, to generate cyano derivatives of *C*-terminal prolines **R67**.[178] In 2019, the same group extended the scope of this decarboxylative process to the *C*-terminal alkynylation of peptides to generate alkyne-containing peptides, like **R69,** under a new set of mild and metal-free conditions in just 30 min at room temperature in a mixture of DMF and water thanks to the EBX reagent **R68**

(**Scheme 44**). However, in the presence of cysteines, chemoselectivity was lost and both residues were functionalized.[179]

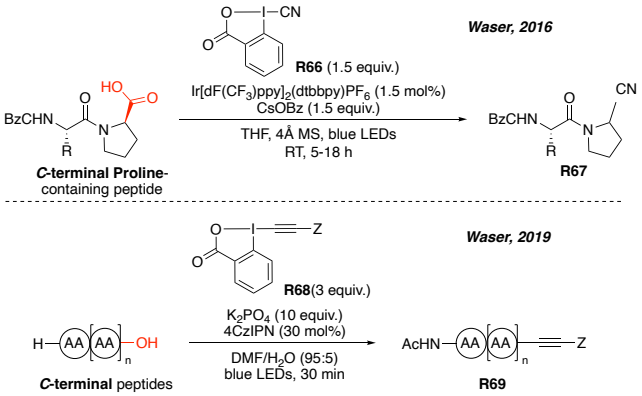

Scheme 44. *C*-termini labelling of small peptides using EBX-CN **R66** reagent for the replacement of the carboxylate group with a cyanide one and incorporation of reagent **R68** for the replacement of the carboxylate group with phenyl alkynyl derivatives. Z stands for various phenyl derivatives.

Finally, hypervalent iodine molecules have been further used for the functionalization of other aliphatic amino acid residues, such as the highly hydrophobic methiones and alanines (**Scheme 45**). However, the use of additives, such as TEMPO/thiourea and acidic pH to prevent decomposition, or the necessary presence of phthalimide groups – in the case of alanine labeling – at the *N*-terminus coupled with incubation under high temperatures, respectively, drastically limited their use and applications.[180,181]

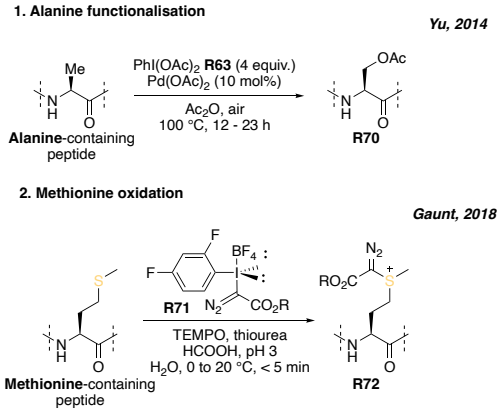

Scheme 45. 1) Alanine labelling using hypervalent iodine reagent PIDA **R63** in the presence of a palladium catalyst. 2) Methionine oxidation using hypervalent iodine reagent **R71**.

2.3.1.4. Conclusion & aim of the project.

Over the last decade, hypervalent iodine (III) molecules have thus shown great potential in chemical biology because of their high reactivity, selectivity and stability. Modification of various types of amino acids – tryptophan, tyrosine, methionine, alanine, *C*- terminal – *via* oxidation, fluoroalkylation, alkynylation, cyanidation, azidation, or alkoxylation have been reported. However, most of these methods were used for the functionalization of small peptides, and only a handful of those found their way towards the labeling of the more complex proteins. The incompatibility of hypervalent iodine reagents with larger proteins could be attributed to their sensitivity to aqueous buffers or their high reactivity, leading either to the degradation of the payload or to chemoselectivity issues, respectively. Building up on these literature precedents, and with the aim of pursuing the efforts in this field, the use of hypervalent iodines was investigated for the chemo-selective modification of cysteine residues in antibodies. This project was held in collaboration with the Waser group, who developed the multifunctional ethynylbenziodazolone (mEBZ) **R73** molecule and evaluated it as a cross-linking reagent of cysteine residues.

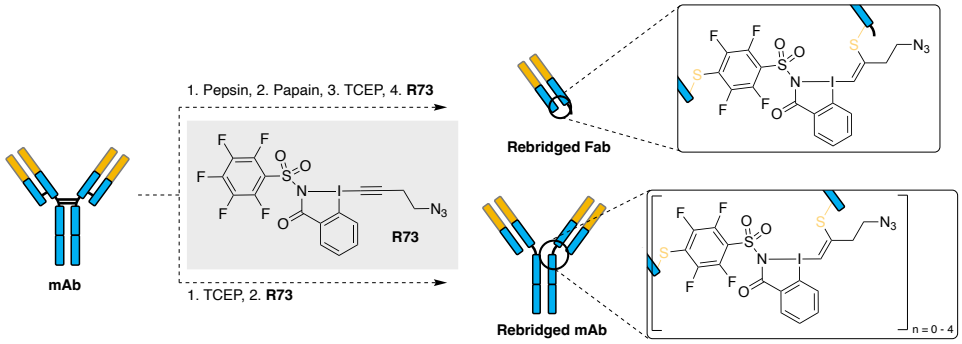

Scheme 46. Summary of this project's objectives.

2.3.2. Multifunctional EBZ

The design of the new crosslinking hypervalent iodine reagent **R73** was based on a nitrogen analogue of EBX **I48** coined EBZ (**Scheme 47**). EBZs have been previously utilized as electrophilic alkynylation reagents for the enantioselective copper-catalyzed oxyalkynylation of diazo compounds, but they have never been used in bioconjugation to date.[182] Compared to EBXs, EBZ reagents have the unique advantage of possessing a nitrogen substituent poised for further diversification. Inspired by the work of the Pentelute lab, who has extensively studied the reactivity of perfluoro aryl groups (see **I87** analogue) in bioconjugation *via* nucleophilic aromatic substitution (S_NAr) reactions,[183] the Waser group designed and synthesized mEBZ **R73**. The reactivity of **R73** is comparable to that of EBX reagent **I48**, enabling a fast (< 10 min at RT) addition of thiols onto the alkyne to give the corresponding vinylbenziodazolone (VBZ) adduct (*v. supra* **R56**). The electron-deficient pentafluorophenyl (*p*fp) group on the sulfonamide can then react in a second step, with another thiol-containing molecule, due its slower kinetics, orders of magnitude slower (i.e., 3-5 h at 37 °C) than the first one, allowing the sequential and orthogonal crosslinking of two thiols. Additional advantage of this new mEBZ crosslinking reagent **R73** is offered by the azide group that it is prone to functionalization prospects *via* click reaction.

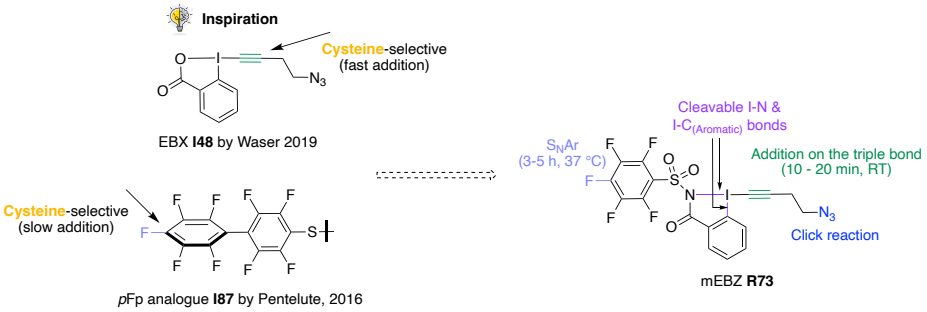

Scheme 47. Design inspiration of mEBZ **R73** reagent and representation of its functionalities.

2.3.3. mEBZ **R73** cross linking of cysteine-containing peptides

After the successful synthesis of mEBZ **R73**, the Waser group evaluated its potential on small cysteine-containing peptides. Reaction of 1.2 equiv. of **R73** with **peptide A** at RT for 20 min in a mixture of 50 mM PB at pH 8 and CAN (1:1, v/v) furnished the desired **VBZ-Peptide A** in average-to-good yields (36 – 82%). The large range in yields was attributed to the influence of the microenvironment surrounding the cysteine residue, since it was noticed that the presence of reactive amino acids such as lysine, or carboxylic acid-containing ones (i.e., aspartate and glutamate) were negatively affecting the conjugation reaction. Presumably, and as discussed before (**Scheme 38**), the VBZ adduct derived from a *β*-thiol-yne addition but a side product, attributed to either a potential *α*-addition or an *α*-elimination followed by 1,2-shift

after the *β*-thiol-yne addition, was also systematically observed. Addition of 1.2 equiv. of another cysteine-containing peptide (**Peptide B)** to the isolated **VBZ-Peptide A** in the same solvent mixture at 37 °C for 4 h gave the expected **cross-linked peptides A & B** in good yields (62 – 89%) (**Scheme 48**).

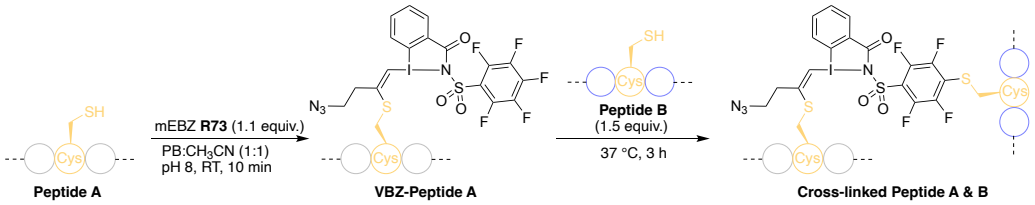

Scheme 48. Sequential cross-linkage of peptides **A & B** with multifunctional EBZ **R73**.

2.3.4. mEBZ **R73** evaluation as a Cys-Cys rebridging agent of native proteins

In an effort to evaluate the potential of mEBZ **R73** as a disulfide crosslinking reagent on more complex substrates, we investigated the rebridging of Fab species, derived from commercial therapeutic mAbs. Reduction of the single interchain disulfide bond to free the cysteines' thiols was carried out following known procedures, using 5 equiv. of TCEP at 37 °C, followed by gel filtration chromatography to eliminate the excess of reagent. Rebridging efficacy was determined by SEC-MS in denaturing conditions (SEC-dMS) – an approach specifically developed for our study –,[184] according to two parameters: *i*) the amount of **Fab** detected, defined as the percentage of Fab species – i.e., both native disulfide-bonded **Fab** and VBZ-rebridged Fab (**Fab-D1**) – *versus* that of LC and Fd sub-species; and *ii*) the average degree of conjugation (avDoC) of Fab, used as a direct indicator of the rebridging efficiency (**Scheme 49**).

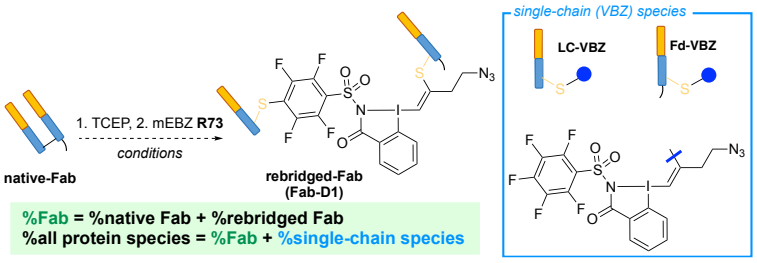

Scheme 49. mEBZ **R73** conjugation with Fab and generation of rebridged Fab **Fab-D1** alongside with LC/Fd species derived from mEBZ's fragmentation.

We began our investigations by applying to our reduced Fab-Trastuzumab similar conditions (2 equiv. mEBZ **R73** in MeCN, PBS 1X buffer, pH 8.5, 37 °C, 2 h) as those previously optimized for the generation of cross-linked peptides by the Waser group. However, to our dismay, this led to poor rebridging due to two main factors: the unexpected generation of

single-chain LC and Fd side-species **LC-frag** and **Fd-Frag**, respectively, bearing only fragments of the expected payload; and the incomplete conversion of native **Fab** to **Fab-D1** (avDoC < 0.3). A plausible explanation behind the formation of **LC-frag** and **Fd-Frag** is the fragmentation of the mEBZ **R73** payload either upon thiolate *α*-addition followed by elimination, or upon thiolate *β*-addition followed by *α*-elimination and 1,2-thiol migration. However, taking into consideration the mechanistic studies initiated by the Waser group in 2014 and 2016 (*v. supra*; **Scheme 38**),[167,168] the latter mechanism should be favoured, due to the alkyne's electron rich alkyl substituent (**Scheme 50**). The reasons behind the observed regio-selectivity of this side reaction, with the alkynyl and sulfonamide fragments being only detected on the **Fd** and the **LC**, respectively, remain poorly understood to this date. A tentative hypothesis, though, is that the regio-selectivity on the LC could be attributed to a spatially close phenylalanine (F208) that could interact with the *p*fp motif and direct the S_NAr – in a similar mechanism as Pentelute's π-clamp (even though they never observed conjugation on Trastuzumab's LC during their own study) –, considering that the bioconjugation reaction of both reactive centers takes place simultaneously.

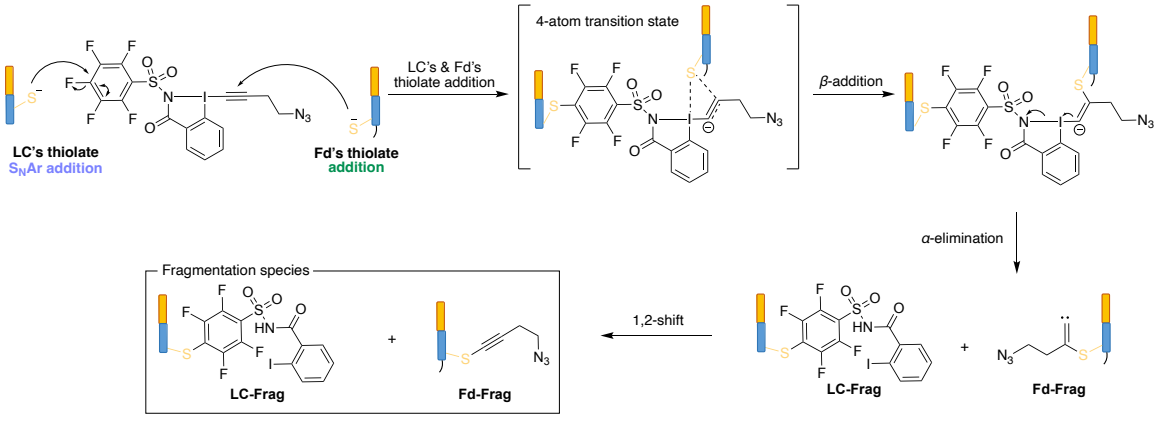

Scheme 50. Mechanistic proposal of mEBZ **R73** fragmentation.

Addition of 6 mM EDTA in an attempt to minimize the reoxidation of cysteines[45] and "playing" on both the reaction time and number of equiv. of **R73** did not have any positive effect (entry **6**; **Table 2**, *page 52*). However, decrease in EDTA's concentration to 2 mM with a simultaneous increase in both reaction time (16 h) and **R73** equiv. (5 equiv.) led to a noticeable improvement of rebridging (i.e., 66% Fab, avDoC 0.52, entry **9**; **Table 2**), whilst maintaining similar amounts of side species **LC-frag** and **Fd-frag**. Interestingly, a stark enhancement was noticed when switching to a borate buffer saline (BBS) (entry **10**; **Table 2**), with 70% of Fab being detected and an avDoC of 0.80, while decreasing the reaction time to 6 h led to improved amounts of Fab but to a less efficient rebridging, as evidenced by its halved avDoC (i.e., 79% Fab, avDoC 0.41, entry **11**; **Table 2**).

Table 2. Representative summary of the different conditions applied for the method development of mEBZ's **R73** conjugation with Fab-Trastuzumab.

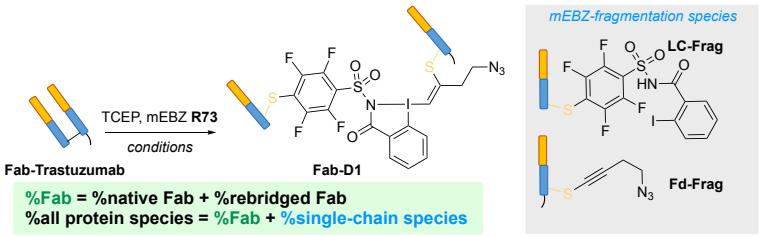

	Entry	Conditions	Fab (%)	avDoC[a]
Two-step reduction-conjugation	1	**R73** (2 equiv. in MeCN), PBS 1X buffer, pH 8.5, 25 °C, 20 min	86	0.34
	2	**R73** (2 equiv. in DMSO), PBS 1X buffer, pH 8.5, 25 °C, 20 min	83	0.33
	3	**R73** (2 equiv. in DMSO), PBS 1X buffer, pH 8, 25 °C, 20 min	92	0.41
	4	**R73** (2 equiv. in DMSO), PBS 1X buffer, pH 8, 37 °C, 20 min	82	0.57
	5	**R73** (2 equiv. in DMSO), PBS 1X buffer, pH 8, 37 °C, 2 h	68	0.28
	6	**R73** (2 equiv. in DMSO), PBS 1X buffer, 6 mM EDTA, pH 8, 37 °C, 2 h	77	0.25
	7	**R73** (2 equiv. in DMSO), PBS 1X buffer, 6 mM EDTA, pH 8, 37 °C, 16 h	74	0.31
	8	**R73** (5 equiv. in DMSO), PBS 1X buffer, 6 mM EDTA, pH 8, 37 °C, 16 h	75	0.30
	9	**R73** (5 equiv. in DMSO), PBS 1X buffer, 2 mM EDTA, pH 8, 37 °C, 16 h	66	0.52
	10	**R73** (5 equiv. in DMSO), BBS buffer, 2 mM EDTA, pH 8, 37 °C, 16 h	70	0.80
	11	**R73** (5 equiv. in DMSO), BBS buffer, 2 mM EDTA, pH 8, 37 °C, 6 h	79	0.41
One-pot reduction-conjugation procedure	12	**R73** (5 equiv. in DMSO), BBS buffer, 2 mM EDTA, pH 8, 37 °C, 6 h	70	1
	13	**R73** (5 equiv. in DMSO), PBS 1X buffer, 2 mM EDTA, pH 8, 37 °C, 6 h	71	0.91
	14	**R73** (5 equiv. in MeCN), PBS 1X buffer, 2 mM EDTA, pH 8, 37 °C, 6 h	69	0.91
	15	**R73** (5 equiv. in DMF), PBS 1X buffer, 2 mM EDTA, pH 8, 37 °C, 6 h	67	0.93
	16	**R73** (5 equiv. in DMSO), Tris buffer, 2 mM EDTA, pH 8, 37 °C, 6 h	82	0.27
	17	**R73** (5 equiv. in MeCN), Tris buffer, 2 mM EDTA, pH 8, 37 °C, 6 h	80	0.36
	18	**R73** (5 equiv. in MeCN), BBS buffer, 2 mM EDTA, pH 8, 37 °C, 6 h	58	0.95
	19	**R73** (5 equiv. in DMF), BBS buffer, 2 mM EDTA, pH 8, 37 °C, 6 h	70	1
	20	**R73** (5 equiv. in DMSO), BBS buffer, 2 mM EDTA, pH 6.5, 37 °C, 6 h	71	1
	21	**R73** (5 equiv. in DMSO), BBS buffer, 2 mM EDTA, pH 7, 37 °C, 6 h	61	1
	22	**R73** (5 equiv. in DMSO), BBS buffer, 2 mM EDTA, pH 7.5, 37 °C, 6 h	62	0.93
	23	**R73** (5 equiv. in DMSO), BBS buffer, 2 mM EDTA, pH 8.5, 37 °C, 6 h	46	0.82
	24	**R73** (5 equiv. in DMSO), BBS buffer, 2 mM EDTA, pH 8, 37 °C, 0.5 h	80	0.69
	25	**R73** (5 equiv. in DMSO), BBS buffer, 2 mM EDTA, pH 8, 37 °C, 1 h	81	0.75
	26	**R73** (5 equiv. in DMSO), BBS buffer, 2 mM EDTA, pH 8, 37 °C, 2 h	82	0.85
	27	**R73** (5 equiv. in DMSO), BBS buffer, 2 mM EDTA, pH 8, 37 °C, 4 h	77	0.93
	28	**R73** (5 equiv. in DMSO), BBS buffer, 2 mM EDTA, pH 8, 37 °C, 5 h	72	1
	29	**R73** (5 equiv. in DMSO), BBS buffer, 2 mM EDTA, pH 8, 25 °C, 6 h	76	0.97
	30	**R73** (5 equiv. in DMSO), BBS buffer, 2 mM EDTA, pH 8, 4 °C, 6 h	69	0.58
	31	**R73** (7.5 equiv. in DMSO), BBS buffer, 2 mM EDTA, pH 8, 25 °C, 6 h	84	1.06[b]
	32	**R73** (10 equiv. in DMSO), BBS buffer, 2 mM EDTA, pH 8, 25 °C, 6 h	77	1.08[b]

At this stage, we hypothesized that the gel purification conducted after the TCEP-mediated reduction step might favour the reoxidation of the thiols, and therefore we evaluated the possibility of conducting both the reduction and the rebridging steps in one pot (see experimental section for procedure, *page 115*). Gratifyingly, this led to full rebridging of Fab-Trastuzumab (i.e., avDoC 1.0), the sole double-chain species detected by denaturing LC-MS (entry **12**; **Table 2**, **Scheme 51**). This excellent stability of the iodine(III) bond toward these reductive conditions is remarkable, and far superior to that of more standard reagents classically used for protein rebridging (*v. supra*). All our subsequent efforts were thus dedicated to improving the percentage of fully rebridged Fab obtained, by minimizing the side reactions leading to the single-chain species.

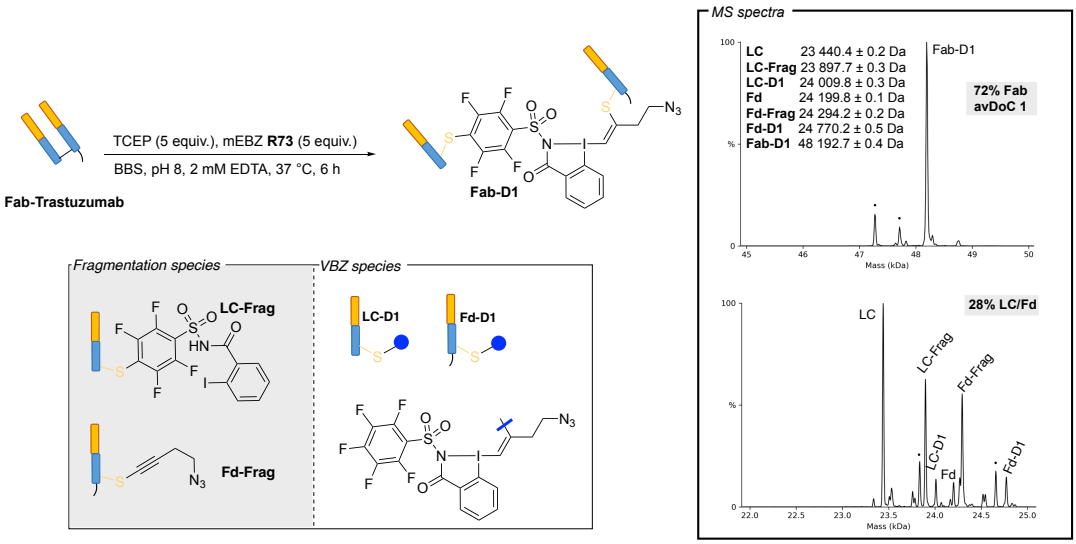

Scheme 51. Labelling of Fab-Trastuzumab with mEBZ **R73** and schematic representation of the different single-chain fragments produced, accompanied with deconvoluted MS-spectra. With dots are represented species generated from the Fab's over-digestion.

Varying buffer and co-solvent led systematically to a decrease in DoC, highlighting the profound influence of solvent effects on conjugation's efficacy (**Figure 9** - **Chart 1**). Increasing pH had a detrimental impact on Fab percentage and DoC, whilst decreasing it had little effect on both terms (**Figure 9** - **Chart 2**). Surprisingly, at pH 7.5, doubly conjugated species were detected, highlighting the enhanced reactivity of mEBZ's alkyne group in comparison with the *pf*P one (*v. supra*) and the necessity of tuning the reaction conditions finely to maintain its chemoselectivity. Following a time-course experiment, we also noted that similar results could be obtained after just 5 h (entry **28**; **Table 2**), but that decreasing the reaction time further led to an erosion of the DoC values and hence the rebridging efficiency (**Figure 9** - **Chart 3**). Lowering the reaction temperature to 25 °C led to an improved amount of Fab with a minimal decrease in avDoC (entry **29**; **Table 2**). Interestingly, formation of side species **LC-frag** and **Fd-frag** could be completely suppressed by working at 4 °C, albeit at the expense of both

avDoC and amount of Fab (entry **30**; **Table 2**; **Figure 9** - **Chart 4**). Any attempt at improving the latter – notably by increasing the number of mEBZ's equiv. (entry **31** & **32**; **Table 2**) – led to a parallel increase of the former, due to the appearance of doubly conjugated Fab species, highlighting again chemoselectivity issues. At this stage, it should be noted that in all cases the yield obtained was quantitative, indicating that mEBZ did not trigger any protein-precipitation issue. This methodology-work led to the development of optimal conditions [35 mM native Fab in BBS, 2 mM EDTA, pH 8, TCEP (5 equiv. in H_2O), **R73** (5 equiv. in DMSO), 5 h, 37 °C], maximizing the percentage of rebridged Fab and minimizing the formation of side species (i.e., 72% Fab, avDoC 1, entry **28**; **Table 2**).

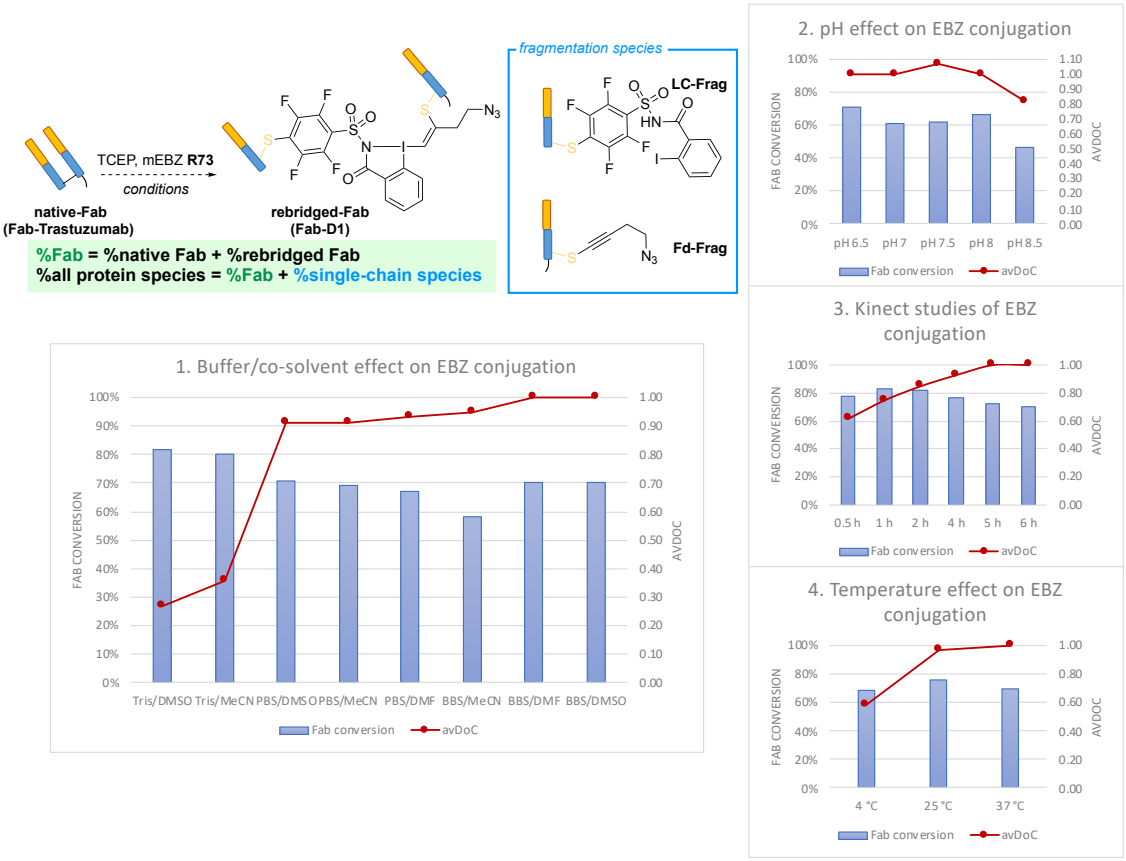

Figure 9. Method development to maximize the rebridging efficacy of **Fab-Trastuzumab**'s conjugation with mEBZ **R73**. Starting conditions were those described in **Scheme 51** – i.e., TCEP (5 equiv.), mEBZ (5 equiv.), BBS, 2 mM EDTA, pH 8, 37 °C, 6 h – and one parameter was varied at a time: buffer/co-solvent in chart 1, pH in chart 2, incubation time in chart 3, and temperature in chart 4.

Having developed optimal conditions on Fab-Trastuzumab, we were keen to apply our protocol to Fab from other mAb sources. Enzymatic digestion of Bevacizumab, Avelumab and Rituximab furnished the desired Fab species in high yield and purity. These were successfully rebridged, with an efficacy similar to that observed with Fab-Trastuzumab (**Scheme 52**), except for Fab-Avelumab, which demonstrated lower conversion rates, perhaps due to the existence of a serine residue (S216) next to the LC's cysteine (C215), negatively affecting EBZ's rebridging efficacy.

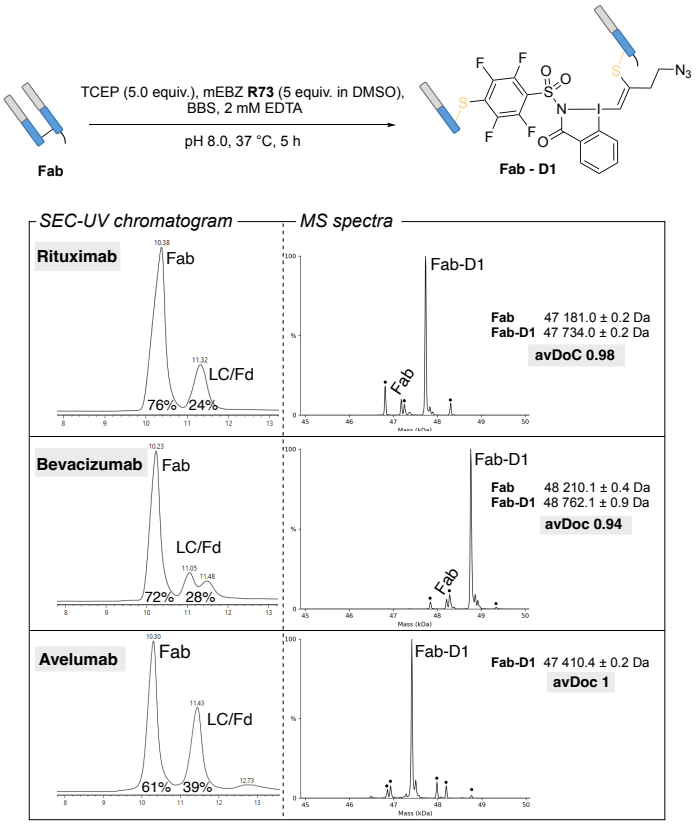

Scheme 52. mEBZ **R73** conjugation with Fabs derived from different sources accompanied by SEC-dMS analysis. With dots are represented species generated from the Fab's over-digestion.

Gratifyingly, we demonstrated that mEBZ **R73** could be also applied to whole mAbs (**Scheme 53**). Under slightly tweaked conditions, Trastuzumab led to 82% of rebridged mAb (avDoC 2.5), with only 11% of half mAb and 7% of LC and HC subspecies, demonstrating the broader applicability of our strategy. For the rebridged mAb, the incorporation of two VBZs was most frequent (**D2**), but insertion of 1, 3 and even 4 VBZs was also observed (**D1**, **D3** and **D4**), while the absence of **D0** species indicated that we achieved full mAb rebridging. Also, this result further supports the previous assumption that the spatial close Phe to the Cys of the LC played a crucial role to the rebridging at the Fab region, as the absence of spatial close Phe residues at the hinge region presumably led to the generation of fewer **D3** and **D4** species, thus favouring the **D2** ones.

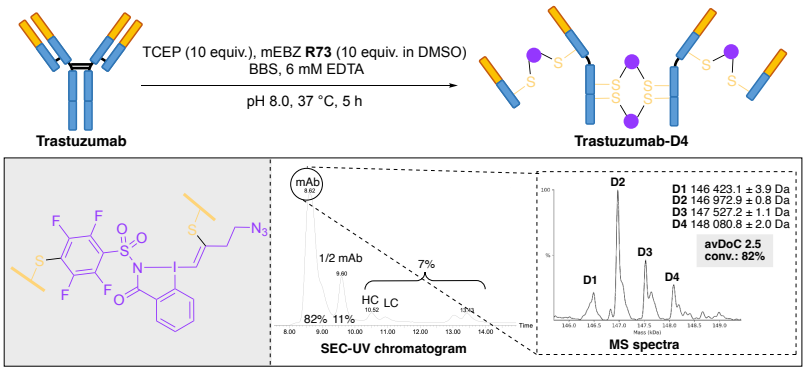

Scheme 53. mEBZ **R73** conjugation with Trastuzumab. The LC chromatogram shows that 82% of the generated species correspond to rebridged species of whole mAb with an avDoC of 2.5 as indicated by the MS spectrum.

Having validated the rebridging step, we next focused our attention on the functionalization of rebridged **Fab-D1** *via* a bioorthogonal click reaction, taking advantage of the azide group on the VBZ payload. Performing this stepwise rebridging/functionalization process on Fab-Trastuzumab with the strained alkyne BCN-Iminobiotin **R74** led to fully rebdriged iminobiotin-containing Fab species **Fab-D1'**, albeit in a lower proportion (62%) (**Scheme 54**). Suspecting that this was caused by the two successive purification steps, we also evaluated the concomitant one-pot reduction/rebridging/functionalization sequence by mixing Fab-Trastuzumab with a mixture of TCEP, **R73** and **R74** under our optimized conjugation conditions at 37 °C. Pleasingly, this led to an increase of rebridged Fab proportion (72%), the only double-chain species detected, as illustrated on the SEC-dMS analysis in **Scheme 54**.

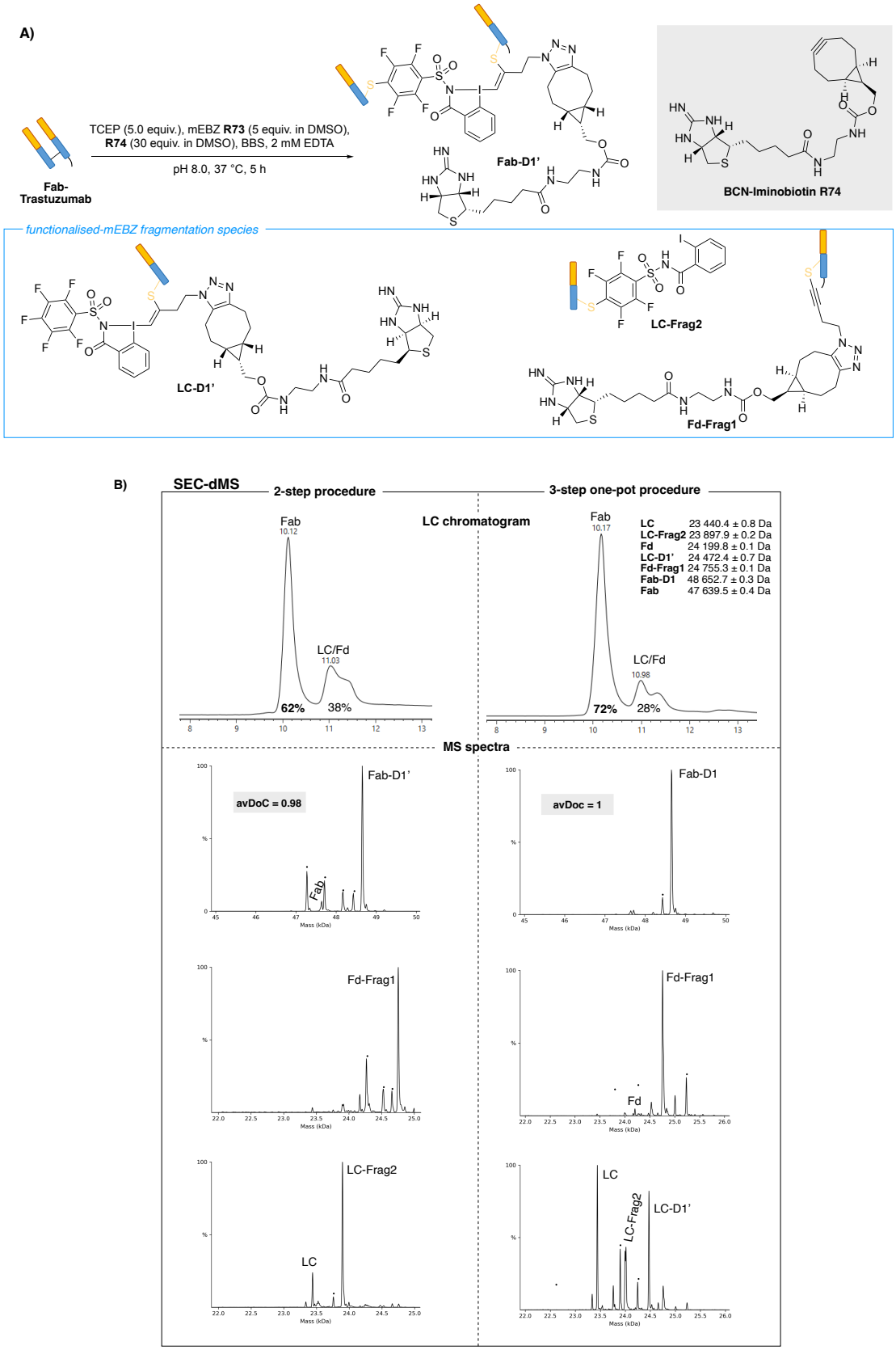

Scheme 54. A) 3-step one-pot reaction between TCEP, mEBZ **R73**, BCN-Iminobiotin **R74** and Fab-Trastuzumab. B) SEC-MS in denaturating conditions demonstrating the difference between the 2-step and the 3-step one-pot procedure of Fab-Trastuzumab, where in the former case 62% Fab and avDoC 0.98 while in latter 72% Fab and avDoC 1 was generated. With dots are represented species generated from the Fab's over-digestion.

In an effort to validate the versatility of our 3-step one-pot approach, we applied it to different mAb sources as we had previously done with the 2-step one-pot procedure (*v. supra*, **Scheme 52**). Delightedly, we observed similar efficacy for Rituximab (Fab 78% & avDoC 1) and Avelumab (Fab 65% & avDoC 1) compared to the results obtained with the 2-step one-pot approach, while Bevacizumab showed both reduced Fab conversion and avDoC values (57% & 0.8, respectively) (see experimental section for the spectra, *page 118*). To the best of our knowledge, this complex chemo-selective ballet between four reactive species has never been reported before and is key in improving both the efficacy and the efficiency of our conjugation sequence. Finally, stability assays of the rebridged Fab-Trastuzumab in human plasma highlighted a perfect stability for 5 days at 37 °C (**Scheme 55**).

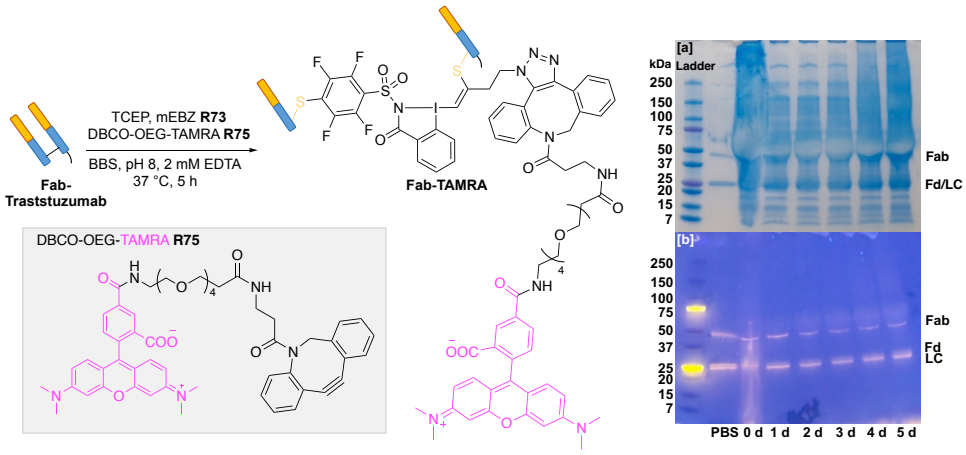

Scheme 55. Stability studies of the rebridged **Fab-TAMRA** in human plasma for up to 5 days at 37 C. [a] SDS-PAGE with Coomassie blue staining. [b] SDS-PAGE under UV light, at 254 nm.

2.3.5. mEBZ **R73** comparison with DBM **R76**

Attempting to perform our optimized one-pot three-step conjugation procedure with a classical dibromomaleimide rebridging reagent **R76** led to mediocre rebridging efficiency (i.e., 92% Fab, avDoC = 0.10), as illustrated in **Scheme 56**, presumably because of TCEP-mediated decomposition of the maleimide motif.[154,185–188]

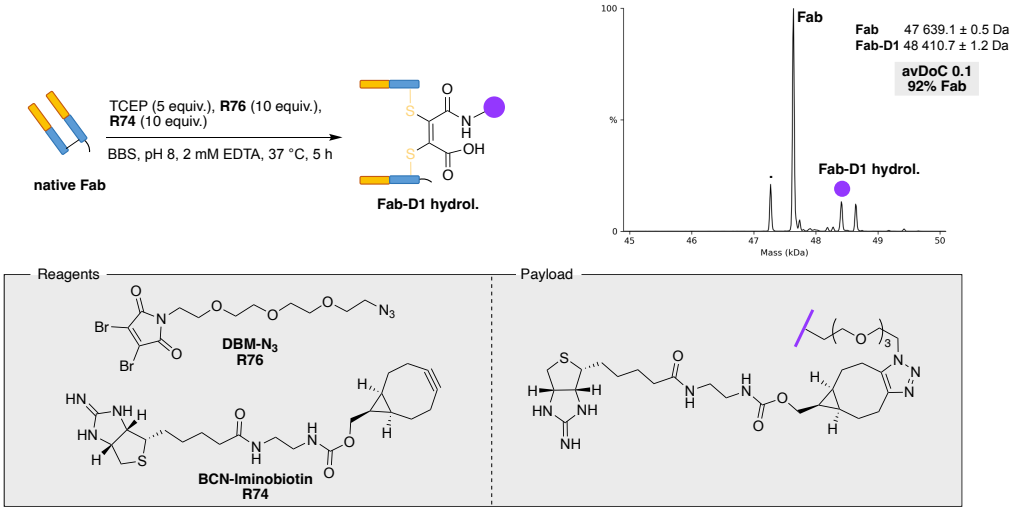

Scheme 56. 3-step one-pot reaction of DBM-N_3 **R76** and BCN-Iminobiotin **R74** with Fab-Trastuzumab incorporating the optimal conditions developed for mEBZ's **R73** conjugation. The deconvoluted MS spectrum shows mainly unreacted Fab species and traces of hydrolyzed maleimide conjugated species. With dots are represented species generated from the Fab's over-digestion

2.3.6. Controlled cleavage of mEBZ **R73**

Next, we wanted to investigate whether we could promote the controlled cleavage of the hypervalent iodine bond of the rebridged **Fab-D1**. Inspired by Ding *et al.* who used copper(I) cyanide for the reduction of the benziodoxole moiety to afford *β*-cyano and -iodo vinyl ethers,[189] we used copper(I) iodide – to prevent the formation of cyano derivatives – in the presence of THPTA, sodium ascorbate and aminoguanidine at 37 °C for 16 h. Satisfyingly, we obtained 90% cleavage of the **Fab-D1** leading to fragmented species **Fd-Red** – the sole Fd fragmentation species detected, which tends to suggest a regio-selective rebridging – and **LC-Red** – the main LC fragmentation species detected –, as determined by denaturing SEC-MS (**Scheme 57**).

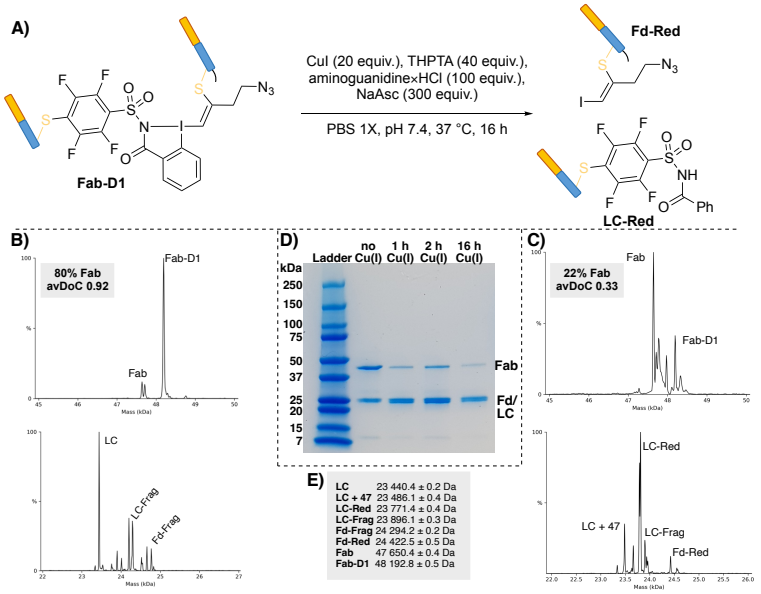

Scheme 57. A) Schematic representation of Fab-D1's reductive cleavage with Cu(I). B) MS (denaturating conditions) of Fab-D1 before Cu(I) treatment. C) MS (denaturating conditions) of Fab-D1 after Cu(I) treatment. D) SDS-PAGE of Fab-D1 cleavage over time. E) Masses of the various species spotted on the MS.

2.3.7. Conclusion

In conclusion, we evaluated a novel heterobifunctional reagent **R73**, bearing EBZ and pentafluorophenyl motifs, as a thiol cross-linker. After extensive method development, we demonstrated that **R73** could be used to rebridge and functionalize various biomolecules in a chemo-selective manner, mainly Fab fragments from various sources with conversion rates above 70% and quantitative yields *via* a one-pot 3-step reaction, but also whole antibodies *via* a one-pot 2-step reaction. The rebridging of Fab was often accompanied with the formation of Fd and LC fragments, derived from the fragmentation of **R73** upon thiolate *β*-addition on its alkyne's portion followed by *α*-elimination and an 1,2-thiol migration. While this side reactivity could be completely suppressed by working at 4 °C, this was however at the expense of both avDoC and amount of Fab. Furthermore, we demonstrated the excellent stability of our rebridged conjugates in human plasma for 5 days at 37 °C and their controlled cleavage in the presence of copper(I) species through iodine(III) reduction. This work has helped to further prove the versatility of hypervalent iodine(III) reagents and their great potential in cystiene bioconjugation.

Having optimised a novel chemo-selective bioconjugation method suitable for the fast rebridging of cysteines in Fab fragments, we then turned our attention to the next stage of complexity in selective strategies: the development of a site-selective method that could be applicable to a broader range of biomolecules. In order to do so, we focused on the conjugation of the side chains of two spatial close amino acids *via* a multicomponent reaction.

3. UGI MULTICOMPONENT REACTION FOR THE SITE-SELECTIVE CONJUGATION OF NATIVE & ARTIFICIAL PROTEINS

3.1. MULTICOMPONENT REACTIONS IN CHEMISTRY

Multicomponent reactions (MCRs) are generally defined as reactions employing at least three chemicals that react in one pot and whose constitutive atoms are (almost) all found in the final product.[190] The usefulness of such reactions is due to their multiple advantages over the traditional, multistep, sequential assembly of complex molecules, namely intrinsic synthetic efficiency and operational simplicity. This is due to vessel-, atom-, and step-economy, saving precious time,[191,192] but also to the facts that MCRs usually do not necessitate stringent conditions (e.g., dry solvent, inert atmosphere) and that the molecules are assembled in a convergent way and not in a linear approach, thus drastically reducing the synthetic effort of traditional multistep synthesis.

Although MCRs are almost as old as organic chemistry itself, being first described as early as 1851,[193] it should be noted that early-day chemists did not recognize the enormous potential of MCRs. Thus, it took another 70 years for Mario Passerini to unveil the first multicomponent reaction employing isocyanides in 1921, and more than 100 until Ivar Ugi discovered his four-component condensation reaction.[194] Up to date, over a dozen MCRs, many of them named after people who discovered them, have been developed, among which, but not limited to, are the Mannich,[195] Biginelli,[196] Ugi,[194] Passerini, Petasis,[197] Groebke-Blackburn-Bienayme (GBB),[198–200] or Orru[201] reaction (**Figure 10**). Reactants such as carbonyls, amines, isonitriles (isocyanides) and carboxylic acids are the most common ones for MCRs, while H_2O and CO_2 are the usual by-products. Recently, many MCRs like the Mannich or the Ugi reaction have gained particular attention due to their ability to take place in water, as they could be used for protein modification.

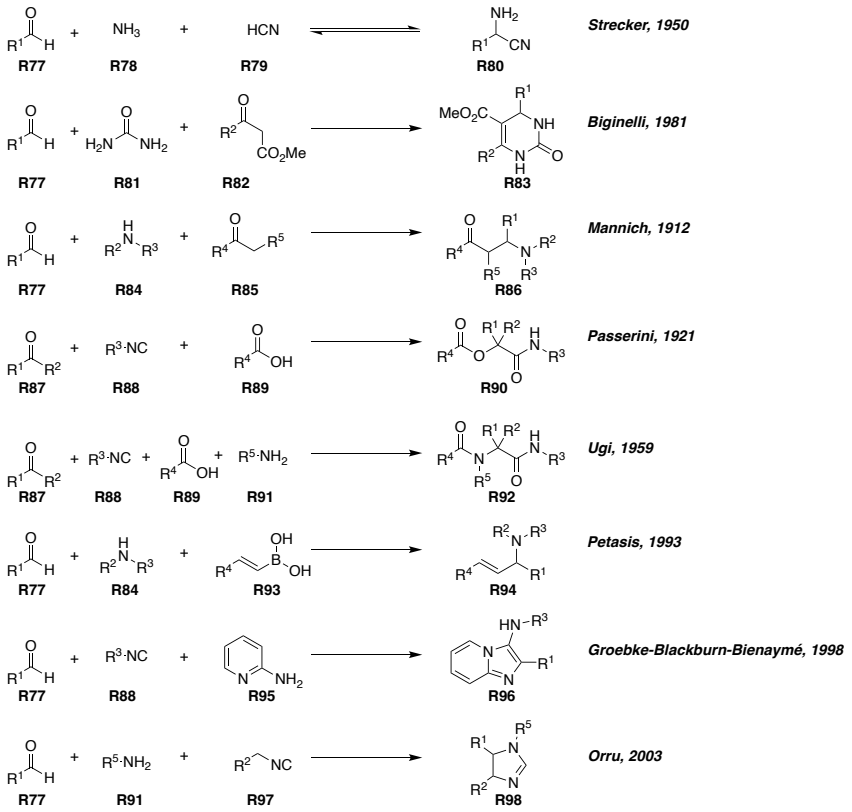

Figure 10. Summary of representative MCRs.

3.2. MULTICOMPONENT REACTIONS IN BIOCONJUGATION

3.2.1. Mannich reaction

As already mentioned in the introduction (i.e., *pages 22 – 23)*, in 2017 and 2018 the Rai group has developed a Mannich multicomponent reaction for the chemo- and regio-selective modification of lysine residues on a small library of proteins. However, these reactions led to small conversions, and necessitated the use of large excess of reagents and the addition of copper catalysts.[104,105]

But the first use of the Mannich reaction in the field of protein conjugation is attributable to the group of Francis in 2004, with the chemo-selective modification of tyrosine residues **R99** through an electrophilic aromatic substitution of their phenol side-chain.[202] Surface-accessible tyrosine residues of different proteins – i.e., chymotrypsinogen A, lysozyme and RNase A – were successfully modified with a large excess of various aldehyde **R100** and aniline derivatives **R101** (1250 equiv.) under mild conditions (i.e., PB, pH 6.5, RT to 37 °C, 18 h) to reach 30 to 66% conversion. Importantly, hydrolysis of undesired imines – resulting from the side reaction of the aldehyde with lysines – was required and was achieved by incubating the conjugated proteins with a solution of hydroxylamine.

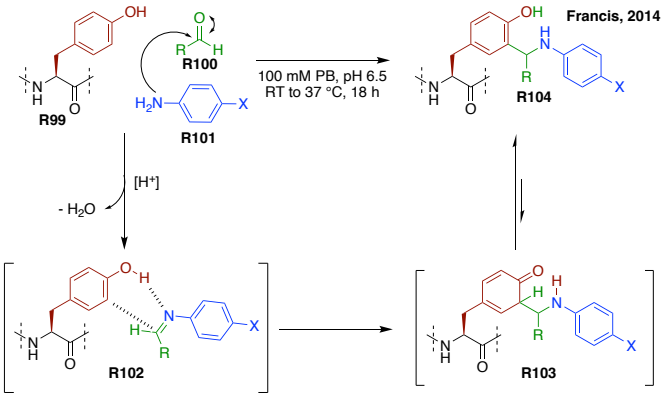

Scheme 58. Chemo-selective labeling of tyrosine residues on proteins *via* a Mannich reaction and mechanism proposed by Francis *et al,* 2014.[202]

Mechanistically, they hypothesized that at pH 6.5, a cyclic transition state **R102** would occur, in which the phenol ring would form a hydrogen bond with the imine's nitrogen, the latter resulting from the condensation between the aniline **R101** and the aldehyde **R100** (**Scheme 58**). This hydrogen bond would enhance the electrophilicity of the imine group, while simultaneously activating the aromatic ring as a nucleophile, thus forming ketone **R103**, in equilibrium with its aromatic enol form **R104**. However, it should be noted that imine formation in water involves numerous equilibrating species, and thus the reaction could proceed through a more complex pathway.[202]

Encouraged by the results obtained with the Mannich reaction as a site-selective approach for the conjugation of proteins, more MCRs were described.

3.2.2. Petasis reaction

The Petasis MCR, also known as the borono-Mannich reaction, is a three-component process comprising the condensation of a carbonyl source **R106**, an amine **R105**, and either an aryl/vinyl boronic acid **R107** or ester. Similar to the Mannich reaction, an imine **R109** is initially formed between the amine **R105** and the carbonyl **R106**, which is subsequently attacked by the boronate complex formed in **R110** (**Scheme 59**). In comparison with the classical Mannich reaction, where the reversibility of the final step limits the number of cases where the yields are synthetically useful, the Petasis reaction offers an interesting and valuable irreversible alternative. In 2019, the Raj group showed that the Petasis reaction could be efficiently used for the conjugation of tripeptides, bioactive peptides and small proteins, by targeting *N*-terminal prolines under mild conditions (PB, pH 7.3, RT, 16 h), furnishing the desired Petasis-modified conjugates with good to excellent conversions.[203]

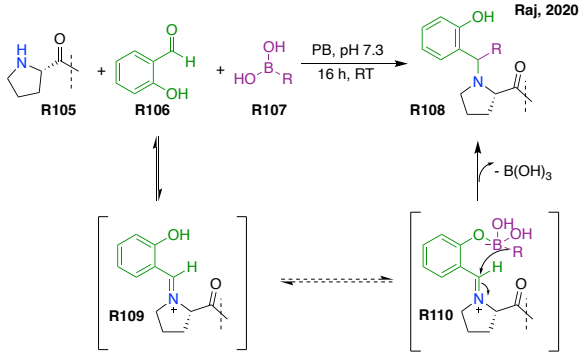

Scheme 59. Labeling of *N*-terminal proline residues *via* Petasis reaction.

Recently, the Rivera and Spring groups have separately described two novel applications of the Petasis reaction for the labelling and stappling of lysine/N-terminal and tryptophan residues, respectively, on small peptides.[204,205] In the case of Rivera's approach, his group utilized various carbonyl **R112** and boronic acid **R113** derivatives to modify single lysine-containing peptides at RT in 24 h (**Scheme 60A**). The carbonyl – boronic acid molecules' combination proved to play a crucial role to the conversion rates of the reaction, ranging from 50 to 100%, as the reactivity of the former was affecting the latter's and *vice versa*. Moreover, they have also applied their strategy to the *N*-terminal of peptides lacking lysine residues, where in this case, microwave irradiation and high temperatures (90 °C) necessitated to reach mediocre conversions (58 – 71%). In the case of Spring group's tryptophan labeling **R115**, high temperatures were required in an effort to accelerate the reaction to reach full conversion, since at room temperature at least 16 h were necessitated to reach the same conversion rates (**Scheme 60B**). Moreover, this reaction was found to be aldehyde, boronic acid and organic solvent dependent, as different combinations of these parameters used to lead from 0 to 100% conversion. In conclusion, although these methods were a nice representation of Petasis

MCR, they required microwave irradiation, high temperatures, and took place only in organic solvents under acidic conditions, thus limiting their application to larger macromolecules.

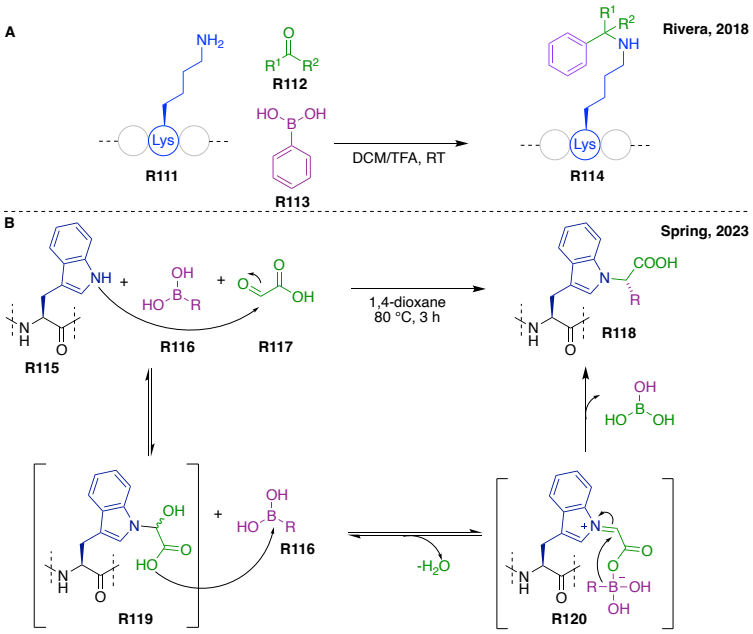

Scheme 60. A) Labeling of lysine residues *via* Petasis reaction by Rivera group. B) Labeling of tryptophan residues *via* Petasis reaction by Spring group.

Contrary to Mannich and Petasis reactions that require three components, the Ugi multicomponent reaction necessitates four, and was thus logically dubbed as the Ugi four-component reaction (U-4CR).

3.2.3. Ugi reaction

As illustrated in

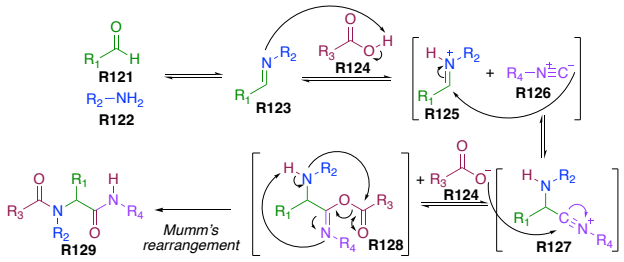

Scheme 61, the U-4CR starts with the formation of imine **R123** upon the condensation between carbonyl **R121** and amine **R122**. Protonation by carboxylic acid **R124** forms iminium ion **R125**, which undergoes a nucleophilic attack from isocyanide **R126** to generate the isonitrilium ion **R127**. The latter reacts with carboxylate **R124**, creating the last intermediate **R128** that partakes in a Mumm rearrangement, *viz*. a *O*-to-*N* acyl shift, yielding the desired Ugi product **R129**. All reaction steps are thought to be reversible, the Mumm rearrangement being the driving force of the whole reaction.

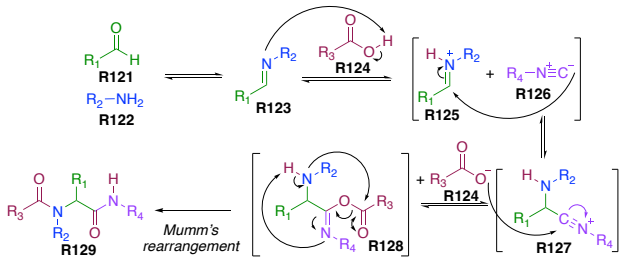

Scheme 61. Ugi's reaction mechanism.

Variations of the U-4CR were described over the years, such as the Ugi-Smiles reaction where a phenol replaces the carboxylic acid, or the Ugi four-center three-component reaction (U-4C-3CR), in which two of the four components necessary for the reaction are borne by the same molecule.

To the best of my knowledge, the utilization of the U-4CR in protein bioconjugation was first reported in 1983 by Marek *et al*. with the immobilization of the enzyme glucose oxidase on a polymeric carrier bearing amine groups **R130**. However, due to the absence of a carbonyl source, the glycoenzyme was first subjected to periodate-mediated oxidative cleavage to generate aldehyde groups in the glycosidic part **R131**. The newly formed aldehydes were next linked to the amino-functionalized glycidyl methacrylate polymers in the presence of acetic acid **R132** and cyclohexyl isocyanide **R133**, delivering the polymer-supported enzyme **R134**, as illustrated on **Scheme 62**.[206]

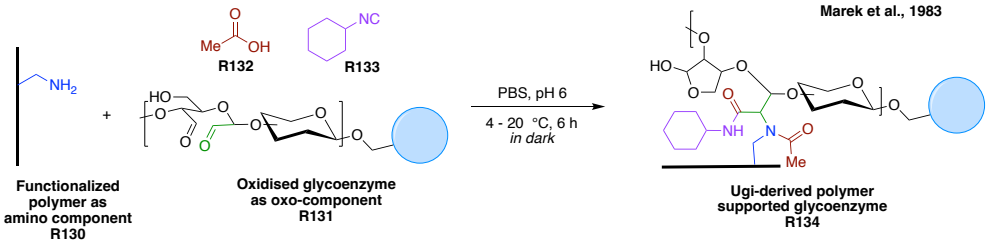

Scheme 62. Immobilization of the enzyme glucose oxidase on a polymeric carrier *via* an U-4CR.

While the glycoenzyme immobilization relied on the generation of aldehydes on the glycan moiety, two other Ugi-reactive functional groups are already present in a protein, i.e., the carboxylic acid and the amine, borne by aspartate/glutamate and lysine residues, respectively. In 2000, the Ziegler group took advantage of this feature and reported the preparation of bovine serum album (BSA) and horseradish peroxidase (HRP) bioconjugates *via* the U-4CR by targeting either aspartate/glutamate or lysine residues (**Scheme 63**).[207] To achieve good conversions, large amount of reactants were necessary – up to 4000 equiv. in isocyanide **R136**, aldehyde **R135**, and amine **R137** or carboxylic acid **R138** derivatives, depending on the targeted residue – as well as long incubation times, typically between 1 to 4 days at 25 °C.

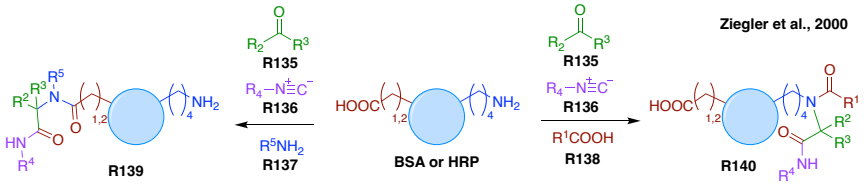

Scheme 63. BSA and HRP modification *via* an U-4CR.

For the development of glycoconjugate vaccine candidates, the Rivera group proposed the utilization of the U-4CR in 2020.[208] Similar to the work of Marek and coworkers, the construction of these vaccines necessitated the oxidation of two bacterial capsular polysaccharides (CPs) from *Streptotoccus Pneumoniae* and *Streptotoccus Typhi*, used as the aldehyde source **R141**. The amine source was provided by lysines of the carrier proteins – tetanus toxoid (TT) or diphteria toxoid (DT) –, while acetic acid **R143** and *tert*-butyl isocyanide **R142** were used as the two remaining components of the reaction. However, due to low conversion rates (41%) even after 48 h of reaction, the side chains of aspartate/glutamate residues were coupled with hydrazine – to bear a more nucleophilic hydrazide group as the amine source – in the presence of N-(3-(dimethylamino)propyl)-N′-ethylcarbodiimide hydrochloride (EDC·HCl) at RT in darkness allowing to reach complete conversion after only 4 h (**Scheme 64**).

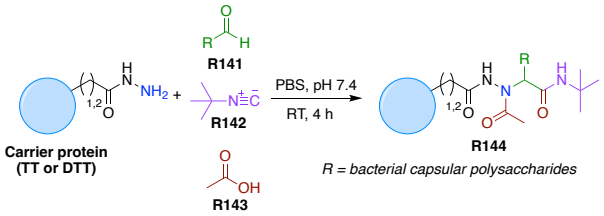

Scheme 64. Modification of Toxoid strains *via* an U-4CR.

Considering the conditions used, it would have been expected to also observe another MCR competing for the conjugation of the proteins, the Passerini reaction, but the authors did not comment on this possibility. This MCR was first reported decades before the Ugi reaction (*v. supra)* and differs from the latter only in the lack of amines utilization, while in this case, the combination of isocyanide, carbonyl and carboxylic acid components lead to *α*-acyloxyamides.

The generally accepted mechanism of the Passerini reaction is shown in **Scheme 65**.[209] According to this concerted mechanism, an H-bonded cluster **R147** would be formed by the interaction of the carboxylic acid **R145** with the carbonyl compound **R146** and would subsequently react with isocyanide **R148** in a single step to give **R149**. The final Mumm-like rearrangement would occur through the cyclic intermediate **R150** to yield the final product **R151**.

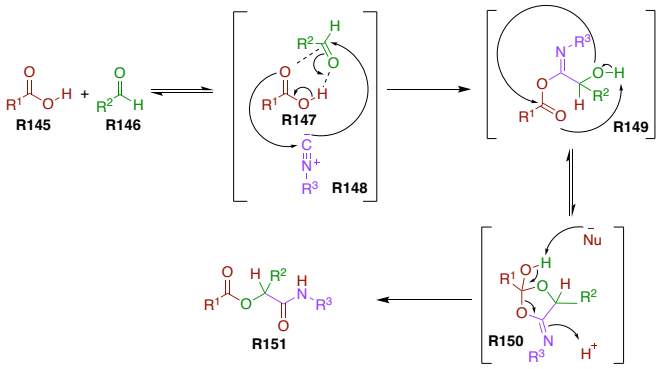

Scheme 65. Passerini's reaction mechanism.

3.3. AIM OF THE PROJECT

Building up on these literature precedents, we investigated the utilization of multicomponent reactions (MCRs) as regio-selective methods in protein bioconjugation. As shown before, the U-4CR represents one of the most well-known and described MCRs in organic chemistry and has been recently employed for that purpose. Inspired by Ziegler *et al.* who targeted amines and carboxylic acids that are abundant in proteins, we envisioned that the addition of a carbonyl and an isocyanide to a model protein could lead to the conjugation of two spatially close lysine and aspartate/glutamate residues – bearing side-chain amine and carboxylate groups, respectively – *via* a three-center four-component Ugi reaction (U-3C-4CR), a variant of the classical U-4CR. This would drastically reduce the number of potential conjugation sites and hence increase our chances to develop a site-selective strategy. This work was initiated by a previous member of our laboratory, Dr Charlotte Sornay, who developed a set of conditions that gave good conversion rates, medium yields, but broad avDoC distribution and the identification of a handful of conjugation sites under one set of conditions. The goal of the current project was the in-depth investigation of this approach by means of comprehensive methodology that would allow a better understanding of the reaction's behavior and, possibly, its improvement with a view to developing a site-selective version.

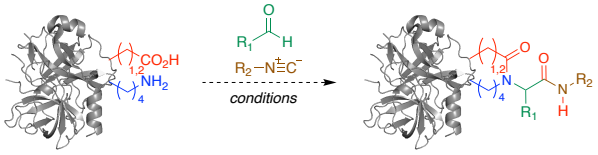

Scheme 66. Application of the three-center four-component Ugi reaction (**U-3C-4CR**) for the bioconjugation of native proteins.

This project was done in close collaboration with PhD students Ms Valentine Vaur, from our laboratory, and Ms Rania Benazza, from the group of Dr Sarah Cianferani, whose laboratory is located at the University of Strasbourg (UMR7178) and is a member of our ITN consortium. They contributed to this work by analyzing our protein conjugates, through native MS and peptide mapping. We also had the opportunity to collaborate with another member of our ITN consortium, the group of Pr Arne Skerra at the TUM, and Ms Carmen Longo and Ms Yağmur Ersoy in particular, who generously provided us with anticalin proteins to test our method.

3.4. UGI REACTION ON TRASTUZUMAB

The model proteins we selected to study our Ugi conjugation reaction were native antibodies, which we reacted with an isocyanide and a carbonyl derivative. In particular, we chose the 150 kDa monoclonal antibody Trastuzumab, currently used in clinics for the treatment of $HER2^+$ breast cancer (*v. supra*). The choice of the isocyanide and the carbonyl source was crucial, and several combinations were evaluated, focusing on three main parameters to evaluate their efficacy: *i*) conversion – i.e., the amount of protein that participated in the Ugi reaction; *ii*) the average degree of conjugation (avDoC) – i.e., the average number of conjugated sites on the protein; and, *iii*), the identity of these conjugation sites. As our goal was to develop an efficient site-selective conjugation reaction, our optimized conditions should ideally lead to complete conversion and narrow DoC distribution, with only one or two conjugation sites identified.

After extensive research conducted previously in our laboratory,[210] it had been identified that cyclohexyl isocyanide **R133** and the azide-PEG_4 aldehyde **R152** were the optimal combination for Trastuzumab conjugation. Mixed in a stoichiometric ratio (45 equiv. of each), these led to an avDoC ~1.5 and a conversion over 80% in almost quantitative yields (> 99%) after 16 h of incubation at 25 °C in PBS (1X, pH 7.5, 137 mM NaCl), according to native mass spectroscopy (native MS). To get rid of any remaining unreacted imines, hydroxylamine was added after the reaction, and incubated at 25 °C for 1.5 h.[202] Since the differences in molecular weights between all protein species were too small after the Ugi conjugation to be well resolved by native MS, a second functionalization step was necessary to increase the molecular weight of the payload. Taking advantage of the azide group borne by the aldehyde, a SPAAC step was realized, using 30 equiv. of strained alkyne BCN-Cy5 **R153** at 25 °C in PBS 1X for 16 h, albeit in mediocre yields. The obtained Ugi-modified Trastuzumab conjugate **R154** was next sent for analysis by LC-MS/MS to determine which sites had been modified. Interestingly, the expected *inter-residue* Ugi adduct between a lysine – K126 – and a carboxylate-containing amino acid – either D122 or E123 (undistinguishable) – was detected. However, a few other sites were also identified, whose conjugation resulted from side reactions; either through the Passerini reaction, resulting in single-residue modification of aspartate/glutamate, or through an unexpected *intra-residue* Ugi reaction between the *N*-terminal *α*-amine and the carboxylate side chains of both E1 and D1 (**Scheme 67**).[210]

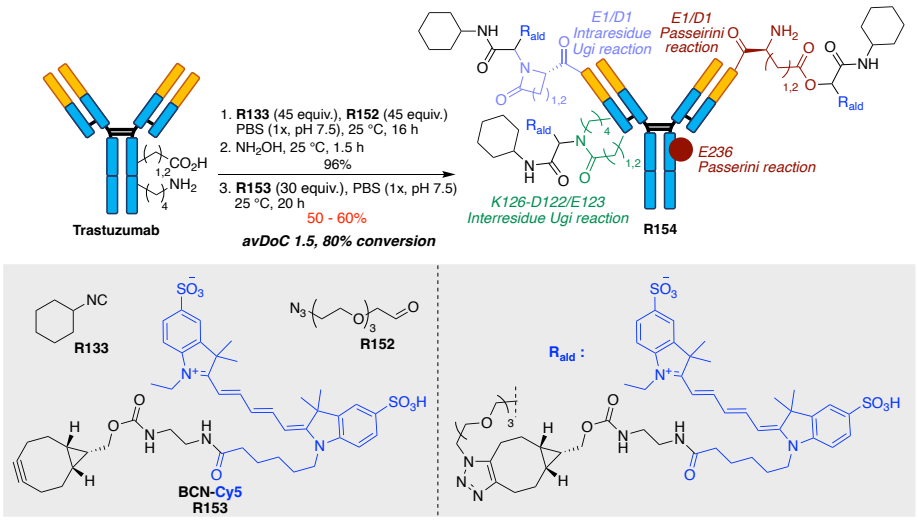

Scheme 67. Ugi reaction on Trastuzumab with the incorporation of cHexNC **R133** and N_3PEG_3CHO **R152**, followed by SPAAC functionalization with BCN-Cy5 **R153** and schematic representation of the various modification sites obtained *via* different reaction mechanisms.[210]

Even though four conjugation sites ended up being detected under the conditions employed, far from the site-selectivity that was initially envisioned, this unexpected *N*-terminus reactivity urged us to carry on this work. We delved into an in-depth study of this transformation, in the hope of identifying key parameters that could favor this intra-residue reaction. In order to do so, my work was based on the following procedure: Trastuzumab conjugates would first be produced through multicomponent conjugation with varying parameters (i.e., nature of reagents, pH, temperature, reaction time, concentration of reagents) before being analyzed by native mass spectrometry and LC-MS/MS, to determine the influence of the studied parameter on the identity of the conjugation site.

3.5. Towards Site-Selective Conditions

3.5.1. SPAAC reaction optimization

This methodology work began by selecting our previously developed conditions – i.e., Trastuzumab (67 µM), aldehyde **R152** (45 equiv.), cyclohexyl isocyanide **R133** (45 equiv.), DMSO / PBS 1X (7:93, v/v), pH 7.5, 25 °C, 16 h, followed by hydroxylamine treatment at 25 °C for 1.5 h to cleave remaining imines – in order to validate the repeatability and reproducibility of the initial results. However, since mediocre yields (50% - 65%) were observed with BCN-Cy5 **R153** during the SPAAC step, due to precipitation of the resulting conjugates attributed to the hydrophobic nature of the cyanine-5 fluorophore (Cy5), our first decision was to opt for a more hydrophilic strained alkyne. Indeed, as both the conversion and avDoC values should only depend on the first conjugation step, any precipitation at the SPAAC stage will inevitably lead to a loss of information about the exact nature and number of conjugation sites and thus to a lack of repeatability. Thus, BCN-Iminobiotin **R74** was selected as our new SPAAC partner, due to its less hydrophobic character, and we were pleased to notice the absence of precipitation in all repeated and reproduced reactions with yields > 95%. Native MS analysis showed an avDoC of 1.1 and 70% conversion with overall yield over 98% in all cases, while peptide mapping studies revealed two inter-residue Ugi reactions (K65-D62 / K277-E275) and a Passerini and an intra-residue Ugi on both *N*-terminal E1 and D1 (see experimental section for MS spectra and peptide mapping results; *pages 125 - 127*). Similar results with this exact set of conditions were obtained by my colleague, Ms Valentine Vaur, who repeated this reaction, and got almost identical results (avDoC 1.0, 64% conversion and the exact same modification sites). Even though small discrepancies were found between these experiments with the one conducted (**Figure 11**) by Dr Sornay, *N*-terminal Passerini- and Ugi-modified E1 and D1 residues were systematically detected. While this could indicate a lack of reproducibility, we hypothesized that this could also be credited to the fact that inter-residue U-4C-3CR accounts for only a small fraction of all conjugation sites, leading to fluctuating detection.

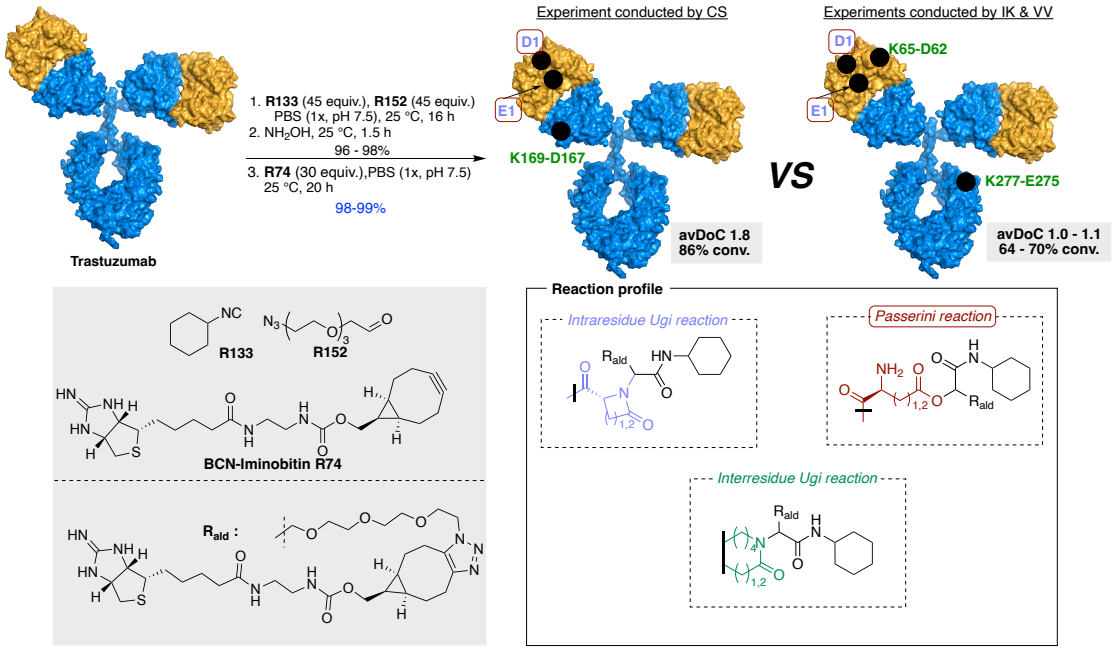

Figure 11. Ugi reaction on Trastuzumab followed by functionalization with BCN-Iminobiotin **R74**. Reaction conditions: 1. Trastuzumab (67 µM), cHexNC **R133** (45 equiv.), N_3PEG_3CHO **R152** (45 equiv.), DMSO / PBS 1X (7:93, v/v), pH 7.5, 25 °C, 16 h; 2. NH_2OH**,** 25 °, 1.5 h; 3. BCN-Iminobiotin **R74** (30 equiv.), PBS 1X, pH 7.5, 25 °C, 20 h. On the left hand-side products' figure, the 3D structure – obtained by Pymol – of Trastuzumab is illustrated, demonstrating the exact sites of modification, after its Ugi reaction with the afore-mentioned conditions conducted by Charlotte Sornay (CS), identified *via* LC-MS/MS. On the right hand-side products' figure, the modification sites from the same experiment conducted by myself (IK) and Valentine Vaur (VV) are displayed. On E1/D1, both intra-residue Ugi and Passerini reactions were detected. On K65-D62, K169-D167 & K277-E275 the inter-residue Ugi reaction was detected.

3.5.2. Reaction conditions optimization

Intrigued by these results, we were engaged into an in-depth methodology work. Preliminary kinetic studies, conducted by Dr Charlotte Sornay, revealed that both Passerini and Ugi reactions already occur after just 1 h of reaction at both *N*-terminal amino acids (E1 & D1), while the inter-residue Ugi reaction between spatial close lysine and aspartate/glutamate residues necessitated at least 8 h before it could be detected (**Chart 1**) (see experimental section for nMS analysis; *page 119*).

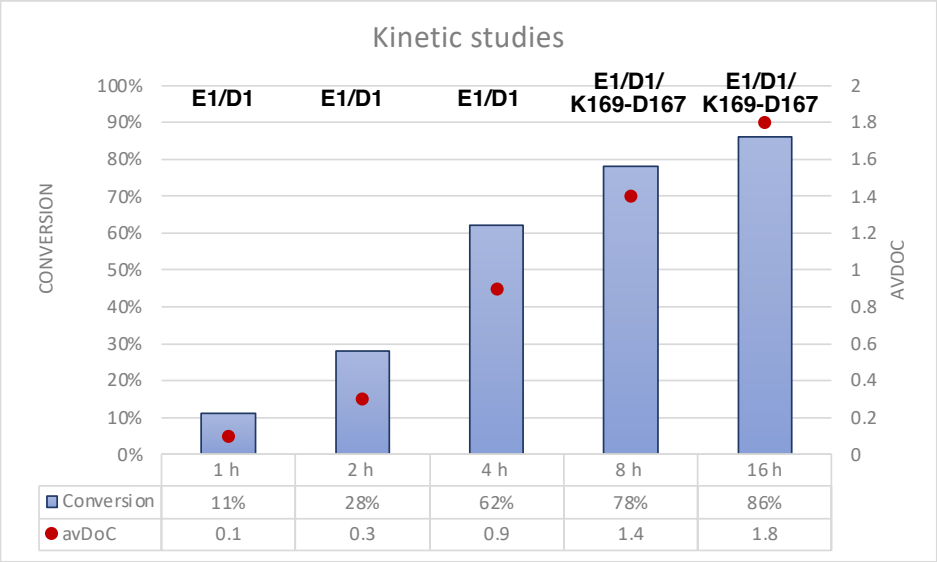

Chart 1. Kinetic studies evaluation over 16 h. Conversion (blue bars) and avDoC (red dots) values were obtained *via* nMS. The exact conjugation sites (letters in black) were determined *via* LC-MS/MS studies. Reaction conditions: 1. Trastuzumab (67 µM), cHexNC **R133** (45 equiv.), N_3PEG_3CHO **R152** (45 equiv.), DMSO / PBS 1X (7:93, v/v), pH 7.5, 25 °C, *time*; 2. NH_2OH, 25 °, 1.5 h; 3. BCN-Iminobiotin **R74** (30 equiv.), PBS 1X, pH 7.5, 25 °C, 20 h.

In this context and inspired by the fact that *N*-terminal conjugation could be favored by variations in pH due to the difference in pK_a between *α*- and *ε*-amines, we then studied its influence on the outcome of the conjugation. Surprisingly, little to no change was detected between all experiments: almost identical conversion and avDoC were obtained, with a maintained *N*-terminal selectivity (**Chart 2**) (see experimental section for nMS analysis; *page 120*). While this demonstrates that the intra-residue U-4C-3CR occurs preferentially over its inter-residue variant with this combination of reagents, competition with Passerini reaction could not be suppressed.

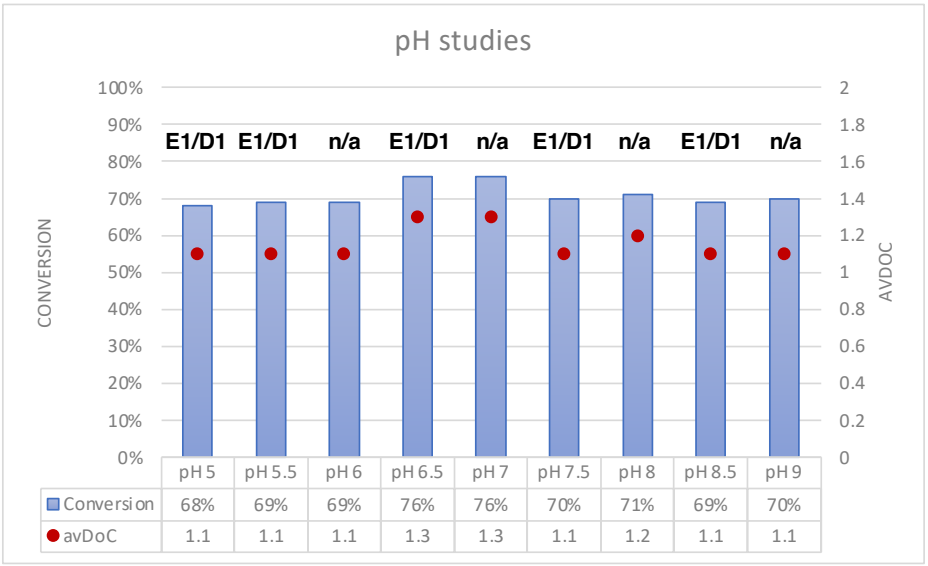

Chart 2. pH studies evaluation in a range from pH 5.5 to pH 9.0. Conversion (blue bars) and avDoC (red dots) values were obtained *via* nMS. The exact conjugation sites (letters in black color) were determined *via* LC-MS/MS studies. Reaction conditions: 1. Trastuzumab (67 μM), cHexNC **R133** (45 equiv.), N_3PEG_3CHO **R152** (45 equiv.), DMSO / PBS 1X (7:93, v/v), *pH*, 25 °C, 16 h; 2. NH_2OH, 25 °, 1.5 h; 3. BCN-Iminobiotin **R74** (30 equiv.), PBS 1X, pH 7.5, 25 °C, 20 h. N/A stands for experiments that were not analyzed *via* LC-MS/MS.

These data suggest that the Ugi reaction with this set of conditions is limited to the Fab region of the antibody. This can be further confirmed by working with the $(Fab')_2$ fragment of Trastuzumab, produced *via* pepsin digestion, which led to similar conversion and avDoC values (avDoC 1.6, 86% conversion) as those observed with the whole antibody under the same conditions. More specifically, peptide mapping analyses revealed three inter-residue Ugi reactions (K65-D62 / K126-D122(E123) / K169-E165(D167/D170)), as well as a competition between a Passerini and an intra-residue Ugi on both E1 and D1 residues (**Figure 12**).

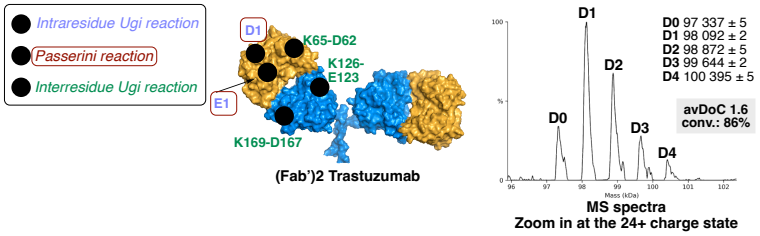

Figure 12. On the 3D figure of $(Fab')_2$ Trastuzumab the conjugation sites, obtained by LC-MS/MS studies, are illustrated. The avDoC and conversion values were obtained *via* nMS. Reaction conditions: 1. $(Fab')_2$ Trastuzumab (67 μM), cHexNC **R133** (45 equiv.), N_3PEG_3CHO **R152** (45 equiv.), DMSO / PBS 1X (7:93, v/v), pH, 25 °C, 16 h; 2. NH_2OH, 25 °, 1.5 h; 3. BCN-Iminobiotin **R74** (30 equiv.), PBS 1X, pH 7.5, 25 °C, 20 h.

3.5.3. Investigation of the aldehyde's and isocyanide's scope

Pursuing this methodology effort, we next varied the structure and identity of both the carbonyl and isocyanide components. On the one hand, two different aldehydes; **R152** and **R155**, were evaluated in combination with bis-isocyanide **R158** (entries **1** & **2**, **Table 3**). While stark variations in conversion and avDoC were seen between these experiments, it also led to more diverse Passerini adducts as evidenced by peptide mapping studies. Interestingly, though, isobutyraldehyde **R155** led again to *N*-terminal selective conjugation, with excellent conversion demonstrating the *N*-terminal selectivity of our approach. Unfortunately, in an effort to improve these conditions by incorporating an azide group onto the isocyanide (isocyanides **R159** and **R160**) to restore a plug-and-play strategy, we noticed that even the slightest structural change had a detrimental effect on either the efficiency or the selectivity of the reaction (entries **3** & **4**, **Table 3**) (see experimental section for nMS analysis; *pages 121 - 122*).

On the other hand, varying the isocyanide component while keeping aldehyde **R152** as a carbonyl source resulted this time in clear fluctuations in the Ugi sites but in Passerini adducts essentially restricted to *N*-terminal glutamate and aspartate residues. Of the three commercially available isocyanides evaluated, ethyl isocyanoacetate **R157** (entry **8**, **Table 3**). was the only one showing an outstanding single-residue selectivity, with the sole modification of E1. Even more remarkable, this was accompanied by an absence of Passerini side reaction, making these conditions not only site- and residue-selective but also "mechanism selective", favouring only the Ugi reaction over the Passerini (see experimental section for nMS and LC-MS/MS analysis, *page 128*).

In an attempt to push the conversion further, we also evaluated the impact of an increased concentration in either the antibody or in both carbonyl and isocyanide. On the one hand, increasing the temperature to 37 °C (entry **9**, **Table 3**) or the number of equiv. of both aldehyde **R152** and ethyl isocyanoacetate **R157** to 75:75 (entry **11**, **Table 3**) resulted in an almost complete conversion but at the expense of site-selectivity; on the other hand, switching from 67 to 102 µM of Trastuzumab successfully resulted in an increased conversion (83%) with avDoC 1.8 and a maintained *N*-terminal selectivity (entry **10**, **Table 3**). Any further attempt at increasing both protein's concentration or reagents' equiv. with simultaneous decrease of incubation time in order to accelerate the reaction, resulted in non-selective U-4C-3CR and lower conversions.

Table 3. Summary of methodology studies for the Ugi reaction towards site-selectivity (in blue) starting from selected set of conditions (in orange), evaluating both the aldehyde and the isocyanide scope. Standard conditions: 1. Trastuzumab (67 µM), isocyanide / aldehyde (45/45 equiv.), DMSO / PBS 1X (7:93, v/v), pH 7.5, 25 °C, 16 h; 2. NH_2OH, 25 °C, 1.5 h; 3. BCN-Iminobiotin **R74** (30 equiv.), PBS 1X, pH 7.5, 25 °C, 20 h.

	Methodology studies			nMS results		Conjugation sites	
Entry	**Variable parameter**	**Aldehyde**	**Isocyanide**	**avDoC**	**Conversion**	**Ugi**	**Passerini**
1	-	Isobutyraldehyde **R155**	bisNC **R158**	1.6	84%	E1	E1/D1
2	-	PEG-N_3 **R152**	bisNC **R158**	0.5	44%	E1	E1/D1
3	-	Isobutyraldehyde **R155**	**R159**	0.8	54%	E1	E1/D1
4	-	Isobutyraldehyde **R155**	**R160**	0.9	59%	E1	E1/D1/D224/D185(E187)
5	-	PEG-N_3 **R152**	cHexNC **R133**	1.1	70%	E1/D1/K65-D62/K277-E275	E1 / D1
6	-	PEG-N_3 **R152**	*i*PrNC **R156**	1.3	81%	E1/D1/K65-D62/ K169-E165(D167/D170)	E1 / D1
7	-	PEG-N_3 **R152**	*t*BuNC **R142**	0.8	52%	E1/D1	E1
8	-	PEG-N_3 **R152**	EtOAcNC **R157**	1.2	69%	E1	-
9	37 °C	PEG-N_3 **R152**	EtOAcNC **R157**	2.5	91%	n/a	n/a
10	102 µM	PEG-N_3 **R152**	EtOAcNC **R157**	1.8	83%	E1	E1/D1
11	75/75 equiv.	PEG-N_3 **R152**	EtOAcNC **R157**	2.5	91%	E1/K65-D62/E275-K277	E1/D1/E6
12	102 µM; Time: 2 h; 100/100 equiv.	PEG-N_3 **R152**	EtOAcNC **R157**	0.5	33%	E1/K65-D62/E275-K277	E1/D1
13	102 µM; Time: 4 h; 100/100 equiv.	PEG-N_3 **R152**	EtOAcNC **R157**	1.2	73%	E1/K65-D62/E275-K277	E1/D1/E6

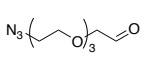
PEG-N_3 R152


isobutyraldehyde R155


cHexNC R133


***i*PrNC R156**


***t*BuNC R142**

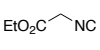
EtOAcNC R157


bisNC R158

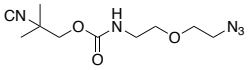
R159

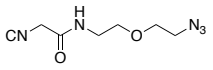
R160

To sum up, two set of effective conjugation conditions were developed, mostly by varying the isocyanide source. The first ones (standard conditions) led to *N*-terminal conjugation by the simultaneous modification of both E1 & D1 *via* both an intra-residue Ugi and a Passerini reaction even though an inter-residue Ugi reaction could sometimes be observed mostly on the $(Fab')_2$ region of Trastuzumab (entry **5**, **Table 3**). The other ones (optimal conditions) led to exclusive E1 modification *via* only an intra-residue Ugi reaction (entry **8**, **Table 3**), a remarkable feature considering the simplicity of our method and its low cost. (**Figure 13**)

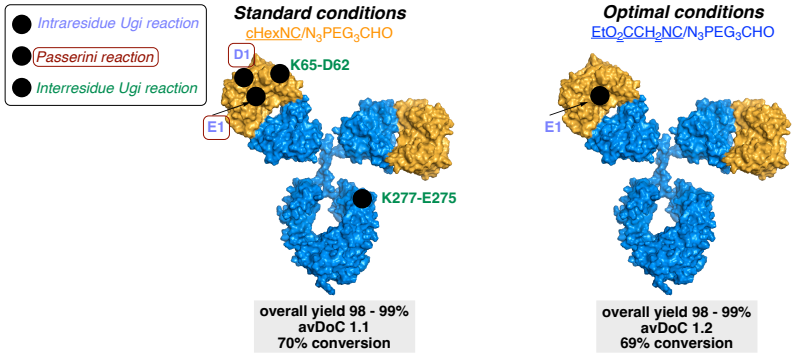

Figure 13. Summary of the established two set of conditions of our (U-3C-4CR) approach on Trastuzumab.

3.6. CONSTRUCTION OF A REGIO-SELECTIVE ADC

Having confirmed by extensive peptide mapping studies the excellent regio-selectivity offered by our Ugi approach, we decided to apply it to the construction of an ADC bearing the cytotoxic maytansine derivative DM1, which would be seen as a site-selective analogue of Kadcyla. This marketed ADC is used to treat $HER2^+$ breast cancer, and is composed of Trastuzumab, covalently linked to DM1 *via* a maleimidomethyl cyclohexane-1-carboxylate (MCC) non-cleavable linker. This linker bears an activated NHS ester on its carboxylate end, ensuring an amine-selective conjugation, yet highly heterogeneous: Wang *et al.* showed that a commercial sample of Kadcyla comprised ~4.5 million different conjugate species for an avDAR of 3.5,[211] all with different pharmacokinetic properties, an enormous limitation that our site-selective approach could help to address.

First, we focused our attention on the attachment of a strained alkyne handle on the DM1 cytotoxic drug that would allow a SPAAC between the azide-bearing group of our Ugi-modified Trastuzumab. In this perspective, we started from commercially available DM1-SMCC **R164** and reacted it with a BCN-amine **R163** – accessed *via* a 2-step procedure starting from **R161**; a strained-alkyne scaffold previously developed in our group –,[212] to furnish BCN-DM1 **R165** in excellent yield (**Scheme 68**).

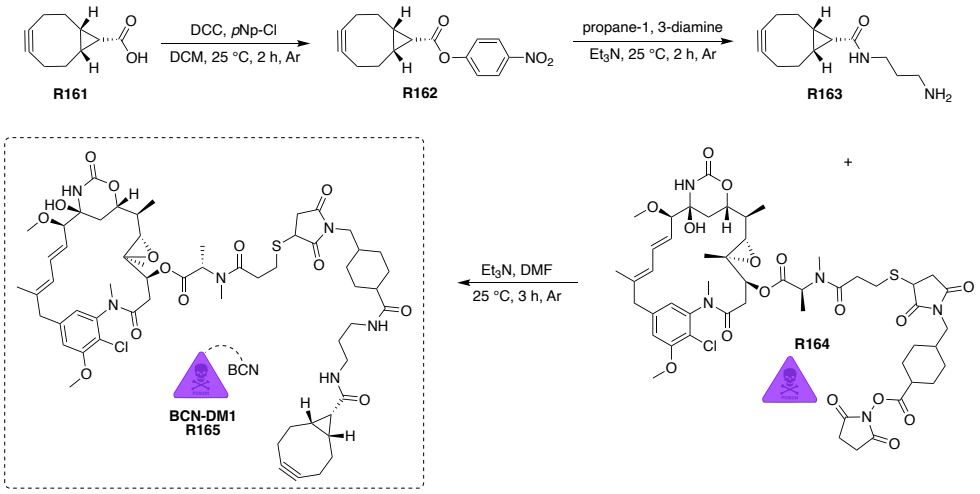

Scheme 68. Synthetic procedure to access BCN-DM1 **R165**.

Following our recently developed optimal conditions – i.e., 1) Trastuzumab (67 µM), EtO_2CCH_2NC **R157** (45 equiv.), N_3PEG_3CHO **R152** (45 equiv.), DMSO / PBS 1X (7:93, v/v), pH 7.5, 25 °C, 16 h; 2) NH_2OH, 25 °C, 1.5 h –, we site-selectively modified *N*-terminal E1 residues *via* an intra-residue Ugi reaction, installing an azide functional handle. We next engaged in a short optimization of the SPPAC step between the latter and BCN-DM1, which is poorly soluble, due to the hydrophobic character of DM1, thus leading to incomplete SPAAC.

We finally managed to construct the desired ADC, accessed in 75% yield, 66% conversion and with an avDoC of 1.1 according to nMS analysis. However, another set of peaks was also detected next to each of the peaks corresponding to D0, D1 and D2 species, indicating the presence of subspecies with a mass increment of 544 Da (**Scheme 69B**). This was attributed to a fragmentation of the linker, which was further confirmed by the analysis of **R165** alone by the Cianferani group, highlighting the amide bond next to the cHex ring as the fragmentation site.

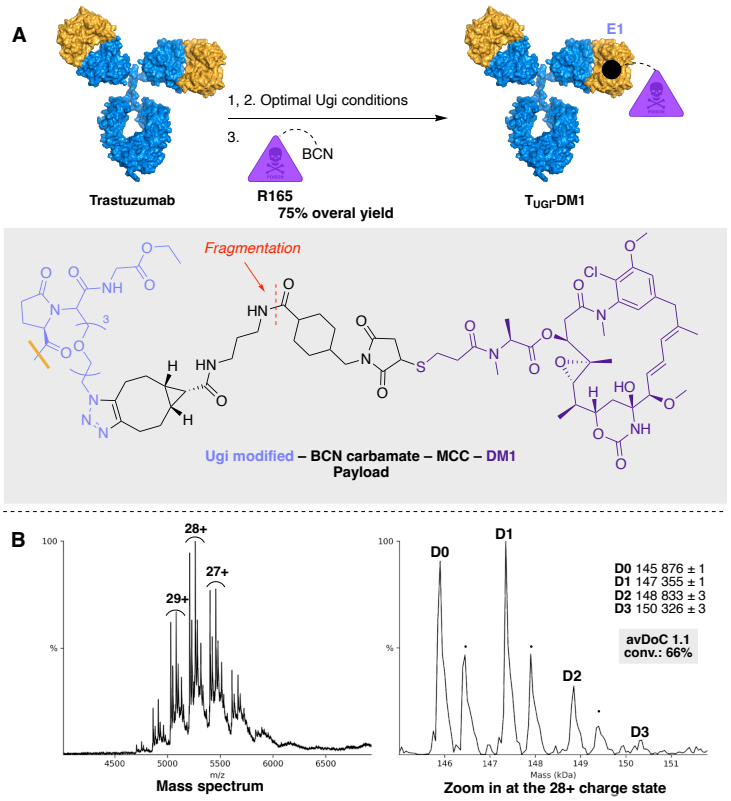

Scheme 69. A) Site-selective ADC **T_{UGI}-DM1**. B) MS deconvoluted spectra of **T_{UGI}-DM1**. The black dots correspond to payload fragmentation. **Optimal Ugi Conditions:** 1. Trastuzumab (67 µM), EtO_2CCH_2NC **R157** (45 equiv.), N_3PEG_3CHO **R152** (45 equiv.), DMSO / PBS 1X (7:93, v/v), pH 7.5, 25 °C, 16 h; 2. NH_2OH, 25 °C, 1.5 h. **SPAAC:** 3. **BCN-DM1** (30 equiv.), PBS 1X, pH 7.5, 37 °C, 48 h, 1 100 rpm constant agitation.

As previously mentioned, this ADC was tested in cell viability assays on both HER2-positive and HER2-negative cell lines (i.e., SKBR-3 and MDA-MB-231, respectively) against the marketed ADC Kadcyla.[213] Despite a 3-fold difference in avDAR, our ADC **T_{Ugi}-DM1** showed a potency comparable to that of Kadcyla, with a subnanomolar toxicity on SKBR-3 cell line (i.e., IC_{50} = 0.9 nM on SKBR-3 *vs* 0.11 nM for Kadcyla), three orders of magnitude higher than that observed on MDA-MB-231 (i.e., IC_{50} = 149.1 nM *vs* 123.8 nM for Kadcyla), as illustrated in **Table 4**.

Table 4. Cytotoxic studies revealing the IC_{50} values of ADCs **T_{UGI}-DM1** and **Kadcyla®** in SKBR-3 and MDA-MB-231 cancer cell lines**.**

		Cell based cytotoxicity IC_{50}	
ADC	**avDAR**	**SKBR3 (HER2 +)**	**MD-MB-231(HER2 -)**
T_{UGI}-DM1	1.1	0.9 nM	149.1 nM
Kadcyla®	3.8	0.1 nM	123.8 nM

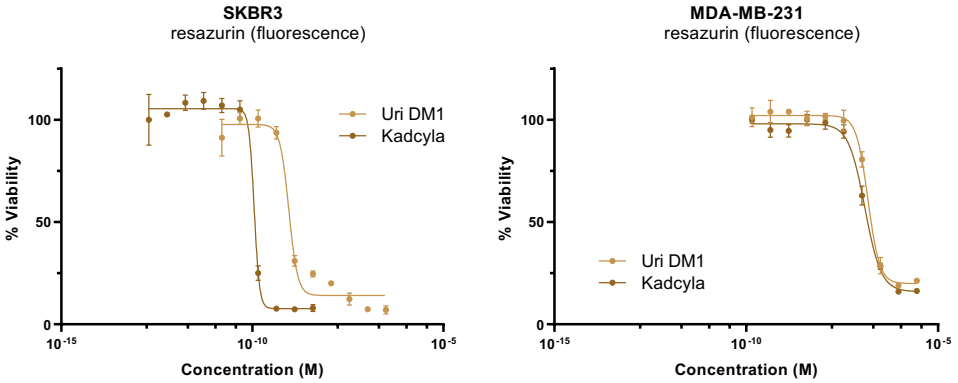

3.7. UGI REACTION ON VARIOUS MAB SOURCES

Having demonstrated that our newly developed site-selective conjugation strategy could lead to valuable Trastuzumab conjugates, we finally concluded our in-depth study by evaluating its application to other proteins. Selecting mAbs with *N*-terminal D1 and E1 – i.e., Bevacizumab and Ramucirumab –, we assessed both our standard and optimal conditions (entries **5** & **8**, respectively, **Table 3**) and found similar results (**Figure 14**). Using cyclohexyl isocyanide **R133** and aldehyde **R152**, Bevacizumab reacted in an almost identical manner as Trastuzumab, which also translated in comparable modification sites. Using the same reagent combination, Ramucirumab conjugation found to be more sluggish but still proceeded with high site-selectivity. Switching to a combination of ethyl isocyanoacetate **R157** and aldehyde **R152** gave *N*-terminal selectivity in all cases, in perfect coherence with what had been previously observed on Trastuzumab. It is also worth stressing at this stage that the use of other biosimilars than Herceptin, such as Ontruzant, had impact on neither the efficiency nor the identity of the conjugation sites. Our conjugation strategy proved also to be tolerant to mAbs deprived of *N*-terminal carboxylates. Rituximab (*N*-ter Q1 on both chains) was successfully conjugated with excellent conversion and avDoC under standard conditions. Peptide mapping studies highlighted two inter-residue Ugi conjugation sites – i.e., K278-E276 and K169-E165 – along with one Passerini site – i.e., E165 –, all of which having been previously detected on other mAbs during the course of this work, suggesting that multicomponent reaction conjugation tends to work only on a handful of hot-spot reactive sites (**Figure 14**; see experimental section for nMS spectra and LC-MS/MS studies, *pages 123 – 124*).

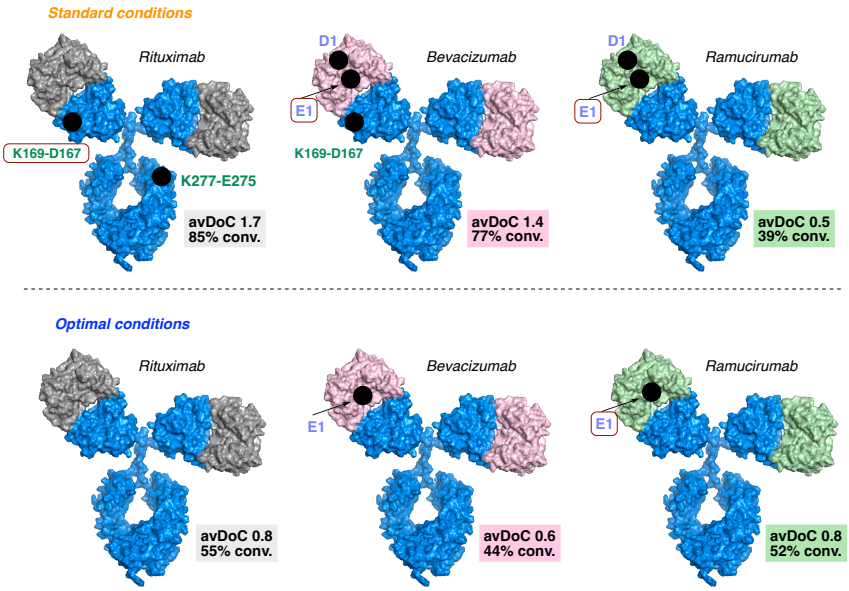

Figure 14. On the 3D figure of each mAb, the conjugation sites, obtained *via* LC-MS/MS studies, are illustrated. Green color indicates that an inter-residue Ugi reaction takes place. Purple color indicates that an intra-residue Ugi reaction takes place. Red circle indicates that a Passerini reaction takes place. The avDoC and conversion values were obtained *via* nMS.

Standard conditions*:** mAb (67 µM), cHexNC **R133** (45 equiv.), N_3PEG_3CHO **R152** (45 equiv.), DMSO / PBS 1X (7:93, v/v), pH 7.5, 25 °C, 16 h; 2. NH_2OH, 25 °C, 1.5 h; 3. BCN-Iminobiotin **R74** (30 equiv.), PBS 1X, pH 7.5, 25 °C, 20 h. ***Optimal conditions: mAb (67 µM), EtO_2CCH_2NC **R157** (45 equiv.), N_3PEG_3CHO **R152** (45 equiv.), DMSO / PBS 1X (7:93, v/v), pH 7.5, 25 °C, 16 h; 2. NH_2OH, 25 °C, 1.5 h; 3. BCN-Iminobiotin **R74** (30 equiv.), PBS 1X, pH 7.5, 25 °C, 20 h.

3.8. UGI REACTION ON NATIVE PROTEINS

While mAbs gave excellent results, we were surprised to notice that several other smaller proteins proved to be unreactive under the same conditions. Indeed, in spite of all our efforts, none of the following proteins led to noticeable conjugation: albumin (neither bovine nor human), *α*-chymotrypsin, myoglobin, lysozyme, ubiquitin. In most if not all cases, the unconjugated protein proved to be the major species detected by nMS, sometimes accompanied with small amounts of higher molecular-weight species whose masses did not match that of the expected adducts (**Figure 15**).

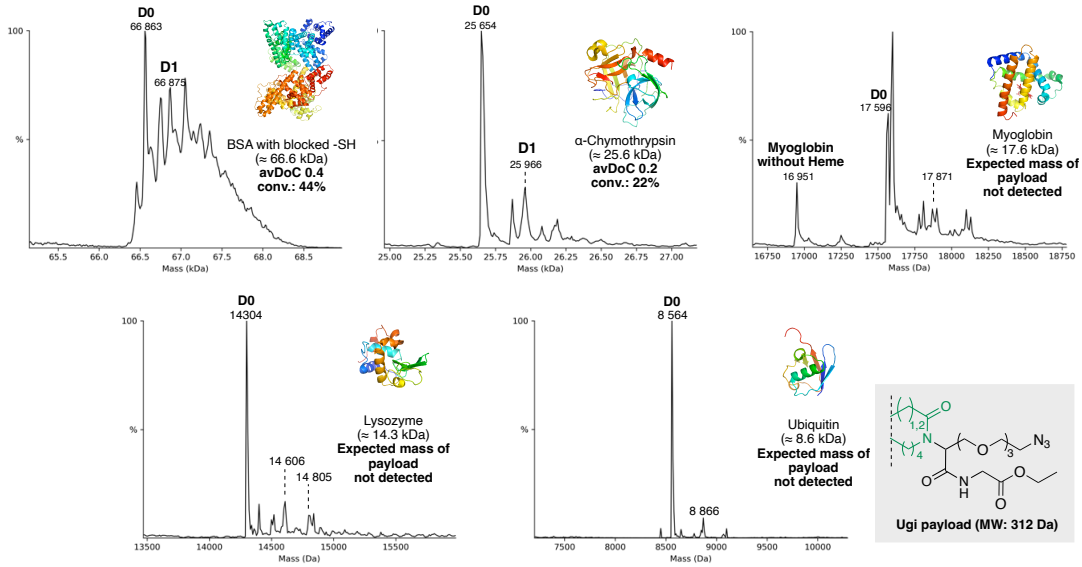

Figure 15. Native MS of various native proteins treated with Ugi reaction. Conditions: 1. 67 µM protein, EtO_2CCH_2NC **R157** (45 equiv.), N_3PEG_3CHO **R152** (45 equiv.), DMSO / PBS 1X (7:93, v/v), pH 7.5, 25 °C, 16 h; 2. NH_2OH, 25 C, 1.5 h.

With these results in hands and considering that some proteins were more prone to conjugation than others, we evaluated the protein-selectivity potential of our approach, that is its ability to conjugate selectively one protein in a mixture of several. Thus, Trastuzumab was mixed with BSA, *α*-chymothrypsin, and lysozyme, all proteins being at the same concentration of 67 µM. This mixture was incubated with 45 equiv. of both **R152** and **R157** in PBS (1X, pH 7.5) for 16 h at 25 °C, before undergoing the same steps as previously described: incubation with hydroxylamine and SPAAC with DBCO-OEG-TAMRA **R75** for 20 h at 25 °C. The fluorescent conjugated species were analyzed by SDS-PAGE (**Figure 16**), which showed that Trastuzumab and BSA had been strongly labelled in all cases, even though all proteins could be more or less detected. This is in coherence with what had been observed before on isolated protein, where conjugation could be detected on almost all proteins, even though it was only partial and extremely limited. Altogether, these results suggest that protein selectivity cannot be achieved with our strategy under the conditions employed, and that Trastuzumab,

despite leading to excellent conversion and avDoC, cannot outcompete other proteins for conjugation.

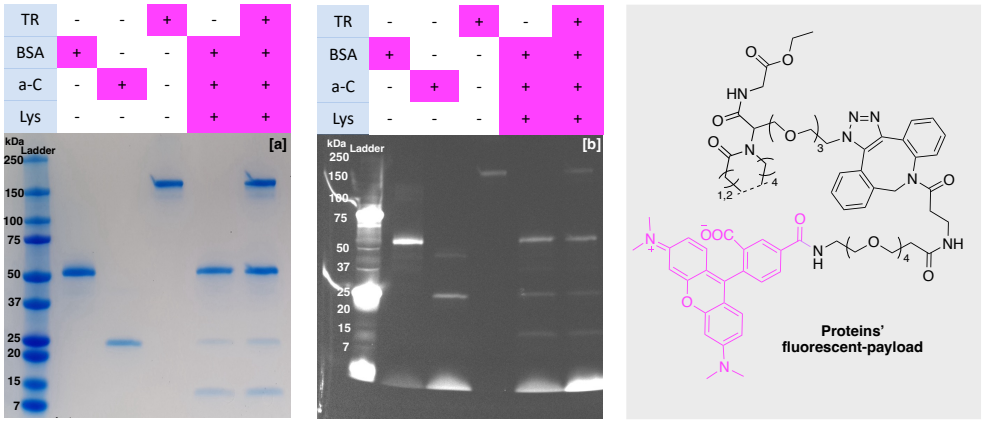

Figure 16. Application of the Ugi reaction in a mixture of four proteins – Trastuzumab, BSA, α-chymothrypsin and lysozyme. Reaction conditions: 1. EtO_2CCH_2NC **R157** (45 equiv.), N_3PEG_3CHO **R152** (45 equiv.), PBS (1X, pH 7.5), 25 °C, 16 h; 2. NH_2OH**,** 25 °C, 1.5 h; 3. DBCO-OEG-TAMRA **R75** (30 equiv.), PBS 1X, pH 7.5, 25 °C, 20 h. On the grey bracket the payload of each protein is demonstrated. The samples were analyzed by SDS-PAGE (0.2 mg/mL concentration of proteins). The gel was revealed by [a] Coomassie blue and [b] fluorescence.

3.9. UGI REACTION ON ANTICALINS

While disappointing on many proteins besides antibodies, we were delighted to notice that our multicomponent conjugation reaction could be successfully applied to anticalin proteins.[214] Anticalins are alternative binding proteins derived from the human lipocalins, which are abundant in plasma and responsible for the transportation of small hydrophobic molecules, and have been extensively studied as binding proteins in the field of oncology and diagnostics.[215] For this work, we employed a recently developed anticalin directed against the human transmembrane glycoprotein CD98hc, dubbed D11vs,[216] which was handed to us thanks to an internal collaboration in the ITN with Pr Arne Skerra at the TUM (*v. supra)*. After an extensive optimization study – varying the nature of reagents, number of equiv., pH, temperature, concentration, and buffer (**Table 5**) –, D11vs led to full conversion and avDoC 1.3 under our optimal conditions, using aldehyde **R152** and cyclohexyl isocyanide **R133**, albeit in a 35:35 equiv. ratio to minimize over-conjugation (entry **3**, **Table 5**). Peptide mapping studies led to the identification of only two conjugation sites: the Passerini-modified D2 (or D6) and the U-4C-3CR between K46 and E44 (or D45 or D47, undistinguishable from each other) residues. Lowering the concentration in anticalins with simultaneous decrease in the number of equiv. of both reagents to 25:25 ratio allowed to maximize single conjugation but at the expense of a partial, yet excellent, conversion, typically ~90%. Batch-to-batch reproducibility was once again demonstrated as well as consistency in peptide mapping results, with the same conjugation sites being detected in triplicate experiments performed on two different batches of D11vs.

Table 5. Conditions optimization for Anticalin D11vs-Strep. In red the altered parameter is highlighted. In blue the optimal conditions are illustrated.

Entry	Anticalin	Conditions	Yield	avDoC	Conversion
1	D11vs, 188 µM	PBS, pH 7.4, 35/35 equiv. EtO_2CCH_2NC-N_3PEG_3CHO, 16 h, 25 °C	82%	1.6	74%
2	D11vs, 188 µM	BBS, pH 8, 2 mM EDTA, 35/35 equiv. cHexNC-N_3PEG_3CHO, 16 h, 25 °C	71%	2.4	98%
3	D11vs, 188 µM	PBS, pH 7.4, 35/35 equiv. cHexNC-N_3PEG_3CHO, 16 h, 25 °C	65%	1.3	100%
4	D11vs, 188 µM	PBS, pH 6.5, 35/35 equiv. cHexNC-N_3PEG_3CHO, 16 h, 25 °C	72%	1.7	91%
5	D11vs, 188 µM	PBS, pH 8.5, 35/35 equiv. cHexNC-N_3PEG_3CHO, 16 h, 25 °C	61%	2.2	98%
6	D11vs, 94 µM	PBS, pH 7.4, 35/35 equiv. cHexNC-N_3PEG_3CHO, 16 h, 25 °C	57%	1.1	95%
7	D11vs, 188 µM	PBS, pH 7.4, 25/25 equiv. cHexNC-N_3PEG_3CHO, 16 h, 25 °C	62%	1.8	97%
8	D11vs, 188 µM	PBS, pH 7.4, 35/35 equiv. cHexNC-N_3PEG_3CHO, 16 h, 20 °C	61%	2.1	96%
9	D11vs, 188 µM	PB 50 mM, pH 7.4, 35/35 equiv. cHexNC-N_3PEG_3CHO, 16 h, 25 °C	62%	2	93%
10	D11vs, 188 µM	Conjugation buffer (40 mM PB, 20 mM NaCl, 6 mM EDTA), pH 7.4, 35/35 equiv. cHexNC-N_3PEG_3CHO, 16 h, 25 °C	72%	1.9	94%
11	D11vs, 188 µM	BBS, pH 7.4, 35/35 equiv. cHexNC-N_3PEG_3CHO, 16 h, 25 °C	62%	2.1	97%
12	D11vs, 94 µM	PBS, pH 7.4, 25/25 equiv. cHexNC-N_3PEG_3CHO, 16 h, 25 °C	77%	1.1	91%
13	D11vs, 94 µM	PBS, pH 7.4, 25/25 equiv. cHexNC-N_3PEG_3CHO, 16 h, 37 °C	74%	1	85%
14	D11vs, 70 µM	PBS, pH 7.4, 25/25 equiv. cHexNC-N_3PEG_3CHO, 16 h, 25 °C	82%	1	85%
15	D11vs, 70 µM	PBS, pH 7.4, 25/25 equiv. cHexNC-N_3PEG_3CHO, 16 h, 37 °C	79%	0.9	82%
16	D11vs, 94 µM	PBS, pH 7.4, 25/25 equiv. EtO_2CCH_2NC-N_3PEG_3CHO, 16 h, 25 °C	79%	0.4	36%
17	D11vs, 94 µM	PBS, pH 7.4, 25/25 equiv. *tBu*NC-N_3PEG_3CHO, 16 h, 25 °C	83%	0.4	34%
18	D11vs, 94 µM	PBS, pH 7.4, 25/25 equiv. BnNC-N_3PEG_3CHO, 16 h, 25 °C	67%	0.8	74%
19	D11vs, 94 µM	PBS, pH 7.4, 25/25 equiv. cHexNC-N_3PEG_3CHO, 16 h, 25 °C	75%	1.1	90%
20	**D11vs(NΔ6)**, 94 µM	PBS, pH 7.4, 25/25 equiv. cHexNC-N_3PEG_3CHO, 16 h, 25 °C	65%	1.1	87%
21	**D11vs(K46R)**, 94 µM	PBS, pH 7.4, 25/25 equiv. cHexNC-N_3PEG_3CHO, 16 h, 25 °C	78%	0.5	42%
22	**D11vs(NΔ6/K46R)**, 94 µM	PBS, pH 7.4, 25/25 equiv. cHexNC-N_3PEG_3CHO, 16 h, 25 °C	76%	0.2	16%

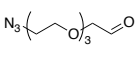

PEG-N_3
R152

BnNC
R166

cHexNC
R133

***t*BuNC**
R142

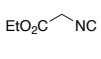

EtOAcNC
R157

In an attempt to further validate these results, our collaborators produced three D11vs mutants: **D11vs(NΔ6)**, with a truncated *N*-terminal region, deprived of D2 and D6 residues; **D11vs(K46R)**, where the key lysine residue had been replaced with an arginine, which should not participate in a U-4C-3CR while maintaining a positive charge in this crucial region; **D11vs(NΔ6/K46R)**, the double mutant featuring both alterations. Interestingly, **D11vs(NΔ6)** led to a similar conjugation profile, with the inter-residue Ugi conjugation being the sole site identified by peptide mapping. This would tend to show that the Passerini reaction is rather marginal in comparison with the U-4C-3CR, or at least occurs at a slowest rate, a hypothesis further reinforced by the limited conjugation observed with the K46R mutant. The high degree of site-selectivity of our method was evidenced when conjugation was barely detected on the double mutant anticalin **D11vs(NΔ6/K46R)**, lacking the two reactive sites previously identified on its parent analogue (see experimental section for nMS spectra and LC-MS/MS studies, *pages 129 – 131*).

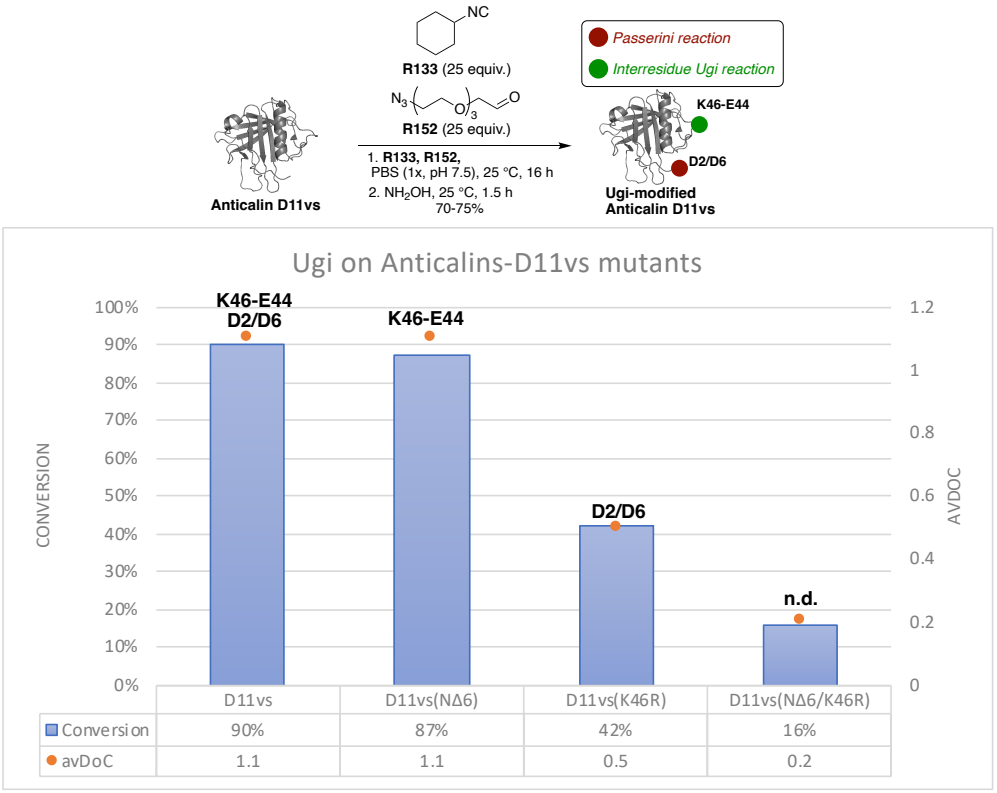

Chart 3. Ugi reaction using the set of standard conditions on Anticalin D11vs and its mutants. Conversion (blue bars) and avDoC (orange dots) values were obtained *via* nMS. The exact conjugation sites (letters in black color) were determined *via* LC-MS/MS studies.

3.10. CONCLUSIONS

In conclusion to this extensive methodology work, all conjugation parameters of the previously developed Ugi conjugation reaction were varied in order to study their impact on the selectivity of this approach on several proteins. We proved that mAbs responded well to this approach, with a handful of key reactive sites being systematically detected. Importantly, we managed to refine some conditions to allow the selective *N*-terminal conjugation of aspartate and glutamate residues, culminating in the precise modification of a single site through an intra-residue U-4C-3CR when commercial ethyl isocyanoacetate was used. Hence, we ended up with two different sets of conditions that we next attempted to apply to various proteins. Nevertheless, when either of these conditions were applied on other native proteins – albumin (either bovine or human), *α*-chymotrypsin, myoglobin, lysozyme, ubiquitin – the unconjugated protein proved to be the major species. Intriguingly, though, when the first set of conditions (i.e., with cyclohexyl isocyanide) was applied on Anticalins, not only site-selective conjugation was achieved but also almost full conversion was detected. In the end, this extensive study showed that some particular combinations of residues/functional groups appear to be extremely reactive, leading to effective conjugation within hours.

3.11. General Conclusions & Future perspectives

This thesis was focused on the development and investigation of novel bioconjugation methods aiming for the chemo- and regio-selective modification of native and artificial proteins. Two of these strategies were focused on the chemo-selective labeling of cysteine residues while the other one was dedicated to the incorporation of an Ugi MCR for the regio-selective modification of spatial close lysine and aspartate/glutamate residues.

Functionalizable non-brominated pyridazinedione molecules, bearing an alkyl-BCN motif on the one N-substituent and an alkyl / phenyl group on the other one, were designed and employed for the investigation of their conjugation / de-conjugation properties on Fab-Trastuzumab. The phenyl analogue was found to be fully de-conjugated from Fab-Trastuzumab after 48 h in contrast with the methyl one that still showed a significant amount of conjugated species, even after 72 h. This demonstrated the versatility of non-brominated PDs and the importance of the *N*-substituent that can either enhance or diminish the de-conjugation rate.

A multifunctional hypervalent iodine (III) reagent, and in particular, an EBZ analogue was next investigated for its potential to be used as a Cys-Cys rebridging reagent. After an extensive methodology work by evaluating various condition-combinations we managed to tune it in such way in order to achieve complete rebridging and functionalization of Fabs and whole mAbs species derived from various sources *via* a one-pot 3-step reaction. However, the rebridging of Fabs was often accompanied with the formation of Fd and LC fragments due to fragmentation of the **mEBZ** reagent. Finally, we demonstrated the excellent stability of our rebridged conjugates in human plasma at 37 °C and their controlled cleavage in the presence of copper(I) species through iodine(III) reduction.

Last but not least, a multicomponent reaction – the Ugi four-component three-centre reaction (U- 4C-3CR) – was investigated as a new regio-selective labelling strategy. After another extensive methodology work, supported by peptide mapping studies, we managed to achieve site-selective conjugation of E1 *N*-terminal of Trastuzumab. Incorporating these site-selective conditions we constructed a homogeneous ADC with an avDAR 1 that showed great cytotoxic profile in comparison with the ADC Kadcyla® with an avDAR 3.5. We next applied this method on other native proteins but with zero to little conjugation detected. However, when we applied the same method with slightly altered conditions on Anticalins, not only site-selective conjugation was detected but also almost full conversion was achieved.

The next logical step related with the latter project, would be the design of a computational model that could predict whether a protein is susceptible for modification *via* our Ugi approach and which residues are more prone for labeling. This would be possible whether this model

could unveil a pattern of the microenvironment surrounding the sites of modification of all the proteins used, so far. These computational studies could also be the foundation of another model that could foresee which aldehyde / isocyanide combination is the most optimal for each protein in order to be site-selectively conjugated.

Finally, the discovery of site-selective conditions for Anticalin D11vs proteins with almost complete conversion can be a promising achievement for the manufacture of PDCs. However, the site of modification (K46) was found to be on the binding site, thus negatively affecting the binding of the protein with the target cell. Hence, an Anticalin D11vs mutant should be designed where K46 would be replaced with an arginine residue (K46R) – in order to maintain the positive charge and prevent the Ugi to take place – and to furthermore examine which site on the Anticalin could be the most optimal for the introduction of two spatial close lysine aspartate/glutamate residues, without disturbing the D11vs' main functions and being at the same time susceptible to Ugi labeling.

4. EXPERIMENTAL SECTION

4.1 MATERIALS & METHODS (UNIVERSITY OF STRASBOURG, FRANCE)

SYNTHETIC CHEMISTRY

All reagents were obtained from commercial sources and used without prior purification. Dry solvents were obtained from Merck. All reactions were carried out under an atmosphere of argon in flame-dried glassware with magnetic stirring. Reactions performed at 0 °C were cooled with an ice and H_2O bath, while those at - 78 °C were cooled with an acetone/dry ice colling bath. Concentration *in vacuo* refers to distillation on a Büchi rotary evaporator, and where appropriate, under high vacuum.

Analytical thin layer chromatography (TLC) was performed using plates cut from aluminum sheets (ALUGRAM Xtra SIL G/UV254) purchased from Macherey-Nagel. Visualization was achieved under a 254 or 365 nm UV light and by immersion in an appropriate staining solution. Column chromatography was carried out as “Flash Chromatography” using silica gel G-80, G-40, G-25, G-12 or G-4 (40-63 µm) columns from Buchi on a Buchi Reveleris X2.

BIOMOLECULES

All reagents, enzymes and solvents were obtained from commercial sources; Sigma Aldrich France, Fischer Scientific France or VWR France, and used without prior purification. Concentrations of protein, antibody or fragment antigen-binding (Fab) solutions were determined by UV absorbance using a NanoDrop spectrophotometer (Thermo Fisher Scientific, Illkirch, France) at 280 nm at ambient temperature. Sample buffer was used as blank for baseline correction.The concentration of antibody conjugates was also measured using a BCA Protein Assay Kit (Thermo Fisher Scientific, Illkirch, France, Ref. 23225).

Buffers List. Buffers were prepared with double-deionized water and filter sterilized (0.20 µm).

- **Phosphate Buffer (PB; 1 M, pH 7.4)** contains a mixture of 1 M NaH_2PO_4 and 1 M Na_2HPO_4 in a 2:21 v/v ratio.
- **Borate Buffer Saline (BBS)** contains 25 mM boric acid (H_3BO_3), 25 mM sodium chloride (NaCl), and the pH was adjusted accordingly.
- **Dulbecco’s Phosphate Buffer Saline 1X** (**DPBS 1X** – calcium and magnesium free, Merck, Ref. D8537-6 × 500 mL) contains 10 mM phosphate, 138 mM NaCl, pH 7.4.
- **Tris buffer** contains 1000 mM Tris base, pH 8.

- **Conjugation buffer** contains 40 mM PB, 20 mM NaCl, 6 mM EDTA, pH 7.4
- **Sodium acetate buffer** contains 20 mM NaOAc, pH 3.1.
- **Digestion buffer 1** contains 50 mM PB, 150 mM NaCl, 1 mM EDTA, pH 6.8.
- **Digestion buffer 2** contains 50 mM PB, 150 mM NaCl, 1 mM EDTA, 10 mM DTT, pH 6.8.
- **Digestion buffer 3** contains 20 mM NaH_2PO_4, 10 mM EDTA, 80 mM cysteine·HCl, pH 7.

Incubation of digestion, reduction and conjugation experiments took place either in an eppendorf thermomixer comfort (catalog # 5355) or in a digital heated shaker dry bath (Ref.: 88880027).

Protein, antibody, or Fab conjugates were **purified by gel filtration chromatography** either on Bio-spin P-30 and P-6 columns obtained from Bio-rad (Hercules, U.S.A) or on Zeba™ Spin Desalting Columns, 7K MWCO, 0.5 mL (Thermo Fisher Scientific, Pierce Biotechnology, USA). Vivaspin micro-concentrators (500 µL, 50 kDa, 30 kDa, 10 kDa and 3 kDa cutoff) from Sartorius (Gottingen, Germany) were used for buffer exchange. Antibody deglycosylation was achieved by incubating Remove-iT® Endo S (New England Biolabs, Ipswich, USA).

Purification by steric exclusion chromatography (SEC) was performed on an ÄKTA Pure system (GE Healthcare) with a Superdex column (S200 10/300 GL), using DPBS 1X, pH 7.4 as eluent at a flow rate of 0.5 mL/min.

Reducing or non-reducing **SDS-PAGE** was performed on 5 – 15% Mini-PROTRIETHYLAMINEN® TGX™ gel (Bio-Rad, Hercules, U.S.A., Ref. 4561094) following standard lab procedures. To the samples containing antibody conjugates (11 µL, 0.2 mg/mL solution in DPBS 1X) was added 3 µL of loading buffer (either reducing or non-reducing Laemmli SDS sample buffer 4X, Alfa Aesar, Ref., J63615.AC) and heated at 90 °C for 10 min. The gel was run at constant voltage (200 V) for 35 min using TRIS 2.5 mM – Glycine 19.2 mM – SDS 0.01% as a running buffer (Bio-rad, Hercules, U.S.A., Ref. 1610772). The fluorescence was visualized on a ImageQuant™ LAS4000 (GE Healthcare) prior to staining with InstantBlue® Protein Stain (Merck, Ref. ISB1L).

SAMPLES PREPARATION FOR NATIVE MASS SPECTROMETRY

Prior to native MS analyses, antibody conjugates were deglycosylated by incubating (37 °C – 2 h) 0.4 unit of Remove-iT® Endo S per microgram of antibody conjugates. Protein concentration was determined by UV absorbance using a NanoDrop spectrophotometer.

STABILITY OF CONJUGATES IN HUMAN PLASMA

Conjugate **Fab-D1** (25 µL in H_2O, 2 mg/mL) was mixed with human plasma (25 µL) and incubated at 37 °C. Every day at certain time points, aliquots (2 µL) were taken, diluted with water (48 µL), frozen in liquid nitrogen and stored at -20 °C. The resulting samples (50 µL) were then subjected to SDS PAGE analysis.

IN VITRO ADC CYTOTOXICITY ASSAY

SKBR-3 (HER2-positive) and MDA-MB-231 (HER2-negative) cell lines were grown in DMEM (Thermo Fisher Scientific, Waltham, MA, USA) supplemented with 10% fetal bovine serum (FBS), Penicillin (100 units/mL), and Streptomycin (100 µg/mL). Cell lines were maintained in a 5% CO_2 humidified atmosphere at 37 °C. The day before experiment, both cell lines were seeded in 96-well plates at 6 000 cells/well in 100 µL fresh cell medium. The day of experiment, the medium was removed carefully and cells were incubated with conjugates in fresh cell medium, 100 µL/well, in triplicate for 96 h. 10 µL of resazurin (Sigma-Aldrich R7017, 0.15 mg/mL in PBS) was added into each well and incubated for 2 – 4 h at 37 °C. Cell viability was measured by quantifying fluorescence (excitation 531/25 nm, emission 595/60 nm) using a plate reader (Perkin Elmer, Victor 2030). EC_{50} values were determined using four-parameter logistic fitting in GraphPad Prism 8.0.

SPECTROSCOPY AND SPECTROMETRY

^{1}H and ^{13}C NMR spectra were recorded at 23 °C on Bruker Advance III – 400 MHz / 500 MHz spectrometers. Recorded shifts are reported in parts per million (δ) and calibrated using residual nondeuterated solvent. Data are represented as follows: chemical shift, multiplicity (s = singlet, d = doublet, t = triplet, q = quartet, m = multiplet, br = broad, app = apparent), coupling constant (*J*, Hz), integration and assignment for ^{1}H NMR data.

Analytical LC-MS analyses were carried out on Waters ARC separations module equipped with Waters 2998 PDA UV detector, Waters Acquity QDa mass detector and XBridge®, 3.5 µm, C18, 50 x 4.6 mm column. The flow rate was 1 mL/min and the solvent system was composed as follows: solvent A: 0.05% TFA in H_2O; solvent B: acetonitrile. The gradient run was: 0 - 5 min. – 5% to 95% B; 5 - 6 min. – 95% B; 6 - 7 min. – 5% B. Mass detector was operated in positive MS Scan mode with 600 °C probe temperature, 1.5 kV capillary voltage and 10 V cone voltage.

High resolution mass spectra (HRMS) were obtained using an Agilent Q-TOF 6520.

Infrared (IR) spectra were recorded in a Thermo-Nicolet FT/IR-380 spectrometer. Spectra were interpreted with OMNIC 9 software and are reporter in cm^{-1}. The abbreviations used are w (weak), m (medium), s (strong).

<u>Initial</u> mass spectrometry analyses of biomolecules were performed using:

- **Native MS *via* LCT** with 20 µg of mAb samples prior buffer exchanged to 150 mM NH_4OAc at pH 7.5 using vivaspin, were performed on a time-of-flight (ToF) LCT mass spectrometer from Micromass (U.K.), which was upgraded for high m/z values by MS vision. The MS was coupled to an automated chip-based nanoESI device (TriVersa NanoMate, Advion, U.S.). The LCT was operated in the positive mode with a sample cone and pressure in the interface region set to V_c = 180 V and P_i = 6 mbar, respectively to ensure good desolvation and transmission of the native structure of the antibodies. Acquisitions of mass spectra were carried out over *m/z* range 1 000 to 10 000 mass range with a 1.5 s scan time. External calibration was performed using singly charged ions produced by a 2 g/L solution of cesium iodide in 2-propanol/water (50/50 v/v). MS data interpretations were performed using Mass Lynx V4.1 (Waters, Manchester, UK).
- **RpLC-MS** with an Agilent 1200 series coupled to a maXis II (Bruker) Q-ToF based mass spectrometer. Nearly 1 µg was injected on a BioResolve™ RP mAb polyphenyl (450 Å, 2,7 µm, 2.1 × 50 mm column, Waters) set at 80 °C. Mobile phases consisted of 0.10% TFA in H2O (mobile phase A) and 0.08% FA in ACN (mobile phase B). The UV chromatograms were acquired with a DAD detector operating from 200 to 400 nm. The gradient was generated at a flow rate of 300 µL/min and the separation was carried out using a gradient from 25% mobile phase B to 75% in 35 min. Then, 2 min of washing was performed at 75% to finally equilibrate for 5 min at 25% mobile phase B. A blank was injected between each sample in the same conditions. The mass spectrometer was operated in positive mode with a capillary voltage of 4.5 kV and CID value was set at 70 eV. Acquisitions were performed on the mass range 500 – 5 000 m/z. Calibration was performed using the singly charged ions produced by a solution of 2 g/L cesium iodide in 2-propanol/water (50/50 v/v). Data interpretation was performed by using Compass DataAnalysis v4.3 software (Bruker Daltonics).

<u>Later</u> mass spectrometry analyses of biomolecules were performed using:

A BioAccord LC-MS system (Waters, Manchester, UK). It comprises an Acquity UPLC M-Class system; including a binary solvent manager, a sample manager at 4 °C, a column oven at room temperature for SEC separation and at 80 °C for rpLC and a UV detector operating at 214 nm and 280 nm, coupled to an RDa detector. The mass spectrometer was calibrated in the 400-7 000 *m/z* range in the positive mode using a solution containing, 50 ng/µL of sodium

iodide in isopropanol/water (80/20 *v/v*) and 0.5 ng/µL of rubidium iodide in isopropanol/water (80/20 *v/v*). A LockMass solution containing 3.75 ng/µL of leucine encephalin, 12.5 ng/µL of caffeine and 2.5 ng/µL of 1-pentanesulfonic acid in ACN/water (80/20 *v/v*) was injected automatically prior to each analysis.

- ***SEC-nMS* –** 5 to 10 µg were injected on a MaxPeak Premier Protein SEC 250 Å, 1.7 µm, 4.6 × 150 mm (Waters, Manchester, UK) used with an isocratic gradient of 150 mM NH_4OAc (pH 6.9) at a flowrate of 250 mL/min over 6 min. The mass spectrometer was operated with a capillary voltage of 3.5 kV and a pressure of 2 mbar. The cone voltage was set to 80 V. Acquisitions were performed on the m/z range 400-7 000 with a 1 s scan time.
- ***rpLC-MS* –** Less than 1 µg was injected on a Bioresolve RP mAb polyphenyl (450 Å, 2.7 µm, 2.1 × 50 mm column, Waters) at a flowrate of 300 µL/min at 80 °C. Mobile phases consisted of 0.1% formic acid (FA) in H_2O (mobile phase A) and 0.1% FA in ACN (mobile phase B). The separation was carried out using a gradient from 5 to 95% of mobile phase B in 25 min. The column was washed with 95% mobile phase B for 1 min and then was equilibrate with 5% mobile phase B for 3 min. The BioAccord was operated in the positive mode with a capillary voltage of 1.5 kV. Desolvation temperature was set to 330 °C, the cone voltage to 60 V and the source pressure was fixed at 2 mbar. Acquisitions were performed on the m/z range 400-7 000 with a 1 s scan time.
- ***dSEC-MS* –** SEC analysis was performed using the AdvanceBioSEC3 (300 Å, 2.5 µm, 4.6 × 150 mm, Agilent) or the Maxpeak Protein SEC (250 Å, 2.5 µm, 4.6 mm × 150 mm, Waters) column kept at room temperature. The separation was carried out using an isocratic gradient of mobile phase (20% ACN+0.1% FA+0.1%TFA) at a flowrate of 0.1 mL/min for 15 min. For *d*SEC-MS, 1 to 3 µg of protein samples were injected. The BioAccord was operated in the same conditions as rpLC-MS. Full scan acquisition was performed on the high mass range (400 – 7 000 m/z) with a 1 s scan time.

Data processing. All MS data interpretations were performed using UNIFI v1.913.9 (Waters, Manchester, UK) and MassLynx V4.1 (Waters, Manchester, UK). The avDoC values were calculated based on the relative peak intensities measured from the raw mass spectra (four charge states) using the equation below:

$$avDoC = \frac{\sum_{k=0}^{n} k \times I_k}{\sum_{k=0}^{n} I_k}$$

Where *k* is the number of drugs and I_k is the relative peak intensity of DoC_k.

In the case of SEC-nMS, when used for the project related with the utilization of the **mEBZ** reagent for the rebridging of Fabs and mAbs, to relatively quantify the amount of by-products

we used integration of the peak areas from UV chromatograms, incorporating the following equation:

$$Amount\ of\ by-products\ (\%) = \frac{\sum Peak\ area_{free\ species}}{\sum Peak\ area_{all\ species}} \times 100$$

Where the free species correspond to to HC, LC, mAb/2 species in the case of mAb rebridging, or LC and Fd in the case of Fab rebridging.

PEPTIDE MAPPING:

Trypsin digestion. 20 µg of sample were solubilized in 150 mM ammonium hydrogen carbonate, 0.1% RapiGest (Waters, Manchester, UK) at pH 7.8, to obtain a final volume of 24 µL. Disulfide reduction was performed by incubating the solution with 5 mM dithiothreitol for 30 min at 57 °C. Alkylation of cysteine residues was performed in 10 mM iodoacetamide in the dark at room temperature for 40 min. The enzyme was prepared by suspending 20 µg of trypsin (Promega, V5111) in 100 µL of water. Digestion was performed by adding 1 µL of trypsin which corresponds to a 1:100 enzyme:substrate ratio. Samples were incubated overnight at 37 °C. The reaction was stopped by 1% of trifluoroacetic acid. RapiGest was eliminated by incubation at 37 °C for 30 min and centrifugation at 10 000 g for 5 min.

NanoLC-MS/MS. The analyses were performed using a nanoACQUITY Ultra-Performance-LC (Waters, Manchester, UK) coupled to a Q Exactive™ Plus Quadrupole-Orbitrap™ Mass Spectrometer (Thermo Fisher Scientific, Bremen, Germany). A volume equivalent to 140 ng of digest were trapped on a Symmetry C18 pre-column (180 µm x 20 mm, 5 µm particle size, Waters) and the peptides were separated on an ACQUITY UPLC® BEH130 C18 separation column (75 µm × 250 mm, 1.7 µm particle size, Waters). The solvent system consisted of 0.1% formic acid in water (solvent A) and 0.1% formic acid in acetonitrile (solvent B). Peptide trapping was performed during 3 min at a flow rate of 5 µL/min with 99% A and 1% B and elution was performed at 60 °C at a flow rate of 350 nL/min from 6% to 40% of B in 43 min. MS and MS/MS acquisition were performed in positive mode, with the following settings: spray voltage 1 800 V and capillary temperature 250 °C. The MS scan had a resolution of 70 000, the AGC target was 3×10^6 and the maximum IT was 50 ms on m/z [300-1 800] range. The MS/MS scans were acquired at a resolution of 17 500, the AGC target was 1×10^5 and the maximum IT was 100 ms with fixed first mass of 100 m/z and Isolation window of 2 m/z. Top 10 HCD was selected with intensity threshold of 5×10^4 and dynamic exclusion of 3 s. The normalized collision energy (NCE) was fixed at 27 V. The complete system was fully controlled by Thermo Scientific™ Xcalibur™ software. Raw data collected were processed and converted with MSConvert into .mgf peak list format.

Peptide identification for antibody samples. Identification of peptides was performed by using the search engine MASCOT 2.6.2 algorithm (Matrix Science, London, UK) and Byos® 5.0 software (Protein Metrics, Cupertino, USA). The search was performed against the amino acid sequence of Trastuzumab. Spectra were searched with a mass tolerance of 10 ppm for MS and 0.05 Da for MS/MS data. The search was made without enzyme specified for MASCOT search, in order to allow the identification of any non-specific peptide cleavage. For Byos® search, trypsin was specified as enzyme with a maximum of three missed cleavages. Variable modifications were specified: carbamidomethylation of cysteine residues, oxidation of methionine residues and adduct of Ugi (769.431 Da for **R154** and 773.389 Dafor **Site-selective Ugi-modified Trastuzumab**) and Passerini (787.442 Da for **R154** and 791.400 Da for **Site-selective Ugi-modified Trastuzumab**) payload on lysine, aspartate and glutamate residues. Peptide identifications were validated with a minimal ion score of 25 for Mascot and 300 for Byos.

Peptides containing Ugi or Passerini payload were validated with the following criteria: *i*) tryptic peptide (no unspecific cleavage); *ii*) retention time higher than that of the unmodified peptide; *iii*) identification of signature fragment ions at m/z 286.172 and 637.343 (characteristic of payload fragmentation); and *iv*) identification with both search engines Byos® and MASCOT.

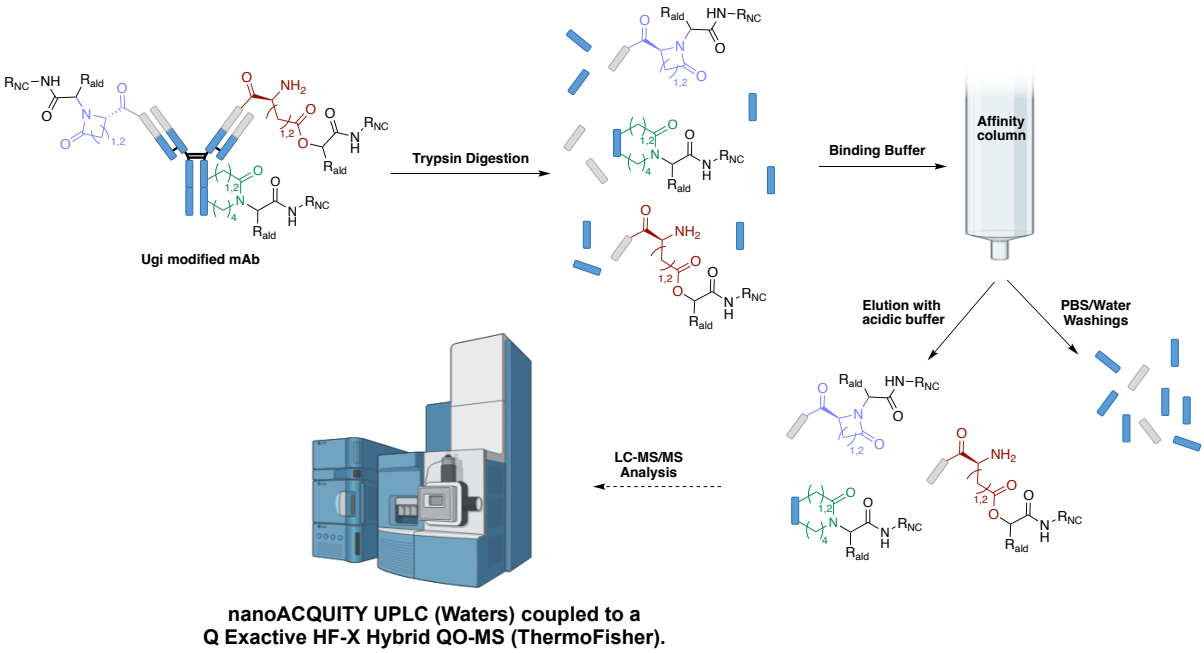

Figure 17. Schematic representation of peptide mapping studies.

Peptide identification for anticalin samples. Identification of peptides was performed by using the search engine MASCOT 2.6.2 algorithm (Matrix Science, London, UK) and Byos® 5.0 software (Protein Metrics, Cupertino, USA). The searches were performed against the amino acid sequence of proteins. Spectra were searched with a mass tolerance of 10 ppm for MS and 0.05 Da for MS/MS data. The search was made without enzyme specified for MASCOT search, in order to allow the identification of any non-specific peptide cleavage. For Byos® search, trypsin was specified as enzyme with a maximum of three missed cleavages. Variable modifications were specified: carbamidomethylation of cysteine residues, oxidation of methionine residues and adduct of Ugi (308.185 Da) and Passerini (326.195 Da) payload on lysine, aspartate and glutamate residues. Peptide identifications were validated with a minimal ion score of 25 for Mascot and 300 for Byos®.

Peptides containing Ugi or Passerini payload were validated with the following criteria: *i*) tryptic peptide (no unspecific cleavage); *ii*) retention time higher than that of the unmodified peptide; *iii*) identification of signature fragment ion at m/z 283.175 (characteristic of payload fragmentation); and *iv*) identification with both search engines Byos® and MASCOT.

4.1.1. Chemical procedures and characterization

1-(2-(2-(2-(2-Azidoethoxy)ethoxy)ethoxy)ethyl)-3,4-dibromo-1*H*-pyrrole-2,5-dione R76

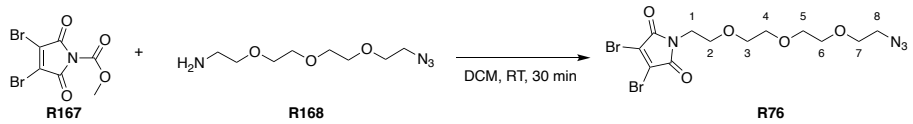

R167 R168 R76

A solution of 2-(2-(2-(2-azidoethoxy)ethoxy)ethoxy)ethanamine **R168** (70 mg, 0.32 mmol, 1 equiv.) in DCM (1.5 mL) was added to a stirred solution of *N*-methoxycarbonyl-3,4-dibromomaleimide **R167** (100 mg, 0.32 mmol, 1 equiv.) in DCM (1.5 mL). 30 min later, DCM (6 mL) was added and the resulting solution was washed with 1 M acetate buffer pH 5 (10 mL), water (10 mL), and the organics were dried over $MgSO_4$, filtered and concentrated *in vacuo*. The crude product was purified *via* flash column chromatography (7:3 cHex/EtOAc) to afford the title compound **R76** (60 mg, 0.13 mmol) as a yellow oil in 55% yield.

Rf 0.34, 7:3 cHex/EtOAc. **Visualization**: PPh_3 and Ninhydrine stain

^{1}H NMR (400 MHz, $CDCl_3$) δ_H 3.81 (t, *J* = 5.6 Hz, 2H, H1), 3.71 – 3.56 (m, 12H, H2-7), 3.39 (t, *J* = 5.1 Hz, 2H, H8).

^{13}C NMR (101 MHz, $CDCl_3$) δ_C 164.0, 129.6, 70.9, 70.8, 70.3, 70.2, 67.8, 50.9, 39.1.

NMR analysis was found to be in agreement with previously reported characterization data.[217]

2-Isocyano-2-methylpropyl (4-nitrophenyl) carbonate R171

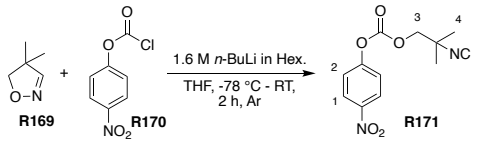

In a flame dry round-bottom flask (RBF), dimethyl oxazoline **R169** (1.046 mL, 9.92 mmol, 1 equiv.) was dissolved in dry THF (20 mL) and the resulted solution was cooled down to - 78 °C under an argon atmosphere. Then, *n*-BuLi (1.6 M in hexanes, 6.2 mL, 9.92 mmol, 1 equiv.) was added dropwise maintaining the temperature below -70 °C and the reaction mixture was stirred for 1 h at -78 °C. This solution was quickly canulated to a three-neck RBF containing a solution of nitrophenyl chloroformate **R170** (2 g, 9.92 mmol, 1 equiv.) in dry THF (20 mL), which has been prior cooled down to -78 °C, and was stirred for 30 min under argon, before it was left to warm up to RT. Afterwards, the resulting reaction mixture was carefully quenched with H_2O (50 mL), maintaining temperature below 4 °C, prior to its evaporation *in vacuo*. The resulted orange solid was dissolved in EtOAc (100 mL), washed with brine (3 × 80 mL), dried over Na_2SO_4, filtered, and concentrated *in vacuo*. The crude product was purified *via* flash column chromatography (100% cHex to 93:7 cHex/EtOAc) to afford the title compound **R171** (1.6 g, 6.43 mmol) as a yellow solid in 65% yield.

Rf 0.15, 9:1 cHex/EtOAc. **Visualization**: UV.

^{1}H NMR (400 MHz, $CDCl_3$) δ_H 8.13 (m, 2H, H1), 7.25 (m, 2H, H2), 4.08 (s, 2H, H3), 1.38 (s, 6H, H4).

^{13}C NMR (101 MHz, $CDCl_3$) δ_C 155.3, 145.6, 126.2, 125.4, 121.8, 115.7, 73.6, 56.3, 25.8.

NMR analysis was found to be in agreement with previously reported characterization data.[218]

2-Isocyano-2-methylpropyl *N*-{2-[2-(2-{[(2-isocyano-2-methylpropoxy)carbonyl]amino} ethoxy)ethoxy]ethyl}carbamate R158

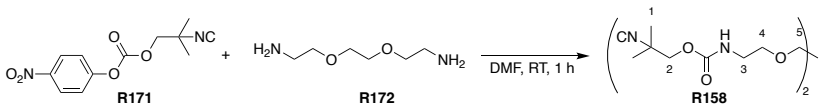

1-{[(2-isocyano-2-methylpropoxy)carbonyl]oxy}-4-nitrobenzene **R171** (109.8 mg, 0.42 mmol, 2.2 equiv.), 1,8-diamino-3,6-dioxaoctane **R172** (27.5 µL, 0.19 mmol, 1 equiv.) and DMF (2 mL) were mixed and stirred at RT. 1 h later, the resulted yellow reaction mixture was partitioned between HCl (0.1 M, 20 mL) and EtOAc (10 mL). The organic layer was washed with brine (5 × 10 mL), dried over Na_2SO_4, filtered and concentrated under reduced pressure at 50 °C.The crude product was purified *via* flash column chromatography (1:4 cHex/EtOAc to 100% EtOAc) to afford the title compound **R158** (8.5 mg, 0.021 mmol) as an orange oil in 11% yield.

^{1}H NMR (400 MHz, $CDCl_3$) δ_H 5.39 (s, br, 2H, NH), 4.10 – 4.00 (s, 4H, H2), 3.63 (d, *J* = 6.6 Hz, 4H, H5), 3.59 (t, *J* = 5.2 Hz, 4H, H4), 3.42 (q, *J* = 5.4 Hz, 4H, H3), 1.42 (s, 12H, H1).

^{13}C NMR (100 MHz, $CDCl_3$) δ_C 155.8 (2C), 155.2 (2C), 70.3 (2C), 69.9 (4C), 56.7 (2C), 40.9 (2C), 25.8 (4C).

NMR analysis was found to be in agreement with previously reported characterization data.[210]

2-Isocyano-2-methylpropyl (2-(2-azidoethoxy)ethyl)carbamate R159

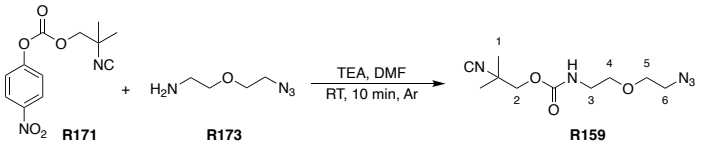

R171 **R173** **R159**

To a solution of commercially available 2-(2-azidoethoxy)ethan-1-amine **R173** (49.3 mg, 0.38 mmol, 2.0 equiv.) in DMF (1 mL) was added triethylamine (53.0 µL, 0.38 mmol, 2.0 equiv.). The resulting solution was stirred at 25 °C under an inert atmosphere of argon for 10 min, before a solution of isocyanide **R171** (50.0 mg, 0.19 mmol, 1.0 equiv.) in DMF (1 mL) was added dropwise and stirred for 3 h. DMF was then removed *in vacuo* and the resulting oil was dissolved in DCM (10 mL) and washed with $NaHCO_3$ (aq., sat., 10 mL). The aqueous layer was extracted with DCM (3 × 10 mL) and the combined organic phases were washed with brine (3 × 20 mL), dried over Na_2SO_4, filtered and concentrated *in vacuo*. The crude product was purified *via* flash column chromatography (1:1 v/v cHex/EtOAc) to afford the title compound **R159** (26.0 mg, 0.10 mmol, 56%) as a yellow oil.

Rf 0.48 (1:1, cHex/EtOAc). **Visualization**: ninhydrine stain with PPh_3.

^{1}H NMR (400 MHz, $CDCl_3$) δ_H 5.26 (s, 1H, NH), 4.07 – 4.01 (m, 2H, H2), 3.67 (t, *J* = 4.9 Hz, 2H, H3), 3.58 (t, *J* = 5.1 Hz, 2H, H6), 3.41 (dt, *J* = 14.6, 5.1 Hz, 4H, H4-5), 1.43 (s, 6H, H1).

^{13}C NMR (101 MHz, $CDCl_3$) δ_C 155.8, 155.4, 70.1, 69.9, 56.7, 50.6, 41.0, 25.8 (2C).

HRMS (ESI$^+$) calcd for $C_{10}H_{18}N_5O_3$ $[M+H]^+$ 256.1404; found 256.1412.

2-(2-(2-(2-Hydroxyethoxy)ethoxy)ethoxy)ethyl 4-methylbenzenesulfonate R175

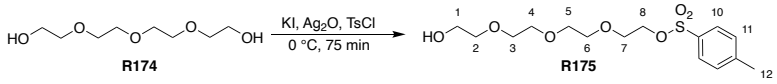

To a solution of tetraethylene glycol **R174** (0.89 mL, 5.15 mmol, 1 equiv.) in DCM (50 mL) at 0 °C, potassium iodide (171 mg, 1.03 mmol, 0.2 equiv.) and silver oxide (1.8 , 7.72 mmol, 1.5 equiv) were added. Subsequently, tosyl chloride (1.03 g, 5.41 mmol, 1.05 equiv.) was added portion-wise in a very slow tempo with vigorous stirring, maintaining temperature at 0 °C. 75 min later, full consumption of SM was validated by TLC. The reaction was stopped, filtered through a pad of Celite® and the filtrates were concentrated to dryness *in vacuo*. The crude product was purified *via* flash chromatography (1:1 cHex/EtOAc to EtOAc to 1:9 MeOH/EtOAc) to afford the title compound **R175** (1.16 g, 3.27 mmol) as a yellow hazy oil in 64% yield

Rf 0.21, 1:4 cHex/EtOAc. Visualization: Dragendorff & UV

^{1}H NMR (400 MHz, $CDCl_3$) δ_H 7.79 (d, *J* = 8.4 Hz, 2H, H10), 7.33 (d, *J* = 8.0 Hz, 2H, H11), 4.15 (t, *J* = 9.8 Hz, 2H, H8), 3.73 – 3.55 (m, 14H, H1-7), 2.58 (s, 1H, OH), 2.43 (s, 3H, H12).

^{13}C NMR (101 MHz, $CDCl_3$) δ_C 144.8, 133.0, 129.8 (2C), 128.0 (2C), 72.5, 70.7, 70.6, 70.5, 70.3, 69.3, 68.7, 61.7, 21.6 (3C).

NMR analysis was found to be in agreement with previously reported characterization data.[162]

2-(2-(2-(2-Azidoethoxy)ethoxy)ethoxy)ethan-1-ol R176

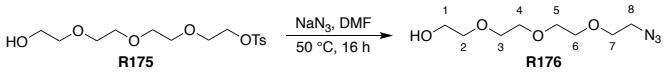

R175 **R176**

To a solution of 2-[2-(2-{2-[(4-methylbenzenesulfonyl)oxy]ethoxy}ethoxy)ethoxy]ethan-1-ol **R175** (1030 mg, 2.96 mmol, 1 equiv.) in DMF (5 mL), sodium azide (288.3 mg, 4.43 mmol, 1.5 equiv) was added and the resulted reaction mixture was heated at 50 °C o/n. 16 h later, TLC confirmed full consumption of SM and the reaction mixture was filtered through a Celite® pad and the filtrates were concentrated to dryness *in vacuo* to remove DMF. A DCM trituration afforded the title compound **R176** (650 mg, 2.96 mmol) as a yellow oil in quantitative yield.

Rf 0.17, 1:4 cHex/EtOAc. **Visualisation**: Dragendorff as a red spot.

^{1}H NMR (400 MHz, $CDCl_3$) δ_H 3.70 (d, *J* = 9.4 Hz, 2H, H1), 3.65 (d, *J* = 10.2 Hz, 10H, H2-6), 3.59 (d, *J* = 9.3 Hz, 2H, H7), 3.37 (t, *J* = 5.1 Hz, 2H, H8), 2.64 (s, 1H, OH).

^{13}C NMR (101 MHz, $CDCl_3$) δ_C 72.5, 70.7, 70.6, 70.5, 70.4, 70.0, 61.7, 50.7.

NMR analysis was found to be in agreement with previously reported characterization data.[219]

2-(2-(2-(2-Azidoethoxy)ethoxy)ethoxy)acetaldehyde R152

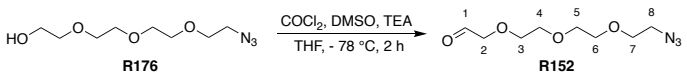

R176 R152

In a flame dry RBF, DMSO (106 µL, 1.49 mmol, 3.0 equiv.) and THF (4 mL) were combined under an argon atmosphere and the resulting colorless solution was cooled down to -78 °C. Then, oxalyl chloride (126.32 mg, 1 mmol, 2.0 equiv.) was added dropwise maintaining the temperature at -78 °C. 15 min later, a cooled 2-(2-(2-(2-azidoethoxy)ethoxy)ethoxy)ethan-1-ol **R176** (109.1 mg, 0.5 mmol, 1 equiv.) in THF (4 mL) solution was added dropwise maintaining the temperature at -78 °C. The resulting colourless solution was left to react at -78 °C for 30 min, followed by dropwise triethylamine (415 µL, 2.99 mmol, 6.0 equiv.) addition. After the completion of triethylamine addition, the resulted white suspension was stirred at -78 °C for 15 min and then the cooling bath was removed, and the reaction mixture was warmed up to RT for 5 – 10 min. The white suspension was filtered and the white pad was washed thoroughly with DCM (3 × 10 mL). The filtrates were concentrated to dryness under reduced pressure at 50 °C, giving an orange solid. This solid was partitioned between DCM (10 mL) and water (10 mL). The organic layer was washed with water (3 × 10 mL) and the combined aqueous layers were extracted with DCM (3 × 10 mL). The combined organics were dried over Na_2SO_4, filtered, concentrated to dryness *in vacuo* and the crude product was purified *via* flash chromatography (1:1 to 3:7 cHex/EtOAc) to afford the title compound **R152** (42.7 mg, 0.2 mmol) as an orange oil in 40% yield.

R_f 0.19, 3:7 cHex/EtOAc. **Visualization**: Dragendorff as a red spot.

^{1}H NMR (400 MHz, $CDCl_3$) δ_H 9.74 (t, *J* = 0.9 Hz, 1H, H1), 4.16 (d, *J* = 0.9 Hz, 2H, H2), 3.78 – 3.63 (m, 10H, H3-6), 3.39 (t, *J* = 5.0 Hz, 2H, H8).

^{13}C NMR (101 MHz, $CDCl_3$) δ_C 201.0, 76.9, 71.3 - 70.1 (5C), 50.7 .

NMR analysis was found to be in agreement with previously reported characterization data.[210]

((1*R*,8*S*,9*S*)-Bicyclo[6.1.0]non-4-yn-9-yl)methyl (4-nitrophenyl) carbonate R178

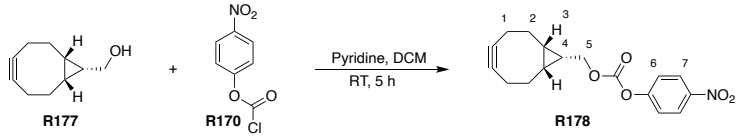

To a solution of [(1*R*,8*S*,9*S*)-bicyclo[6.1.0]non-4-yn-9-yl]methanol **R177** (600 mg, 3.99 mmol, 1 equiv.) in DCM (1 mL), *p*-nitrophenol chloroformate **R170** (966 mg, 4.79 mmol, 1.2 equiv.) was added, followed by pyridine (3.23 mL, 39.94 mmol, 10 equiv., 0.978 g/mL) addition and the resulting yellow reaction mixture was left to react at RT. 5 h later, the reaction was completed, according to TLC, and was quenched with NH_4Cl (60 mL, aq., sat.). The resulting biphasic mixture was transferred into a separating funnel and the layers were separated. The aqueous layer was extracted with DCM (3 × 50 mL). The combined organics were washed with brine (1 × 60 mL), dried over Na_2SO_4 for 20 min, filtered and evaporated to dryness under reduced pressure at 55 °C. The crude product was purified *via* flash column chromatography (100% cHex to 9:1 cHex/EtOAc) to afford the title compound **R178** (534 mg, 1.7 mmol) as a yellow oil that solidified at RT in 44% yield.

Rf 0.32, 9:1 cHex/EtOAc. **Visualization**: Ninhydrine as a yellow spot, UV.

^{1}H NMR (400 MHz, $CDCl_3$) δ_H 8.33 – 8.24 (m, 2H, H7), 7.43 – 7.35 (m, 2H,H 6), 4.41 (d, *J* = 8.3 Hz, 2H, H5), 2.40 – 2.20 (m, 6H, H1-2), 1.68 – 1.58 (m, 2H, H2'), 1.55 – 1.45 (m, 1H, H4), 1.13 – 1.00 (m, 2H, H3).

^{13}C NMR (101 MHz, $CDCl_3$) δ_C 155.6, 152.6, 145.4, 125.3 (2C), 121.8 (2C), 98.7 (2C), 68.0, 29.1, 21.4 (2C), 20.5 (2C), 17.3 (2C).

NMR analysis was found to be in agreement with previously reported characterization data.[220]

((1*R*,8*S*,9*S*)-Bicyclo[6.1.0]non-4-yn-9-yl)methyl *N*-(2-aminoethyl)carbamate R179

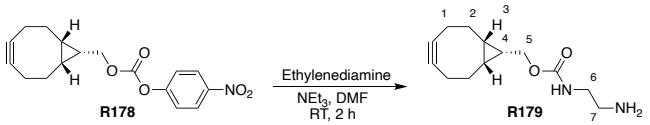

To a solution of ethylene diamine (0.44 mL, 6.5 mmol, 10 equiv.) in DMF (4 mL) and triethylamine (0.904 mL, 6.5 mmol, 10 equiv.), a solution of [(1*R*,8*S*,9*S*)-bicyclo[6.1.0]non-4-yn-9-yl]methyl 4-nitrophenyl carbonate **R178** (205 mg, 0.65 mmol, 1 equiv.) in DMF (1 mL) was added dropwise at RT. The reaction mixture was stirred for 3 h at RT and the completion of the reaction was confirmed by TLC. Then, it was concentrated *in-vacuo* at 60 °C and the obtained yellow oil was partitioned between NaH_2PO_4 (1 M, 50 mL) and DCM (20 mL). The aqueous layer was extracted with DCM (3 × 20 mL). The aqueous layer was basified to pH 9 with NaOH 1 M and was further extracted with DCM (3 × 20 mL). The combined organic layers were washed with brine (1 × 80 mL), dried over Na_2SO_4, filtered and evaporated to dryness under reduced pressure at 50 °C to afford a yellow oil. The crude product was purified by column chromatography (100% DCM to 1:9 MeOH/DCM cont. 1% NH_4OH) to afford the title compound **R179** (105 mg, 0.44 mmol) as a yellow solid in 68% yield.

Rf 0.12, 1:9 MeOH/DCM cont. 1% NH_4OH. **Visualization**: Ninhydrine as a magenta spot.

1H NMR (400 MHz, $CDCl_3$) δ_H 5.07 (s, 1H, NH), 4.15 (d, *J* = 8.1 Hz, 2H, H5), 3.24 (t, *J* = 5.8 Hz, 2H, H6), 2.84 (m, 2H, H7), 2.36 – 2.12 (m, 6H, H1-2), 1.67 – 1.50 (m, 2H, H2'), 1.42 – 1.31 (m, 1H, H4), 1.01 – 0.89 (m, 2H, H3).

^{13}C NMR (101 MHz, $CDCl_3$) δ_C 157.1, 98.8 (2C), 67.1, 42.7, 41.5, 29.1, 21.4 (2C), 20.2 (2C), 17.8 (2C).

NMR analysis was found to be in agreement with previously reported characterization data.[221]

BCN-iminobiotin R74

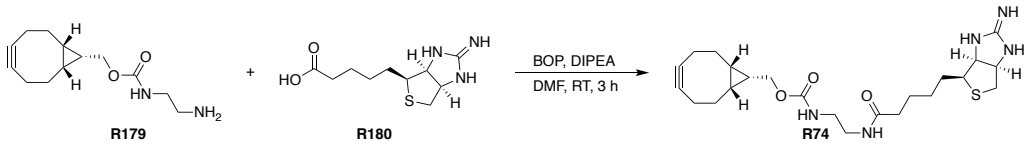

R179 R180 R74

To a stirred solution of 2-Iminobiotin **R180** (20.3 mg, 0.083 mmol, 1 equiv.) in DMF (2 mL), DIPEA (44 µL, 0.25 mmol, 3 equiv.) and BOP (44.28 mg, 0.1 mmol, 1.2 equiv.) were added. After 30 min, ((1*R*,8*S*,9*S*)-bicyclo[6.1.0]non-4-yn-9-yl) methyl (2-aminoethyl)carbamate **R179** (19.7 mg, 0.083 mmol, 1 equiv.) was added and the reaction was stirred for 3 h at RT. The reaction mixture was concentrated to dryness at 60 °C to remove DMF and it was then partitioned between EtOAc (10 mL) and NH_4Cl (60 mL, aq., sat.). The layers were separated, the organics were washed with $NaHCO_3$ (50 mL, aq., sat.) and brine (50 mL), dried over Na_2SO_4, filtered and concentrated to dryness to afford the crude product as an orange viscous oil. The crude product was purified by column chromatography (1:9 MeOH/DCM) to afford the title compound **R74** (2 mg, 0.004 mmol) as a yellow oil in 5% yield.

Rf 0.16, 1:9 MeOH / DCM. **Visualization** PMA as a black spot.

HRMS (ESI$^+$) calcd for $C_{23}H_{35}N_5O_3S^+$ [M+H$^+$] 461.2464; found 461.2461.

MS analysis were found to be in agreement with previously reported characterization data.[210]

4-Nitrophenyl bicyclo[6.1.0]non-4-yne-9-carboxylate R162

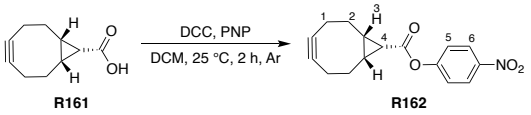

R161 **R162**

To a solution of (1*R*,8*S*,9*S*)-bicyclo[6.1.0]non-4-yne-9-carboxylic acid **R161** (100 mg, 0.61 mmol, 1 equiv.) and 4-nitrophenol (101.7 mg, 0.73 mmol, 1.2 equiv.) in DCM (8 mL), DCC (150.8 mg, 0.73 mmol, 1.2 equiv.) was added, and the resulting reaction was stirred at RT under argon atmosphere. 2 h later, the reaction mixture was filtreted, and the filtrates were quenched with NH_4Cl (aq., sat., 10 mL). The aqueous layer was extracted with DCM (4 × 20 mL) and the organics were washed with brine (3 × 20 mL), dried over Na_2SO_4 and concentrated *in vacuo*. The crude residue was purified *via* flash column chromatography (4:1 cHex/EtOAc) to afford the title compound **R162** (125 mg, 0.44 mmol) as a yellowish viscous oil, that solidified to a yellowish solid after it was left at RT, in 72% yield.

Rf 0.84, 7:3 cHex/EtOAc. **Visualization**: Ninhydrine as a yellow spot, UV.

^{1}H NMR (400 MHz, $CDCl_3$) δ_H 8.31 – 8.20 (m, 2H, H6), 7.31 – 7.24 (m, 2H, H5), 2.42 – 2.11 (m, 9H, H1-2, H4), 1.62 – 1.50 (m, 2H, H3).

^{13}C NMR (101 MHz, $CDCl_3$) δ_C 169.4, 155.6, 145.1, 125.1 (2C), 122.6 (2C), 98.4 (2C), 27.4, 26.6 (2C), 21.3 (2C), 20.9 (2C).

ν_{max} (thin film) /cm^{-1} 2925 (w), 2858 (w), 2359 & 2341 (s, disubstituted), 1748 (m), 1615 (w), 1592 (w), 1520 (s), 1345 (s), 1214 (m), 1108 (s), 1068 (m).

HRMS (ESI$^+$) calcd for $C_{16}H_{15}NO_4^+$ [M+H$^+$] 285.1000; found 285.1001.

***N*-(3-aminopropyl)bicyclo[6.1.0]non-4-yne-9-carboxamide R163**

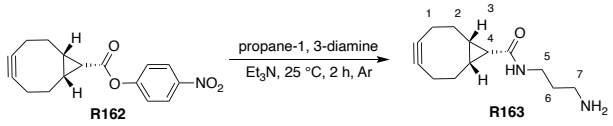

A solution of 4-nitrophenyl bicyclo[6.1.0]non-4-yne-9-carboxylate **R162** (285.3 mg, 0.35 mmol, 1.0 equiv.), propane-1,3-diamine (300 µL, 3.51 mmol, 10 equiv.) and triethylamine (490 µL, 3.51 mmol, 10 equiv.) was stirred at RT. 2 h later, the mixture was partitioned between H_2O (10 mL) and DCM (5 mL) and the aqueous layer was extracted with DCM (4 × 20 mL). The combined organics were washed with brine (3 × 20 mL), dried over Na_2SO_4 and concentrated *in vacuo*, to afford the title compound **R163** (70 mg, 0.32 mmol) as a yellow viscous oil in 91% yield.

Rf 0.15, 1:1 cHex/EtOAc. **Visualization**: Ninhydrine as a magenta spot.

^{1}H NMR (400 MHz, DMSO) δ_H 7.96 (t, *J* = 5.8 Hz, 1H, NH), 3.32 (m, 2H, H5), 3.07 (td, *J* = 6.8, 5.6 Hz, 2H, H7), 2.59 – 2.51 (m, 2H, H6), 2.33 – 2.07 (m, 6H, H1, H3), 1.95 – 1.85 (m, 2H, NH2), 1.69 (t, *J* = 9.0 Hz, 1H, H4), 1.45 (p, *J* = 6.8 Hz, 2H, H2), 1.18 – 1.03 (m, 2H, H2').

^{13}C NMR (101 MHz, DMSO) δ_C 171.1, 99.3 (2C), 36.4, 32.6, 27.9, 26.8 (2C), 23.5 (2C), 22.4 (2C), 21.1 (2C).

ν_{max} (thin film) /cm^{-1} 3295 (br), 2911 (w), 2857 (w), 2359 & 2341 (s, disubstituted), 1636 (m), 1540 (m), 1435 (w), 1233 (w).

HRMS (ESI$^+$) calcd for $C_{13}H_{20}N_2O^+$ [M+H$^+$] 220.1575; found 220.1576.

BCN-DM1 R165

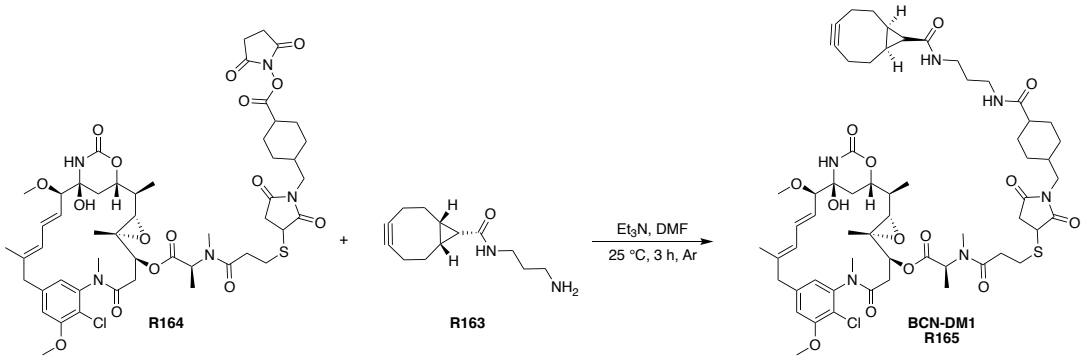

To a stirring solution of SMCC-DM1 **R164** (4 mg, 0.0037 mmol, 1 equiv.) in DMF (0.5 mL), a solution of (1*R*,8*S*,9*S*)-*N*-(3-aminopropyl)bicyclo[6.1.0]non-4-yne-9-carboxamide **R163** (0.83 mg, 0.0038 mmol, 1.01 equiv.) in DMF (0.5 mL) and Et_3N (0.58 µL, 0.004 mmol, 1.1 equiv.) was added. The resulting yellow solution was left to react at RT under argon. 3 h later, the reaction mixture was evaporated to dryness *in vacuo* and was purified by reverse phase column chromatography (9.5:0.5 to 0.5:9.5 H_2O-ACN) to afford the title compound **R165** (2.4 mg, 0.0027 mmol) as a white powder in 75% yield.

HRMS (ESI$^+$) calc. for $C_{60}H_{81}ClN_6O_{14}S$ ([M+H]$^+$): 1176.5206; found: ([M+H]$^+$): 1176.5220.

4.1.2. Bioconjugation procedures

GENERAL PROCEDURES

Preparation of Fab- Trastuzumab & Avelumab fragments

A solution (1 mL, 107 µM in H_2O) of the monoclonal antibody (mAb) was buffer exchanged into **sodium acetate buffer** *via* ultrafiltration (10 kDa MWCO), followed by determination of concentration by NanoDrop.

Thermo Scientific™ Immobilized Pepsin (Agarose Resin) (732 µL) was split in two ways, each of which was loaded onto a Pierce™ centrifuge column and washed with sodium acetate buffer three times. Waste was discarded.

A solution of buffer-swapped mAb (0.50 mL) was then added to the activated pepsin and the mixture was incubated at 37 °C for 5 h under constant agitation (1 100 rpm). The resin was then removed from the digest using a Pierce™ centrifuge column and was washed three times with 0.5 mL of **digestion buffer 1** (i.e., **without DTT**). The filtrates from the washes containing $F(ab')_2$ were combined, concentrated with 15 mL Falcon viva spin tubes (10 kDa MWCO) before the volume was adjusted to 0.5 mL.

At the beginning of the 4th h of pepsin incubation, Thermo Scientific™ Immobilized Papain (Agarose Resin) (1.22 mL) was split in three ways, each of which was loaded onto a separate Pierce™ centrifuge column, concentrated and washed three times with 0.5 mL of **digestion buffer 2**. The resulted papain in **digestion buffer 2** was then incubated at 37 °C for 90 min under constant agitation (1 100 ppm) before it was washed ten times with 0.5 mL of **digestion buffer 1** using a Pierce™ centrifuge column, in order to remove DTT before adding the antibody.

The 0.5 mL of $F(ab')_2$ solution obtained before was added to the Pierce™ centrifuge column containing the activated papain and the mixture was incubated at 37 °C for 16 h under constant agitation (1 100 rpm). Effective Fab formation was confirmed by SDS-PAGE analysis. The resin was then separated and washed four times with 0.5 mL of PBS X pH 7.5. The filtrates were combined, concentrated with a 15 mL Falcon viva spin tube (10 kDa MWCO) and purified via steric exclusion chromatography (SEC) on an ÄKTA pure system. Aliquots of Trastuzumab/Avelumab-Fabs were stored at -20 °C for up to 6 months.

Preparation of Rituximab Fab fragment

Immobilized papain (0.3 mL, 0.25 mg/mL) was loaded onto a Pierce™ centrifuge column, concentrated, and washed 3 times with **digestion buffer 2**. The resin-bound papain in **digestion buffer 2** was then incubated at 37 °C under constant agitation (1 100 pm) for 1 h before the resin was washed six times with 0.5 mL of **digestion buffer 1**. Rituximab (3 mg in 0.5 mL of digestion buffer) was then added to the resin-bound papain and the mixture was incubated for 16 h at 37 °C under constant agitation (1 100 rpm). The resin was then separated from the digested Rituximab by washing the Pierce™ centrifuge column 4 times with 0.5 mL of **Pierce™ protein A binding buffer** (100 mM phosphate, 150 mM NaCl, pH 7.2). The filtrates containing digested Rituximab were combined and buffer exchanged to **protein A binding buffer** – in order to get rid of **digestion buffer 1** – and the volume adjusted to 1.5 mL before it was loaded onto a NAb™ protein A column (Thermo Scientific, France) and incubated at 20 °C with end-over-end mixing for 10 min. Filtration of the NAb™ protein A column followed by three washes with protein A binding buffer delivered Rituximab Fab (concentration determined by NanoDrop), whose aliquots were stored at -20 °C for up to 6 months.

Preparation of Fab-Bevacizumab fragment

Bevacizumab (0.5 mL, 10 mg/mL) was buffer exchanged into **digestion buffer 3**. Thermo Scientific™ Immobilized Papain (Agarose Resin) (0.5 mL, 0.25 mg/mL) was loaded onto a Pierce™ centrifuge column, concentrated and washed three times with **digestion buffer 3**. The previously made Bevacizumab solution was added to the resin-bound papain and the mixture was incubated at 37 °C for 4 h under constant agitation (1 100 rpm). The resin was then separated from the digested Bevacizumab by washing the Pierce™ centrifuge column four times with 0.5 mL of **Pierce™ protein A binding buffer**. The filtrates were combined and completely buffer exchanged to **Pierce™ protein A binding buffer** while the volume was adjusted to 1.5 mL. The sample was then loaded onto a NAb™ protein A column (Thermo Scientific, France) and incubated at 20 °C with end-over-end mixing for 10 min. The Fab-Bevacizumab was finally obtained after filtration of the protein A column followed by three washes with 0.5 mL of **Pierce™ protein A binding buffer**. The filtrates were combined, concentrated using a 15 mL Falcon viva spin tube (10 kDa MWCO) and purified by steric exclusion chromatography (SEC). Concentration in Fab-Bevacizumab was determined by NanoDrop and the resulting aliquots were stored at -20 °C for up to 6 months.

MEBZ R73 CONJUGATION

Step-wise conjugation-functionalization procedure

Reduction of Fab fragments

To a solution of Fab (30 – 40 µM in PBS 1X with 1% EDTA, pH 7.5, 1 equiv.) was added TCEP (15 mM in H_2O, 5 equiv.). The reaction mixture was then incubated for 1.5 h at 37 °C with constant agitation (650 rpm), before the excess of reagent was removed by gel filtration chromatography on Zeba™ Spin Desalting Columns, 7K MWCO, pre-equilibrated with BBS (25 mM borate, 25 mM NaCl, 2 mM EDTA, pH 8) to give a solution of reduced Fab in BBS, whose concentration was determined by NanoDrop.

Conjugation step

To a solution of reduced Fab (30 – 40 µM in the desired buffer containing EDTA, 1 equiv.) was added EBZ reagent **R73** (10 mM solution in I the desired organic solvent). The resulting solution was then incubated at either 4 °C, 25 °C or 37 °C, with constant agitation (650 rpm), before the excess of reagent was removed by gel filtration chromatography on Zeba™ Spin Desalting Columns, 7K MWCO pre-equilibrated with PBS 1X pH 7.5 to give a solution of rebridged Fab **Fab-D1**.

Functionalization step (SPAAC reaction)

To a solution of rebridged Fab – **Fab-D1** – (30 – 40 µM, 1 equiv., 50 µL in PBS 1X, pH 7.5) was added BCN-Iminobiotin **R74** (10 M solution in DMSO, 30 equiv.). The resulting mixture was then incubated for 24 h at 25 °C before the excess of reagent was removed by gel filtration chromatography on Zeba™ Spin Desalting Columns, 7K MWCO.

One-pot reduction-conjugation procedure

To a solution of Fab (30 – 40 µM in BBS, 2 mM EDTA, pH 8, 1 equiv.) was added TCEP (15 mM in H_2O, 5 equiv.) and EBZ reagent **R73** (10 mM solution in DMSO, 5 equiv). The resulting solution was then incubated for 5 h at 37 °C with constant agitation (650 rpm), before the excess of reagent was removed by gel filtration chromatography on Zeba™ Spin Desalting Columns, 7K MWCO, to give a solution of rebridged Fab **Fab-D1**.

One-pot reduction-conjugation-functionalization procedure

To a solution of Fab (30 – 40 µM in BBS, 2 mM EDTA, pH 8, 1 equiv.) was added TCEP (15 mM in H_2O, 5 equiv.), EBZ reagent **R73** (10 mM solution in DMSO, 5 equiv) and BCN-Iminobiotin **R74** (10 mM solution in DMSO, 20 equiv.). The resulting solution was then incubated for 5 h at 37 °C with constant agitation (650 rpm), before the excess of reagent was removed by gel filtration chromatography on Zeba™ Spin Desalting Columns, 7K MWCO, to give a solution of functionalized Fab-Trastuzumab **Fab-D1'**.

One-pot reduction-conjugation procedure (mAb)

To a solution of Trastuzumab (17 µM in BBS, 6 mM EDTA, pH 8, 1 equiv.) was added TCEP (15 mM in H_2O, 10 equiv.) and EBZ reagent **R73** (10 mM solution in DMSO, 10 equiv.). The resulting solution was then incubated for 5 h at 37 °C with constant agitation (650 rpm), before the excess of reagent was removed by gel filtration chromatography on Zeba™ Spin Desalting Columns, 7K MWCO, to give a solution of functionalized Trastuzumab.

Copper(I)-mediated reduction procedure

A solution of copper(I) iodide (15 mM in H_2O, 20 equiv.), THPTA (160 mM in H_2O, 40 equiv.), aminoguanidine hydrochloride (100 mM in H_2O, 100 equiv.) and sodium ascorbate (400 mM in H_2O, 300 equiv.) was first prepared and incubated for 10 min at 25 °C without agitation, before it was added to a solution of rebridged Fab-Trastuzumab **Fab-D1** (32 µM in PBS 1X, pH 7.4, 1 equiv.). The resulting reaction mixture was then incubated at 37 °C for 16 h with constant agitation (650 rpm), before the excess of reagent was removed by gel filtration chromatography on Zeba™ Spin Desalting Columns, 7K MWCO.

UGI CONJUGATION

Ugi reaction on proteins (General procedure)

To a solution of a protein (67 µM; 97 µM for Anticalins in PBS 1X, pH 7.4, 1 equiv.) was added aldehyde (as a 0.1 M solution in DMSO) and cyanide (as a 0.1 M solution in DMSO). The reaction mixture was then incubated for 16 h at 25 °C,after which a 50 wt% solution of hydroxylamine in H_2O (730 equiv.) was added. The resulting solution was incubated for 1 h at 25 °C, before the excess of reagent was removed by gel filtration chromatography using Bio-spin P-30 or P-6 columns pre-equilibrated with PBS 1X, pH 7.5 to give a solution of protein-azide which was further derivatized.

SPAAC reaction (General procedure)

To a solution of Ugi-modified-protein bearing an azide group in PBS 1X was added a BCN-derivative (as a 0.1 M solution in DMSO, 30 equiv.). The resulting solution was incubated for 20 h at 25 °C, before the excess of reagent was removed by gel filtration chromatography using Bio-spin P-30 or P- 6 columns pre-equilibrated with PBS 1X, pH 7.5 to give a solution of conjugated protein that was further analyzed by native mass spectrometry.

SPAAC reaction with BCN-DM1

To a solution of Trastuzumab-azide in PBS 1X, pH 7.5 (34 µM) was added a BCN-DM1 **R165** (as a 0.05 M solution in DMSO, 30 equiv.). The resulting solution was incubated for 48 h at 37 °C with 1 100 rpm constant agitation, before the excess of reagent was removed by gel filtration chromatography using Bio-spin P-30 columns pre-equilibrated with PBS 1X, pH 7.5 to give a solution of the ADC that was further analyzed by native mass spectrometry.

4.1.3. dSEC-MS analyses

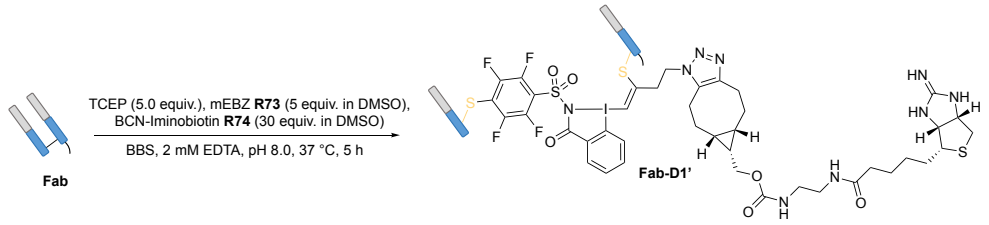

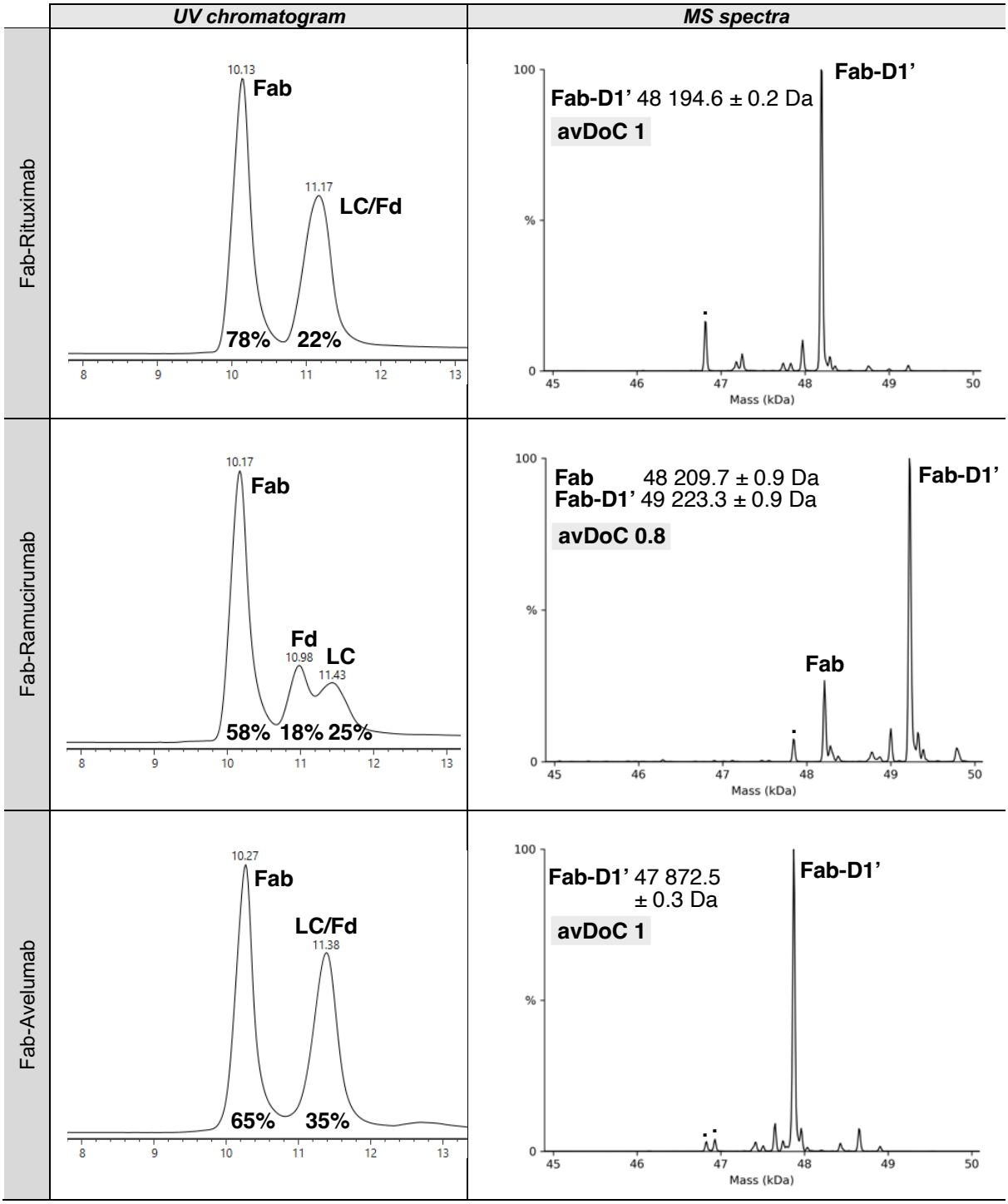

Figure 18. dSEC-MS spectra of the 3-step one-pot reaction between mEBZ **R73**, BCN-Iminobiotin **R74** and various Fab-sources.

4.1.4. Native MS analyses

4.1.4.1. Time-course experiments

The influence of the reaction time on the average degree of conjugation (avDoC), conversion rate and conjugation site was evaluated. The spectra of these samples analysed by nMS and the conjugation sites provided by peptide mapping are illustrated in **Figure 19**.

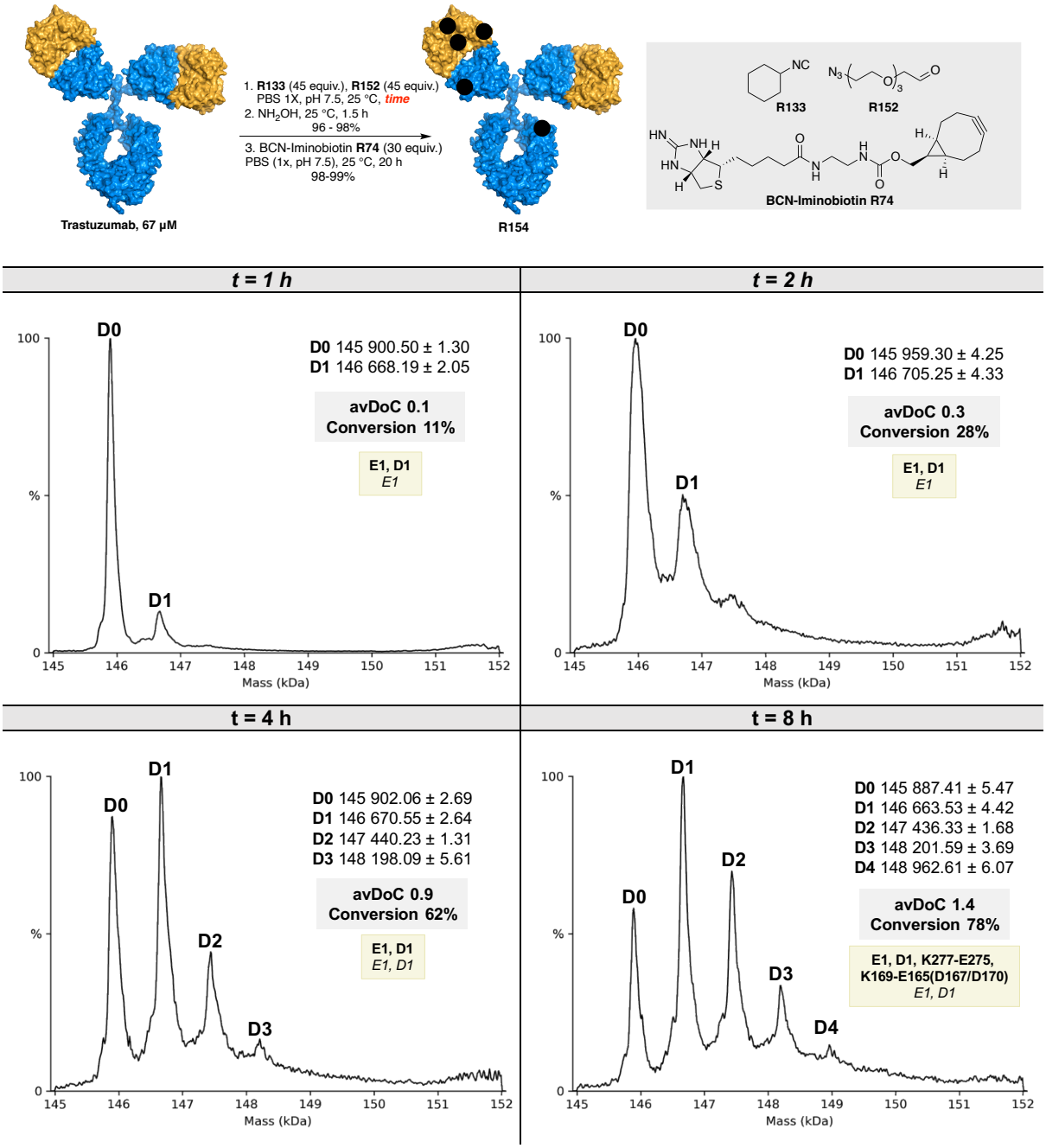

Figure 19. Native mass spectra of samples from time-course experiments study. Conversion, avDoC, and conjugation sites (**Ugi** and *Passerini*) are given.

4.1.4.2. pH experiments

The influence of pH on the average degree of conjugation (avDoC), conversion rate and conjugation site was evaluated. The spectra of these samples analysed by nMS and the conjugation sites provided by peptide mapping are illustrated in **Figure 20**.

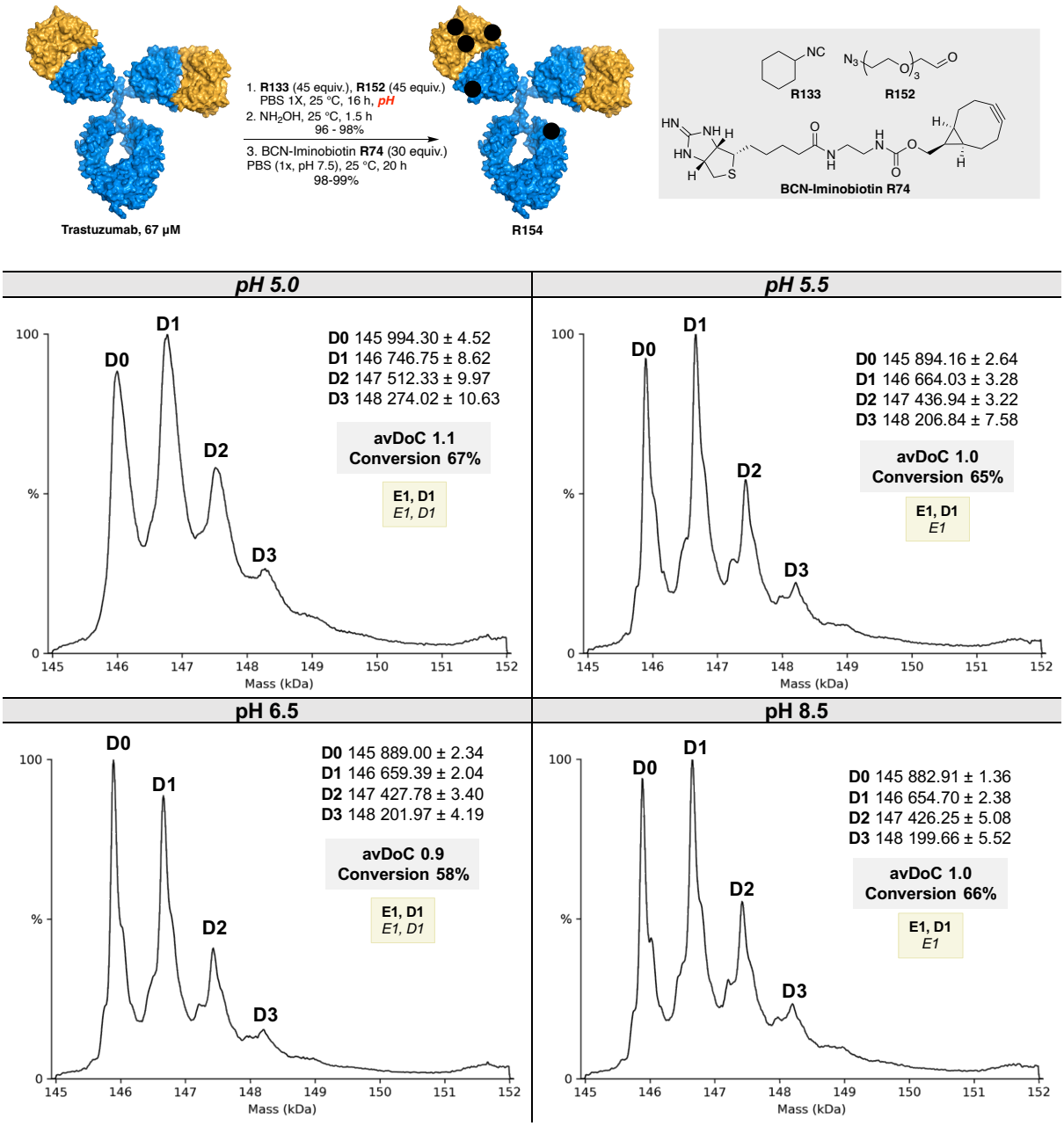

Figure 20. Native mass spectra of samples from pH experiments study. Conversion, avDoC, and conjugation sites (**Ugi** and *Passerini*) are given.

4.1.4.3. Aldehyde & Isocyanide scope

The influence of the isocyanide and the aldehyde structure on the average degree of conjugation (avDoC), conversion rate and conjugation site was evaluated. The spectra of these samples analysed by nMS and the conjugation sites provided by peptide mapping are illustrated in **Figure 21**.

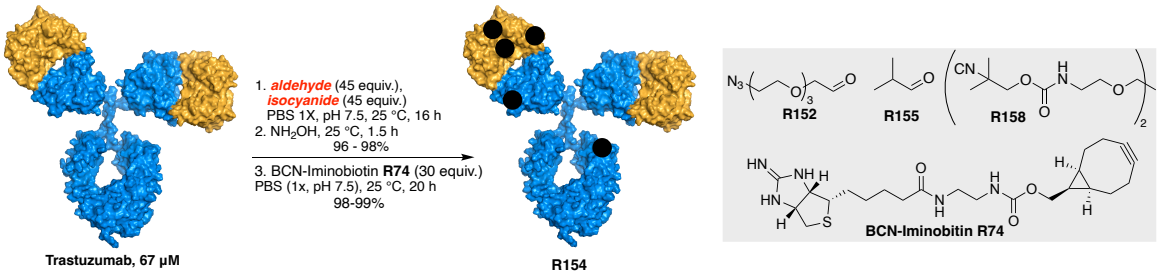

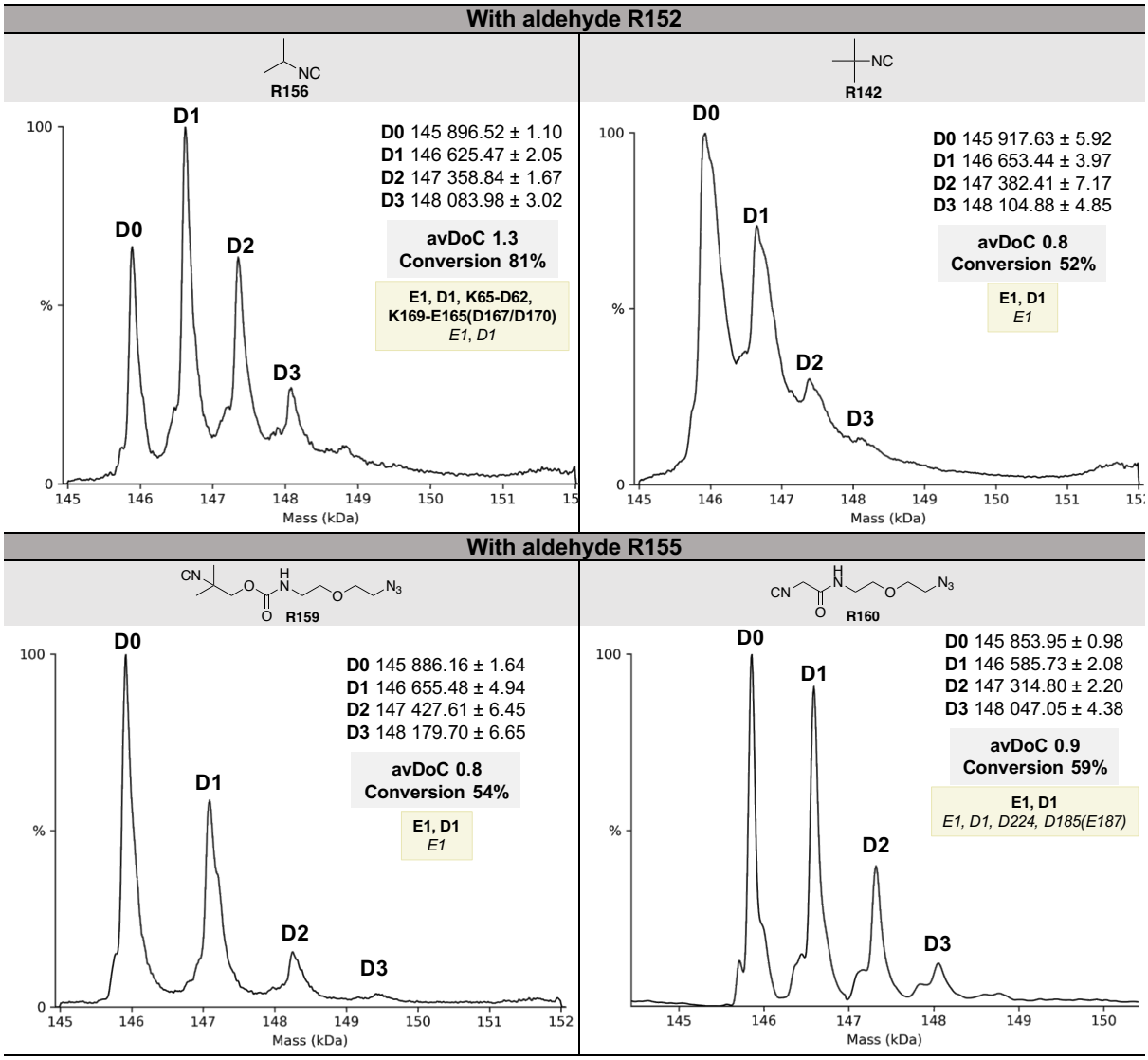

With isocyanide R158

R155

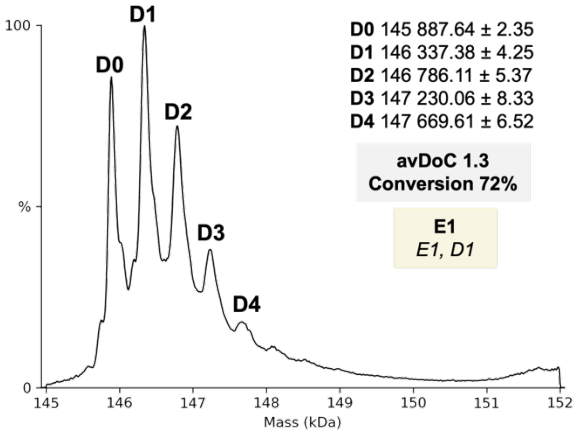

Figure 21. Native mass spectra of samples from the isocyanide and the aldehyde scope. Conversion, avDoC, and conjugation sites (**Ugi** and *Passerini*) are given.

4.1.4.4. mAb scope

4.1.4.4.1. Using aldehyde **R152** and cyclohexyl isocyanide **R133**

The influence of the mAb source on the average degree of conjugation (avDoC), conversion rate and conjugation site was evaluated. The spectra of these samples analysed by nMS and the conjugation sites provided by peptide mapping are illustrated in **Figure 22**.

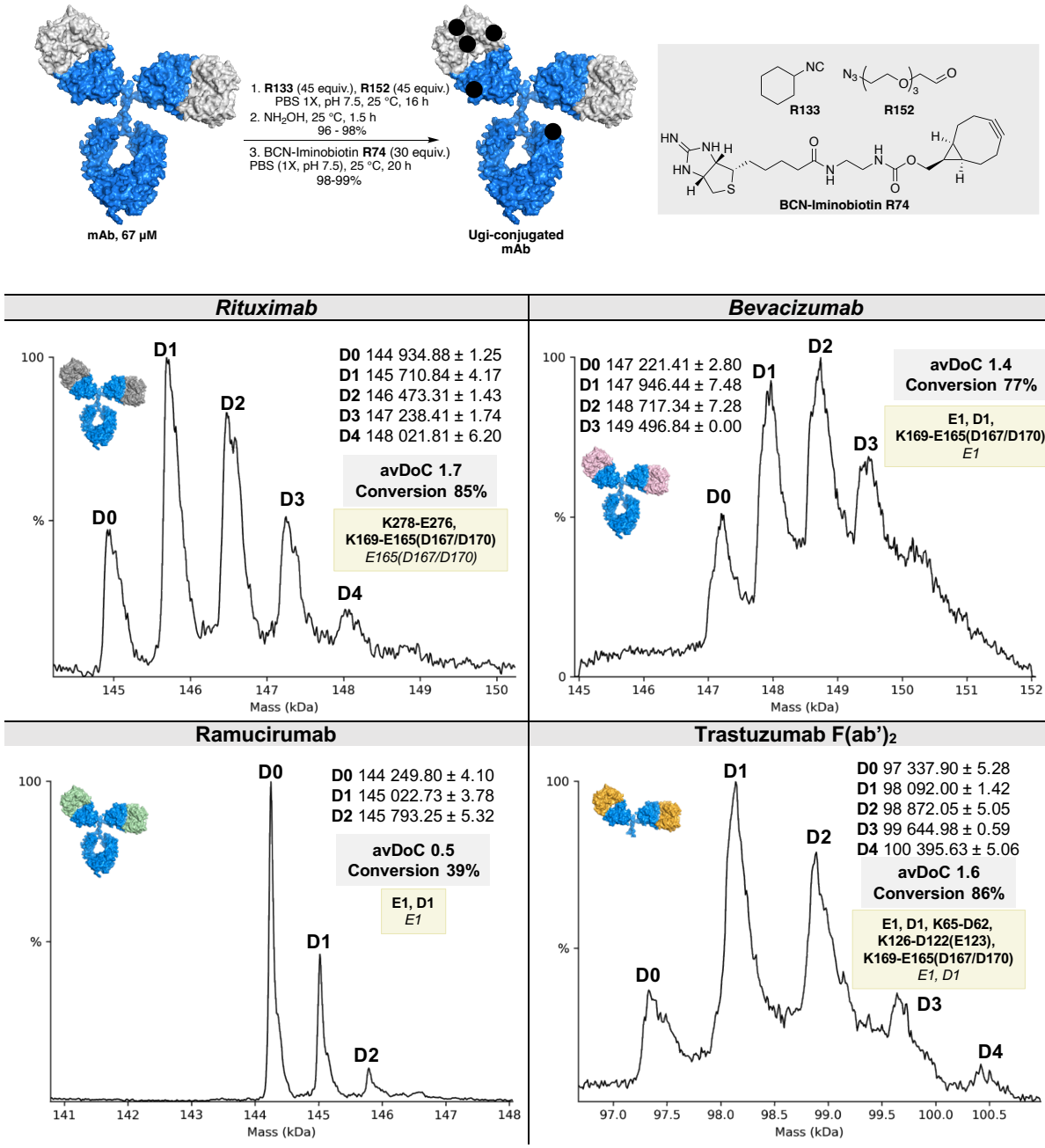

Figure 22. Native mass spectra of samples from the mAb scope using aldehyde 2 and isocyanide 1. Conversion, avDoC, and conjugation sites (**Ugi** and *Passerini*) are given.

4.1.4.4.2. Using aldehyde **R152** and ethyl isocyanoacetate **R157**

The influence of the mAb source on the average degree of conjugation (avDoC), conversion rate and conjugation site was evaluated. The spectra of these samples analysed by nMS and the conjugation sites provided by peptide mapping are illustrated in **Figure 23**.

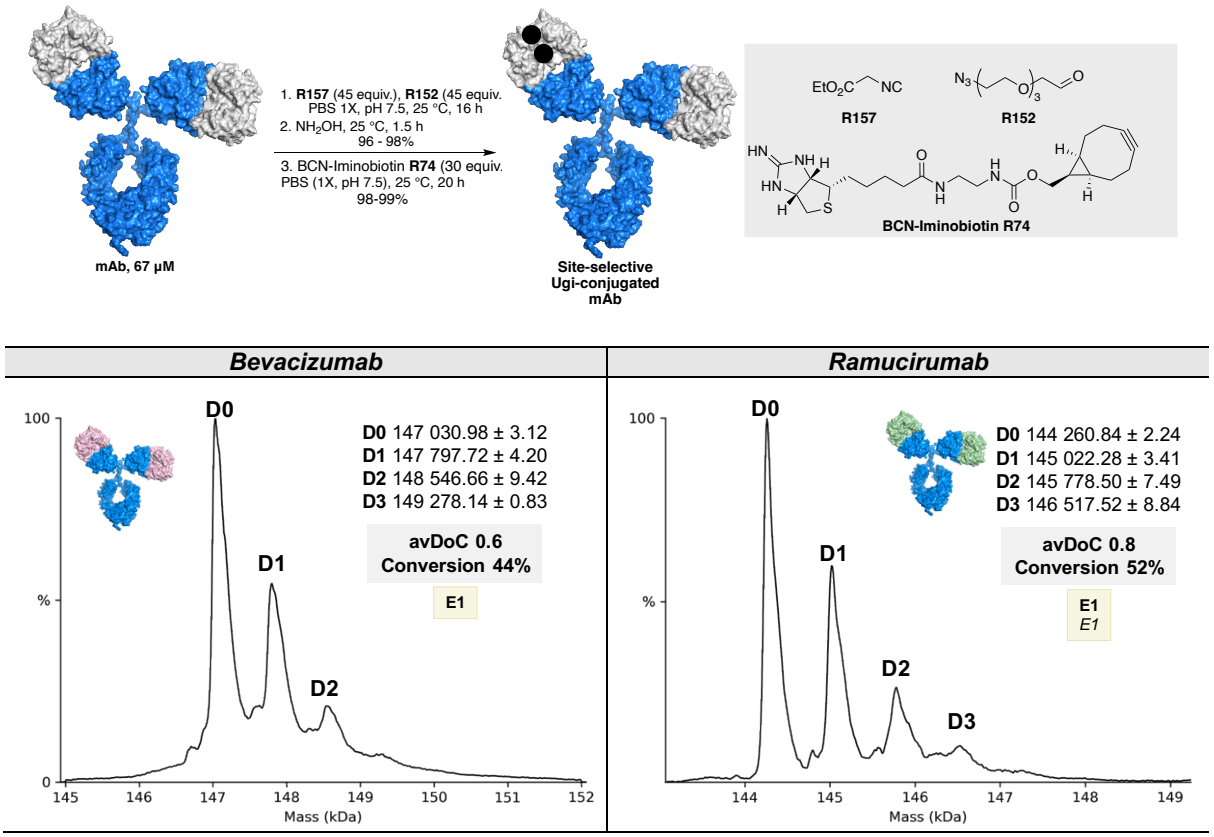

Figure 23. Native mass spectra of samples from the mAb scope using aldehyde 2 and isocyanide 4. Conversion, avDoC, and conjugation sites (**Ugi** and *Passerini*) are given.

4.1.5. Peptide mapping analyses

Peptide identification for Trastuzumab samples

Table 6. Conjugation sites observed by peptide mapping for the ugi reaction on Trastuzumab. U for ugi reaction, p for passerini reaction.

	Conjugation sites				
Samples	E1 (HC)	D1 (LC)	D62-K64 (HC)	E275-K277 (HC)	K169-D170 (LC)
cHexNC	U, P	U, P	U	U	U
EtO_2CCH_2NC	U	-	-	-	-

Chemo-selective conditions

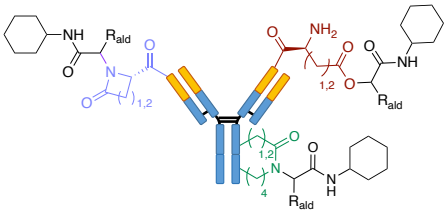

Ugi modified mAb R154

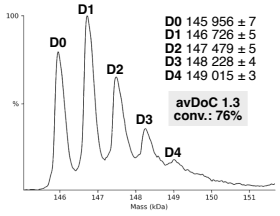

MS profile by LCT

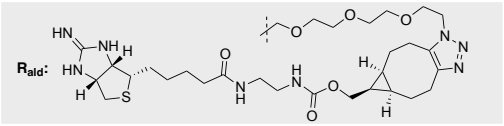

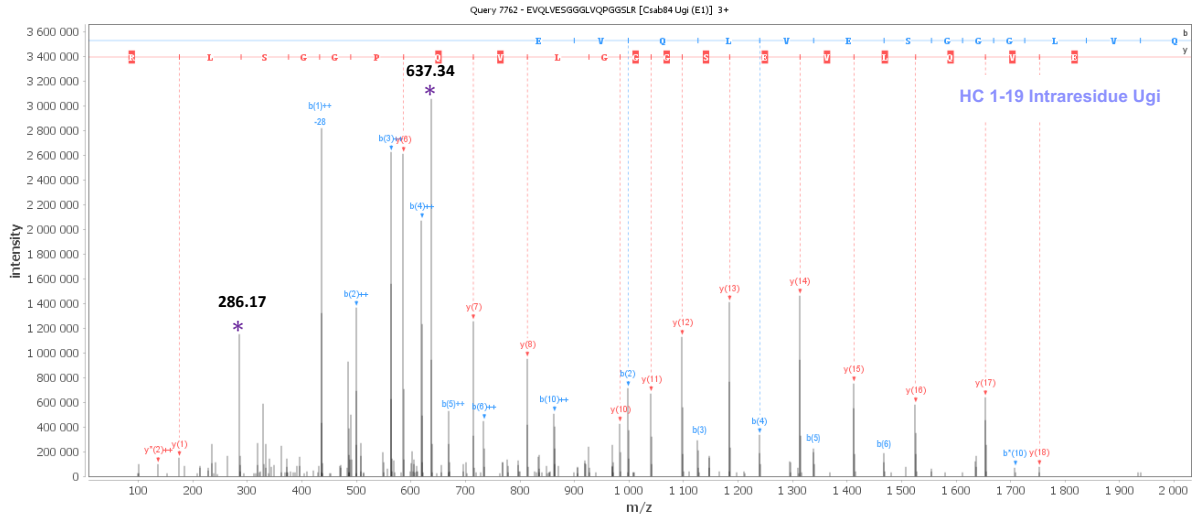

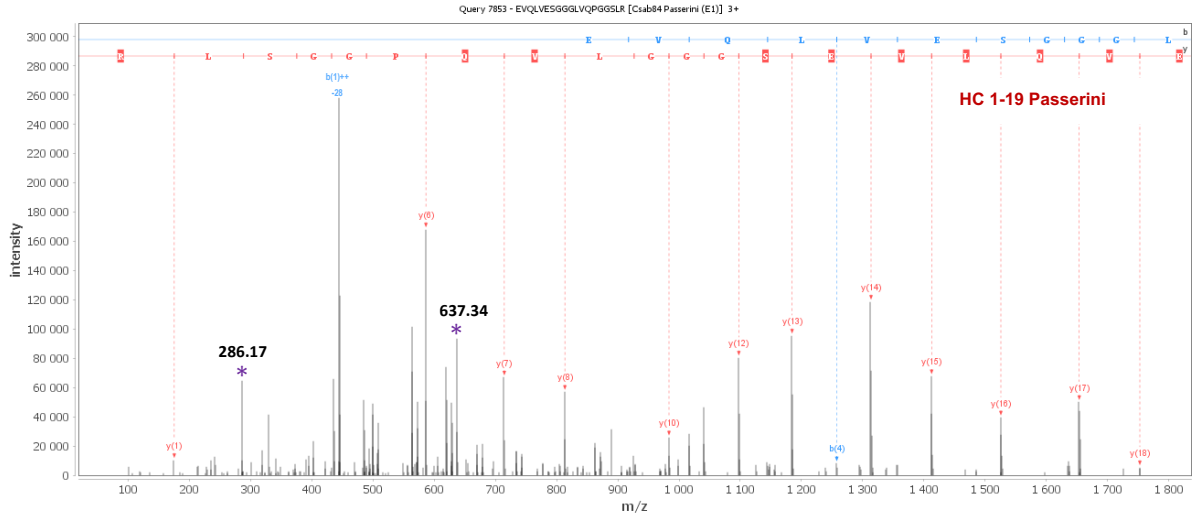
Query 7853 - EVQLVESGGGLVQPGGSLR [Csab84 Passerini (E1)] 3+
HC 1-19 Passerini
637.34
286.17
intensity
m/z

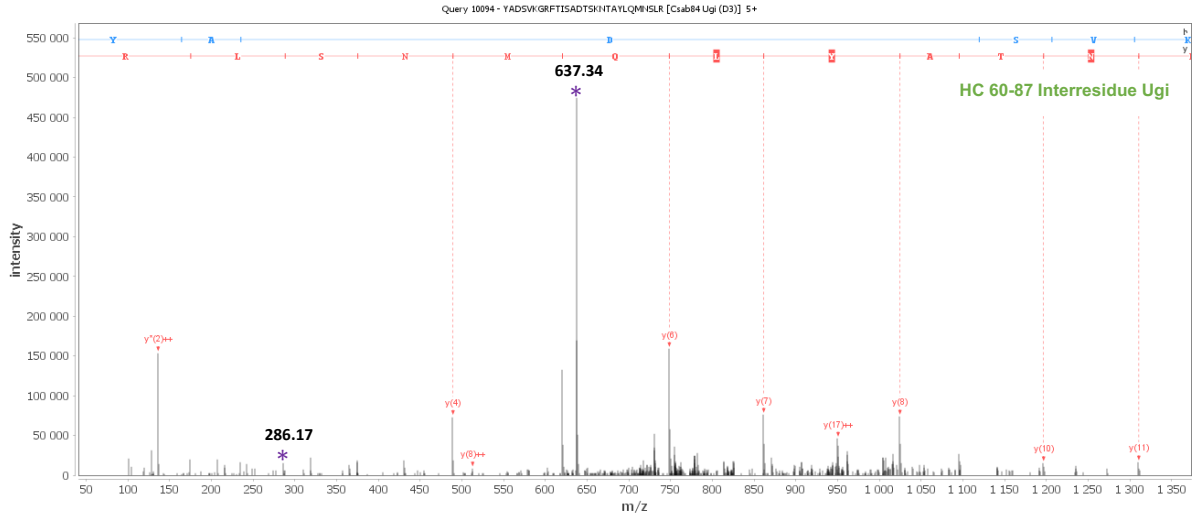
Query 10094 - YADSVKGRFTISADTSKNTAYLQMNSLR [Csab84 Ugi (D3)] 5+
HC 60-87 Interresidue Ugi
637.34
286.17
intensity
m/z

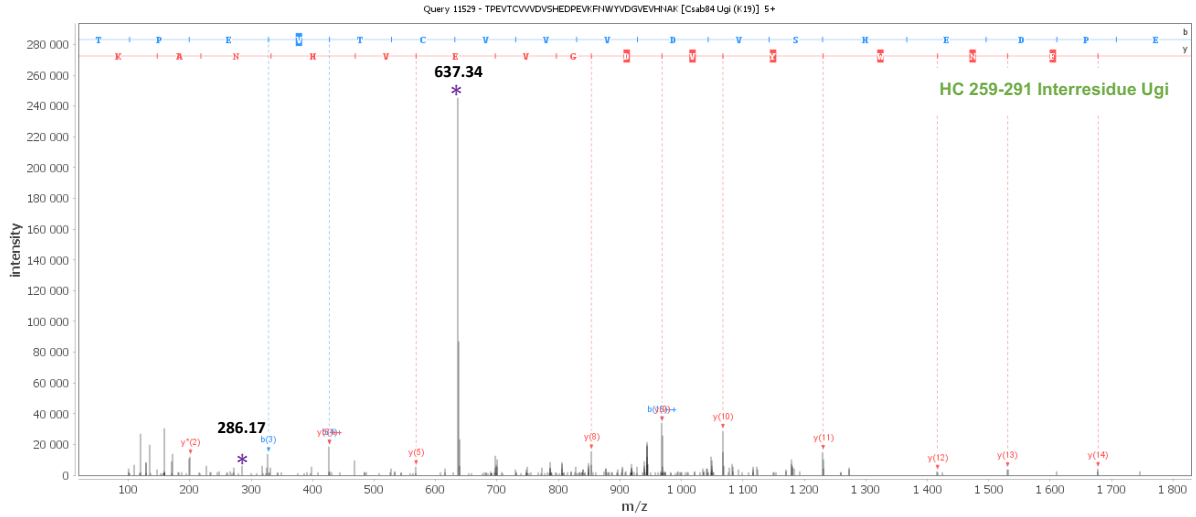
Query 11529 - TPEVTCVVVDVSHEDPEVKFNWYVDGVEVHNAK [Csab84 Ugi (K19)] 5+
HC 259-291 Interresidue Ugi
637.34
286.17
intensity
m/z

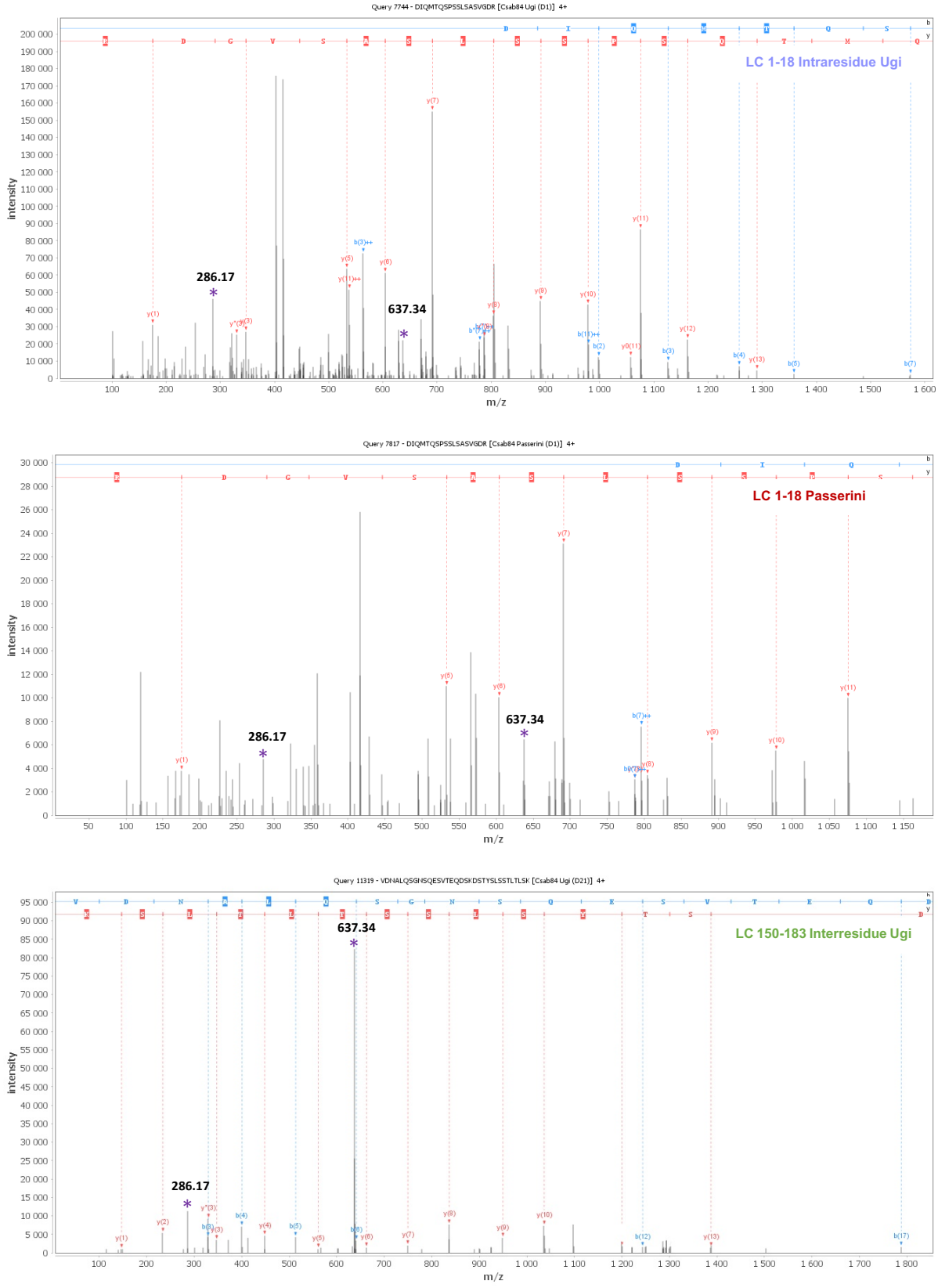

Figure 24. MS/MS spectra of each conjugated peptides validated by peptide mapping for Trastuzumab modified by cHex-NC **R133** / N_3PEG_3CHO **R152** (45/45 equiv.) and functionalized by BCN-Iminobiotin **R74** (30 equiv.). Three types of reactions were identified here; an intraresidue Ugi reaction on the E1/D1 between the *N*-terminal and the

carboxylate group, a Passerini reaction on the carboxylate group of E1/D1& and interresidue Ugi reaction between special close Lysine and Aspartate/Glutamate.

Regio-selective conditions

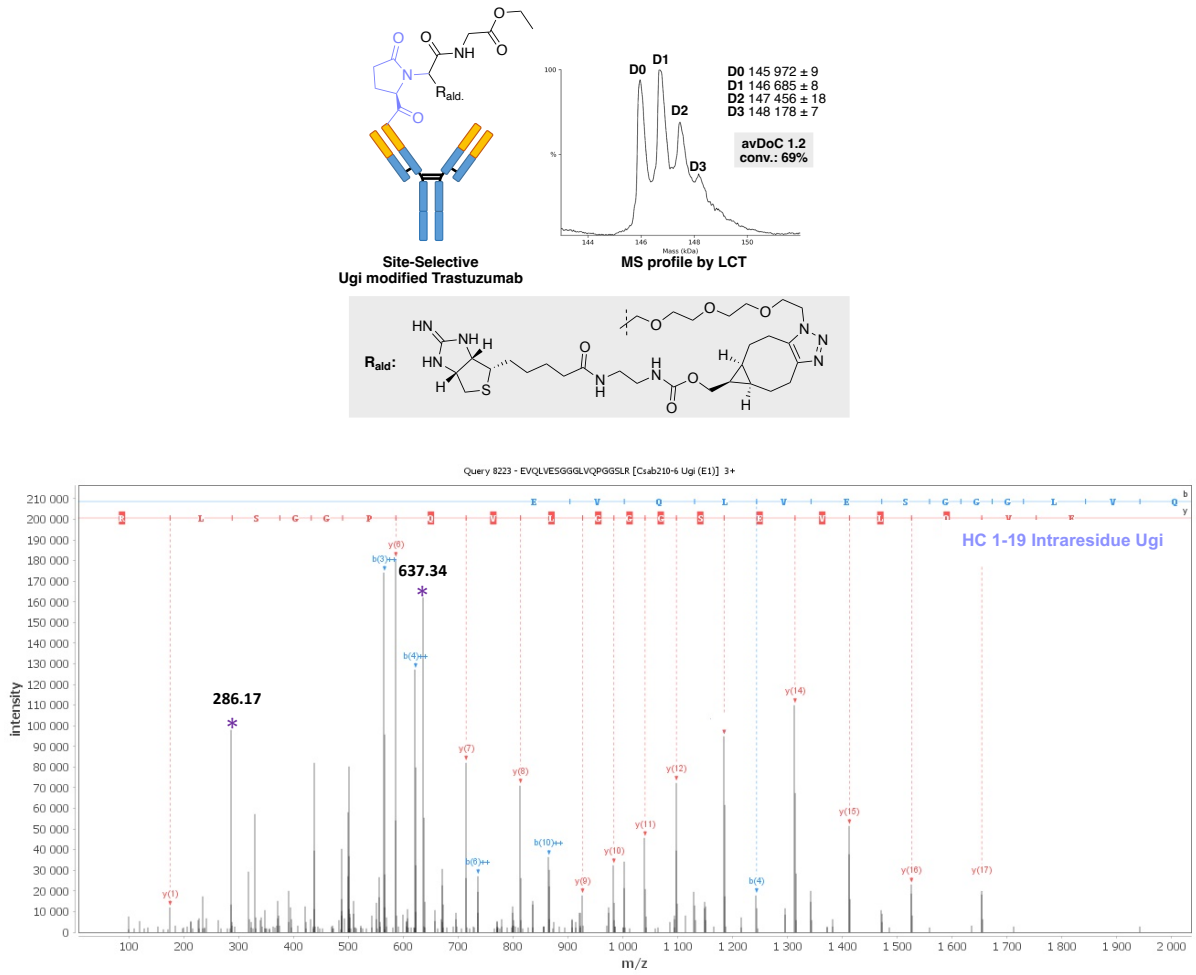

Figure 25. MS/MS spectra of each conjugated peptides validated by peptide mapping for Trastuzumab modified by EtO_2CCH_2-NC **R157** / N_3PEG_3CHO **R152** (45/45 equiv.) and functionalized by BCN-Iminobiotin **R74** (30 equiv.). Only one type of reaction was identified here; an intraresidue Ugi reaction on the E1 between the *N*-terminal and the carboxylate group.

Peptide identification for Anticalin samples

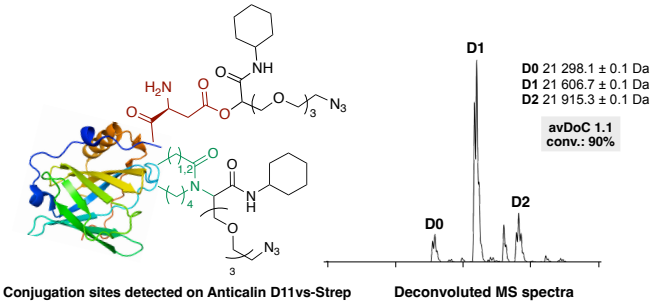

Conjugation sites detected on Anticalin D11vs-Strep Deconvoluted MS spectra

Table 7. Conjugation sites observed by peptide mapping for the Ugi reaction on Trastuzumab. U for Ugi reaction, P for Passerini reaction.

	Conjugation sites	
Anticalin	D2 / D6	D45-K46
D11vs	P	U
D11vs(NΔ6)	-	U
D11vs(K46R)	P	-
D11vs(NΔ6/K46R)	-	-

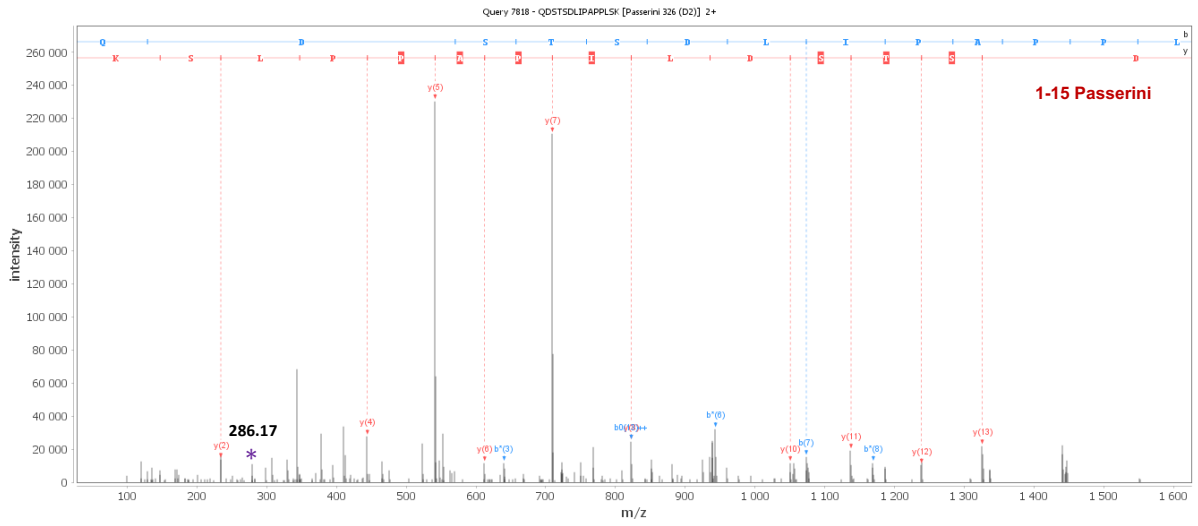

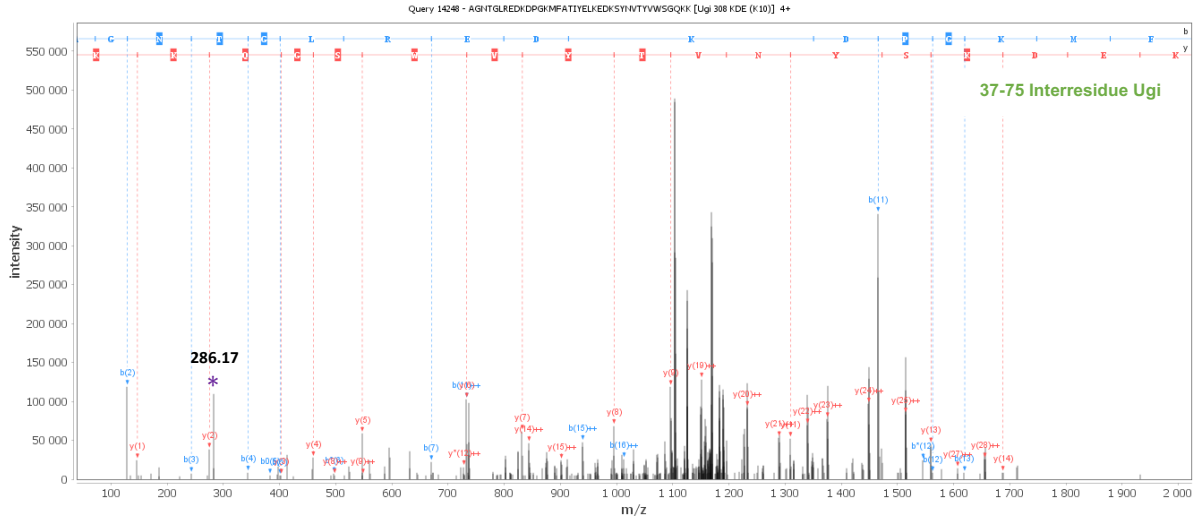

Figure 26. MS/MS spectra of each conjugated peptides validated by peptide mapping for Anticalin D11vs-Strep modified by cHex-NC **R133** / N_3PEG_3CHO **R152** (25/25 equiv.). A Passerini reaction on the carboxylate group of either D2 or D6 & an interresidue Ugi reaction between special close K46 and D45 was identified.

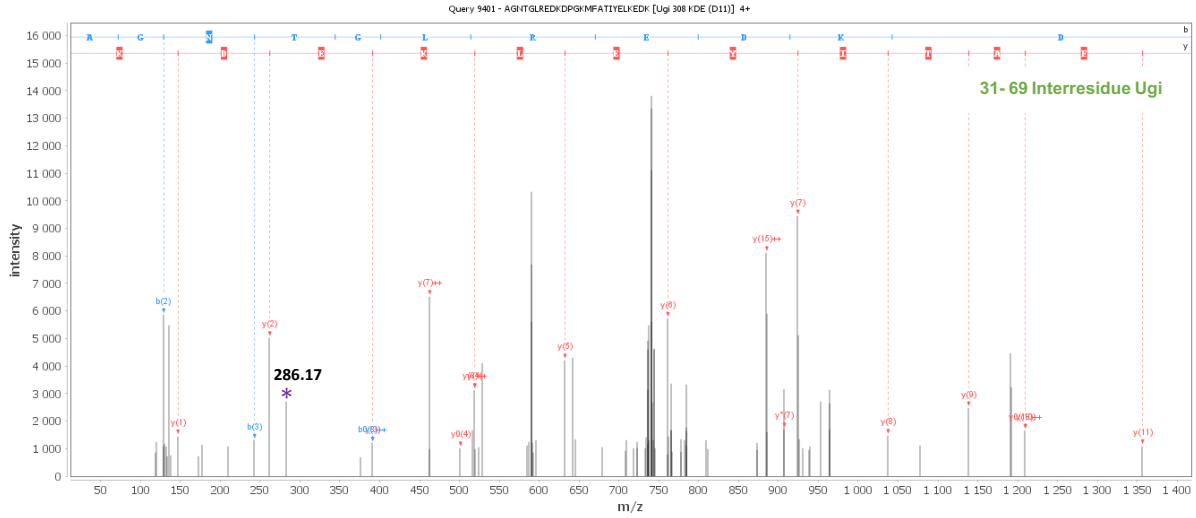

Figure 27. MS/MS spectra of each conjugated peptides validated by peptide mapping for Anticalin D11vs-SDM-(Q1-D6)N.-Strep modified by cHex-NC **R133** / N_3PEG_3CHO **R152** (25/25 equiv.). On this mutant only an interresidue Ugi reaction between special close K46 and D45 was identified.

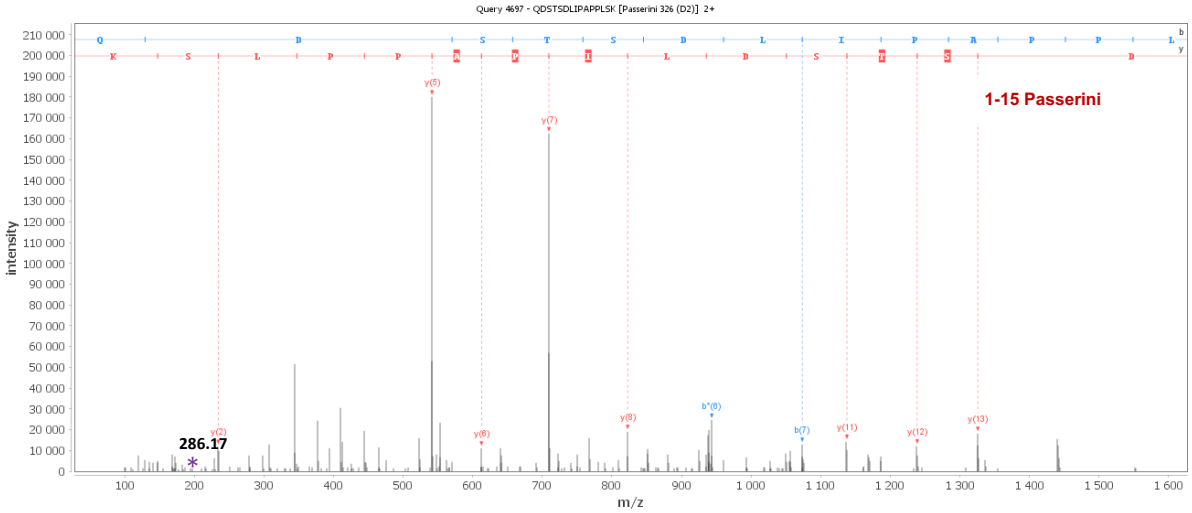

Figure 28. MS/MS spectra of each conjugated peptides validated by peptide mapping for Anticalin D11vs-SDM.K46R.-Strep modified by cHex-NC **R133** / N_3PEG_3CHO **R152** (25/25 equiv.). On this mutant only a Passerini reaction on the carboxylate group of either D2 or D6 was detected.

4.2. MATERIALS AND METHODS (UNIVERSITY COLLEGE LONDON, UNITED KINGDOM)

SYNTHETIC CHEMISTRY

All chemical reagents were purchased from commercial sources such as Sigma Aldrich (Merck), Fischer Scientific or Alfa Aesar and were used without prior purification. All reactions were carried out under an atmosphere of argon in flame-dried glassware with magnetic stirring. Reactions performed at 0 °C were cooled with an ice and H_2O bath. Concentration *in vacuo* refers to distillation on a Büchi rotary evaporator, and where appropriate, under high vacuum.

Analytical thin layer chromatography (TLC) was performed using pre-coated silica gel plates 60 F254 purchased from VWR. TLC plates were initially examined under a 254 or 365 nm UV light and then developed using aqueous potassium permanganate or ninhydrin stains, when appropriate. Flash column chromatography was carried out with pre-loaded FlashPure® silica flash cartridges on a Biotage® Isolera Spektra One flash chromatography system.

BIOMOLECULES

All reagents, enzymes and solvents were obtained from commercial sources; Sigma Aldrich, UK, Fischer Scientific UK or VWR UK, and were used without prior purification. UV-Vis spectroscopy was used to determine protein concentrations by a NanoDrop spectrophotometer (Thermo Fisher Scientific, London, UK) at 280 nm at ambient temperature. Sample buffer was used as blank for baseline correction. Extinction coefficients for proteins (at A_{280}) and payloads (at A_{MAX}) are listed below. A correction factor was applied in the event that the conjugated payload had a competing absorption at A_{280}, which is listed in the table below.

Table 8. Extinction coefficients for proteins (at A280).

Protein	Extinction Coefficient ε_{280} (M^{-1} cm^{-1})
Trastuzumab	215 000
Trastuzumab Fab	68 590

Table 9. Extinction coefficient for the conjugated payloads on proteins (at A280) alongside with their correction factor.

Payload	Extinction Coefficient (M^{-1} cm^{-1})			Correction Factor
	ε_{280}	ε_{335}	ε_{495}	
Pyridazinedione Scaffolds	2 275	9 100	-	0.25
AlexaFluor-488	8 030	-	73 000	0.11

Corrected A_{280} = Experimental A_{280} – (A_{MAX} × Correction Factor)

Buffers were prepared with double-deionized H_2O and filter sterilized (0.20 µm). Conjugation buffer contains 40 mM phosphate, 20 mM NaCl, 6 mM ethylenediaminetetraacetic acid (EDTA), pH 7.4. Incubation of digestion, reduction and conjugation experiments took place either in an eppendorf thermomixer comfort (catalog # 5355) or in a Digital heated shaker dry bath (Ref.: 88880027).

Protein, antibody, or fragment antigen-binding (Fab) conjugates were purified by gel filtration chromatography on Zeba™ Spin Desalting Columns, 7K MWCO, 0.5 mL (Thermo Fisher Scientific, Pierce Biotechnology, USA). Vivaspin micro-concentrators (500 µL, 50 kDa, 30 kDa, 10 kDa and 3 kDa cutoff) from Sartorius (Gottingen, Germany) were used for buffer exchange. Antibody deglycosylation was achieved by incubating PNGAse F (ThermoFischer, UK)

SPECTROSCOPY AND SPECTROMETRY

^{1}H NMR spectra were obtained at 400, 500 or 600 MHz. **^{13}C NMR** spectra were obtained at 150 MHz. All results were obtained using Bruker NMR instruments, the models are as follows: Avance III 600, DRX 500 and Avance III 400. All samples were run at the default number of scan and at ambient temperature. Chemical shifts (δ) for ^{1}H and ^{13}C NMR are quoted relative to residual signal of the solvent on a parts per million (ppm) scale. Where amide rotamers are the case, and when possible, only the major rotamer has been assigned for chemical shifts, and areas underneath all rotameric peaks have been considered for integration calculations. Coupling constants (*J* values) are reported in Hertz (Hz) and are reported as *JH-H* couplings.

IR were obtained on a Perkin Elmer Spectrum 100 FTIR spectrometer operating in ATR mode.

Analytical LC-MS analysis of small molecules was obtained from the UCL mass spectroscopy service on either an Agilent 6 510 QTOF LC-MS system or Waters Acquity uPLC mass spectrometer.

Molecular masses of proteins were measured using an Agilent 6 510 QTOF LC-MS system (Agilent, UK). Agilent 1 200 HPLC system was equipped with an Agilent PLRP-S, 1 000 A, 8 µM, 150 mm × 2.1 mm column. 10 µL of a protein sample (diluted to 0.2 mg/mL in d.d. H_2O) was separated on the column using mobile phase A (H_2O-0.1% formic acid) and B (acetonitrile - 0.1% formic acid) with an eluting gradient (as shown below) at a flow rate of 0.3 mL/min. The oven temperature was maintained at 60 °C.

Table 10. LC-MS mobile phase gradient for A/B elution:

Time (min)	Solvent A (%)	Solvent B (%)
0	85	15
2	85	15
3	68	32
4	68	32
14	65	35
18	5	95
20	5	95
22	85	15
25	85	15

Agilent 6510 QTOF mass spectrometer was operated in a positive polarity mode, coupled with an ESI ion source. The ion source parameters were set up with a VCap of 3 500 V, a gas temperature at 350 °C, a dry gas flow rate at 10 L/min and a nebulizer of 30 psig. MS-TOF was acquired under conditions of a fragmentor at 350 V, a skimmer at 65 V and an acquisition rate at 0.5 spectra/s in a profile mode, within a scan range between 700 and 4 500 *m/z*. The data was then analysed by deconvoluting a spectrum to a zero-charge mass spectrum using a maximum entropy deconvolution algorithm within the MassHunter software version B.07.00.

Deconvoluted spectra were avoided where possible in the quantification of conjugates due to differing ionisation tendencies between species with significantly different masses.

Non-reducing glycine-SDS-PAGE at 12% acrylamide running were performed following standard lab procedures. A 6% stacking gel was used and a broad-range molecular weight (MW) marker (10-250 kDa, Prestained Pageruler Plus Protein Standards, Bio-RAD) was co-run to estimate protein weights. Samples (10 µL at ~7 µM) were mixed with loading buffer (2 µL, composition for 5 × SDS: 1 g SDS, 3 mL glycerol, 6 mL 0.5 M Tris buffer pH 6.8, 2 mg bromophenol blue in 10 mL), heated at 75 °C for 5 min. Samples were subsequently loaded into the wells in a volume of 5 µL. The gels were run at 70 V for 15 – 30 min and then 150 V for 30 min. Gels were stained using Coomassie blue dye.

4.2.1. Chemical procedures and characterizations

Di-*tert*-butyl-1-methylhydrazine-1,2-dicarboxylate R7

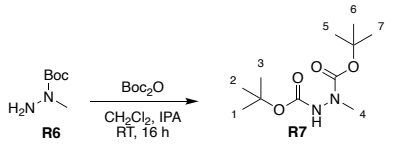

To a solution of N-methyl(tert-butoxy)carbohydrazide **R6** (2.03 mL, 13.68 mmol, 1 equiv.) in IPA (9.6 mL), was added drop wise di-*tert*-butyl dicarbonate (3.14 g, 14.36 mmol, 1.05 equiv.) pre-dissolved in DCM (3.2 mL) over 30 min. The reaction was stirred at 21 °C for 16 h, before the solvents were removed *in vacuo* and the crude residue was purified *via* column chromatography (100% cHex to 4:1 cHex/EtOAc) to afford the title compound **R7** (3 g, 12.18 mmol) as a white solid in 89% yield.

^{1}H NMR (600 MHz, $CDCl_3$, rotamers) δ_H 6.41–6.16 (s, NH) 3.11 (s, 3H, H4), 1.47–1.46 (m, H1-3, H5-7).

^{13}C NMR (150 MHz, $CDCl_3$, rotamers) δ_C 155.9 (2C), 81.3 (2C), 37.5, 28.3 (6C).

NMR analysis was found to be in agreement with previously reported characterization data.[126]

Di-*tert*-butyl-1-(3-tert-butoxy)-3-oxopropyl)-2-methylhydrazine-1,2-dicarboxylate R11

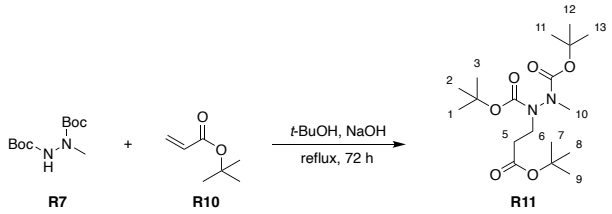

To a solution of di-*tert*-butyl-1-methylhydrazine-1,2-dicarboxylate **R7** (3 g, 12.18 mmol, 1 equiv.) in *tert*-butanol (20 mL), was added 2 M NaOH (0.4 mL) and the resulted mixture was stirred at 21 °C for 10 min. Then, *tert*-butyl acrylate **R10** (5.3 mL, 36.54 mmol, 3 equiv.) was added and the reaction mixture was heated to 82 °C. 7 h later, the solvent was removed *in vacuo* and the crude residue was dissolved in EtOAc (150 mL) and washed with H_2O (3 × 50 mL). The organic layer was dried over Na_2SO_4 and concentrated *in vacuo* to afford the title compound **R11** (4.35 g, 11.62 mmol as a yellow oil in 95% yield.

^{1}H NMR (600 MHz, $CDCl_3$, rotamers) δ_H 3.84-3.51 (m, 2H, H6), 3.06-2.99 (m, 3H, H10), 2.55-2.49 (m, 2H, H5), 1.48-1.42 (m, H1-3, H7-9, H11-13).

^{13}C NMR (150 MHz, $CDCl_3$, rotamers) δ_C 169.2, 153.6, 152.5, 79.2 (3C), 42.7, 34.8, 32.3, 26.5 (9C).

NMR analysis was found to be in agreement with previously reported characterization data.[126]

3-(2-Methyl-3,6-dioxo-3,6-dihydropyridazin-1(2*H*)-yl)propanoic acid R13

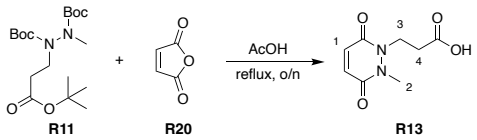

R11 R20 R13

Maleic anhydride **R20** (0.68 g, 6.89 mmol, 1.2 equiv.) was dissolved in acetic acid (65 mL) and heated to 130 °C for 30 min. To this solution, di-tert-butyl-1-(3-(*tert*-butoxy)-3-oxopropyl)-2-methylhydrazine-1,2- dicarboxylate **R11** (2.15 g, 5.74 mmol, 1 equiv.) was added and the reaction was left to react at 130 °C for 16 h. Then, the reaction mixture was concentrated *in vacuo* with toluene co-evaporation (3 × 30 mL, as an azeotrope) and the crude residue was purified *via* flash column chromatography (100% EtOAc to 1:4 MeOH/EtOAc, cont. 1% AcOH) to afford the title compound **R13** (330 mg, 1.67 mmol) as a light brownish solid in 29% yield.

^{1}H NMR (500 MHz, DMSO) δ_H 12.44 (s, 1H, OH), 6.92 (dd, *J* = 13.3, 10.1 Hz, 2H, H1), 4.22 (t, *J* = 7.4 Hz, 2H, H3), 3.51 (s, 3H, H2), 2.58 (t, *J* = 7.4 Hz, 2H, H4).

^{13}C NMR (126 MHz, DMSO) δ_C 171.9, 156.6, 156.5, 134.5, 134.2, 41.2 (*C*H_3), 32.5, 32.0.

νmax (thin film) /cm^{-1} 3077, 1715, 1594, 1560.

HRMS (ESI$^+$) calcd for $C_8H_{11}N_2O_4^+$ $[M+H]^+$ 199.0719, found 199.0715.

2,5-Dioxopyrrolidin-1-yl 3-(2-methyl-3,6-dioxo-3,6-dihydropyridazin-1(2*H*)-yl) propanoate R15

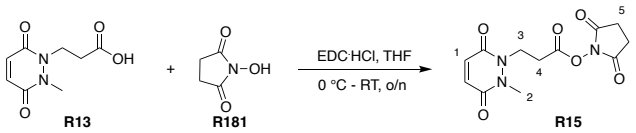

To a solution of 3-(2-methyl-3,6-dioxo-3,6-dihydropyridazin-1(2*H*)-yl)propanoic acid **R13** (250 mg, 1.26 mmol, 1 equiv.) in THF (45 mL), pre-cooled to 0 °C, *N*,*N*'-dicyclohexylcarbodiimide (266 mg, 1.39 mmol, 1.1 equiv.) was added. The homogenous solution was stirred at 0 °C for 30 min. Subsequently, *N*-hydroxysuccinimide **R181** (166.96 mg, 1.45 mmol, 1.15 equiv.) was added and the reaction was stirred at 21 °C for a further 16 h. The newly formed heterogenous mixture was filtered through a Celite® pad and the filtrates were concentrated *in vacuo*. Purification of the crude residue *via* flash column chromatography (1:1 cHex/EtOAc to 100% EtOAc) afforded the title compound **R15** (162 mg, 0.55 mmol) as a beige solid in 43% yield.

^{1}H NMR (500 MHz, $CDCl_3$) δ_H 6.90 (dd, *J* = 25.5, 10.1 Hz, 2H, H1), 4.43 (t, *J* = 7.0 Hz, 2H, H3), 3.60 (s, 3H, H2), 3.05 (q, *J* = 6.3 Hz, 2H, H4), 2.84 (s, 4H, H5).

^{13}C NMR (150 MHz, $CDCl_3$) δ_C 168.8, 166.1 (2C), 157.5, 157.4, 135.3, 134.2, 41.2, 33.3, 29.2, 25.7 (2C).

νmax (thin film) /cm^{-1} 2936, 1817, 1782, 1736, 1625, 1583.

((1*R*,8*S*,9*S*)-Bicyclo[6.1.0]non-4-yn-9-yl)methyl (2-(2-(2-(3-(2-methyl-3,6-dioxo-3,6-dihydropyridazin-1(2*H*)-yl)propanamido)ethoxy)ethoxy)ethyl)carbamate R18

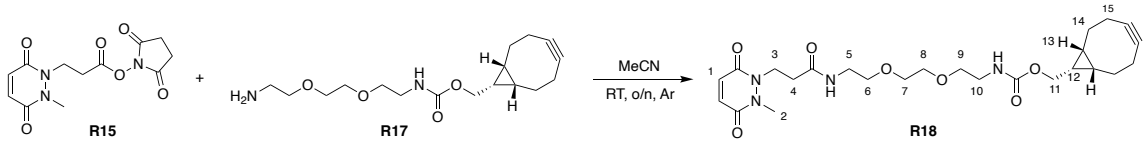

R15 R17 R18

To a solution of 2,5-dioxopyrrolidin-1-yl 3-(2-methyl-3,6-dioxo-1,2,3,6-tetrahydropyridazin-1-yl)propanoate **R15** (39.95 mg, 0.11 mmol, 1 equiv.) in acetonitrile (10 mL), *N*- [(1*R*,8*S*,9*S*)-bicyclo[6.1.0]non-4-yn-9-ylmethyloxycarbonyl]-1,8-diamino-3,6-dioxaoctane **R17** (36 mg, 0.11 mmol, 1 equiv.) was added and the reaction was stirred at 21 °C for 16 h. Then, acetonitrile was removed *in vacuo* and the crude residue was partitioned between chloroform (50 mL) and H_2O (30 mL). The organic layer was washed with H_2O (1 × 30 mL), K_2CO_3 (1 × 30 mL, aq., sat.), dried over $MgSO_4$ and concentrated *in vacuo.* Purification of the crude residue *via* flash column chromatography (100% EtOAc to 1.5:8.5 MeOH/EtOAc) afforded the title compound **R18** (47.3 mg, 0.094 mmol) as an orangish oil in 84% yield.

^{1}H NMR (600 MHz, $CDCl_3$) δ_H 6.88 (dd, *J* = 22.5, 10.4 Hz, 2H, H1), 6.36 (s, 1H, NH), 5.33 (s, 1H, NH), 4.38 (t, *J* = 7.2 Hz, 2H, H3), 4.14 (dd, *J* = 21.6, 13.0 Hz, 2H, H11), 3.65 (s, 3H, H2), 3.63 – 3.48 (m, 8H, H6-9), 3.44 (q, *J* = 5.3 Hz, 2H, H5), 3.41 – 3.33 (m, 2H, H10), 2.59 (t, *J* = 7.3 Hz, 2H, H4), 2.29 – 2.19 (m, 4H, H15), 1.65 – 1.32 (m, 4H, H14), 1.01 – 0.89 (m, 2H, H13), 0.89 – 0.80 (m, 1H, H12).

^{13}C NMR (126 MHz, $CDCl_3$) δ_C 169.3, 156.9, 153.0 (2C), 135.4 (2C), 98.9, 70.3 (4C) 66.7, 44.6, 40.9, 39.5, 35.2, 34.1, 29.8, 29.1, 22.8, 20.2, 17.9.

νmax (thin film) /cm^{-1} 3311, 3073, 2917, 2850, 1708, 1629, 1537, 1247, 1098, 729.

HRMS (ESI$^+$) calcd for $C_{25}H_{36}N_4O_7^+$ $[M+H]^+$ 505.2657; found 502.2652.

Di-*tert*-butyl 1-phenylhydrazine-1,2-dicarboxylate R9

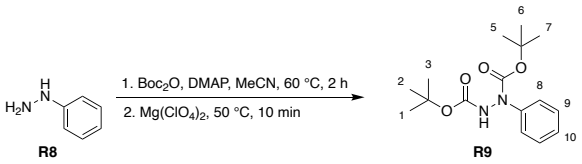

To a solution of phenylhydrazine **R8** (0.99 mL, 10 mmol, 1 equiv.) in acetonitrile (27 mL), di-*tert*-butyl dicarbonate (9.17 g, 42 mmol, 4.2 equiv.) and 4-dimethylaminopyridine (cat.) were added and the reaction was stirred at 60 °C for 2 h. Then, the heating was dropped to 50 °C, magnesium perchlorate (0.45 g, 2 mmol, 0.2 equiv.) was added, and the reaction was completed 10 min later. The reaction mixture was then cooled down to RT and was quenched with a 100 mL 1:3 mixture $Na_2S_2O_4$ (sat., aq.) / brine. The resulted biphasic solution was extracted with EtOAc (2 × 100 mL). The combined organics were washed with $NaHCO_3$ (aq., sat., 150 mL) and brine (150 mL), dried over Na_2SO_4 and concentrated *in vacuo*. The crude product was triturated in EtOH at -10 °C to afford the title compound **R9** (2.9 g, 9.4 mmol) as a white solid in 94% yield.

^{1}H NMR (600 MHz, $CDCl_3$, rotamers) δ_H 7.42 (d, *J* = 12.6 Hz, 2H, H8), 7.31 (t, *J* = 7.8 Hz, 2H, H9), 7.15 (t, *J* = 7.4 Hz, 1H, H10), 6.76 (s, 1H, NH), 1.49 (s, 18H, H1-3, H5-7).

^{13}C NMR (151 MHz, $CDCl_3$) δ_C 155.5, 153.8, 142.3, 128.6 (2C), 125.7 (2C), 123.8, 82.4, 81.7, 28.3 (d, 9C).

ν_{max} (thin film) /cm^{-1} 3283, 2980, 1713, 1509, 1249, 1148, 692.

HRMS (**(ESI$^+$)** calcd for $C_{16}H_{24}N_2O_4Na^+$ $[M+Na]^+$ 331.1628; found 331.1623.

Di-*tert*-butyl 1-(3-(*tert*-butoxy)-3-oxopropyl)-2-phenylhydrazine-1,2-dicarboxylate R11

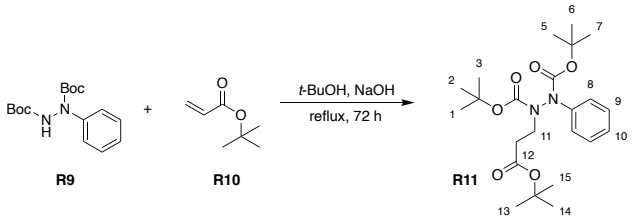

To a solution of di-*tert*-butyl 1-phenylhydrazine-1,2-dicarboxylate **R9** (500 mg, 1.62 mmol, 1 equiv.) in *tert*-butanol (2.6 mL), was added 2 M NaOH (0.05 mL) and the reaction mixture was stirred at 21 °C for 10 min. *Tert*-butyl acrylate **R10** (0.706 mL, 4.86 mmol, 3 equiv.) was then added to the above solution and the reaction mixture was refluxed at 82 °C. 72 h later, the volatiles were removed *in vacuo* and the crude residue was partitioned between EtOAc (100 mL) and H_2O (3 × 50 mL). The organic layer was washed with H_2O (3 × 50 mL), dried over Na_2SO_4 and concentrated *in vacuo* to afford the title compound **R11** (549 mg, 1.26 mmol) as a yellow oil in 78% yield.

^{1}H NMR (600 MHz, DMSO) δ_H 7.32 (m, 4H, H8-9), 7.17 – 7.11 (t, *J* = 6.6 Hz, 1H, H10), 3.79 – 3.66 (m, 2H, H11), 2.59 – 2.44 (m, 2H, H12), 1.53 (d, *J* = 18.4 Hz, 9H, H13-15), 1.48 (d, *J* = 8.7 Hz, 9H, H5-7), 1.38 (d, *J* = 7.3 Hz, 9H, H1-3).

^{13}C NMR (151 MHz, $CDCl_3$) δ_C 170.9, 153.0 (2C), 141.1, 128.6 (2C), 125.5 (2C), 122.5, 82.3, 81.9, 45.5, 33.9, 28.5 (3C), 28.4 (6C).

ν_{max} (thin film) /cm^{-1} 3370, 2977, 2931, 1722, 1368, 1152.

HRMS (ESI$^+$) calcd for $C_{23}H_{36}N_2O_6^+$ $[M+H]^+$ 437.2646; found 437.2640.

3-(3,6-Dioxo-2-phenyl-3,6-dihydropyridazin-1(2*H*)-yl)propanoic acid R14

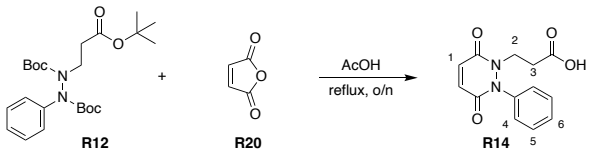

R12 R20 R14

Maleic anhydride **R20** (76.37 mg, 0.78 mmol, 1.7 equiv.) was dissolved in acetic acid (5 mL) and heated to 130 °C for 30 min. To this solution, di-*tert*-butyl-1-(3-(tert-butoxy)-3-oxopropyl)-2-phenyllhydrazine-1,2- dicarboxylate **R12** (200 mg, 0.46 mmol, 1 equiv.) was added and the reaction was left to react at 130 °C. 16 h later, the reaction mixture was concentrated *in vacuo* with toluene co-evaporation (3 × 30 mL, as an azeotrope) and the crude residue was purified *via* flash column chromatography (100% EtOAc to 1:4 MeOH/EtOAc, cont. 1% AcOH)) to afford the title compound **R14** (50 mg, 0.19 mmol) as a white solid in 42% yield.

^{1}H NMR (600 MHz, DMSO) δ_H 12.38 (s, 1H, OH), 7.52 (dd, *J* = 31.8, 8.0 Hz, 5H, H5-7), 7.04 (dd, *J* = 33.4, 10.7 Hz, 2H, H1), 3.73 (t, *J* = 7.5 Hz, 2H, H2), 2.39 (t, *J* = 7.4 Hz, 2H, H3).

^{13}C NMR (151 MHz, DMSO) δ_C 171.6, 157.3, 157.0, 136.1), 136.0, 135.0, 129.5 (2C), 129.4 (2C), 128.8, 42.2, 31.2.

νmax (thin film) /cm^{-1} 3174, 2969, 1704, 1620, 1414, 692.

HRMS (ESI^{+}) calcd for $C_{13}H_{11}N_2O_4^-$ $[M-H]^-$ 259.0724; found 259.0724.

2,5-Dioxopyrrolidin-1-yl 3-(3,6-dioxo-2-phenyl-3,6-dihydropyridazin-1(2*H*)-yl)propanoate R16

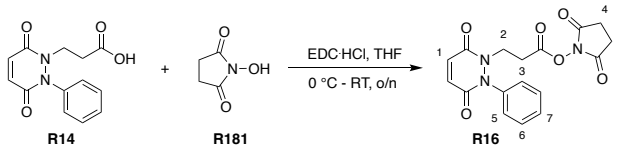

To a solution of 3-(3,6-dioxo-2-phenyl-3,6-dihydropyridazin-1(2*H*)-yl)propanoic acid **R14** (45 mg, 0.27 mmol, 1 equiv.) in THF (6.2 mL) at 0 °C, EDC·HCl (36.46 mg, 0.19 mmol, 1.1 equiv.) was added. The resulted solution was then stirred at 0 °C for 30 min. Subsequently, N-hydroxysuccinimide **R181** (29.85 mg, 0.26 mmol, 1.5 equiv.) was added and the reaction was stirred at 21 °C.16 h later, the reaction mixture was filtered through a Celite® pad and the filtrates were concentrated *in vacuo*. Purification of the crude residue *via* flash column chromatography (1:1 cHex/EtOAc to 100% EtOAc) afforded the title compound **R16** (44.8 mg, 0.13 mmol) as a beige solid in 73% yield.

^{1}H NMR (600 MHz, $CDCl_3$) δ_H 7.55 (t, *J* = 7.6 Hz, 2H, H6), 7.49 (t, *J* = 7.5 Hz, 1H, H7), 7.37 (d, *J* = 8.6 Hz, 2H, H5), 6.97 (m, 2H, H1), 4.05 (t, *J* = 7.1 Hz, 2H, H2), 2.88 (t, *J* = 7.1 Hz, 2H, H3), 2.80 (s, 4H, H4).

^{13}C NMR (151 MHz, $CDCl_3$) δ_C 168.8, 165.7 (2C), 158.0, 157.8 , 135.8 (2C),135.4 (*2C*), 130.1 (2C), 128.3, 42.1, 28.6 , 25.7 (2C).

νmax (thin film) /cm^{-1} 3359, 3069, 2978, 1702, 1618, 1508, 759.

HRMS (ESI$^+$) calcd for $C_{17}H_{16}N_3O_6^+$ $[M+H]^+$ 358.1034; found 358.1030.

((1*R*,8*S*,9*S*)-Bicyclo[6.1.0]non-4-yn-9-yl)phenyl(2-(2-(2-(3-(3,6-dioxo-2-phenyl-3,6-dihydropyridazin-1(2*H*)-yl)propanamido)ethoxy)ethoxy)ethyl)carbamate R19

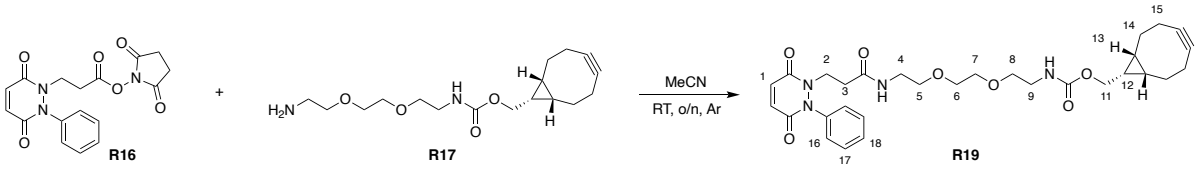

R16 R17 R19

To a solution of 2,5-dioxopyrrolidin-1-yl 3-(3,6-dioxo-2-phenyl-3,6-dihydropyridazin-1(2*H*)-yl)propanoate **R16** (33.92 mg, 0.095 mmol, 1 equiv.) in acetonitrile (6.2 mL), *N*- [(1*R*,8*S*,9*S*)-bicyclo[6.1.0]non-4-yn-9-ylmethyloxycarbonyl]-1,8-diamino-3,6-dioxaoctane **R17** (30.8 mg, 0.095 mmol, 1 equiv.) was added and the reaction was stirred at 21 °C. 16 h later, acetonitrile was removed *in vacuo* and the crude residue was partitioned between chloroform (50 mL) and H_2O (30 mL). The organic layer was washed with H_2O (30 mL) and K_2CO_3 (30 mL aq., sat.), dried over $MgSO_4$ and concentrated *in vacuo.* Purification of the crude residue *via* flash column chromatography (100% EtOAc to 1.5:8.5 MeOH/EtOAc) afforded the title compound **R19** (24 mg, 0.042 mmol) as an orangish oil in 45% yield.

^{1}H NMR (600 MHz, $CDCl_3$) δ_H 7.54 (t, *J* = 7.6 Hz, 2H, H17), 7.48 (t, *J* = 7.8 Hz, 1H, H18), 7.37 (d, *J* = 7.7 Hz, 2H, H16), 6.97 (dd, *J* = 20.3, 10.1 Hz, 2H, H1), 6.31 (s, 1H, NH), 5.34 (s, 1H, NH), 4.14 (dd, *J* = 32.7, 24.6 Hz, 2H, H11), 3.97 (t, *J* = 7.3 Hz, 2H, H2), 3.62 – 3.47 (m, 8H, H5-8), 3.37 (q, *J* = 5.3 Hz, 4H, H4, H9), 2.42 (t, *J* = 7.4 Hz, 2H, H3), 2.30 – 2.18 (m, 5H, H15), 1.67 – 1.26 (m, 4H, H14), 1.00 – 0.90 (m, 2H, H13), 0.90 – 0.80 (m, 1H, H12).

^{13}C NMR (151 MHz, $CDCl_3$) δ_C 171.8, 169.2, 157.9 (2C), 157.0, 135.8 (2C), 135.5 (2C), 130.1 (2C), 128.4, 99.0 (2C), 70.8 (4C), 69.8, 43.9, 40.9, 39.4, 33.9, 29.8, 29.2, 22.8 (2C), 20.2 (2C), 17.9 (2C).

***ν*max (thin film) /cm^{-1}** 3318, 3068, 2918, 1640, 1528, 1248, 1099, 697.

HRMS (ESI$^+$) calcd for $C_{30}H_{39}N_4O_7^+$ $[M+H]^+$ 567.2813; found 567.2810.

1-Phenyl-1,2-dihydropyridazine-3,6-dione R21

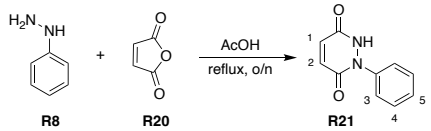

R8 R20 R21

Maleic anhydride **R20** (4.5 g, 46 mmol, 1 equiv.) was dissolved in glacial acetic acid (20 mL) and heated to 130 °C for 30 min. To this solution, phenylhydrazine **R8** (5 mL, 50.4 mmol, 1.1 equiv.) was added and the reaction was left to react at 130 °C. 16 h later, the reaction mixture was concentrated *in vacuo* with toluene co-evaporation (3 × 30 mL, as an azeotrope) and the crude residue was triturated in EtOH to afford the title compound **R21** (3.2 g, 16.8 mmol) as a yellowish powder in 33% yield.

^{1}H NMR (600 MHz, DMSO) δ_H 11.32 (s, 1H, NH), 7.55 (d, *J* = 7.9 Hz, 2H, H3), 7.46 (t, *J* = 7.7 Hz, 2H, H4), 7.36 (t, *J* = 7.4 Hz, 1H, H5), 7.17 (d, *J* = 9.7 Hz, 1H, H1), 7.01 (d, *J* = 9.7 Hz, 1H, H2).

^{13}C NMR (151 MHz, DMSO) δ_C 157.8, 152.8, 141.5, 134.0, 128.5, 127.7, 127.4 (2C), 125.5 (2C).

ν_{max} (thin film) /cm^{-1} 3059, 1659, 1243, 827.

HRMS (ESI$^+$) calcd for $C_{10}H_9N_2O_2^+$ $[M+H]^+$ 189.0659; found 189.0656.

1,2-Diphenyl-1,2-dihydropyridazine-3,6-dione R23

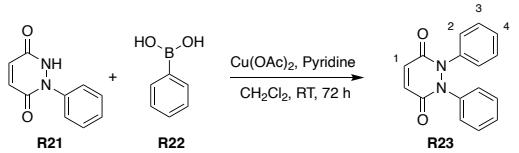

R21 R22 R23

In a right size flask, phenylboronic acid **R22** (2.43 g, 19.9 mmol, 2.5 equiv.), 1-phenyl-1,2,3,6-tetrahydropyridazine-3,6-dione **R21** (1.5 g, 8 mmol, 1 equiv.), anhydrous cupric acetate (2.17 g, 11.96 mmol, 1.5 equiv.), 750 mg activated 4 Å molecular sieves, DCM (50 mL) and pyridine (1.29 mL, 16 mmol, 2 equiv.) were charged, following this order. The reaction was stirred under air at 21 °C for 72 h. Purification of the crude product *via* flash column chromatography (4:1 to 3:7 cHex/EtOAc cont. 1% AcOH)) afforded the title compound **R23** (500 mg, 0.38 mmol,) as a yellow solid in 25% yield.

^{1}H NMR (600 MHz, DMSO) δ_H 7.33 (d, *J* = 6.9 Hz, 4H, H1, H4), 7.24 (t, *J* = 7.9 Hz, 4H, H3), 7.16 (d, *J* = 6.6 Hz, 4H, H2).

^{13}C NMR (151 MHz, DMSO) δ_C 156.7 (2C), 136.9, 135.8 (2C), 129.3 (2C), 128.5 (2C), 128.34.

ν_{max} (thin film) /cm^{-1} 3068, 2918, 2850, 1639, 760.

HRMS (ESI$^+$) calcd for $C_{16}H_{13}N_2O_2^+$ $[M+H]^+$ 265.0972; found 265.0965.

Methyl-*N*-(*tert*-butoxycarbonyl)-*S*-(3,6-dioxo-1,2-diphenylhexahydropyridazin-4-yl)-*L*-cysteinate R25

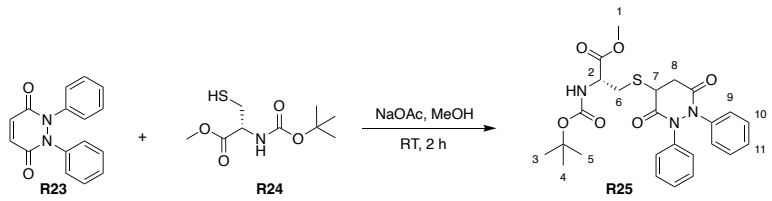

R23 R24 R25

To a solution of 1,2-diphenyl-1,2-dihydropyridazine-3,6-dione **R23** (30 mg, 0.1 mmol, 1 equiv.) in MeOH (2 mL), methyl (2*R*)-2-{[(tert-butoxy)carbonyl]amino}-3-sulfanylpropanoate **R24** (26.71 mg, 0.11 mmol, 1 equiv.) and sodium acetate (27.94 mg, 0.34 mmol, 3Âequiv.) were added and the reaction was stirred at 21 °C for 2 h. The crude product was purified *via* flash column chromatography (100% cHex to 3:7 cHex/EtOAc cont. 1% AcOH) to afford the title compound **R25** (41 mg, 0.082 mmol) as a white solid in 75% yield.

HRMS (ESI$^+$) calcd for $C_{25}H_{30}N_3O_6\,^{32}S$ $[M+H]^+$ 500.18498, observed 500.1846.

((5a*R*,6*S*,6a*S*)-1-(2-Oxo-6,9,12-trioxa-3-azatetradecan-14-yl)-1,4,5,5a,6,6a,7,8-octahydrocyclopropa[5,6]cycloocta[1,2-*d*][1,2,3]triazol-6-yl)methyl (2-(2-(2-(3-(2-methyl-3,6-dioxo-3,6-dihydropyridazin-1(2*H*)yl)propanamido)ethoxy)ethoxy)ethyl)carbamate R27

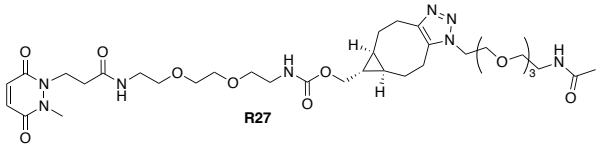

To a solution of *N*-(*2*-(*2*-(*2*-azidoethoxy)ethoxy)ethoxy)ethyl)acetamide **R26** (10 mg, 0.038 mmol) in MeCN (1 mL), was added **R18** (20 mg, 0.038 mmol) in MeCN (1 mL). The reaction mixture was stirred at RT for 2 h, prior to *in vacuo* evaporation. The crude product was purified *via* reverse phase flash column chromatography (0 to 100% acetonitrile/water) to afford the title compound **R27** (21 mg, 0.028 mmol,) as a colourless oil in 72% yield.

HRMS (ESI) calcd for $C_{35}H_{56}N_8O_{11}$ $[M+H]^+$ 765.4141, observed 765.4141.

((5a*R*,6*S*,6a*S*)-1-(2-Oxo-6,9,12-trioxa-3-azatetradecan-14-yl)-1,4,5,5a,6,6a,7,8-octahydrocyclopropa[5,6]cycloocta[1,2-*d*][1,2,3]triazol-6-yl)methyl (2-(2-(2-(3-(3,6-dioxo-2-phenyl-3,6-dihydropyridazin-1(2*H*)-yl)propanamido)ethoxy)ethoxy)ethyl)carbamate R28

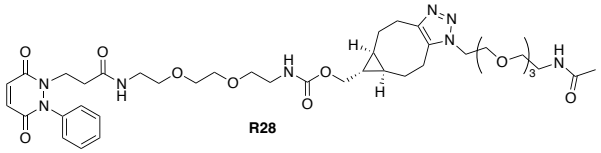

To a solution of *N*-(*2*-(*2*-(*2*-azidoethoxy)ethoxy)ethoxy)ethyl)acetamide **R26** (10 mg, 0.038 mmol, 1 equiv.) in MeCN (1 mL), was added **R19** (22 mg, 0.038 mmol, 1 equiv.) in MeCN (1 mL). The reaction mixture was stirred at RT for 2 h, prior to *in vacuo* evaporation. The crude product was purified *via* reverse phase flash column chromatography (0 to 100% acetonitrile/water) to afford the title compound **R28** (26 mg, 0.031 mmol,) as a yellow oil in 81% yield.

HRMS (ESI) calcd for $C_{40}H_{58}N_8O_{11}$ $[M+H]^+$ 827.4294, observed 827.4298.

4.2.2. Bioconjugation - Labelling of cysteine residues with pyridazinedione derivatives

GENERAL PROCEDURE FOR THE PREPARATION OF TRASTUZUMAB (ONTRUZANT) FAB FRAGMENT FOLLOWED BY DECONJUGATION

The same procedure, as the one described at 6.1.1 chapter for Trastuzumab (Trazimera), was followed here.

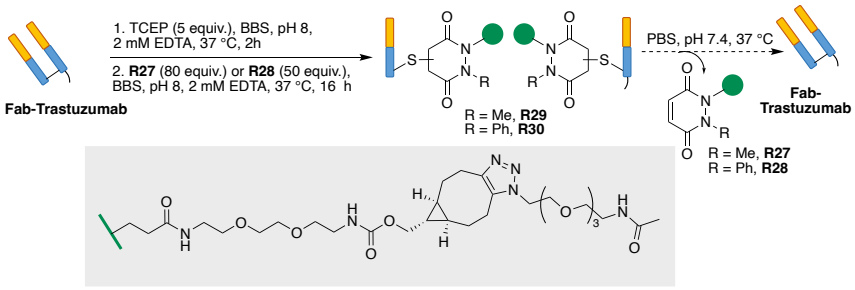

Reduction step

To a solution of Fab-Trastuzumab (100 µM, 20 µL) in BBS (25 mM sodium borate, 25 mM NaCl, 2 mM EDTA, pH 8), TCEP.HCl (0.7 µL, 150 mM in H_2O, 5 equiv.) was added. The mixture was incubated for 2 h at 37 °C under constant agitation (300 rpm). Excess of TCEP was removed by gel filtration chromatography on Zeba™ Spin Desalting Columns, 7K MWCO, pre-equilibrated with BBS (25 mM sodium borate, 25 mM NaCl, 2 mM EDTA, pH .0), to give a solution of reduced Fab.

Conjugation step

PD **R27** or **R28** (3 µL for **R28** and 4.8 µL for **R27**, 20 mM in MeCN, 50 or 80 equiv.) to a solution of reduced Fab-Trastuzumab (25 µM, 50 µL) in BBS (25 mM sodium borate, 25 mM NaCl, 2 mM EDTA, pH 8), and the reaction was incubated at 37 °C for 16 h. Excess of small molecules was removed by buffer-exchange in DI water using Zeba™ Spin Desalting column for LC-MS analysis.

De-conjugation step

2 supplementary Zeba™ Spin Desalting columns were used to remove all the excess and buffer-swapped in PBS pH 7.4. Deconjugation of **R27** and **R28** were followed by LC-MS by taking timepoints after 2.5 h, 6.5 h, 24 h, 48 h and 72 h.

Expected masses of native fragments: 23,439 Da (LC), 24,202 Da (HC), 47,639 Da (Fab).

FAB DECONJUGATION STUDY

Fab-Trastuzumab

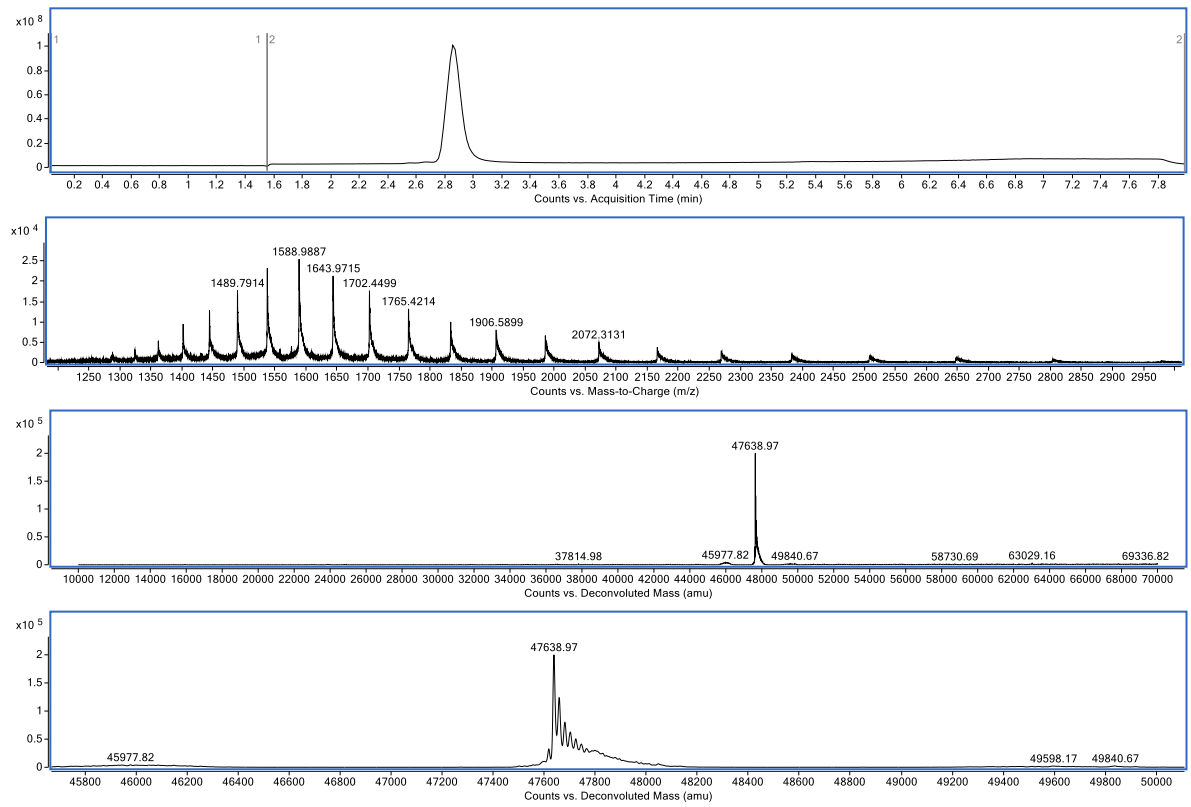

Figure 29. LC-MS spectra of native **Fab-Trastuzumab**. UV signal trace (top), non-deconvoluted MS trace (upper middle), wide range deconvoluted MS data (bottom middle) & zoom in deconvoluted data for Fab region (bottom).

Conjugate **R29**

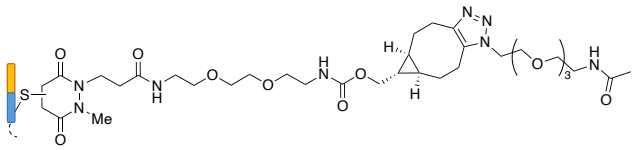

Expected masses: 22 206 Da (LC + **R27**); 24 967 Da (HC + **R27**)

Timepoint 0 h

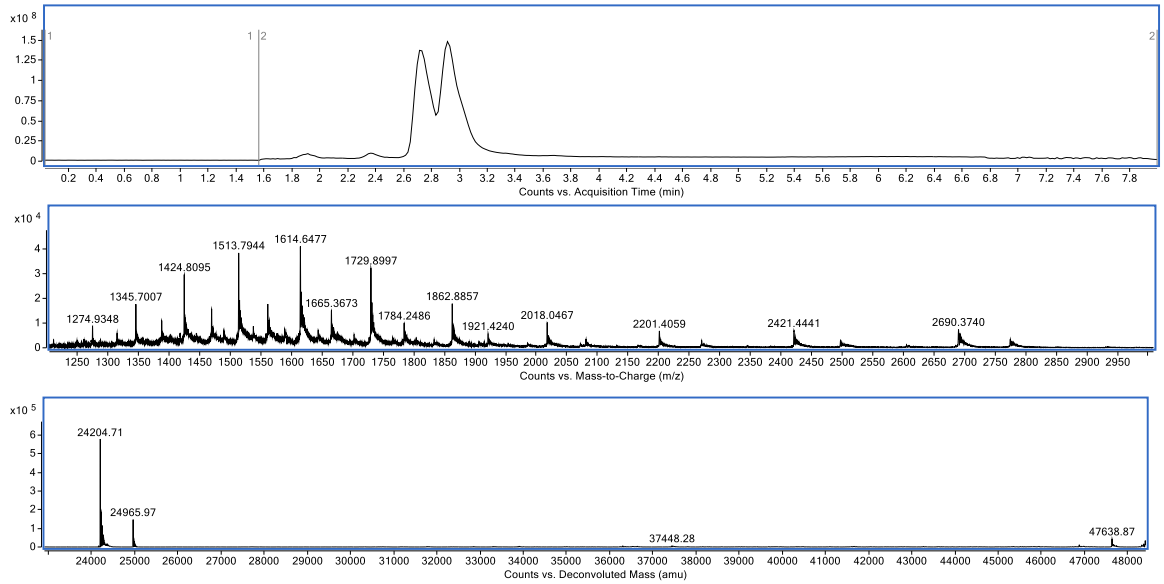

Timepoint 2.5 h

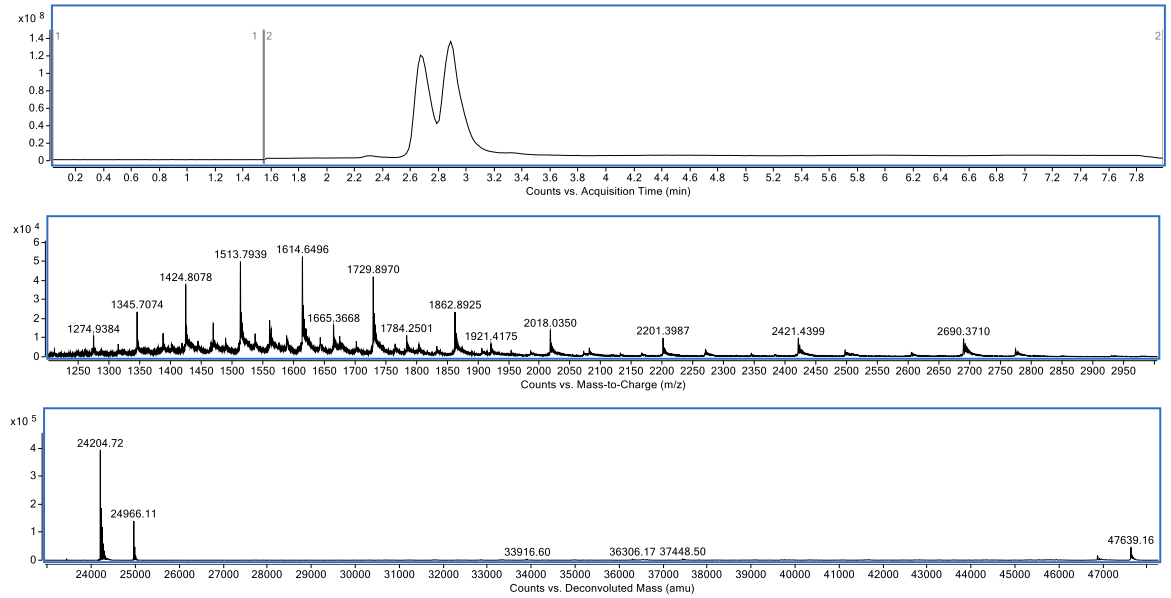

Timepoint 6.5 h

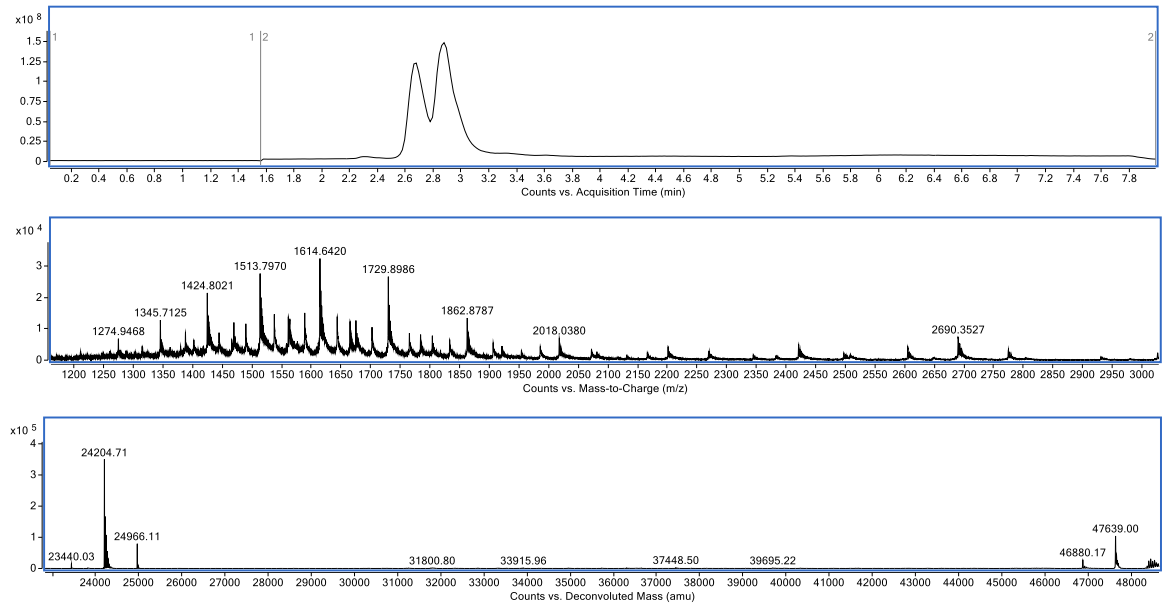

Timepoint 24 h

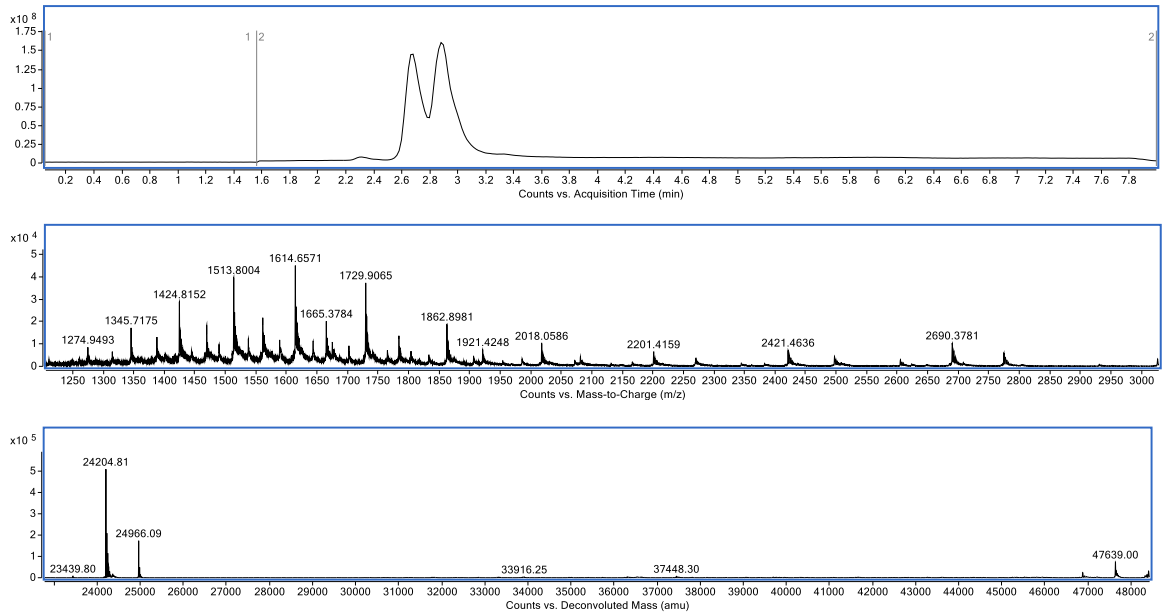

Timepoint 48 h

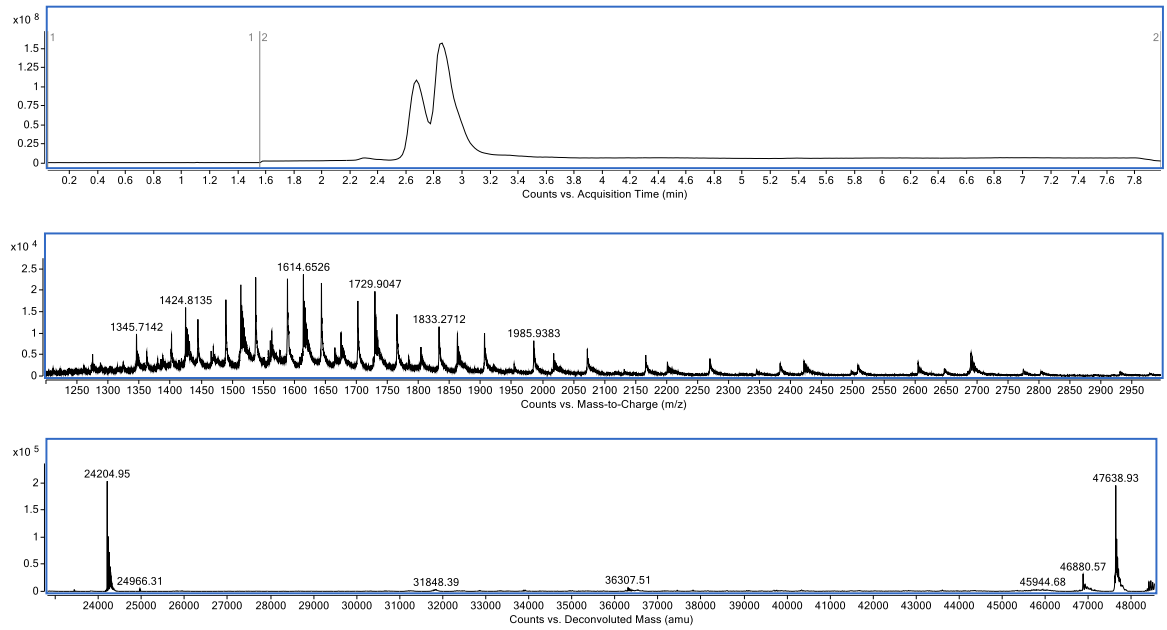

Timepoint 72 h

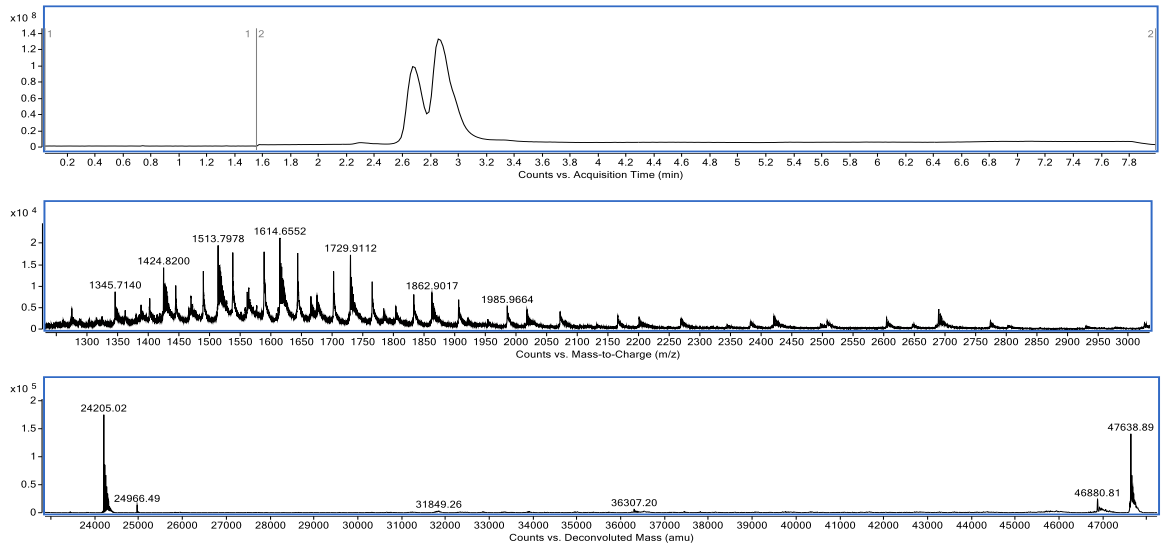

Figure 30. Deconjugation study over time of conjugate **R29** *via* LC-MS. UV signal trace (top), non-deconvoluted MS trace (middle), wide range deconvoluted MS data (bottom).

Conjugate **R30**

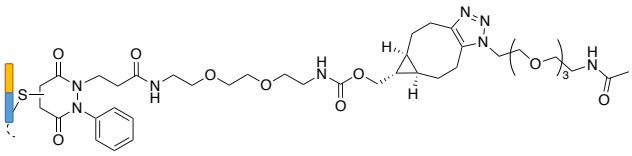

Expected masses: 24,268 Da (LC + **R28**), 25,029 Da (HC + **R28**)

Timepoint 0 h

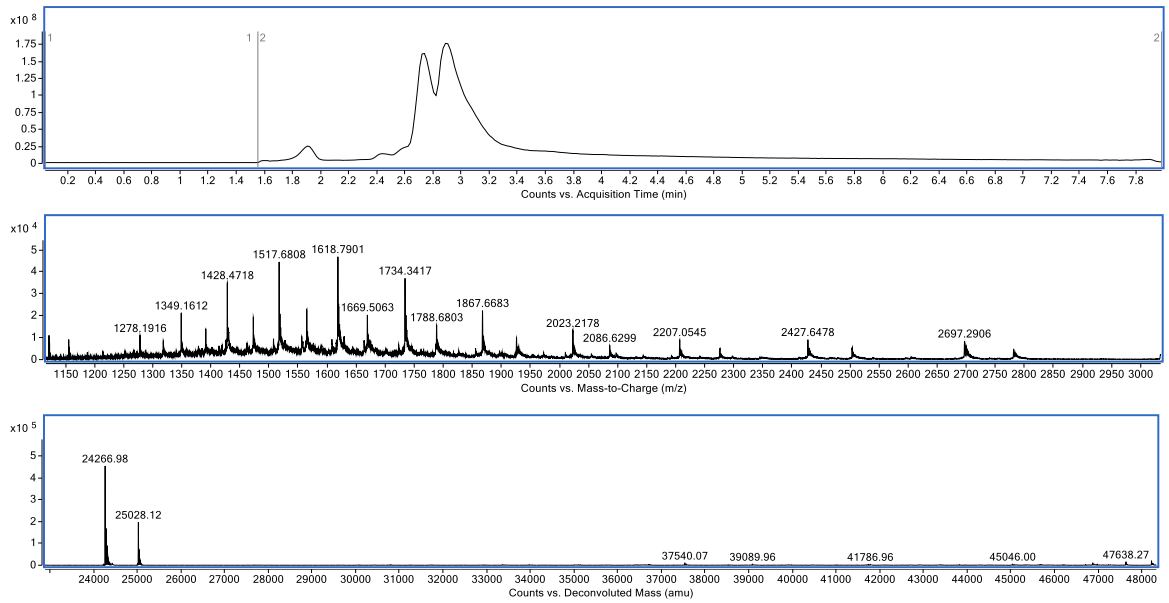

Timepoint 2.5 h

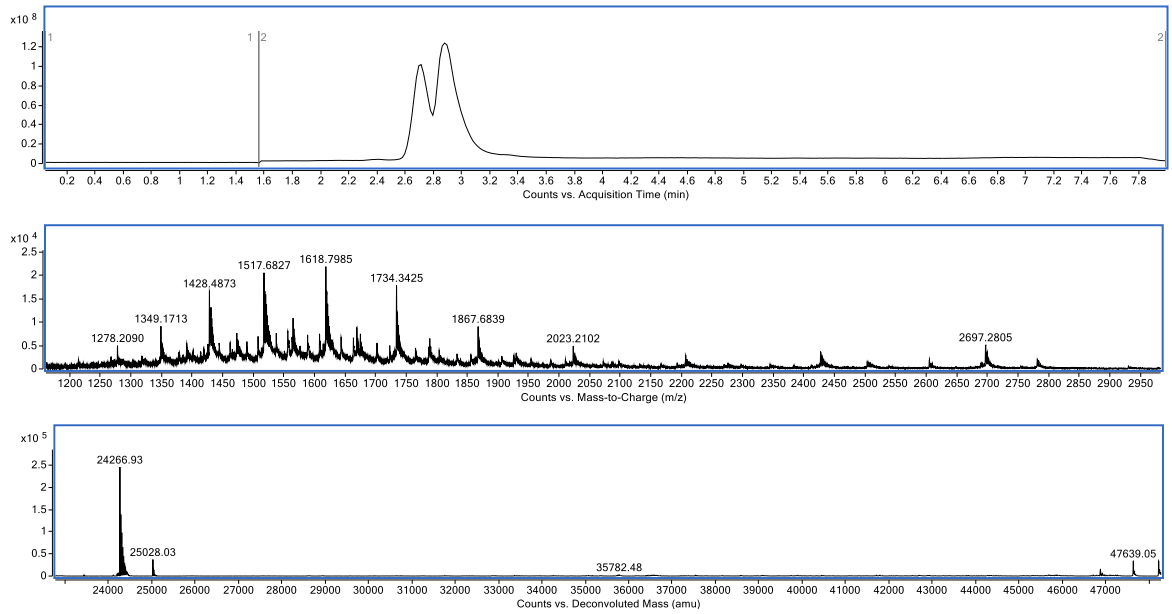

Timepoint 6.5 h

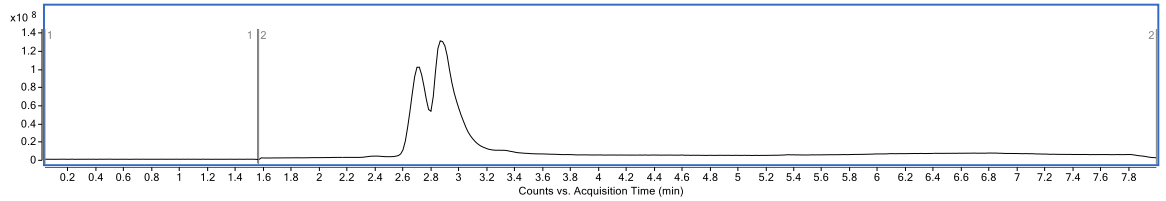

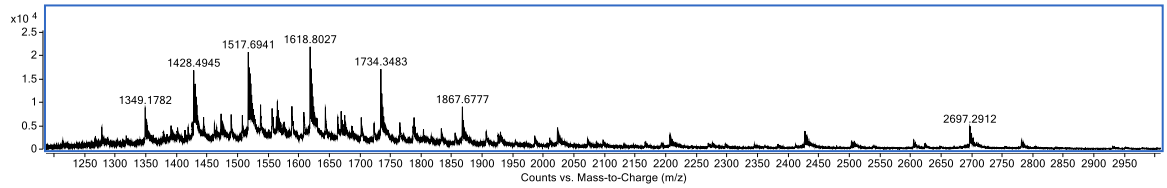

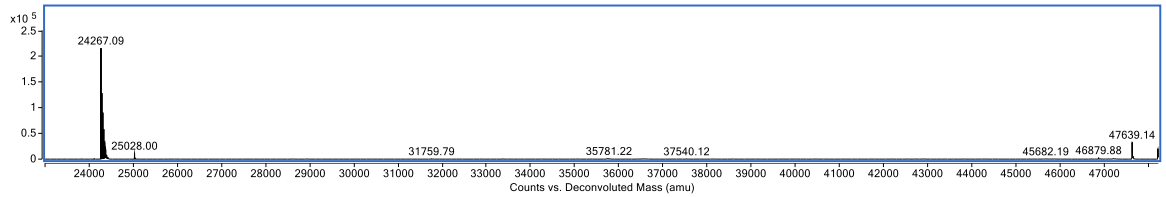

Timepoint 24 h

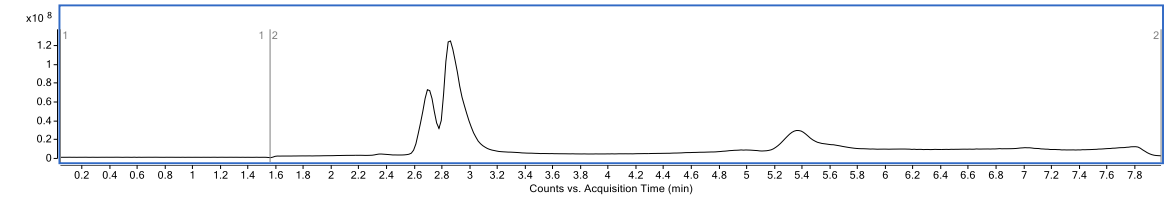

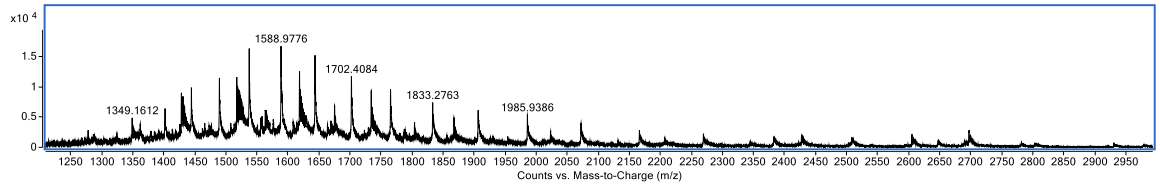

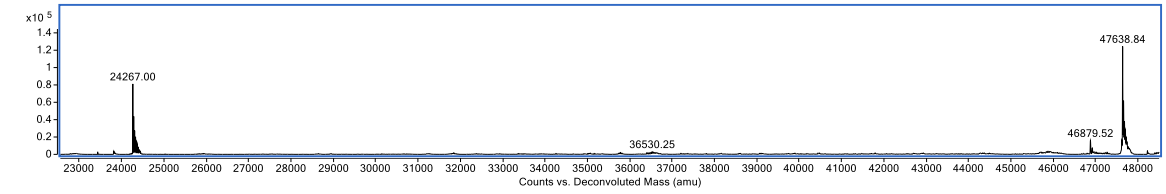

Timepoint 48 h

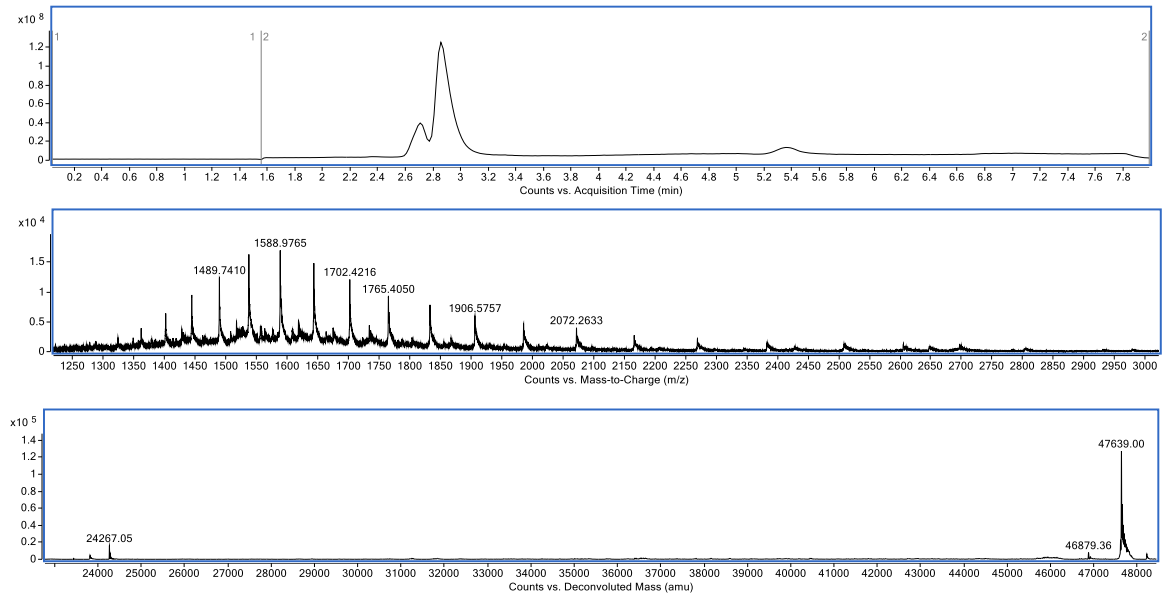

Timepoint 72 h

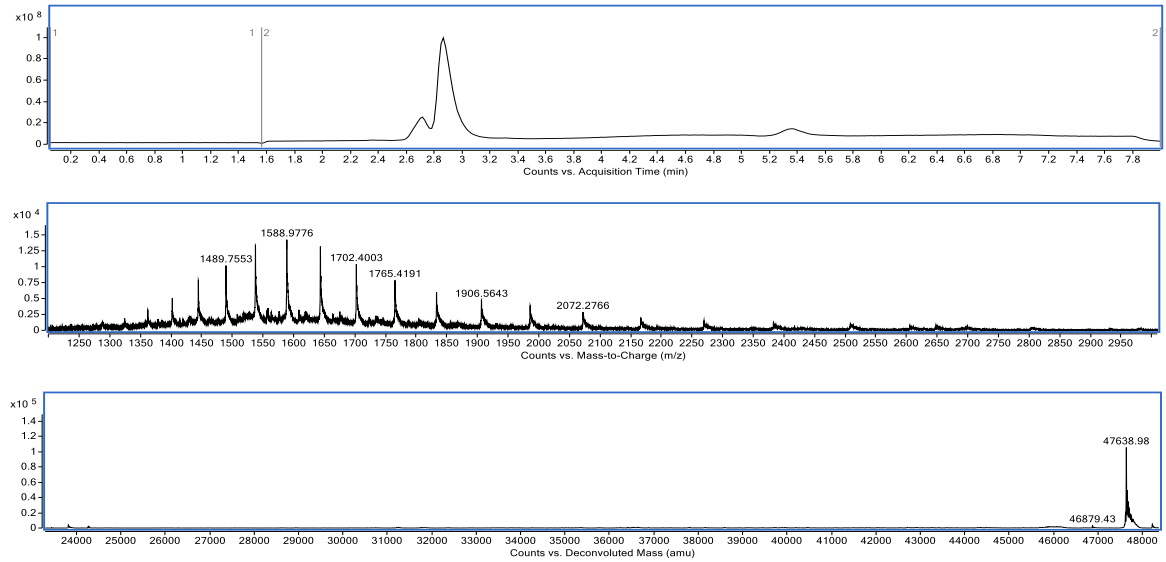

Figure 31. Deconjugation study over time of conjugate **R30** *via* LC-MS. UV signal trace (top), non-deconvoluted MS trace (middle), wide range deconvoluted MS data (bottom).

ANNEX (SYNTHETIC WORK IN SPIROCHEM, AG)

MATERIALS AND METHODS

SYNTHETIC CHEMISTRY

All reactions were performed with oven-dried glassware and under an inert atmosphere (nitrogen) unless otherwise stated. All solvents were used as purchased unless otherwise stated. Commercial reagents were used as purchased without further purification. Organic solutions were concentrated under reduced pressure on a Büchi rotary evaporator.

Thin-layer chromatography was carried out using Merck Kieselgel 60 F254 (230–400 mesh) fluorescent treated silica and were visualized under UV light (250 and 354 nm) and/or by staining with aqueous potassium permanganate solution. Medium pressure liquid chromatography (MPLC) was performed on a Biotage Isolera Four with builtin UV-detector and fraction collector with Agela technologies silica gel columns.

SPECTROSCOPY AND SPECTROMETRY

^{1}H NMR spectra were recorded in deuterated solvents on Bruker spectrometer at 400 MHz or 300 MHz Nanalysis NMReady-60 PRO spectrometer at 60 MHz, with residual protic solvent as the internal standard. **^{13}C NMR** spectra were recorded in deuterated solvents on Bruker spectrometer at 100 MHz or 75 MHz, with the central peak of the deuterated solvent as the internal standard. The ^{1}H NMR spectra are reported as δ/ppm downfield from tetramethylsilane (multiplicity, number of protons, coupling constant *J*/*Hz*). The ^{13}C NMR spectra are reported as *δ*/*ppm*. Data are reported as follows : s = singlet, d = doublet, t = triplet, q = quartet, p = quintet, m = multiplet, coupling constants *J* in Hz.

Mass spectra by ESI-MS were recorded on Shimadzu LC-MS-2020, coupled with Shimadzu LC-2040C. TLC–MS data was obtained on Advion Expression CMS coupled with Plate Express TLC-plate Reader (APCI method).

High Intensity Photoreactors were custom designed and built in coordination with the mechanical workshop in the Department of Chemistry and Biosciences at ETH Zürich having blue LEDs, equally spaced in a circle design, powered by a 10.3 A power supply, emitting 350 W of light. The LEDs were water cooled and further cooled by built-in fans to maintain an ambient temperature. Photochemistry reactions using 365 nm LEDs were performed in a EvoluChem PhotoRedOx Box.

2-phenylacrylaldehyde A2

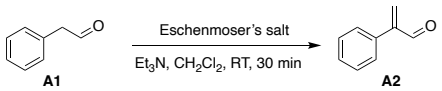

To a solution of phenylacetaldehyde **A1** (10 g, 9.7 mL, 1 equiv., 83 mmol) in Et_3N (120 mL, 10 equiv., 830 mmol) and DCM (500 mL), Eschenmoser's salt (32 g, 2.05 equiv., 170 mmol) was added in one portion. The resulting orange slurry, which turned into a yellowish solution after 10 min, was stirred at RT for 30 min. The reaction mixture was transferred into a separating funnel and was washed with $NaHCO_3$ (2 × 200 mL, aq., sat.) and brine (200 mL). The organic layer was dried over Na_2SO_4, filtered, and concentrated under reduced pressure (note: the temperature of the rotary evaporator bath should not exceed 20 °C to avoid polymerization) to afford the title compound **A2** (13 g, 89 mmol, 90 wt%) as a yellow oil in 99% yield. The crude product was taken directly to the next step, without purification, to avoid polymerization.

Rf 0.45, 9:1 cHex/EtOAc.

^{1}H NMR (400 MHz, $CDCl_3$) δ_H 9.83 (s, 1H), 7.49 – 7.45 (m, 2H), 7.41 – 7.38 (m, 2H), 7.28 (t, *J* = 0.8 Hz, 1H), 6.64 (d, *J* = 0.7 Hz, 1H), 6.19 (d, *J* = 0.6 Hz, 1H).

LRMS (APCI) calcd for $C_9H_8O^+$ [M+H$^+$] 133.06; found 133.21.

2-phenylhexa-1,5-dien-3-ol A3

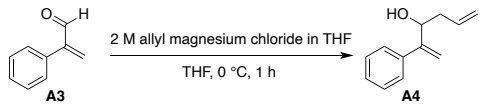

To a solution of 2-phenylacrylaldehyde **A3** (13 g, 1 equiv., 89 mmol, 90 wt%) in THF (350 mL) at 0 °C, allylmagnesium chloride (2.0 M in THF, 93 mL, 2.1 equiv., 190 mmol) was added dropwise, maintaining T < 5 °C. The resulting brownish solution was stirred at 0 °C for 1 hr. The reaction was quenched carefully with NH_4Cl (900 mL, aq., sat.), maintaining T < 10 °C. The resulted biphasic mixture was extracted with EtOAc (3 × 500 mL). The combined organic layers were washed with brine (500 mL), dried over Na_2SO_4 , filtered and evaporated under reduced pressure (T = 38 °C) and the crude was purified *via* flash chromatography (9:1 cHex/EtOAc) to afford the title compound **A4** (8.3 g, 47 mmol) as an orange oil in 53% yield. The crude product was taken directly to the next step, without purification, to avoid polymerization.

Rf_{ROH} 0.24, **$Rf_{polymer}$** 0.55, 9:1 cHex/EtOAc.

^{1}H NMR (400 MHz, $CDCl_3$) δ_H 7.42 – 7.28 (m, 5H), 5.89 – 5.74 (m, 1H), 5.39 (t, *J* = 1.4 Hz, 1H), 5.33 (t, *J* = 1.0 Hz, 1H), 5.17 – 5.09 (m, 2H), 4.71 (dd, *J* = 7.8, 4.2 Hz, 1H), 2.41 (dddt, *J* = 14.3, 6.8, 4.2, 1.3 Hz, 1H), 2.23 (dtt, *J* = 14.2, 7.5, 1.2 Hz, 1H), 1.99 (s, 1H).

LRMS (APCI) calcd for $C_{12}H_{14}O^+$ [M+H$^+$] 174.24; found 175.31

2-phenylhexa-1,5-dien-3-one A5

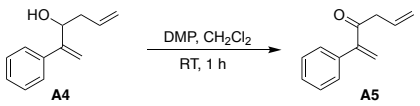

To a solution of 2-phenylhexa-1,5-dien-3-ol **A4** (6 g, 1 equiv., 30 mmol) in dry DCM (300 mL), DMP (30 g, 2 equiv., 70 mmol) was added in one portion and it was stirred for 1 h at RT. The reaction mixture was quenched with 100 mL of an 1:1 mixture of $NaHCO_3$ (aq., sat.) and $Na_2S_2O_3$ (aq., 10 wt%) and the resulting biphasic mixture was left stirring for 15 min before it was transferred into a separating funnel. The aqueous layer was extracted with DCM (3 × 200 mL) and the combined organics were washed with brine (400 mL), dried over Na_2SO_4, filtered, and concentrated under reduced pressure to afford the title compound **A5** (6 g, 44 mmol, 82 wt%) as an orange oil in 80% yield. The crude product was taken to the next step without further purification to avoid polymerization.

Rf 0.24, 9:1 cHex/EtOAc.

^{1}H NMR (400 MHz, $CDCl_3$) δ_H 7.40 – 7.29 (m, 5H), 6.14 (d, *J* = 0.6 Hz, 1H), 6.00 (ddt, *J* = 17.1, 10.2, 6.8 Hz, 1H), 5.93 (d, *J* = 0.6 Hz, 1H), 5.23 – 5.10 (m, 2H), 3.53 (dt, *J* = 6.8, 1.4 Hz, 2H).

LRMS (APCI) calcd for $C_{12}H_{12}O^+$ [M+H$^+$] 172.23; found 173.05.

***N*-methoxy-*N*-methyl-2-phenylacrylamide A7**

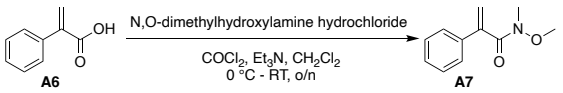

To solution of the commercially available 2-phenylacrylic acid **A6** (10 g, 1 equiv., 67 mmol) in dry DCM (450 mL) and cat. DMF (1 mL, 0.2 equiv., 0.01 mol) at 0 °C, oxalyl chloride (10 g, 7.1 mL, 1.2 equiv., 81 mmol) was added dropwise and the resulting yellow solution was stirred at RT. 90 min later, TLC confirmed the formation of the carbonyl chloride derivative and temperature was dropped again at 0 °C, before triethylamine (20 g, 28 mL, 3 equiv., 0.20 mol) and *N,O*-dimethylhydroxylamine hydrochloride (7.2 g, 1.1 equiv., 74 mmol) were added portion wise, by controlling the produced pressure, and the resulted red solution that subsequently turned into an orange one was allowed to warm up to RT overnight. The reaction mixture was quenched with H_2O (500 mL) the resulted biphasic mixture was transferred into a separation funnel. The aqueous layer was extracted with DCM (3 × 250 mL) and the combined organic layers were dried over Na_2SO_4 and concentrated *in vacuo*. The crude was purified *via* flash chromatography (4:1 cHex/EtOAc) to afford the title compound **A7** (12 g, 63 mmol) as a yellow oil in 92% yield.

Rf 0.2, 1:1 cHex/EtOAc.

^{1}H NMR (300 MHz, $CDCl_3$) δ_H 7.45 – 7.18 (m, 5H), 5.66 (s, 1H), 5.45 (s, 1H), 3.43 (s, 3H), 3.20 (s, 3H).

^{13}C NMR (75 MHz, $CDCl_3$) δ_C 144.9, 136.2, 128.6, 128.4, 125.9, 115.3, 61.0.

LRMS (APCI) calcd for $C_{11}H_2NO_2^+$ [M+H$^+$] 191.09; found 192.24.

2-phenylhexa-1,5-dien-3-one A5

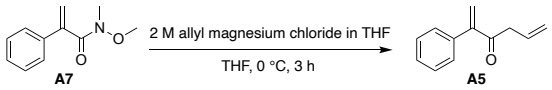

To a solution of *N*-methoxy-*N*-methyl-2-phenylacrylamide **A7** (12 g, 1 equiv., 58 mmol) in THF (210 mL) at 0 °C, allyl magnesium chloride (2 M in THF, 43 mL, 1.5 equiv., 87 mmol) was added dropwise, over 35 min, maintaining T < 8 °C. The resulting brownish solution was stirred at 0 °C for 3 h. The reaction mixture was quenched carefully with NH_4Cl (500 mL, aq., sat.); till the white suspension turns into a clear orangish biphasic solution, maintaining T < 15 °C, which was allowed to warm up to RT over 1 h. The resulted biphasic mixture was extracted with EtOAc (2 × 500 mL). The combined organics were washed with brine (300 mL), dried over Na_2SO_4 , filtered and evaporated under reduced pressure (T = 38 °C) to afford the title compound **A5** (12 g, 58 mmol, 83 wt%) as an orange oil in 100% yield. The crude product was taken to the next step with no further purification.

Rf 0.24, 9:1 cHex/EtOAc.

^{1}H NMR (400 MHz, $CDCl_3$) δ_H 7.40 – 7.29 (m, 5H), 6.14 (d, *J* = 0.6 Hz, 1H), 6.00 (ddt, *J* = 17.1, 10.2, 6.8 Hz, 1H), 5.93 (d, *J* = 0.6 Hz, 1H), 5.23 – 5.10 (m, 2H), 3.53 (dt, *J* = 6.8, 1.4 Hz, 2H).

LRMS (APCI) calcd for $C_{12}H_{12}O^+$ [M+H$^+$] 172.23; found 173.05.

1-phenylbicyclo[2.1.1]hexan-2-one A8

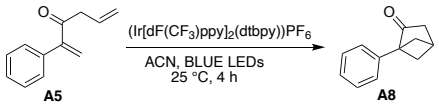

To a solution of 2-phenylhexa-1,5-dien-3-one **A5** (6 g, 1 equiv., 28.6 mmol, 82 wt%) in acetonitrile (380 mL) (4,4'-Di-*t*-butyl-2,2'-bipyridine)bis[3,5-difluoro-2-(5-trifluoromethyl-2-pyridinyl-kN)phenyl-kC]iridium(III) hexafluorophosphate (320 mg, 2 mol %, 286 µmol) and the mixture was degassed with nitrogen for 5 min before being irradiated with blue LEDs in a photoreactor (400 W). After 4 h of stirring, the volatiles were evaporated under reduced pressure and the crude was purified *via* flash chromatography (9:1 cHex/EtOAc) to afford the title compound **A8** (4.5 g, 25 mmol) as a white solid in 89% yield.

Rf 0.23, 9:1 cHex/EtOAc.

^{1}H NMR (300 MHz, $CDCl_3$) δ_H 7.40 – 7.31 (m, 2H), 7.31 – 7.23 (m, 1H), 7.14 (dt, 2H), 2.86 (h, *J* = 1.6 Hz, 1H), 2.42 (dtt, *J* = 5.4, 3.1, 1.2 Hz, 4H), 2.11 (dd, *J* = 4.5, 2.1 Hz, 2H).

^{13}C NMR (75 MHz, $CDCl_3$) δ_C 211.7, 136.8, 128.3, 127.1, 126.7, 68.1, 44.8, 42.5, 30.9.

νmax (thin film) /cm^{-1} 1749 (s), 1501 (w), 1252 (w), 1101 (w), 779 (m), 700 (m).

LRMS (APCI) calcd for $C_{12}H_{12}O^+$ [M+H$^+$] 173.23; found 174.05.

1-phenylbicyclo[2.1.1]hexan-2-ol A9

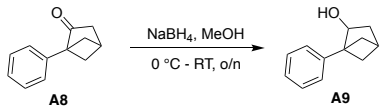

To a solution of 1-phenylbicyclo[2.1.1]hexan-2-one **A8** (400 mg, 1 equiv., 2.32 mmol) in MeOH (11.6 mL) at 0 °C, sodium boron tetrahydride (176 mg, 2 equiv., 4.64 mmol) was added portion-wise and the resulting mixture was allowed to warm to RT overnight. Upon completion of the reaction, the volatiles were evaporated under reduced pressure and the resulting residue was partitioned between H_2O (50 mL) and EtOAc (50 mL). The aqueous layer was washed with EtOAc (3 × 50 mL) and the combined organics were dried over Na_2SO_4, filtered, and evaporated under reduced pressure to afford the title compound **A9** (405 mg, 2.24 mmol) as a white solid in 97% yield.

Rf 0.25, 9:1 cHex/EtOAc.

^{1}H NMR (300 MHz, $CDCl_3$) δ_H 7.45 – 7.19 (m, 5H), 4.36 (dt, *J* = 7.3, 1.8 Hz, 1H), 2.53 (tt, *J* = 3.0, 1.5 Hz, 1H), 2.32 (dddd, *J* = 11.5, 7.3, 2.6, 1.5 Hz, 1H), 2.04 (dd, *J* = 9.5, 6.7 Hz, 1H), 1.90 – 1.80 (m, 2H), 1.74 – 1.52 (m, 4H).

^{13}C NMR (75 MHz, $CDCl_3$) δ_C 141.8, 128.3, 126.4, 126.2, 76.0, 59.1, 43.7, 39.2, 37.4, 34.9.

LRMS (APCI) calcd for $C_{12}H_{12}O^+$ [M+H$^+$] 175.24; found 176.49

2-oxobicyclo[2.1.1]hexane-1-carboxylic acid A10

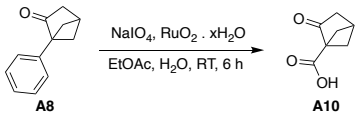

A8 **A10**

Sodium periodate (7.17 g, 15 equiv., 33.5 mmol) was added to a vigorously stirring biphasic solution of 1-phenylbicyclo[2.1.1]hexan-2-one **A8** (397 mg, 1 equiv., 2.24 mmol) in a 1:3 mixture of EtOAc (22.8 mL) / water (68.4 mL) at RT. Ruthenium(IV) oxide hydrate (33.8 mg, 0.1 equiv., 224 µmol) was then added in a single portion, and the light yellow mixture was allowed to react at RT for 6 h. The resulting biphasic mixture was transferred into a separating funnel and extracted with EtOAc (2 × 100 mL). The combined organics were washed twice with a 100 mL of 10:1 brine/sodium sulfite solution (aq., 10 wt%). The combined aqueous layers obtained from the latter separation were acidified to pH 1-2 and extracted with EtOAc (3 x 50 mL). The combined organics from this separation were washed brine (1 × 70 mL), dried over Na_2SO_4, filtered and concentrated *in vacuo* at 45 °C to afford the title compound **A10** (220 mg, 1.57 mmol) as a yellow crystalline solid in 70% yield.

Rf 0.11, 9:1 EtOAc/MeOH, **Visualization**: UV, bromocresol.

^{1}H NMR (300 MHz, DMSO) δ_H 12.57 (s, 1H), 2.63 (p, *J* = 2.3 Hz, 1H), 2.42 – 2.32 (m, 2H), 2.29 – 2.21 (m, 2H), 1.87 (dd, *J* = 4.7, 2.2 Hz, 2H).

^{13}C NMR (75 MHz, DMSO) δ_C 208.5, 170.9, 66.9, 43.4, 41.3, 30.5.

2-phenylbicyclo[2.1.1]hexan-2-ol A11

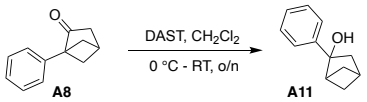

To a solution of 1-phenylbicyclo[2.1.1]hexan-2-ol **A8** (200 mg, 1 equiv., 1.15 mmol) in DCM (10 mL), diethylaminosulfur trifluoride (227 µL, 1.5 equiv., 1.72 mmol) was added dropwise at 0 °C, under an argon atmosphere. 45 min later, the cooling bath was removed and the reaction mixture was allowed to warm up to RT overnight, before it was quenched with 10 mL $NaHCO_3$ (aq., sat.). The biphasic mixture was transferred into a separating funnel and the aqueous layer was extracted with DCM (3 × 10 mL). The combined organics were washed with brine (20 mL), dried over Na_2SO_4, filtered and concentration *in vacuo* at 38 °C and the crude was purified *via* flash chromatography (4:1 cHex/EtOAc) to afford the title compound **A11** (55 mg, 0.32 mmol) as a yellow oil in 30% yield.

Rf 0.25, 9:1 cHex/EtOAc.

^{1}H NMR (300 MHz, $CDCl_3$) δ_H 7.57 – 7.44 (m, 2H), 7.42 – 7.32 (m, 2H), 7.32 – 7.21 (m, 2H), 2.88 (dt, *J* = 6.8, 2.6 Hz, 1H), 2.52 (dtt, *J* = 7.1, 2.9, 1.5 Hz, 1H), 2.36 (ddd, *J* = 11.4, 2.5, 1.5 Hz, 1H), 2.01 (ddd, *J* = 11.4, 3.5, 1.4 Hz, 1H), 1.90 – 1.70 (m, 4H), 1.14 (ddd, *J* = 9.2, 7.1, 1.1 Hz, 1H).

^{13}C NMR (75 MHz, $CDCl_3$) δ_C 146.5, 128.4, 127.2, 126.6, 81.2, 49.5, 43.8, 40.3, 38.3, 37.4.

LRMS (APCI) calcd for $C_{12}H_{12}O^+$ [M+H$^+$] 175.24; found 176.49.

2-methoxy-2-phenylbicyclo[2.1.1]hexane A12

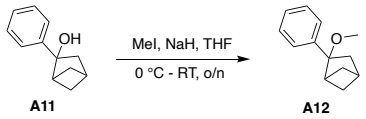

To a solution of 2-phenylbicyclo[2.1.1]hexan-2-ol **A11** (20 mg, 1 equiv., 0.11 mmol) in THF (1 mL) at 0 °C, sodium hydride (6.9 mg, 60 wt%, 1.5 equiv., 0.17 mmol) was added and the resulting grey suspension was stirred at 0 °C for 2.5 h under an argon atmosphere. Then, methyl iodide (44 mg, 19 µL, 2.7 equiv., 0.31 mmol) was added and the resulted reaction mixture was allowed to warm up to RT overnight. The grey suspension was filtered through a Celite® pad, which was washed thoroughly with EtOAc and the filtrates were evaporated to dryness. The crude was purified *via* flash chromatography (9.5:0.5 cHex/EtOAc) to afford the title compound **A12** (0.06 mmol, 11 mg) as a yellowish solid in 51% yield.

Rf 0.64, 9:1 cHex/EtOAc.

^{1}H NMR (300 MHz, $CDCl_3$) δ_H 7.48 – 7.40 (m, 2H), 7.40 – 7.31 (m, 2H), 7.29 – 7.22 (m, 1H), 3.08 – 2.98 (m, 1H), 2.92 (s, 3H), 2.51 (dddd, *J* = 6.8, 4.1, 2.4, 1.4 *Hz*, 1H), 2.20 (dt, *J* = 11.3, 1.8 *Hz*, 1H), 2.03 (ddd, *J* = 11.3, 3.5, 1.4 *Hz*, 1H), 1.81 – 1.70 (m, 3H), 1.17 – 1.07 (m, 1H).

^{13}C NMR (75 MHz, $CDCl_3$) δ_C 143.2, 128.0, 127.9, 126.9, 86.4, 50.6, 45.7, 41.9, 39.4, 38.0, 36.7.

LRMS (APCI) calcd for $C_{13}H_{16}O^+$ [M+H$^+$] 188.11; found 189.21.

4-methyl-*N*'-(1-phenylbicyclo[2.1.1]hexan-2-ylidene)benzenesulfonohydrazide A13

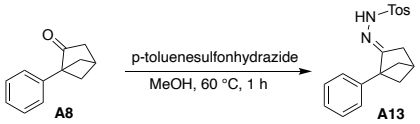

A solution of *p*-toluenesulfonhydrazide (216 mg, 1.0 equiv., 1.16 mmol) in anhydrous MeOH (2.32 mL) was stirred and heated to 60 °C until *p*-toluenesulfonhydrazine was completely dissolved. Then, 1- phenylbicyclo[2.1.1]hexan-2-one **A8** (200 mg, 1.0 equiv., 1.16 mmol) was added to the stirring mixture. 1 h later, the desired product precipitated and the resulted slurry was filtered. The recovered solid was washed with cold cHex to afford the title compound **A13** (0.79 mmol, 270 mg) as a white solid in 68% yield.

^{1}H NMR (300 MHz, DMSO-d_6) δ_H 10.01 (s, 1H), 7.62 – 7.52 (m, 2H), 7.40 – 7.30 (m, 4H), 7.29 – 7.23 (m, 1H), 7.06 – 6.99 (m, 2H), 2.60 (dq, *J* = 3.2, 1.6 *Hz*, 1H), 2.43 (q, *J* = 1.9 *Hz*, 2H), 2.40 (s, 3H), 2.14 (q, *J* = 3.3 *Hz*, 2H), 1.69 (dd, *J* = 4.3, 2.1 *Hz*, 2H).

^{13}C NMR (75 MHz, DMSO-d_6) δ_C 166.5, 143.0, 138.2, 136.2, 129.1, 127.7, 127.5, 127.0, 126.5, 61.3, 45.4, 34.9, 31.1, 21.0.

LRMS (APCI) calcd for $C_{19}H_{20}N_2O_2S^+$ [M+H$^+$] 340.12; found 341.23.

NMR and MS analysis were found to be in agreement with previously reported characterization data.[1]

REFERENCES

(1) Herter, L.; Koutsopetras, I.; Turelli, L.; Fessard, T.; Salomé, C. Preparation of New Bicyclo[2.1.1]Hexane Compact Modules: An Opening towards Novel Sp3-Rich Chemical Space. *Org. Biomol. Chem.* **2022**, *20* (46), 9108–9111. https://doi.org/10.1039/D2OB01669A.

(2) Harlan, J. W.; Feairheller, S. H. Chemistry of the Crosslinking of Collagen during Tanning. In *Protein Crosslinking: Biochemical and Molecular Aspects*; Friedman, M., Ed.; Springer US: Boston, MA, **1977**; pp 425–440. https://doi.org/10.1007/978-1-4684-3282-4_27.

(3) Yadav, D. K.; Yadav, N.; Khurana, S. M. P. Chapter 26 - Vaccines: Present Status and Applications. In *Animal Biotechnology*; Verma, A. S., Singh, A., Eds.; Academic Press: San Diego, **2014**; pp 491–508. https://doi.org/10.1016/B978-0-12-416002-6.00026-2.

(4) Metz, B.; Michiels, T.; Uittenbogaard, J.; Danial, M.; Tilstra, W.; Meiring, H. D.; Hennink, W. E.; Crommelin, D. J. A.; Kersten, G. F. A.; Jiskoot, W. Identification of Formaldehyde-Induced Modifications in Diphtheria Toxin. *J. Pharm. Sci.* **2020**, *109* (1), 543–557. https://doi.org/10.1016/j.xphs.2019.10.047.

(5) Means, G. E.; Feeney, R. E. Chemical Modifications of Proteins: History and Applications. *Bioconjug. Chem.* **1990**, *1* (1), 2–12. https://doi.org/10.1021/bc00001a001.

(6) Cohen, L. A. Group-Specific Reagents in Protein Chemistry. *Annu. Rev. Biochem.* **1968**, *37* (1), 695–726. https://doi.org/10.1146/annurev.bi.37.070168.003403.

(7) Lamson, R. W. THE VAN SLYKE METHOD FOR THE DETERMINATION OF AMINO-ACID NITROGEN AS APPLIED TO THE STUDY OF BACTERIAL CULTURES. *J. Bacteriol.* **1924**, *9* (3), 307–313.

(8) Haynes, R.; Osuga, D. T.; Feeney, R. E. Modification of Amino Groups in Inhibitors of Proteolytic Enzymes*. *Biochemistry* **1967**, *6* (2), 541–547. https://doi.org/10.1021/bi00854a023.

(9) Fields, R. [38] The Rapid Determination of Amino Groups with TNBS. In *Methods in Enzymology*; Academic Press, **1972**; Vol. 25, pp 464–468. https://doi.org/10.1016/S0076-6879(72)25042-X.

(10) Ellman, G. L. Tissue Sulfhydryl Groups. *Arch. Biochem. Biophys.* **1959**, *82* (1), 70–77. https://doi.org/10.1016/0003-9861(59)90090-6.

(11) Fujioka, M.; Takata, Y.; Konishi, K.; Ogawa, H. Function and Reactivity of Sulfhydryl Groups of Rat Liver Glycine Methyltransferase. *Biochemistry* **1987**, *26* (18), 5696–5702. https://doi.org/10.1021/bi00392a018.

(12) Horton, H. R.; Koshland, D. E. [65] Reactions with Reactive Alkyl Halides. In *Methods in Enzymology*; Academic Press, **1967**; Vol. 11, pp 556–565. https://doi.org/10.1016/S0076-6879(67)11067-7.

(13) Hang, H. C.; Yu, C.; Kato, D. L.; Bertozzi, C. R. A Metabolic Labeling Approach toward Proteomic Analysis of Mucin-Type O-Linked Glycosylation. *Proc. Natl. Acad. Sci. U. S. A.* **2003**, *100* (25), 14846–14851. https://doi.org/10.1073/pnas.2335201100.

(14) Prescher, J. A.; Bertozzi, C. R. Chemistry in Living Systems. *Nat. Chem. Biol.* **2005**, *1* (1), 13–21. https://doi.org/10.1038/nchembio0605-13.

(15) Kozlowski, L. P. Proteome-pI: Proteome Isoelectric Point Database. *Nucleic Acids Res.* **2017**, *45* (D1), D1112–D1116. https://doi.org/10.1093/nar/gkw978.

(16) Sornay, C.; Vaur, V.; Wagner, A.; Chaubet, G. An Overview of Chemo- and Site-Selectivity Aspects in the Chemical Conjugation of Proteins. *R. Soc. Open Sci.* **2022**, *9* (1), 211563. https://doi.org/10.1098/rsos.211563.

(17) Rosen, C. B.; Francis, M. B. Targeting the N Terminus for Site-Selective Protein Modification. *Nat. Chem. Biol.* **2017**, *13* (7), 697–705. https://doi.org/10.1038/nchembio.2416.

(18) Jentoft, N.; Dearborn, D. G. Labeling of Proteins by Reductive Methylation Using Sodium Cyanoborohydride. *J. Biol. Chem.* **1979**, *254* (11), 4359–4365. https://doi.org/10.1016/S0021-9258(17)30016-9.

(19) Gildersleeve, J. C.; Oyelaran, O.; Simpson, J. T.; Allred, B. Improved Procedure for Direct Coupling of Carbohydrates to Proteins via Reductive Amination. *Bioconjug. Chem.* **2008**, *19* (7), 1485–1490. https://doi.org/10.1021/bc800153t.

(20) Tuls, J.; Geren, L.; Millett, F. Fluorescein Isothiocyanate Specifically Modifies Lysine 338 of Cytochrome P-450scc and Inhibits Adrenodoxin Binding. *J. Biol. Chem.* **1989**, *264* (28), 16421–16425. https://doi.org/10.1016/S0021-9258(19)84723-3.

(21) Jorbágy, A.; Király, K. Chemical Characterization of Fluorescein Isothiocyanate-Protein Conjugates. *Biochim. Biophys. Acta BBA - Gen. Subj.* **1966**, *124* (1), 166–175. https://doi.org/10.1016/0304-4165(66)90325-4.

(22) Stark, G. R. Reactions of Cyanate with Functional Groups of Proteins. III. Reactions with Amino and Carboxyl Groups*. *Biochemistry* **1965**, *4* (6), 1030–1036. https://doi.org/10.1021/bi00882a008.

(23) Hettick, J. M.; Ruwona, T. B.; Siegel, P. D. Structural Elucidation of Isocyanate-Peptide Adducts Using Tandem Mass Spectrometry. *J. Am. Soc. Mass Spectrom.* **2009**, *20* (8), 1567–1575. https://doi.org/10.1016/j.jasms.2009.04.016.

(24) *Site-Specific Protein Labeling: Methods and Protocols*; Gautier, A., Hinner, M. J., Eds.; Methods in Molecular Biology; Springer: New York, NY, **2015**; Vol. 1266. https://doi.org/10.1007/978-1-4939-2272-7.

(25) Kalkhof, S.; Sinz, A. Chances and Pitfalls of Chemical Cross-Linking with Amine-Reactive N-Hydroxysuccinimide Esters. *Anal. Bioanal. Chem.* **2008**, *392* (1), 305–312. https://doi.org/10.1007/s00216-008-2231-5.

(26) Leavell, M. D.; Novak, P.; Behrens, C. R.; Schoeniger, J. S.; Kruppa, G. H. Strategy for Selective Chemical Cross-Linking of Tyrosine and Lysine Residues. *J. Am. Soc. Mass Spectrom.* **2004**. https://doi.org/10.1016/j.jasms.2004.07.018.

(27) Hermanson, G. T. *Bioconjugate Techniques*; Academic Press, **2013**.

(28) Chalker, J. M.; Bernardes, G. J. L.; Lin, Y. A.; Davis, B. G. Chemical Modification of Proteins at Cysteine: Opportunities in Chemistry and Biology. *Chem. – Asian J.* **2009**, *4* (5), 630–640. https://doi.org/10.1002/asia.200800427.

(29) Gunnoo, S. B.; Madder, A. Chemical Protein Modification through Cysteine. *ChemBioChem* **2016**, *17* (7), 529–553. https://doi.org/10.1002/cbic.201500667.

(30) Mthembu, S. N.; Sharma, A.; Albericio, F.; de la Torre, B. G. Breaking a Couple: Disulfide Reducing Agents. *ChemBioChem* **2020**, *21* (14), 1947–1954. https://doi.org/10.1002/cbic.202000092.

(31) Chin, C. C. Q.; Wold, F. Some Chemical Properties of Carboxymethyl Derivatives of Amino Acids. *Arch. Biochem. Biophys.* **1975**, *167* (2), 448–451. https://doi.org/10.1016/0003-9861(75)90486-5.

(32) Wawrzynow, A.; Collins, J. H.; Coan, C. An Iodoacetamide Spin-Label Selectively Labels a Cysteine Side Chain in an Occluded Site on the Sarcoplasmic Reticulum Calcium-ATPase. *Biochemistry* **1993**, *32* (40), 10803–10811. https://doi.org/10.1021/bi00091a035.

(33) Brune, D. C. Alkylation of Cysteine with Acrylamide for Protein Sequence Analysis. *Anal. Biochem.* **1992**, *207* (2), 285–290. https://doi.org/10.1016/0003-2697(92)90013-W.

(34) Friedman, M.; Krull, L. H.; Cavins, J. F. The Chromatographic Determination of Cystine and Cysteine Residues in Proteins as S-β-(4-Pyridylethyl)Cysteine. *J. Biol. Chem.* **1970**, *245* (15), 3868–3871. https://doi.org/10.1016/S0021-9258(18)62930-8.

(35) Sechi, S.; Chait, B. T. Modification of Cysteine Residues by Alkylation. A Tool in Peptide Mapping and Protein Identification. *Anal. Chem.* **1998**, *70* (24), 5150–5158. https://doi.org/10.1021/ac9806005.

(36) *ANTIMITOTIC ACTION OF MALEIMIDE AND RELATED SUBSTANCES - FRIEDMANN - **1949** - British Journal of Pharmacology and Chemotherapy - Wiley Online Library*. https://bpspubs-onlinelibrary-wiley-com.scd-rproxy.u-strasbg.fr/doi/10.1111/j.1476-5381.1949.tb00521.x (accessed 2023-06-22).

(37) Friedmann, E. Spectrophotometric Investigation of the Interaction of Glutathione with Maleimide and N-Ethylmaleimide. *Biochim. Biophys. Acta* **1952**, *9*, 65–75. https://doi.org/10.1016/0006-3002(52)90121-2.

(38) Szijj, P. A.; Bahou, C.; Chudasama, V. Minireview: Addressing the Retro-Michael Instability of Maleimide Bioconjugates. *Antib. - Drug Conjug. ADC* **2018**, *30*, 27–34. https://doi.org/10.1016/j.ddtec.2018.07.002.

(39) Wu, C.-W.; Yarbrough, L. R.; Wu, F. Y. H. N-(1-Pyrene)Maleimide: A Fluorescent Crosslinking Reagent. *Biochemistry* **1976**, *15* (13), 2863–2868. https://doi.org/10.1021/bi00658a025.

(40) Christie, R. J.; Fleming, R.; Bezabeh, B.; Woods, R.; Mao, S.; Harper, J.; Joseph, A.; Wang, Q.; Xu, Z.-Q.; Wu, H.; Gao, C.; Dimasi, N. Stabilization of Cysteine-Linked Antibody Drug Conjugates with N-Aryl Maleimides. *J. Controlled Release* **2015**, *220*, 660–670. https://doi.org/10.1016/j.jconrel.2015.09.032.

(41) Lyon, R. P.; Setter, J. R.; Bovee, T. D.; Doronina, S. O.; Hunter, J. H.; Anderson, M. E.; Balasubramanian, C. L.; Duniho, S. M.; Leiske, C. I.; Li, F.; Senter, P. D. Self-Hydrolyzing Maleimides Improve the Stability and Pharmacological Properties of Antibody-Drug Conjugates. *Nat. Biotechnol.* **2014**, *32* (10), 1059–1062. https://doi.org/10.1038/nbt.2968.

(42) Fontaine, S. D.; Reid, R.; Robinson, L.; Ashley, G. W.; Santi, D. V. Long-Term Stabilization of Maleimide–Thiol Conjugates. *Bioconjug. Chem.* **2015**, *26* (1), 145–152. https://doi.org/10.1021/bc5005262.

(43) Dovgan, I.; Kolodych, S.; Koniev, O.; Wagner, A. 2-(Maleimidomethyl)-1,3-Dioxanes (MD): A Serum-Stable Self-Hydrolysable Hydrophilic Alternative to Classical Maleimide Conjugation. *Sci. Rep.* **2016**, *6* (1), 30835. https://doi.org/10.1038/srep30835.

(44) Maruani, A.; Alom, S.; Canavelli, P.; Lee, M. T. W.; Morgan, R. E.; Chudasama, V.; Caddick, S. A Mild TCEP-Based Para-Azidobenzyl Cleavage Strategy to Transform Reversible Cysteine Thiol Labelling Reagents into Irreversible Conjugates. *Chem. Commun.* **2015**, *51* (25), 5279–5282. https://doi.org/10.1039/C4CC08515A.

(45) Bahou, C.; J. Spears, R.; E. Aliev, A.; Maruani, A.; Fernandez, M.; Javaid, F.; A. Szijj, P.; R. Baker, J.; Chudasama, V. Use of Pyridazinediones as Extracellular Cleavable Linkers through Reversible Cysteine Conjugation. *Chem. Commun.* **2019**, *55* (98), 14829–14832. https://doi.org/10.1039/C9CC08362F.

(46) Sebastiano, R.; Citterio, A.; Lapadula, M.; Righetti, P. G. A New Deuterated Alkylating Agent for Quantitative Proteomics. *Rapid Commun. Mass Spectrom.* **2003**, *17* (21), 2380–2386. https://doi.org/10.1002/rcm.1206.

(47) Seki, H.; Walsh, S. J.; Bargh, J. D.; Parker, J. S.; Carroll, J.; Spring, D. R. Rapid and Robust Cysteine Bioconjugation with Vinylheteroarenes. *Chem. Sci.* **2021**, *12* (26), 9060–9068. https://doi.org/10.1039/D1SC02722K.

(48) Lipka, B. M.; Betti, V. M.; Honeycutt, D. S.; Zelmanovich, D. L.; Adamczyk, M.; Wu, R.; Blume, H. S.; Mendina, C. A.; Goldberg, J. M.; Wang, F. Rapid Electrophilic Cysteine Arylation with Pyridinium Salts. *Bioconjug. Chem.* **2022**, *33* (11), 2189–2196. https://doi.org/10.1021/acs.bioconjchem.2c00419.

(49) Kasper, M.-A.; Glanz, M.; Stengl, A.; Penkert, M.; Klenk, S.; Sauer, T.; Schumacher, D.; Helma, J.; Krause, E.; Cardoso, M. C.; Leonhardt, H.; Hackenberger, C. P. R. Cysteine-Selective Phosphonamidate Electrophiles for Modular Protein Bioconjugations. *Angew. Chem. Int. Ed.* **2019**, *58* (34), 11625–11630. https://doi.org/10.1002/anie.201814715.

(50) Baumann, A. L.; Schwagerus, S.; Broi, K.; Kemnitz-Hassanin, K.; Stieger, C. E.; Trieloff, N.; Schmieder, P.; Hackenberger, C. P. R. Chemically Induced Vinylphosphonothiolate Electrophiles for Thiol–Thiol Bioconjugations. *J. Am. Chem. Soc.* **2020**, *142* (20), 9544–9552. https://doi.org/10.1021/jacs.0c03426.

(51) Abegg, D.; Frei, R.; Cerato, L.; Prasad Hari, D.; Wang, C.; Waser, J.; Adibekian, A. Proteome-Wide Profiling of Targets of Cysteine Reactive Small Molecules by Using Ethynyl Benziodoxolone Reagents. *Angew. Chem. Int. Ed.* **2015**, *54* (37), 10852–10857. https://doi.org/10.1002/anie.201505641.

(52) Tessier, R.; Ceballos, J.; Guidotti, N.; Simonet-Davin, R.; Fierz, B.; Waser, J. “Doubly Orthogonal” Labeling of Peptides and Proteins. *Chem* **2019**, *5* (8), 2243–2263. https://doi.org/10.1016/j.chempr.2019.06.022.

(53) Tessier, R.; Nandi, R. K.; Dwyer, B. G.; Abegg, D.; Sornay, C.; Ceballos, J.; Erb, S.; Cianférani, S.; Wagner, A.; Chaubet, G.; Adibekian, A.; Waser, J. Ethynylation of Cysteine Residues: From Peptides to Proteins in Vitro and in Living Cells. *Angew. Chem. Int. Ed.* **2020**, *59* (27), 10961–10970. https://doi.org/10.1002/anie.202002626.

(54) Gazvoda, M.; Dhanjee, H. H.; Rodriguez, J.; Brown, J. S.; Farquhar, C. E.; Truex, N. L.; Loas, A.; Buchwald, S. L.; Pentelute, B. L. Palladium-Mediated Incorporation of Carboranes into Small Molecules, Peptides, and Proteins. *J. Am. Chem. Soc.* **2022**, *144* (17), 7852–7860. https://doi.org/10.1021/jacs.2c01932.

(55) Tilden, J. A. R.; Lubben, A. T.; Reeksting, S. B.; Kociok-Köhn, G.; Frost, C. G. Pd(II)-Mediated C−H Activation for Cysteine Bioconjugation. *Chem. – Eur. J.* **2022**, *28* (11), e202104385. https://doi.org/10.1002/chem.202104385.

(56) Tamura, T.; Hamachi, I. Recent Progress in Design of Protein-Based Fluorescent Biosensors and Their Cellular Applications. *ACS Chem. Biol.* **2014**, *9* (12), 2708–2717. https://doi.org/10.1021/cb500661v.

(57) Nischan, N.; Hackenberger, C. P. R. Site-Specific PEGylation of Proteins: Recent Developments. *J. Org. Chem.* **2014**, *79* (22), 10727–10733. https://doi.org/10.1021/jo502136n.

(58) Turecek, P. L.; Bossard, M. J.; Schoetens, F.; Ivens, I. A. PEGylation of Biopharmaceuticals: A Review of Chemistry and Nonclinical Safety Information of Approved Drugs. *J. Pharm. Sci.* **2016**, *105* (2), 460–475. https://doi.org/10.1016/j.xphs.2015.11.015.

(59) Lambert, J. M.; Berkenblit, A. Antibody–Drug Conjugates for Cancer Treatment. *Annu. Rev. Med.* **2018**, *69* (1), 191–207. https://doi.org/10.1146/annurev-med-061516-121357.

(60) Beck, A.; Goetsch, L.; Dumontet, C.; Corvaïa, N. Strategies and Challenges for the next Generation of Antibody–Drug Conjugates. *Nat. Rev. Drug Discov.* **2017**, *16* (5), 315–337. https://doi.org/10.1038/nrd.2016.268.

(61) Schumacher, D.; Hackenberger, C. P. R.; Leonhardt, H.; Helma, J. Current Status: Site-Specific Antibody Drug Conjugates. *J. Clin. Immunol.* **2016**, *36* (1), 100–107. https://doi.org/10.1007/s10875-016-0265-6.

(62) Gautier, V.; Boumeester, A. J.; Lössl, P.; Heck, A. J. R. Lysine Conjugation Properties in Human IgGs Studied by Integrating High-Resolution Native Mass Spectrometry and Bottom-up Proteomics. *PROTEOMICS* **2015**, *15* (16), 2756–2765. https://doi.org/10.1002/pmic.201400462.

(63) Hoyt, E. A.; Cal, P. M. S. D.; Oliveira, B. L.; Bernardes, G. J. L. Contemporary Approaches to Site-Selective Protein Modification. *Nat. Rev. Chem.* **2019**, *3* (3), 147–171. https://doi.org/10.1038/s41570-019-0079-1.

(64) Junutula, J. R.; Bhakta, S.; Raab, H.; Ervin, K. E.; Eigenbrot, C.; Vandlen, R.; Scheller, R. H.; Lowman, H. B. Rapid Identification of Reactive Cysteine Residues for Site-Specific Labeling of Antibody-Fabs. *J. Immunol. Methods* **2008**, *332* (1), 41–52. https://doi.org/10.1016/j.jim.2007.12.011.

(65) Junutula, J. R.; Raab, H.; Clark, S.; Bhakta, S.; Leipold, D. D.; Weir, S.; Chen, Y.; Simpson, M.; Tsai, S. P.; Dennis, M. S.; Lu, Y.; Meng, Y. G.; Ng, C.; Yang, J.; Lee, C. C.; Duenas, E.; Gorrell, J.; Katta, V.; Kim, A.; McDorman, K.; Flagella, K.; Venook, R.; Ross, S.; Spencer, S. D.; Lee Wong, W.; Lowman, H. B.; Vandlen, R.; Sliwkowski, M. X.; Scheller, R. H.; Polakis, P.; Mallet, W. Site-Specific Conjugation of a Cytotoxic Drug to an Antibody Improves the Therapeutic Index. *Nat. Biotechnol.* **2008**, *26* (8), 925–932. https://doi.org/10.1038/nbt.1480.

(66) Sadowsky, J. D.; Pillow, T. H.; Chen, J.; Fan, F.; He, C.; Wang, Y.; Yan, G.; Yao, H.; Xu, Z.; Martin, S.; Zhang, D.; Chu, P.; dela Cruz-Chuh, J.; O'Donohue, A.; Li, G.; Del Rosario, G.; He, J.; Liu, L.; Ng, C.; Su, D.; Lewis Phillips, G. D.; Kozak, K. R.; Yu, S.-F.; Xu, K.; Leipold, D.; Wai, J. Development of Efficient Chemistry to Generate Site-Specific Disulfide-Linked Protein– and Peptide–Payload Conjugates: Application to THIOMAB Antibody–Drug Conjugates. *Bioconjug. Chem.* **2017**, *28* (8), 2086–2098. https://doi.org/10.1021/acs.bioconjchem.7b00258.

(67) Hofer, T.; Thomas, J. D.; Burke, T. R.; Rader, C. An Engineered Selenocysteine Defines a Unique Class of Antibody Derivatives. *Proc. Natl. Acad. Sci.* **2008**, *105* (34), 12451–12456. https://doi.org/10.1073/pnas.0800800105.

(68) Hofer, T.; Skeffington, L. R.; Chapman, C. M.; Rader, C. Molecularly Defined Antibody Conjugation through a Selenocysteine Interface. *Biochemistry* **2009**, *48* (50), 12047–12057. https://doi.org/10.1021/bi901744t.

(69) Hatfield, D. L.; Tsuji, P. A.; Carlson, B. A.; Gladyshev, V. N. Selenium and Selenocysteine: Roles in Cancer, Health, and Development. *Trends Biochem. Sci.* **2014**, *39* (3), 112–120. https://doi.org/10.1016/j.tibs.2013.12.007.

(70) Driscoll, D. M.; Copeland, P. R. MECHANISM AND REGULATION OF SELENOPROTEIN SYNTHESIS. *Annu. Rev. Nutr.* **2003**, *23* (1), 17–40. https://doi.org/10.1146/annurev.nutr.23.011702.073318.

(71) Li, X.; Nelson, C. G.; Nair, R. R.; Hazlehurst, L.; Moroni, T.; Martinez-Acedo, P.; Nanna, A. R.; Hymel, D.; Burke, T. R.; Rader, C. Stable and Potent Selenomab-Drug Conjugates. *Cell Chem. Biol.* **2017**, *24* (4), 433-442.e6. https://doi.org/10.1016/j.chembiol.2017.02.012.

(72) Wang, L.; Gruzdys, V.; Pang, N.; Meng, F.; Sun, X.-L. Primary Arylamine-Based Tyrosine-Targeted Protein Modification. *RSC Adv.* **2014**, *4* (74), 39446–39452. https://doi.org/10.1039/C4RA05413J.

(73) Wong, C.-Y.; Chung, L.-H.; Lin, S.; Chan, D. S.-H.; Leung, C.-H.; Ma, D.-L. A Ruthenium(II) Complex Supported by Trithiacyclononane and Aromatic Diimine Ligand as Luminescent Switch-On Probe for Biomolecule Detection and Protein Staining. *Sci. Rep.* **2014**, *4* (1), 7136. https://doi.org/10.1038/srep07136.

(74) Seki, Y.; Ishiyama, T.; Sasaki, D.; Abe, J.; Sohma, Y.; Oisaki, K.; Kanai, M. Transition Metal-Free Tryptophan-Selective Bioconjugation of Proteins. *J. Am. Chem. Soc.* **2016**, *138* (34), 10798–10801. https://doi.org/10.1021/jacs.6b06692.

(75) Solomatina, A. I.; Chelushkin, P. S.; Krupenya, D. V.; Podkorytov, I. S.; Artamonova, T. O.; Sizov, V. V.; Melnikov, A. S.; Gurzhiy, V. V.; Koshel, E. I.; Shcheslavskiy, V. I.; Tunik, S. P. Coordination to Imidazole Ring Switches on Phosphorescence of Platinum Cyclometalated Complexes: The Route to Selective Labeling of Peptides and Proteins via Histidine Residues. *Bioconjug. Chem.* **2017**, *28* (2), 426–437. https://doi.org/10.1021/acs.bioconjchem.6b00598.

(76) Agard, N. J.; Prescher, J. A.; Bertozzi, C. R. A Strain-Promoted [3 + 2] Azide−Alkyne Cycloaddition for Covalent Modification of Biomolecules in Living Systems. *J. Am. Chem. Soc.* **2004**, *126* (46), 15046–15047. https://doi.org/10.1021/ja044996f.

(77) Kularatne, S. A.; Deshmukh, V.; Ma, J.; Tardif, V.; Lim, R. K. V.; Pugh, H. M.; Sun, Y.; Manibusan, A.; Sellers, A. J.; Barnett, R. S.; Srinagesh, S.; Forsyth, J. S.; Hassenpflug, W.; Tian, F.; Javahishvili, T.; Felding-Habermann, B.; Lawson, B. R.; Kazane, S. A.; Schultz, P. G. A CXCR4-Targeted Site-Specific Antibody–Drug Conjugate. *Angew. Chem. Int. Ed.* **2014**, *53* (44), 11863–11867. https://doi.org/10.1002/anie.201408103.

(78) Zimmerman, E. S.; Heibeck, T. H.; Gill, A.; Li, X.; Murray, C. J.; Madlansacay, M. R.; Tran, C.; Uter, N. T.; Yin, G.; Rivers, P. J.; Yam, A. Y.; Wang, W. D.; Steiner, A. R.; Bajad, S. U.; Penta, K.; Yang, W.; Hallam, T. J.; Thanos, C. D.; Sato, A. K. Production of Site-Specific Antibody–Drug Conjugates Using Optimized Non-Natural Amino Acids in a Cell-Free Expression System. *Bioconjug. Chem.* **2014**, *25* (2), 351–361. https://doi.org/10.1021/bc400490z.

(79) VanBrunt, M. P.; Shanebeck, K.; Caldwell, Z.; Johnson, J.; Thompson, P.; Martin, T.; Dong, H.; Li, G.; Xu, H.; D'Hooge, F.; Masterson, L.; Bariola, P.; Tiberghien, A.; Ezeadi, E.; Williams, D. G.; Hartley, J. A.; Howard, P. W.; Grabstein, K. H.; Bowen, M. A.; Marelli, M. Genetically Encoded Azide Containing Amino Acid in Mammalian Cells Enables Site-Specific Antibody–Drug Conjugates Using Click Cycloaddition Chemistry. *Bioconjug. Chem.* **2015**, *26* (11), 2249–2260. https://doi.org/10.1021/acs.bioconjchem.5b00359.

(80) Wu, Y.; Zhu, H.; Zhang, B.; Liu, F.; Chen, J.; Wang, Y.; Wang, Y.; Zhang, Z.; Wu, L.; Si, L.; Xu, H.; Yao, T.; Xiao, S.; Xia, Q.; Zhang, L.; Yang, Z.; Zhou, D. Synthesis of Site-Specific Radiolabeled Antibodies for Radioimmunotherapy via Genetic Code Expansion. *Bioconjug. Chem.* **2016**, *27* (10), 2460–2468. https://doi.org/10.1021/acs.bioconjchem.6b00412.

(81) Roy, G.; Reier, J.; Garcia, A.; Martin, T.; Rice, M.; Wang, J.; Prophet, M.; Christie, R.; Dall'Acqua, W.; Ahuja, S.; Bowen, M. A.; Marelli, M. Development of a High Yielding Expression Platform for the Introduction of Non-Natural Amino Acids in Protein Sequences. *mAbs* **2020**, *12* (1), 1684749. https://doi.org/10.1080/19420862.2019.1684749.

(82) Oller-Salvia, B.; Kym, G.; Chin, J. W. Rapid and Efficient Generation of Stable Antibody–Drug Conjugates via an Encoded Cyclopropene and an Inverse-Electron-Demand Diels–Alder Reaction. *Angew. Chem. Int. Ed.* **2018**, *57* (11), 2831–2834. https://doi.org/10.1002/anie.201712370.

(83) St. Amant, A. H.; Huang, F.; Lin, J.; Rickert, K.; Oganesyan, V.; Lemen, D.; Mao, S.; Harper, J.; Marelli, M.; Wu, H.; Gao, C.; Read de Alaniz, J.; Christie, R. J. A Diene-Containing Noncanonical Amino Acid Enables Dual Functionality in Proteins: Rapid Diels–Alder Reaction with Maleimide or Proximity-Based Dimerization. *Angew. Chem. Int. Ed.* **2019**, *58* (25), 8489–8493. https://doi.org/10.1002/anie.201903494.

(84) Isenegger, P. G.; Davis, B. G. Concepts of Catalysis in Site-Selective Protein Modifications. *J. Am. Chem. Soc.* **2019**, *141* (20), 8005–8013. https://doi.org/10.1021/jacs.8b13187.

(85) Ojida, A.; Tsutsumi, H.; Kasagi, N.; Hamachi, I. Suzuki Coupling for Protein Modification. *Tetrahedron Lett.* **2005**, *46* (19), 3301–3305. https://doi.org/10.1016/j.tetlet.2005.03.094.

(86) Brustad, E.; Bushey, M. L.; Lee, J. W.; Groff, D.; Liu, W.; Schultz, P. G. A Genetically Encoded Boronate-Containing Amino Acid. *Angew. Chem. Int. Ed.* **2008**, *47* (43), 8220–8223. https://doi.org/10.1002/anie.200803240.

(87) Chalker, J. M.; Wood, C. S. C.; Davis, B. G. A Convenient Catalyst for Aqueous and Protein Suzuki−Miyaura Cross-Coupling. *J. Am. Chem. Soc.* **2009**, *131* (45), 16346–16347. https://doi.org/10.1021/ja907150m.

(88) Spicer, C. D.; Davis, B. G. Palladium-Mediated Site-Selective Suzuki–Miyaura Protein Modification at Genetically Encoded Aryl Halides. *Chem. Commun.* **2011**, *47* (6), 1698–1700. https://doi.org/10.1039/C0CC04970K.

(89) Li, J.; Lin, S.; Wang, J.; Jia, S.; Yang, M.; Hao, Z.; Zhang, X.; Chen, P. R. Ligand-Free Palladium-Mediated Site-Specific Protein Labeling Inside Gram-Negative Bacterial Pathogens. *J. Am. Chem. Soc.* **2013**, *135* (19), 7330–7338. https://doi.org/10.1021/ja402424j.

(90) Kodama, K.; Fukuzawa, S.; Nakayama, H.; Sakamoto, K.; Kigawa, T.; Yabuki, T.; Matsuda, N.; Shirouzu, M.; Takio, K.; Yokoyama, S.; Tachibana, K. Site-Specific Functionalization of Proteins by Organopalladium Reactions. *ChemBioChem* **2007**, *8* (2), 232–238. https://doi.org/10.1002/cbic.200600432.

(91) *Regioselective Carbon–Carbon Bond Formation in Proteins with Palladium Catalysis; New Protein Chemistry by Organometallic Chemistry - Kodama - **2006** - ChemBioChem - Wiley Online Library*. https://chemistry-europe-onlinelibrary-wiley-com.scd-rproxy.u-strasbg.fr/doi/10.1002/cbic.200500290 (accessed 2023-07-10).

(92) Keppler, A.; Gendreizig, S.; Gronemeyer, T.; Pick, H.; Vogel, H.; Johnsson, K. A General Method for the Covalent Labeling of Fusion Proteins with Small Molecules in Vivo. *Nat. Biotechnol.* **2003**, *21* (1), 86–89. https://doi.org/10.1038/nbt765.

(93) Gautier, A.; Juillerat, A.; Heinis, C.; Corrêa, I. R.; Kindermann, M.; Beaufils, F.; Johnsson, K. An Engineered Protein Tag for Multiprotein Labeling in Living Cells. *Chem. Biol.* **2008**, *15* (2), 128–136. https://doi.org/10.1016/j.chembiol.2008.01.007.

(94) Yang, G.; de Castro Reis, F.; Sundukova, M.; Pimpinella, S.; Asaro, A.; Castaldi, L.; Batti, L.; Bilbao, D.; Reymond, L.; Johnsson, K.; Heppenstall, P. A. Genetic Targeting of Chemical Indicators in Vivo. *Nat. Methods* **2015**, *12* (2), 137–139. https://doi.org/10.1038/nmeth.3207.

(95) Los, G. V.; Encell, L. P.; McDougall, M. G.; Hartzell, D. D.; Karassina, N.; Zimprich, C.; Wood, M. G.; Learish, R.; Ohana, R. F.; Urh, M.; Simpson, D.; Mendez, J.; Zimmerman, K.; Otto, P.; Vidugiris, G.; Zhu, J.; Darzins, A.; Klaubert, D. H.; Bulleit, R. F.; Wood, K. V. HaloTag: A Novel Protein Labeling Technology for Cell Imaging and Protein Analysis. *ACS Chem. Biol.* **2008**, *3* (6), 373–382. https://doi.org/10.1021/cb800025k.

(96) Hori, Y.; Ueno, H.; Mizukami, S.; Kikuchi, K. Photoactive Yellow Protein-Based Protein Labeling System with Turn-On Fluorescence Intensity. *J. Am. Chem. Soc.* **2009**, *131* (46), 16610–16611. https://doi.org/10.1021/ja904800k.

(97) Hori, Y.; Norinobu, T.; Sato, M.; Arita, K.; Shirakawa, M.; Kikuchi, K. Development of Fluorogenic Probes for Quick No-Wash Live-Cell Imaging of Intracellular Proteins. *J. Am. Chem. Soc.* **2013**, *135* (33), 12360–12365. https://doi.org/10.1021/ja405745v.

(98) Zhang, C.; Welborn, M.; Zhu, T.; Yang, N. J.; Santos, M. S.; Van Voorhis, T.; Pentelute, B. L. π-Clamp-Mediated Cysteine Conjugation. *Nat. Chem.* **2016**, *8* (2), 120–128. https://doi.org/10.1038/nchem.2413.

(99) Zhang, C.; Dai, P.; Vinogradov, A. A.; Gates, Z. P.; Pentelute, B. L. Site-Selective Cysteine–Cyclooctyne Conjugation. *Angew. Chem. Int. Ed.* **2018**, *57* (22), 6459–6463. https://doi.org/10.1002/anie.201800860.

(100) Walsh, S. J.; Bargh, J. D.; Dannheim, F. M.; Hanby, A. R.; Seki, H.; Counsell, A. J.; Ou, X.; Fowler, E.; Ashman, N.; Takada, Y.; Isidro-Llobet, A.; Parker, J. S.; Carroll, J. S.; Spring, D. R. Site-Selective Modification Strategies in Antibody–Drug Conjugates. *Chem. Soc. Rev.* **2021**, *50* (2), 1305–1353. https://doi.org/10.1039/D0CS00310G.

(101) Chen, X.; Muthoosamy, K.; Pfisterer, A.; Neumann, B.; Weil, T. Site-Selective Lysine Modification of Native Proteins and Peptides via Kinetically Controlled Labeling. *Bioconjug. Chem.* **2012**, *23* (3), 500–508. https://doi.org/10.1021/bc200556n.

(102) Pham, G. H.; Ou, W.; Bursulaya, B.; DiDonato, M.; Herath, A.; Jin, Y.; Hao, X.; Loren, J.; Spraggon, G.; Brock, A.; Uno, T.; Geierstanger, B. H.; Cellitti, S. E. Tuning a Protein-Labeling Reaction to Achieve Highly Site Selective Lysine Conjugation. *ChemBioChem* **2018**, *19* (8), 799–804. https://doi.org/10.1002/cbic.201700611.

(103) Matos, M. J.; Oliveira, B. L.; Martínez-Sáez, N.; Guerreiro, A.; Cal, P. M. S. D.; Bertoldo, J.; Maneiro, M.; Perkins, E.; Howard, J.; Deery, M. J.; Chalker, J. M.; Corzana, F.; Jiménez-Osés, G.; Bernardes, G. J. L. Chemo- and Regioselective Lysine Modification on Native Proteins. *J. Am. Chem. Soc.* **2018**, *140* (11), 4004–4017. https://doi.org/10.1021/jacs.7b12874.

(104) Chilamari, M.; Purushottam, L.; Rai, V. Site-Selective Labeling of Native Proteins by a Multicomponent Approach. *Chem. – Eur. J.* **2017**, *23* (16), 3819–3823. https://doi.org/10.1002/chem.201605938.

(105) Chilamari, M.; Kalra, N.; Shukla, S.; Rai, V. Single-Site Labeling of Lysine in Proteins through a Metal-Free Multicomponent Approach. *Chem. Commun.* **2018**, *54* (53), 7302–7305. https://doi.org/10.1039/C8CC03311K.

(106) Dawson, P. E.; Muir, T. W.; Clark-Lewis, I.; Kent, S. B. H. Synthesis of Proteins by Native Chemical Ligation. *Science* **1994**, *266* (5186), 776–779. https://doi.org/10.1126/science.7973629.

(107) Forte, N.; Benni, I.; Karu, K.; Chudasama, V.; Baker, J. R. Cysteine-to-Lysine Transfer Antibody Fragment Conjugation. *Chem. Sci.* **2019**, *10* (47), 10919–10924. https://doi.org/10.1039/C9SC03825F.

(108) Adusumalli, S. R.; Rawale, D. G.; Thakur, K.; Purushottam, L.; Reddy, N. C.; Kalra, N.; Shukla, S.; Rai, V. Chemoselective and Site-Selective Lysine-Directed Lysine Modification Enables Single-Site Labeling of Native Proteins. *Angew. Chem. Int. Ed.* **2020**, *59* (26), 10332–10336. https://doi.org/10.1002/anie.202000062.

(109) Matsuda, Y.; Malinao, M.-C.; Robles, V.; Song, J.; Yamada, K.; Mendelsohn, B. A. Proof of Site-Specificity of Antibody-Drug Conjugates Produced by Chemical Conjugation Technology: AJICAP First Generation. *J. Chromatogr. B* **2020**, *1140*, 121981. https://doi.org/10.1016/j.jchromb.2020.121981.

(110) Yamada, K.; Shikida, N.; Shimbo, K.; Ito, Y.; Khedri, Z.; Matsuda, Y.; Mendelsohn, B. A. AJICAP: Affinity Peptide Mediated Regiodivergent Functionalization of Native Antibodies. *Angew. Chem. Int. Ed.* **2019**, *58* (17), 5592–5597. https://doi.org/10.1002/anie.201814215.

(111) Matsuda, Y.; Mendelsohn, B. A. An Overview of Process Development for Antibody-Drug Conjugates Produced by Chemical Conjugation Technology. *Expert Opin. Biol. Ther.* **2021**, *21* (7), 963–975. https://doi.org/10.1080/14712598.2021.1846714.

(112) Fujii, T.; Matsuda, Y.; Seki, T.; Shikida, N.; Iwai, Y.; Ooba, Y.; Takahashi, K.; Isokawa, M.; Kawaguchi, S.; Hatada, N.; Watanabe, T.; Takasugi, R.; Nakayama, A.; Shimbo, K.; Mendelsohn, B. A.; Okuzumi, T.; Yamada, K. AJICAP Second Generation: Improved Chemical Site-Specific Conjugation Technology for Antibody–Drug Conjugate Production. *Bioconjug. Chem.* **2023**, *34* (4), 728–738. https://doi.org/10.1021/acs.bioconjchem.3c00040.

(113) Liberatore, F. A.; Comeau, R. D.; McKearin, J. M.; Pearson, D. A.; Belonga, B. Q. I.; Brocchini, S. J.; Kath, J.; Phillips, T.; Oswell, K.; Lawton, R. G. Site-Directed Chemical Modification and Crosslinking of a Monoclonal Antibody Using Equilibrium Transfer Alkylating Crosslink Reagents. *Bioconjug. Chem.* **1990**, *1* (1), 36–50. https://doi.org/10.1021/bc00001a005.

(114) Del Rosario, R. B.; Wahl, R. L.; Brocchini, S. J.; Lawton, R. G.; Smith, R. H. Sulfhydryl Site-Specific Crosslinking and Labeling of Monoclonal Antibodies by a Fluorescent Equilibrium Transfer Alkylation Crosslink Reagent. *Bioconjug. Chem.* **1990**, *1* (1), 51–59. https://doi.org/10.1021/bc00001a006.

(115) Bird, M.; Nunes, J.; Frigerio, M. Bridged Cysteine Conjugations. In *Antibody-Drug Conjugates: Methods and Protocols*; Tumey, L. N., Ed.; Methods in Molecular Biology; Springer US: New York, NY, **2020**; pp 113–129. https://doi.org/10.1007/978-1-4939-9929-3_8.

(116) Forte, N.; Livanos, M.; Miranda, E.; Morais, M.; Yang, X.; Rajkumar, V. S.; Chester, K. A.; Chudasama, V.; Baker, J. R. Tuning the Hydrolytic Stability of Next Generation Maleimide Cross-Linkers Enables Access to Albumin-Antibody Fragment Conjugates and Tri-scFvs. *Bioconjug. Chem.* **2018**, *29* (2), 486–492. https://doi.org/10.1021/acs.bioconjchem.7b00795.

(117) Feuillâtre, O.; Gély, C.; Huvelle, S.; Baltus, C. B.; Juen, L.; Joubert, N.; Desgranges, A.; Viaud-Massuard, M.-C.; Martin, C. Impact of Maleimide Disubstitution on Chemical and Biological Characteristics of HER2 Antibody–Drug Conjugates. *ACS Omega* **2020**, *5* (3), 1557–1565. https://doi.org/10.1021/acsomega.9b03510.

(118) Schumacher, F. F.; Nunes, J. P. M.; Maruani, A.; Chudasama, V.; Smith, M. E. B.; Chester, K. A.; Baker, J. R.; Caddick, S. Next Generation Maleimides Enable the Controlled Assembly of Antibody–Drug Conjugates via Native Disulfide Bond Bridging. *Org. Biomol. Chem.* **2014**, *12* (37), 7261–7269. https://doi.org/10.1039/C4OB01550A.

(119) Chudasama, V.; Smith, M. E. B.; Schumacher, F. F.; Papaioannou, D.; Waksman, G.; Baker, J. R.; Caddick, S. Bromopyridazinedione-Mediated Protein and Peptide Bioconjugation. *Chem. Commun.* **2011**, *47* (31), 8781–8783. https://doi.org/10.1039/C1CC12807H.

(120) Lee, M. T. W.; Maruani, A.; Chudasama, V. The Use of 3,6-Pyridazinediones in Organic Synthesis and Chemical Biology. *J. Chem. Res.* **2016**, *40* (1), 1–9. https://doi.org/10.3184/174751916X14495034614855.

(121) Robinson, E.; Nunes, J. P. M.; Vassileva, V.; Maruani, A.; Nogueira, J. C. F.; Smith, M. E. B.; Pedley, R. B.; Caddick, S.; Baker, J. R.; Chudasama, V. Pyridazinediones Deliver Potent, Stable, Targeted and Efficacious Antibody–Drug Conjugates (ADCs) with a Controlled Loading of 4 Drugs per Antibody. *RSC Adv.* **2017**, *7* (15), 9073–9077. https://doi.org/10.1039/C7RA00788D.

(122) Spears, R. J.; McMahon, C.; Shamsabadi, M.; Bahou, C.; Thanasi, I. A.; Rochet, L. N. C.; Forte, N.; Thoreau, F.; Baker, J. R.; Chudasama, V. A Novel Thiol-Labile Cysteine Protecting Group for Peptide Synthesis Based on a Pyridazinedione (PD) Scaffold. *Chem. Commun.* **2022**, *58* (5), 645–648. https://doi.org/10.1039/D1CC03802H.

(123) Lee, M. T. W.; Maruani, A.; Baker, J. R.; Caddick, S.; Chudasama, V. Next-Generation Disulfide Stapling: Reduction and Functional Re-Bridging All in One. *Chem. Sci.* **2015**, *7* (1), 799–802. https://doi.org/10.1039/C5SC02666K.

(124) Maruani, A.; Smith, M. E. B.; Miranda, E.; Chester, K. A.; Chudasama, V.; Caddick, S. A Plug-and-Play Approach to Antibody-Based Therapeutics via a Chemoselective Dual Click Strategy. *Nat. Commun.* **2015**, *6* (1), 6645. https://doi.org/10.1038/ncomms7645.

(125) Lee, M. T. W.; Maruani, A.; Richards, D. A.; Baker, J. R.; Caddick, S.; Chudasama, V. Enabling the Controlled Assembly of Antibody Conjugates with a Loading of Two Modules without Antibody Engineering. *Chem. Sci.* **2017**, *8* (3), 2056–2060. https://doi.org/10.1039/C6SC03655D.

(126) Bahou, C.; Richards, D. A.; Maruani, A.; Love, E. A.; Javaid, F.; Caddick, S.; Baker, J. R.; Chudasama, V. Highly Homogeneous Antibody Modification through Optimisation of the Synthesis and Conjugation of Functionalised Dibromopyridazinediones. *Org. Biomol. Chem.* **2018**, *16* (8), 1359–1366. https://doi.org/10.1039/C7OB03138F.

(127) Greene, M. K.; Richards, D. A.; Nogueira, J. C. F.; Campbell, K.; Smyth, P.; Fernández, M.; Scott, C. J.; Chudasama, V. Forming Next-Generation Antibody–Nanoparticle Conjugates through the Oriented Installation of Non-Engineered Antibody Fragments. *Chem. Sci.* **2017**, *9* (1), 79–87. https://doi.org/10.1039/C7SC02747H.

(128) Thoreau, F.; Szijj, P. A.; Greene, M. K.; Rochet, L. N. C.; Thanasi, I. A.; Blayney, J. K.; Maruani, A.; Baker, J. R.; Scott, C. J.; Chudasama, V. Modular Chemical Construction of IgG-like Mono- and Bispecific Synthetic Antibodies (SynAbs). *ACS Cent. Sci.* **2023**. https://doi.org/10.1021/acscentsci.2c01437.

(129) Counsell, A. J.; Walsh, S. J.; Robertson, N. S.; Sore, H. F.; Spring, D. R. Efficient and Selective Antibody Modification with Functionalised Divinyltriazines. *Org. Biomol. Chem.* **2020**, *18* (25), 4739–4743. https://doi.org/10.1039/D0OB01002B.

(130) Hanby, A. R.; Walsh, S. J.; Counsell, A. J.; Ashman, N.; Mortensen, K. T.; Carroll, J. S.; Spring, D. R. Antibody Dual-Functionalisation Enabled through a Modular Divinylpyrimidine Disulfide Rebridging Strategy. *Chem. Commun.* **2022**, *58* (67), 9401–9404. https://doi.org/10.1039/D2CC02515A.

(131) Dannheim, F. M.; Walsh, S. J.; Orozco, C. T.; Hansen, A. H.; Bargh, J. D.; Jackson, S. E.; Bond, N. J.; Parker, J. S.; Carroll, J. S.; Spring, D. R. All-in-One Disulfide Bridging Enables the Generation of Antibody Conjugates with Modular Cargo Loading. *Chem. Sci.* **2022**, *13* (30), 8781–8790. https://doi.org/10.1039/D2SC02198F.

(132) Chrzastek, A.; Thanasi, I. A.; Irving, J. A.; Chudasama, V.; Baker, J. R. Dual Reactivity Disulfide Bridging Reagents; Enabling New Approaches to Antibody Fragment Bioconjugation. *Chem. Sci.* **2022**, *13* (39), 11533–11539. https://doi.org/10.1039/D2SC04531A.

(133) Gilmore, J. M.; Scheck, R. A.; Esser-Kahn, A. P.; Joshi, N. S.; Francis, M. B. N-Terminal Protein Modification through a Biomimetic Transamination Reaction. *Angew. Chem. Int. Ed.* **2006**, *45* (32), 5307–5311. https://doi.org/10.1002/anie.200600368.

(134) Witus, L. S.; Netirojjanakul, C.; Palla, K. S.; Muehl, E. M.; Weng, C.-H.; Iavarone, A. T.; Francis, M. B. Site-Specific Protein Transamination Using N-Methylpyridinium-4-Carboxaldehyde. *J. Am. Chem. Soc.* **2013**, *135* (45), 17223–17229. https://doi.org/10.1021/ja408868a.

(135) MacDonald, J. I.; Munch, H. K.; Moore, T.; Francis, M. B. One-Step Site-Specific Modification of Native Proteins with 2-Pyridinecarboxyaldehydes. *Nat. Chem. Biol.* **2015**, *11* (5), 326–331. https://doi.org/10.1038/nchembio.1792.

(136) Adumeau, P.; Sharma, S. K.; Brent, C.; Zeglis, B. M. Site-Specifically Labeled Immunoconjugates for Molecular Imaging—Part 1: Cysteine Residues and Glycans. *Mol. Imaging Biol.* **2016**, *18* (1), 1–17. https://doi.org/10.1007/s11307-015-0919-4.

(137) F. Schumacher, F.; M. Nunes, J. P.; Maruani, A.; Chudasama, V.; B. Smith, M. E.; A. Chester, K.; R. Baker, J.; Caddick, S. Next Generation Maleimides Enable the Controlled Assembly of Antibody–Drug Conjugates via Native Disulfide Bond Bridging. *Org. Biomol. Chem.* **2014**, *12* (37), 7261–7269. https://doi.org/10.1039/C4OB01550A.

(138) Küppers, J.; Kürpig, S.; Bundschuh, R. A.; Essler, M.; Lütje, S. Radiolabeling Strategies of Nanobodies for Imaging Applications. *Diagnostics* **2021**, *11* (9), 1530. https://doi.org/10.3390/diagnostics11091530.

(139) Serafimova, I. M.; Pufall, M. A.; Krishnan, S.; Duda, K.; Cohen, M. S.; Maglathlin, R. L.; McFarland, J. M.; Miller, R. M.; Frödin, M.; Taunton, J. Reversible Targeting of Noncatalytic Cysteines with Chemically Tuned Electrophiles. *Nat. Chem. Biol.* **2012**, *8* (5), 471–476. https://doi.org/10.1038/nchembio.925.

(140) Weissman, M. R.; Winger, K. T.; Ghiassian, S.; Gobbo, P.; Workentin, M. S. Insights on the Application of the Retro Michael-Type Addition on Maleimide-Functionalized Gold Nanoparticles in Biology and Nanomedicine. *Bioconjug. Chem.* **2016**, *27* (3), 586–593. https://doi.org/10.1021/acs.bioconjchem.5b00600.

(141) Hoare, T. R.; Kohane, D. S. Hydrogels in Drug Delivery: Progress and Challenges. *Polymer* **2008**, *49* (8), 1993–2007. https://doi.org/10.1016/j.polymer.2008.01.027.

(142) Mauri, E.; Veglianese, P.; Papa, S.; Mariani, A.; Paola, M. D.; Rigamonti, R.; F. Chincarini, G. M.; Vismara, I.; Rimondo, S.; Sacchetti, A.; Rossi, F. Double Conjugated Nanogels for Selective Intracellular Drug Delivery. *RSC Adv.* **2017**, *7* (48), 30345–30356. https://doi.org/10.1039/C7RA04584K.

(143) Schneider, E. L.; Henise, J.; Reid, R.; Ashley, G. W.; Santi, D. V. Hydrogel Drug Delivery System Using Self-Cleaving Covalent Linkers for Once-a-Week Administration of Exenatide. *Bioconjug. Chem.* **2016**, *27* (5), 1210–1215. https://doi.org/10.1021/acs.bioconjchem.5b00690.

(144) Chen, G.; Li, J.; Cai, Y.; Zhan, J.; Gao, J.; Song, M.; Shi, Y.; Yang, Z. A Glycyrrhetinic Acid-Modified Curcumin Supramolecular Hydrogel for Liver Tumor Targeting Therapy. *Sci. Rep.* **2017**, *7* (1), 44210. https://doi.org/10.1038/srep44210.

(145) Mauri, E.; Rossetti, A.; Mozetic, P.; Schiavon, C.; Sacchetti, A.; Rainer, A.; Rossi, F. Ester Coupling of Ibuprofen in Hydrogel Matrix: A Facile One-Step Strategy for Controlled Anti-Inflammatory Drug Release. *Eur. J. Pharm. Biopharm.* **2020**, *146*, 143–149. https://doi.org/10.1016/j.ejpb.2019.11.002.

(146) Santi, D. V.; Schneider, E. L.; Reid, R.; Robinson, L.; Ashley, G. W. Predictable and Tunable Half-Life Extension of Therapeutic Agents by Controlled Chemical Release from Macromolecular Conjugates. *Proc. Natl. Acad. Sci. U. S. A.* **2012**, *109* (16), 6211–6216. https://doi.org/10.1073/pnas.1117147109.

(147) Greenwald, R. B.; Choe, Y. H.; McGuire, J.; Conover, C. D. Effective Drug Delivery by PEGylated Drug Conjugates. *Adv. Drug Deliv. Rev.* **2003**, *55* (2), 217–250. https://doi.org/10.1016/S0169-409X(02)00180-1.

(148) Shen, B.-Q.; Xu, K.; Liu, L.; Raab, H.; Bhakta, S.; Kenrick, M.; Parsons-Reponte, K. L.; Tien, J.; Yu, S.-F.; Mai, E.; Li, D.; Tibbitts, J.; Baudys, J.; Saad, O. M.; Scales, S. J.; McDonald, P. J.; Hass, P. E.; Eigenbrot, C.; Nguyen, T.; Solis, W. A.; Fuji, R. N.; Flagella, K. M.; Patel, D.; Spencer, S. D.; Khawli, L. A.; Ebens, A.; Wong, W. L.; Vandlen, R.; Kaur, S.; Sliwkowski, M. X.; Scheller, R. H.; Polakis, P.; Junutula, J. R. Conjugation Site Modulates the in Vivo Stability and Therapeutic Activity of Antibody-Drug Conjugates. *Nat. Biotechnol.* **2012**, *30* (2), 184–189. https://doi.org/10.1038/nbt.2108.

(149) Liu, Z.; Chen, X. Simple Bioconjugate Chemistry Serves Great Clinical Advances: Albumin as a Versatile Platform for Diagnosis and Precision Therapy. *Chem. Soc. Rev.* **2016**, *45* (5), 1432–1456. https://doi.org/10.1039/C5CS00158G.

(150) Baldwin, A. D.; Kiick, K. L. Tunable Degradation of Maleimide–Thiol Adducts in Reducing Environments. *Bioconjug. Chem.* **2011**, *22* (10), 1946–1953. https://doi.org/10.1021/bc200148v.

(151) Bahou, C.; Spears, R. J.; Aliev, A. E.; Maruani, A.; Fernandez, M.; Javaid, F.; Szijj, P. A.; Baker, J. R.; Chudasama, V. Correction: Use of Pyridazinediones as Extracellular Cleavable Linkers through Reversible Cysteine Conjugation. *Chem. Commun.* **2022**, *58* (91), 12740–12740. https://doi.org/10.1039/D2CC90389J.

(152) Nahta, R.; Esteva, F. J. Trastuzumab: Triumphs and Tribulations. *Oncogene* **2007**, *26* (25), 3637–3643. https://doi.org/10.1038/sj.onc.1210379.

(153) Zhao, Y.; Gutshall, L.; Jiang, H.; Baker, A.; Beil, E.; Obmolova, G.; Carton, J.; Taudte, S.; Amegadzie, B. Two Routes for Production and Purification of Fab Fragments in Biopharmaceutical Discovery Research: Papain Digestion of mAb and Transient Expression in Mammalian Cells. *Protein Expr. Purif.* **2009**, *67* (2), 182–189. https://doi.org/10.1016/j.pep.2009.04.012.

(154) Castañeda, L.; Maruani, A.; Schumacher, F. F.; Miranda, E.; Chudasama, V.; Chester, K. A.; Baker, J. R.; Smith, M. E. B.; Caddick, S. Acid-Cleavable Thiomaleamic Acid Linker for Homogeneous Antibody–Drug Conjugation. *Chem. Commun.* **2013**, *49* (74), 8187–8189. https://doi.org/10.1039/C3CC45220D.

(155) Brudno, Y.; Silva, E. A.; Kearney, C. J.; Lewin, S. A.; Miller, A.; Martinick, K. D.; Aizenberg, M.; Mooney, D. J. Refilling Drug Delivery Depots through the Blood. *Proc. Natl. Acad. Sci. U. S. A.* **2014**, *111* (35), 12722–12727. https://doi.org/10.1073/pnas.1413027111.

(156) Brudno, Y.; Pezone, M. J.; Snyder, T. K.; Uzun, O.; Moody, C. T.; Aizenberg, M.; Mooney, D. J. Replenishable Drug Depot to Combat Post-Resection Cancer Recurrence. *Biomaterials* **2018**, *178*, 373–382. https://doi.org/10.1016/j.biomaterials.2018.05.005.

(157) Zhao, J.; Santino, F.; Giacomini, D.; Gentilucci, L. Integrin-Targeting Peptides for the Design of Functional Cell-Responsive Biomaterials. *Biomedicines* **2020**, *8* (9), 307. https://doi.org/10.3390/biomedicines8090307.

(158) Yoshimura, A.; Zhdankin, V. V. Advances in Synthetic Applications of Hypervalent Iodine Compounds. *Chem. Rev.* **2016**, *116* (5), 3328–3435. https://doi.org/10.1021/acs.chemrev.5b00547.

(159) Eisenberger, P.; Gischig, S.; Togni, A. Novel 10-I-3 Hypervalent Iodine-Based Compounds for Electrophilic Trifluoromethylation. *Chem. – Eur. J.* **2006**, *12* (9), 2579–2586. https://doi.org/10.1002/chem.200501052.

(160) Kieltsch, I.; Eisenberger, P.; Togni, A. Mild Electrophilic Trifluoromethylation of Carbon- and Sulfur-Centered Nucleophiles by a Hypervalent Iodine(III)–CF3 Reagent. *Angew. Chem. Int. Ed.* **2007**, *46* (5), 754–757. https://doi.org/10.1002/anie.200603497.

(161) Matoušek, V.; Václavík, J.; Hájek, P.; Charpentier, J.; Blastik, Z. E.; Pietrasiak, E.; Budinská, A.; Togni, A.; Beier, P. Expanding the Scope of Hypervalent Iodine Reagents for Perfluoroalkylation: From Trifluoromethyl to Functionalized Perfluoroethyl. *Chem. – Eur. J.* **2016**, *22* (1), 417–424. https://doi.org/10.1002/chem.201503531.

(162) Václavík, J.; Zschoche, R.; Klimánková, I.; Matoušek, V.; Beier, P.; Hilvert, D.; Togni, A. Irreversible Cysteine-Selective Protein Labeling Employing Modular Electrophilic Tetrafluoroethylation Reagents. *Chem. – Eur. J.* **2017**, *23* (27), 6490–6494. https://doi.org/10.1002/chem.201700607.

(163) Charpentier, J.; Früh, N.; Togni, A. Electrophilic Trifluoromethylation by Use of Hypervalent Iodine Reagents. *Chem. Rev.* **2015**, *115* (2), 650–682. https://doi.org/10.1021/cr500223h.

(164) Commare, B.; Togni, A. Hypervalent Iodine Reagents: Thiol Derivatization with a Tetrafluoroethoxy Coumarin Residue for UV Absorbance Recognition. *Helv. Chim. Acta* **2017**, *100* (5), e1700059. https://doi.org/10.1002/hlca.201700059.

(165) Frei, R.; Waser, J. A Highly Chemoselective and Practical Alkynylation of Thiols. *J. Am. Chem. Soc.* **2013**, *135* (26), 9620–9623. https://doi.org/10.1021/ja4044196.

(166) Frei, R.; Wodrich, M. D.; Hari, D. P.; Borin, P.-A.; Chauvier, C.; Waser, J. Fast and Highly Chemoselective Alkynylation of Thiols with Hypervalent Iodine Reagents Enabled through a Low Energy Barrier Concerted Mechanism. *J. Am. Chem. Soc.* **2014**, *136* (47), 16563–16573. https://doi.org/10.1021/ja5083014.

(167) Frei, R.; Wodrich, M. D.; Hari, D. P.; Borin, P.-A.; Chauvier, C.; Waser, J. Fast and Highly Chemoselective Alkynylation of Thiols with Hypervalent Iodine Reagents Enabled through a Low Energy Barrier Concerted Mechanism. *J. Am. Chem. Soc.* **2014**, *136* (47), 16563–16573. https://doi.org/10.1021/ja5083014.

(168) Wodrich, M. D.; Caramenti, P.; Waser, J. Alkynylation of Thiols with Ethynylbenziodoxolone (EBX) Reagents: α- or β- π-Addition? *Org. Lett.* **2016**, *18* (1), 60–63. https://doi.org/10.1021/acs.orglett.5b03241.

(169) Ceballos, J.; Grinhagena, E.; Sangouard, G.; Heinis, C.; Waser, J. Cys–Cys and Cys–Lys Stapling of Unprotected Peptides Enabled by Hypervalent Iodine Reagents. *Angew. Chem. Int. Ed.* **2021**, *60* (16), 9022–9031. https://doi.org/10.1002/anie.202014511.

(170) Rahimidashaghoul, K.; Klimánková, I.; Hubálek, M.; Korecký, M.; Chvojka, M.; Pokorný, D.; Matoušek, V.; Fojtík, L.; Kavan, D.; Kukačka, Z.; Novák, P.; Beier, P. Reductant-Induced Free Radical Fluoroalkylation of Nitrogen Heterocycles and Innate Aromatic Amino Acid Residues in Peptides and Proteins. *Chem. – Eur. J.* **2019**, *25* (69), 15779–15785. https://doi.org/10.1002/chem.201902944.

(171) Rahimidashaghoul, K.; Klimánková, I.; Hubálek, M.; Matoušek, V.; Filgas, J.; Slavíček, P.; Slanina, T.; Beier, P. Visible-Light-Driven Fluoroalkylation of Tryptophan Residues in Peptides. *ChemPhotoChem* **2021**, *5* (1), 43–50. https://doi.org/10.1002/cptc.202000214.

(172) Brand, J. P.; Charpentier, J.; Waser, J. Direct Alkynylation of Indole and Pyrrole Heterocycles. *Angew. Chem. Int. Ed.* **2009**, *48* (49), 9346–9349. https://doi.org/10.1002/anie.200905419.

(173) Tolnai, G. L.; Brand, J. P.; Waser, J. Gold-Catalyzed Direct Alkynylation of Tryptophan in Peptides Using TIPS-EBX. *Beilstein J. Org. Chem.* **2016**, *12* (1), 745–749. https://doi.org/10.3762/bjoc.12.74.

(174) Hansen, M. B.; Hubálek, F.; Skrydstrup, T.; Hoeg-Jensen, T. Chemo- and Regioselective Ethynylation of Tryptophan-Containing Peptides and Proteins. *Chem. – Eur. J.* **2016**, *22* (5), 1572–1576. https://doi.org/10.1002/chem.201504462.

(175) Wang, P.; Cheng, Y.; Wu, C.; Zhou, Y.; Cheng, Z.; Li, H.; Wang, R.; Su, W.; Fang, L. Tyrosine-Specific Modification via a Dearomatization–Rearomatization Strategy: Access to Azobenzene Functionalized Peptides. *Org. Lett.* **2021**, *23* (11), 4137–4141. https://doi.org/10.1021/acs.orglett.1c01013.

(176) Noble, A.; McCarver, S. J.; MacMillan, D. W. C. Merging Photoredox and Nickel Catalysis: Decarboxylative Cross-Coupling of Carboxylic Acids with Vinyl Halides. *J. Am. Chem. Soc.* **2015**, *137* (2), 624–627. https://doi.org/10.1021/ja511913h.

(177) Bloom, S.; Liu, C.; Kölmel, D. K.; Qiao, J. X.; Zhang, Y.; Poss, M. A.; Ewing, W. R.; MacMillan, D. W. C. Decarboxylative Alkylation for Site-Selective Bioconjugation of Native Proteins via Oxidation Potentials. *Nat. Chem.* **2018**, *10* (2), 205–211. https://doi.org/10.1038/nchem.2888.

(178) Vaillant, F. L.; Wodrich, M. D.; Waser, J. Room Temperature Decarboxylative Cyanation of Carboxylic Acids Using Photoredox Catalysis and Cyanobenziodoxolones: A Divergent Mechanism Compared to Alkynylation. *Chem. Sci.* **2017**, *8* (3), 1790–1800. https://doi.org/10.1039/C6SC04907A.

(179) Garreau, M.; Le Vaillant, F.; Waser, J. C-Terminal Bioconjugation of Peptides through Photoredox Catalyzed Decarboxylative Alkynylation. *Angew. Chem. Int. Ed.* **2019**, *58* (24), 8182–8186. https://doi.org/10.1002/anie.201901922.

(180) Taylor, M. T.; Nelson, J. E.; Suero, M. G.; Gaunt, M. J. A Protein Functionalization Platform Based on Selective Reactions at Methionine Residues. *Nature* **2018**, *562* (7728), 563–568. https://doi.org/10.1038/s41586-018-0608-y.

(181) Gong, W.; Zhang, G.; Liu, T.; Giri, R.; Yu, J.-Q. Site-Selective C(Sp3)–H Functionalization of Di-, Tri-, and Tetrapeptides at the N-Terminus. *J. Am. Chem. Soc.* **2014**, *136* (48), 16940–16946. https://doi.org/10.1021/ja510233h.

(182) Hari, D. P.; Schouwey, L.; Barber, V.; Scopelliti, R.; Fadaei-Tirani, F.; Waser, J. Ethynylbenziodazolones (EBZ) as Electrophilic Alkynylation Reagents for the Highly Enantioselective Copper-Catalyzed Oxyalkynylation of Diazo Compounds. *Chem. – Eur. J.* **2019**, *25* (40), 9522–9528. https://doi.org/10.1002/chem.201900950.

(183) Vinogradova, E. V.; Zhang, C.; Spokoyny, A. M.; Pentelute, B. L.; Buchwald, S. L. Organometallic Palladium Reagents for Cysteine Bioconjugation. *Nature* **2015**, *526* (7575), 687–691. https://doi.org/10.1038/nature15739.

(184) Benazza, R.; Koutsopetras, I.; Vaur, V.; Chaubet, G.; Hernandez-Alba, O.; Cianferani, S. SEC-MS in Denaturing Conditions (dSEC-MS) for In-Depth Analysis of Rebridged Monoclonal Antibody-Based Formats. ChemRxiv June 7, **2023**. https://doi.org/10.26434/chemrxiv-2023-jmp5n.

(185) Nunes, J. P. M.; Morais, M.; Vassileva, V.; Robinson, E.; Rajkumar, V. S.; Smith, M. E. B.; Pedley, R. B.; Caddick, S.; Baker, J. R.; Chudasama, V. Functional Native Disulfide Bridging Enables Delivery of a Potent, Stable and Targeted Antibody–Drug Conjugate (ADC). *Chem. Commun.* **2015**, *51* (53), 10624–10627. https://doi.org/10.1039/C5CC03557K.

(186) Schumacher, F. F.; Sanchania, V. A.; Tolner, B.; Wright, Z. V. F.; Ryan, C. P.; Smith, M. E. B.; Ward, J. M.; Caddick, S.; Kay, C. W. M.; Aeppli, G.; Chester, K. A.; Baker, J. R. Homogeneous Antibody Fragment Conjugation by Disulfide Bridging Introduces 'Spinostics.' *Sci. Rep.* **2013**, *3* (1), 1525. https://doi.org/10.1038/srep01525.

(187) Smith, M. E. B.; Schumacher, F. F.; Ryan, C. P.; Tedaldi, L. M.; Papaioannou, D.; Waksman, G.; Caddick, S.; Baker, J. R. Protein Modification, Bioconjugation, and Disulfide Bridging Using Bromomaleimides. *J. Am. Chem. Soc.* **2010**, *132* (6), 1960–1965. https://doi.org/10.1021/ja908610s.

(188) Bryden, F.; Maruani, A.; Savoie, H.; Chudasama, V.; Smith, M. E. B.; Caddick, S.; Boyle, R. W. Regioselective and Stoichiometrically Controlled Conjugation of Photodynamic Sensitizers to a HER2 Targeting Antibody Fragment. *Bioconjug. Chem.* **2014**, *25* (3), 611–617. https://doi.org/10.1021/bc5000324.

(189) Ding, W.; Chai, J.; Wang, C.; Wu, J.; Yoshikai, N. Stereoselective Access to Highly Substituted Vinyl Ethers via Trans-Difunctionalization of Alkynes with Alcohols and Iodine(III) Electrophile. *J. Am. Chem. Soc.* **2020**, *142* (19), 8619–8624. https://doi.org/10.1021/jacs.0c04140.

(190) Ugi, I.; Dömling, A.; Hörl, W. Multicomponent Reactions in Organic Chemistry. *Endeavour* **1994**, *18* (3), 115–122. https://doi.org/10.1016/S0160-9327(05)80086-9.

(191) Zarganes-Tzitzikas, T.; Dömling, A. Modern Multicomponent Reactions for Better Drug Syntheses. *Org. Chem. Front.* **2014**, *1* (7), 834–837. https://doi.org/10.1039/C4QO00088A.

(192) Zhi, S.; Ma, X.; Zhang, W. Consecutive Multicomponent Reactions for the Synthesis of Complex Molecules. *Org. Biomol. Chem.* **2019**, *17* (33), 7632–7650. https://doi.org/10.1039/C9OB00772E.

(193) Strecker, A. Ueber Die Künstliche Bildung Der Milchsäure Und Einen Neuen, Dem Glycocoll Homologen Körper; *Justus Liebigs Ann. Chem.* **1850**, *75* (1), 27–45. https://doi.org/10.1002/jlac.18500750103.

(194) Versammlungsberichte. *Angew. Chem.* **1959**, *71* (11), 373–388. https://doi.org/10.1002/ange.19590711110.

(195) Mannich, C.; Krösche, W. Ueber Ein Kondensationsprodukt Aus Formaldehyd, Ammoniak Und Antipyrin. *Arch. Pharm. (Weinheim)* **1912**, *250* (1), 647–667. https://doi.org/10.1002/ardp.19122500151.

(196) Biginelli, P. Ueber Aldehyduramide Des Acetessigäthers. *Berichte Dtsch. Chem. Ges.* **1891**, *24* (1), 1317–1319. https://doi.org/10.1002/cber.189102401228.

(197) Petasis, N. A.; Akritopoulou, I. The Boronic Acid Mannich Reaction: A New Method for the Synthesis of Geometrically Pure Allylamines. *Tetrahedron Lett.* **1993**, *34* (4), 583–586. https://doi.org/10.1016/S0040-4039(00)61625-8.

(198) Bienaymé, H.; Bouzid, K. A New Heterocyclic Multicomponent Reaction For the Combinatorial Synthesis of Fused 3-Aminoimidazoles. *Angew. Chem. Int. Ed.* **1998**, *37* (16), 2234–2237. https://doi.org/10.1002/(SICI)1521-3773(19980904)37:16<2234::AID-ANIE2234>3.0.CO;2-R.

(199) Blackburn, C.; Guan, B.; Fleming, P.; Shiosaki, K.; Tsai, S. Parallel Synthesis of 3-Aminoimidazo[1,2-a]Pyridines and Pyrazines by a New Three-Component Condensation. *Tetrahedron Lett.* **1998**, *39* (22), 3635–3638. https://doi.org/10.1016/S0040-4039(98)00653-4.

(200) Groebke, K.; Weber, L.; Mehlin, F. Synthesis of Imidazo[1,2-a] Annulated Pyridines, Pyrazines and Pyrimidines by a Novel Three-Component Condensation. *Synlett* **1998**, *1998* (06), 661–663. https://doi.org/10.1055/s-1998-1721.

(201) Bon, R. S.; Hong, C.; Bouma, M. J.; Schmitz, R. F.; de Kanter, F. J. J.; Lutz, M.; Spek, A. L.; Orru, R. V. A. Novel Multicomponent Reaction for the Combinatorial Synthesis of 2-Imidazolines. *Org. Lett.* **2003**, *5* (20), 3759–3762. https://doi.org/10.1021/ol035521g.

(202) Joshi, N. S.; Whitaker, L. R.; Francis, M. B. A Three-Component Mannich-Type Reaction for Selective Tyrosine Bioconjugation. *J. Am. Chem. Soc.* **2004**, *126* (49), 15942–15943. https://doi.org/10.1021/ja0439017.

(203) Sim, Y. E.; Nwajiobi, O.; Mahesh, S.; Cohen, R. D.; Reibarkh, M. Y.; Raj, M. Secondary Amine Selective Petasis (SASP) Bioconjugation. *Chem. Sci.* **2019**, *11* (1), 53–61. https://doi.org/10.1039/C9SC04697F.

(204) Ricardo, M. G.; Llanes, D.; Wessjohann, L. A.; Rivera, D. G. Introducing the Petasis Reaction for Late-Stage Multicomponent Diversification, Labeling, and Stapling of Peptides. *Angew. Chem. Int. Ed.* **2019**, *58* (9), 2700–2704. https://doi.org/10.1002/anie.201812620.

(205) Krajcovicova, S.; Spring, D. R. Tryptophan in Multicomponent Petasis Reactions for Peptide Stapling and Late-Stage Functionalisation. *Angew. Chem. Int. Ed.* **2023**, *62* (34), e202307782. https://doi.org/10.1002/anie.202307782.

(206) Marek, M.; Jarý, J.; Valentová, O.; Vodrážka, Z. Immobilization of Glycoenzymes by Means of Their Glycosidic Components. *Biotechnol. Lett.* **1983**, *5* (10), 653–658. https://doi.org/10.1007/BF01386357.

(207) Ziegler, T.; Gerling, S.; Lang, M. Preparation of Bioconjugates through an Ugi Reaction. *Angew. Chem. Int. Ed.* **2000**, *39* (12), 2109–2112. https://doi.org/10.1002/1521-3773(20000616)39:12<2109::AID-ANIE2109>3.0.CO;2-9.

(208) Humpierre, A. R.; Zanuy, A.; Saenz, M.; Garrido, R.; Vasco, A. V.; Pérez-Nicado, R.; Soroa-Milán, Y.; Santana-Mederos, D.; Westermann, B.; Vérez-Bencomo, V.; Méndez, Y.; García-Rivera, D.; Rivera, D. G. Expanding the Scope of Ugi Multicomponent Bioconjugation to Produce Pneumococcal Multivalent Glycoconjugates as Vaccine Candidates. *Bioconjug. Chem.* **2020**, *31* (9), 2231–2240. https://doi.org/10.1021/acs.bioconjchem.0c00423.

(209) Müller, T. J. J.; Schaumann, E.; Arévalo, M. J.; Ayaz, M.; Banfi, L.; Basso, A.; Bernardi, L.; Berrée, F.; Carboni, B.; Chebanov, V. A.; Moliner, F. D.; Dömling, A.; Gorobets, N. Y.; Huang, Y.; Hulme, C.; Kaluđerović, G. N.; Lavilla, R.; Gall, E. L.; Lemanski, G.; Li, C.-J.; Matveeva, E. D.; Mayence, A.; Menon, R. S.; Morales, G. A.; Morejon, M. C.; Müller, T. J. J.; Nair, V.; Filho, R. A. W. N.; Ricci, A.; Riva, R.; Sedash, Y. V.; Shuvalov, M. V.; Eynde, J. J. V.; Wessjohann, L. A.; Yoo, W.-J.; Zefirov, N. S.; Zhao, L.; Ziegler, T. *Multicomponent Reactions, Volume 1*, 2014th ed.; Thieme Verlag, **2014**. https://doi.org/10.1055/b-003-125816.

(210) Sornay, C.; Hessmann, S.; Erb, S.; Dovgan, I.; Ehkirch, A.; Botzanowski, T.; Cianférani, S.; Wagner, A.; Chaubet, G. Investigating Ugi/Passerini Multicomponent Reactions for the Site-Selective Conjugation of Native Trastuzumab**. *Chem. – Eur. J.* **2020**, *26* (61), 13797–13805. https://doi.org/10.1002/chem.202002432.

(211) Wang, L.; Amphlett, G.; Blättler, W. A.; Lambert, J. M.; Zhang, W. Structural Characterization of the Maytansinoid–Monoclonal Antibody Immunoconjugate, huN901–DM1, by Mass Spectrometry. *Protein Sci.* **2005**, *14* (9), 2436–2446. https://doi.org/10.1110/ps.051478705.

(212) Rady, T.; Mosser, M.; Nothisen, M.; Erb, S.; Dovgan, I.; Cianférani, S.; Wagner, A.; Chaubet, G. Bicyclo[6.1.0]Nonyne Carboxylic Acid for the Production of Stable Molecular Probes. *RSC Adv.* **2021**, *11* (58), 36777–36780. https://doi.org/10.1039/D1RA07905K.

(213) Barok, M.; Joensuu, H.; Isola, J. Trastuzumab Emtansine: Mechanisms of Action and Drug Resistance. *Breast Cancer Res.* **2014**, *16* (2), 209. https://doi.org/10.1186/bcr3621.

(214) Richter, A.; Eggenstein, E.; Skerra, A. Anticalins: Exploiting a Non-Ig Scaffold with Hypervariable Loops for the Engineering of Binding Proteins. *FEBS Lett.* **2014**, *588* (2), 213–218. https://doi.org/10.1016/j.febslet.2013.11.006.

(215) Deuschle, F.-C.; Ilyukhina, E.; Skerra, A. Anticalin® Proteins: From Bench to Bedside. *Expert Opin. Biol. Ther.* **2021**, *21* (4), 509–518. https://doi.org/10.1080/14712598.2021.1839046.

(216) Deuschle, F.-C.; Morath, V.; Schiefner, A.; Brandt, C.; Ballke, S.; Reder, S.; Steiger, K.; Schwaiger, M.; Weber, W.; Skerra, A. Development of a High Affinity Anticalin® Directed against Human CD98hc for Theranostic Applications. *Theranostics* **2020**, *10* (5), 2172–2187. https://doi.org/10.7150/thno.38968.

(217) Castañeda, L.; Maruani, A.; Schumacher, F. F.; Miranda, E.; Chudasama, V.; Chester, K. A.; Baker, J. R.; Smith, M. E. B.; Caddick, S. Acid-Cleavable Thiomaleamic Acid Linker for Homogeneous Antibody–Drug Conjugation. *Chem. Commun.* **2013**, *49* (74), 8187–8189. https://doi.org/10.1039/C3CC45220D.

(218) Stöckmann, H.; Neves, A. A.; Stairs, S.; Brindle, K. M.; Leeper, F. J. Exploring Isonitrile-Based Click Chemistry for Ligation with Biomolecules. *Org. Biomol. Chem.* **2011**, *9* (21), 7303–7305. https://doi.org/10.1039/C1OB06424J.

(219) Ursuegui, S.; Schneider, J. P.; Imbs, C.; Lauvoisard, F.; Dudek, M.; Mosser, M.; Wagner, A. Expedient Synthesis of Trifunctional Oligoethyleneglycol-Amine Linkers and Their Use in the Preparation of PEG-Based Branched Platforms. *Org. Biomol. Chem.* **2018**, *16* (44), 8579–8584. https://doi.org/10.1039/C8OB02097C.

(220) Dommerholt, J.; Schmidt, S.; Temming, R.; Hendriks, L. J. A.; Rutjes, F. P. J. T.; van Hest, J. C. M.; Lefeber, D. J.; Friedl, P.; van Delft, F. L. Readily Accessible Bicyclononynes for Bioorthogonal Labeling and Three-Dimensional Imaging of Living Cells. *Angew. Chem. Int. Ed.* **2010**, *49* (49), 9422–9425. https://doi.org/10.1002/anie.201003761.

(221) D'Alessandro, P. L.; Buschmann, N.; Kaufmann, M.; Furet, P.; Baysang, F.; Brunner, R.; Marzinzik, A.; Vorherr, T.; Stachyra, T.-M.; Ottl, J.; Lizos, D. E.; Cobos-Correa, A. Bioorthogonal Probes for the Study of MDM2-P53 Inhibitors in Cells and Development of High-Content Screening Assays for Drug Discovery. *Angew. Chem. Int. Ed.* **2016**, *55* (52), 16026–16030. https://doi.org/10.1002/anie.201608568.

(222) Walsh, C. T.; Garneau-Tsodikova, S.; Gatto Jr., G. J. Protein Posttranslational Modifications: The Chemistry of Proteome Diversifications. *Angew. Chem. Int. Ed.* **2005**, *44* (45), 7342–7372. https://doi.org/10.1002/anie.200501023.

(223) Prescher, J. A.; Dube, D. H.; Bertozzi, C. R. Chemical Remodelling of Cell Surfaces in Living Animals. *Nature* **2004**, *430* (7002), 873–877. https://doi.org/10.1038/nature02791.

(224) Fu, Z.; Li, S.; Han, S.; Shi, C.; Zhang, Y. Antibody Drug Conjugate: The "Biological Missile" for Targeted Cancer Therapy. *Signal Transduct. Target. Ther.* **2022**, *7* (1), 93. https://doi.org/10.1038/s41392-022-00947-7.

(225) Morales-Kastresana, A.; Siegemund, M.; Haak, S.; Peper-Gabriel, J.; Neiens, V.; Rothe, C. Chapter Four - Anticalin®-Based Therapeutics: Expanding New Frontiers in Drug Development. In *International Review of Cell and Molecular Biology*; Aranda, F., Berraondo, P., Galluzzi, L., Eds.; Academic Press, **2022**; Vol. 369, pp 89–106. https://doi.org/10.1016/bs.ircmb.2022.03.009.

(226) Deuschle, F.-C.; Morath, V.; Schiefner, A.; Brandt, C.; Ballke, S.; Reder, S.; Steiger, K.; Schwaiger, M.; Weber, W.; Skerra, A. Development of a High Affinity Anticalin® Directed against Human CD98hc for Theranostic Applications. *Theranostics* **2020**, *10* (5), 2172–2187. https://doi.org/10.7150/thno.38968.

RESUME

Les modifications post-traductionnelles (PTM) sont le principal outil dont dispose la nature pour générer rapidement un large éventail de protéines diverses aux activités variées à partir d'un précurseur commun.[222] Pour tenter d'imiter la nature, les chimistes ont mis au point plusieurs méthodes chimiques permettant de modifier les protéines sur des sites prédéterminés, afin d'y installer des modifications soigneusement sélectionnées en vue d'applications biologiques et thérapeutiques. Par exemple, le marquage des protéines avec des fluorophores permet de les suivre à la fois in vitro et in vivo,[223] tandis que la conjugaison d'agents cytotoxiques puissants à des anticorps permet d'obtenir de nouveaux médicaments anticancéreux avec une efficacité améliorée et des effets secondaires réduits. Pour cette dernière application, le contrôle précis du nombre de molécules cytotoxiques conjuguées par anticorps (c'est-à-dire le degré de conjugaison, DoC) est d'une importance majeure et deux approches principales ont été conçues pour y parvenir.[224]

Des stratégies chimiosélectives - c'est-à-dire ciblant sélectivement une seule famille de résidus d'acides aminés - ont été tout d'abord développées avec succès pour la conjugaison de presque tous les acides aminés réactifs. Malgré des applications majeures et une myriade de méthodes puissantes, cette approche tend à conduire à des mélanges hétérogènes de conjugués avec des DoC variables, limitant leurs applications industrielles. Ceci est une conséquence directe de la grande taille des anticorps et de la présence de multiples copies du même résidu d'acide aminé à leur surface. Une solution à ce problème a consisté à étudier des stratégies dites site-sélectives - régiosélectives - ciblant une seule copie d'un acide aminé précis. Cela a notamment été réalisé par des modifications biochimiques, en utilisant des proteines mutantes portant des acides aminés naturels (ou non) qui peuvent être séléctivement conjugués par des réactions adaptées. Ces réactions sont souvent bioorthogonales. Il en résulte généralement des conjugués homogènes présentant une reproductibilité d'un lot à l'autre, une pharmacocinétique bien définie, une grande efficacité et souvent une meilleure tolérance. Pourtant, ces méthodes peuvent s'avérer fastidieuses et couteuses, ces conjugués pouvant formerdes agrégats en raison de modifications de leur séquence d'acides aminés. Une alternative intéressante mais plus difficile à mettre en oeuvre consistait donc à étudier le développement d'approches régiosélectives rutilisant des protéines natives.[16,100]

L'objectif principal de mon doctorat était donc de poursuivre nos efforts en vue de développer de nouvelles stratégies chimiques pour la conjugaison de protéines natives. Ce travail a été réalisé dans le cadre d'un projet Innovative Training Network (ITN) qui a bénéficié d'un

financement du programme de recherche Horizon 2020 de l'Union européenne (Actions Marie Skłodowska Curie ; N° 859458).

Évaluation de réactifs hétérofonctionnels à base d'iode(III) hypervalent comme agent de pontage de résidus cystéine

Une méthode de bioconjugaison très populaire et largement utilisée se concentre sur les modifications des résidus cystéine en raison de leur présence limitée à la surface des anticorps monoclonaux (mAb). En effet, seuls huit résidus sont généralement accessibles dans les anticorps, sous la forme de liaisons disulfure, reliant les différentes chaînes de l'anticorps de manière covalente. Les stratégies de conjugaison cystéine sont déjà bien développées et notre groupe a participé aux progrès dans ce domaine en rapportant le triméthylsilyl-éthynylbenziodoxolone (TMS-EBX **I50**) comme réactif chimiosélectif en 2020 (**Figure 32A**) dans le cadre d'une collaboration avec le groupe du Professeur Jérôme Waser à l'École polytechnique fédérale de Lausanne (EPFL).[53] Poursuivant cette collaboration, nous avons voulu évaluer l'application de ces réactifs d'iode(III) hypervalents au *rebridging* de motifs cystines - c'est-à-dire, la double conjugaison de deux résidus cystéines avec un seul réactif. Dans cette optique, le groupe du Professeur Waser a synthétisé l'éthynylbenziodazolone EBZ **R73**, portant deux sites électrophiles différents, et l'a appliqué avec succès au pontage de petits peptides. Au cours de leur étude d'optimisation, ils ont remarqué que la β-addition des thiols libres sur le groupe éthynyle se produisait d'abord et assez rapidement, en seulement 10 min à température ambiante, mais que la deuxième étape, la réaction de substitution nucléophile aromatique des thiols sur le cycle pentafluorophényle, nécessitait des températures plus élevées et un temps de réaction prolongé pour atteindre une conversion complète et fournir les **Peptides** pontés **A & B** (**Figure 32C**).

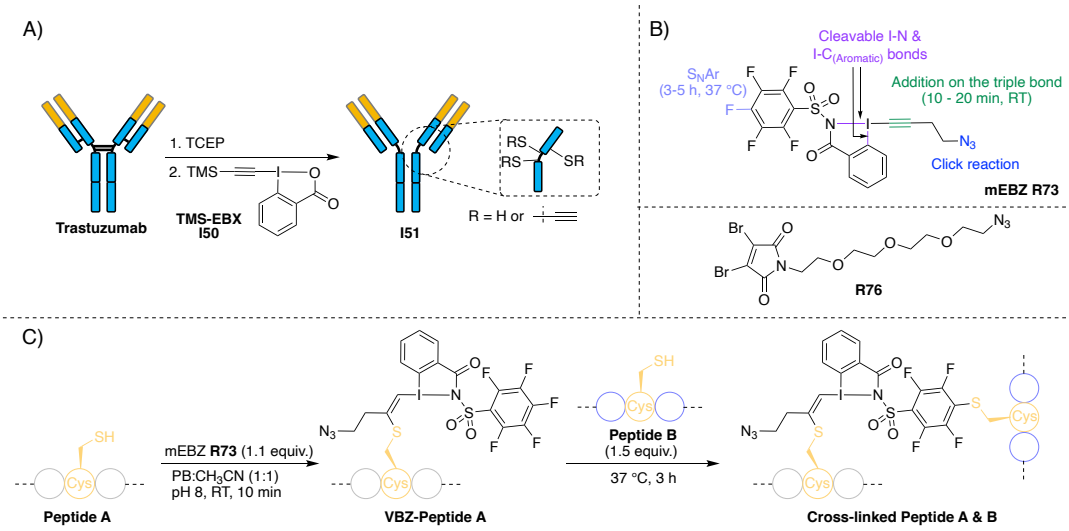

Figure 32. A) Application du TMS-EBX **I50** à la conjugaison d'anticorps B) Structure de l'mEBZ **R73** et du dérivé dibromomaléimide **R76**, C) Pontage du **Peptide A** via l'mEBZ **R73**.

Pour évaluer le potentiel de l'mEBZ **R73** en tant que réactif de pontage sur des substrats plus complexes, nous avons sélectionné des fragments d'anticorps se liant à l'antigène (Fab). Les Fab ne contiennent qu'une seule liaison disulfure inter-chaîne mais possèdent une affinité maintenue avec l'antigène, ce qui en fait des fragments attrayants avec leur penetration tissulaire accrue. Les Fab dérivées du Trastuzumab ont été produits après deux étapes de digestion consécutives par la pepsine et la papaïne et nous avons commencé à évaluer sa conjugaison après la réduction préliminaire de la liaison disulfure à l'aide de *tris*(2-carboxyéthyl)phosphine (TCEP) afin de libérer les fonctions thiols des cystéines.[217] Les conjugués Fab ont été analysés par LC-MS dénaturante, en collaboration avec le groupe Cianferani, membre du projet ITN, nous permettant de déterminer l'efficacité du pontage, basée sur la quantité de Fab détectée (exprimée en pourcentage), et son degré de conjugaison moyen (avDoC).

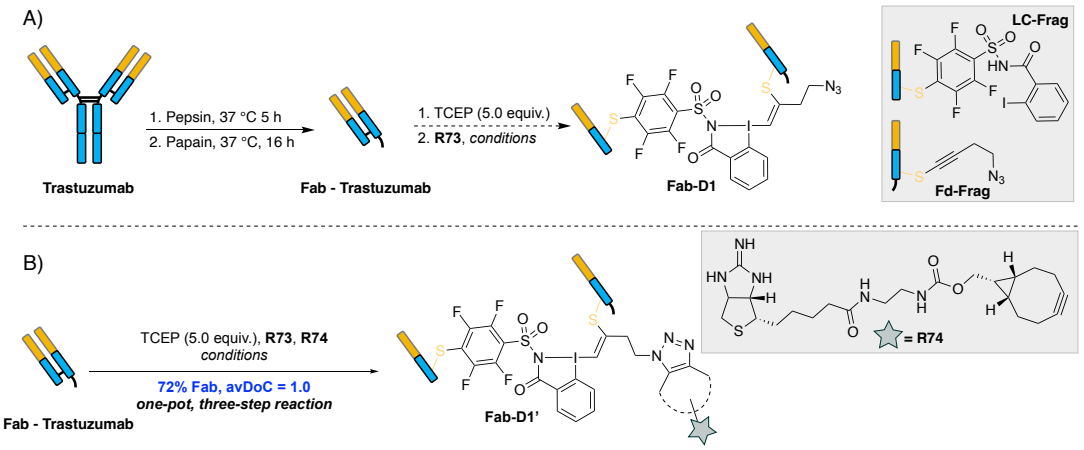

Figure 33. A) Fragmentation de l'mEBZ **R73** après conjugaison avec le Fab. B) Réaction en trois étapes "one-pot".

Nous avons rapidement constaté une faible efficacité du pontage en raison de deux problèmes principaux : la génération des espèces secondaires **LC-Frag** et **Fd-Frag**, ne portant que des fragments du produit de conjugaison attendu et la conjugaison incomplète de **Fab**. En passant en revue plusieurs conditions, nous avons réussi à déterminer que la composition du solvant et la présence d'EDTA étaient les deux paramètres cruciaux pour obtenir une réaction efficace, permettant d'accéder à 72% d'espèces pontées **Fab-D1** avec un avDoC 1 en une seule étape et en seulement 5 heures, avec les étapes de réduction et de conjugaison effectuées simultanément et en *one-pot*. En outre, nous avons réussi à montrer qu'une nouvelle procédure où les trois étapes (c'est-à-dire réduction-conjugaison-fonctionnalisation via SPAAC) étaient réalisées simultanément permettait d'obtenir le **Fab** en seulement 5 heures avec un bon rendement et un pontage extrêmement efficace, chose impossible à réaliser avec le réactif classique de pontage de type dibromomaléimide (DBM) **R76**. À notre connaissance, cela fait de cette approche une méthode de bioconjugaison sans précédent en une seule étape, réduisant le temps de réaction et les étapes de purification, comme le montre la **Figure 33B**.

Utilisation de réactions multicomposantes comme méthode régiosélective pour la bioconjugaison de protéines

Le deuxième projet de mon doctorat concerne l'étude des réactions multicomposantes (MCR) en tant que méthodes régiosélectives pour la bioconjugaison de protéines. L'une des MCR les plus connues et décrites en chimie organique est la réaction à quatre composants d'Ugi (U-4CR) entre une amine, un acide carboxylique, un carbonyle et un isonitrile pour former un bis-amide. Comme les amines et les acides carboxyliques sont abondants dans les protéines, nous avons imaginé que l'ajout d'un carbonyle et d'un isonitrile à une protéine modèle pourrait conduire à la conjugaison de deux résidus lysine et aspartate/glutamate spatialement proches via une réaction d'Ugi à trois centres et quatre composants (U-3C-4CR), une variante de la U-4CR classique. Nous avons choisi l'anticorps Trastuzumab comme protéine modèle et, après des recherches approfondies, avons identifié l'aldéhyde azoture **R152** et l'isocyanure de cyclohexyle **R133** comme réactifs optimaux. Après 16 heures à 25 °C dans du tampon phosphate (PBS 1X, pH 7.5, 137 mM NaCl), nous avons été ravis d'observer un avDoC d'environ 1.0 et des taux de conversion supérieurs à 70% lorsque 45 équivalents de chaque réactif ont été utilisés. Ces valeurs ont été déterminées par spectrométrie de masse native (native MS), grâce à une collaboration avec le groupe du Dr Sarah Cianferani. Le groupe azoture incorporé par cette réaction d'Ugi est particulièrement intéressant, car il permet de fonctionnaliser davantage nos conjugués par cycloaddition de Huisgen entre un azoture et un alcyne tendu (SPAAC). Après 16 heures à 25 °C dans du PBS, des conjugués de Trastuzumab

équipés de charges utiles d'intérêt - telles qu'une iminobiotine **R74** ou un fluorophore - ont pu être facilement isolés avec un excellent rendement (**Figure 34**).[210]

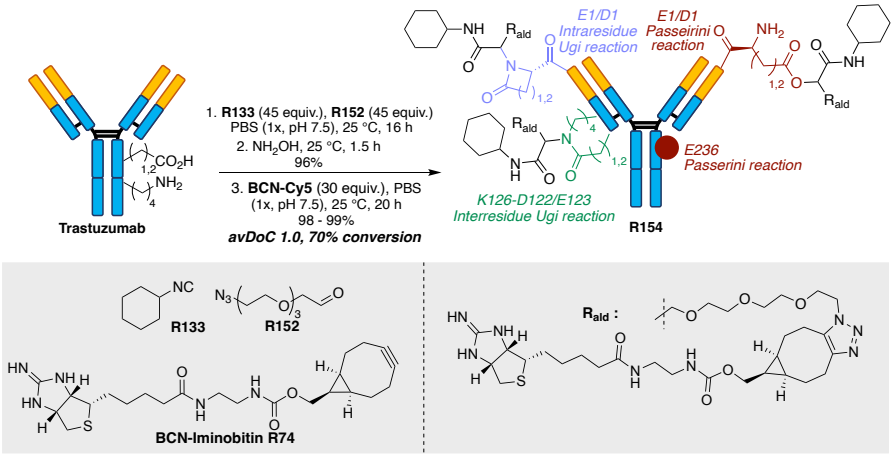

Figure 34. Réaction d'Ugi sur le Trastuzumab et les trois types de réaction détectés par analyse LC-MS/MS.

Motivés par ces résultats, nous avons voulu vérifier si notre approche était effectivement régiosélective et nous avons entrepris des études par LC-MS/MS afin d'identifier les sites de conjugaison précis – une approche nommée peptide mapping. Nous avons ainsi pu détecter un adduit Ugi attendu entre une lysine - K169 - et un acide aminé contenant un carboxylate - soit E165, D167 ou D170 (indiscernable). Cependant, une poignée d'autres sites ont également été identifiés, dont la conjugaison résulte de réactions secondaires, soit par la réaction de Passerini, qui entraîne la modification d'un seul résidu d'aspartate/glutamate, soit par une réaction inattendue de Ugi dite "intrarésidu" entre l'amine *N*-terminale et le carboxylate porté par les chaînes latérales des résidus E1 et D1. Intéressés par ces résultats, nous avons entrepris un travail méthodologique approfondi pour mieux comprendre les facteurs régissant la chimiosélectivité et la régiosélectivité de ces MCR.

Au cours de nos investigations et après avoir passé en revue divers réactifs et conditions, nous avons découvert que l'isocyanoacétate d'éthyle **R158** conduisait exclusivement à la conjugaison E1, dite "intrarésidu", avec un taux de conversion de 65% et avDAR d'environ 1.1, des conditions réactionnelles offrant une parfaite régiosélectivité encore jamais documentée pour une telle approche. Nous continuons d'étudier à ce jour toutes les possibilités offertes par cette stratégie et notamment la production de conjugués anticorps-médicaments (ADC) homogènes afin d'évaluer si cette conjugaison sélective peut améliorer leur activité par rapport à des analogues conjugués de manière stochastique (**Figure 35**).

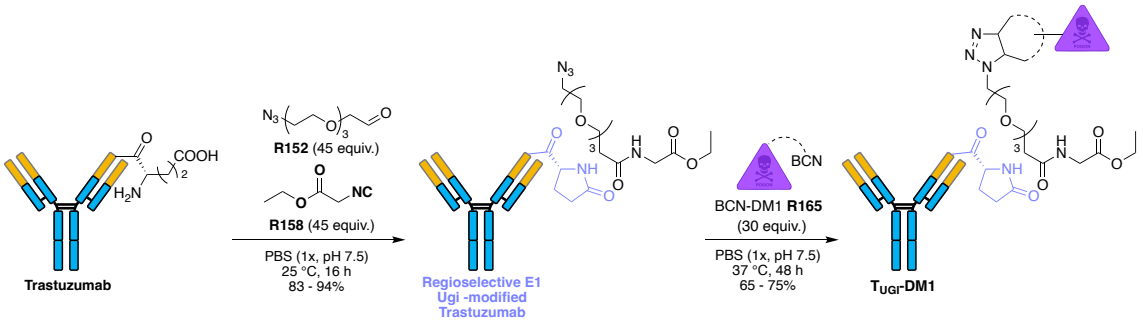

Figure 35. Réaction d'Ugi régiosélective sur le Trastuzumab suivi de la production d'un ADC.

Afin d'évaluer l'applicabilité de notre réaction de conjugaison Ugi, nous avons décidé de l'évaluer sur une autre famille de protéines : les anticalines. Les anticalines sont des protéines artificielles dérivées des lipocalines, abondantes dans le plasma et responsables du transport de petites molécules hydrophobes. Elles présentent des propriétés très intéressantes, telles qu'un faible coût de production, une spécificité de cible, une perméabilité cellulaire améliorée par rapport aux anticorps et ont démontré un potentiel thérapeutique intéressant dans les premières études cliniques d'immuno-oncologie.[225,226] Grâce à une collaboration interne à l'ITN avec le professeur Arne Skerra de l'Université technique de Munich, nous avons appliqué nos conditions de réaction optimisées à une anticaline modèle et avons été ravis d'observer un avDoC de 1.1 avec une conversion complète après une brève optimisation. Les analyses LC-MS/MS ont permis d'identifier la lysine K46 et le glutamate E44 (ou l'aspartate D47) comme principal site de conjugaison, ainsi que l'aspartate D2 ou D6, modifié via une réaction secondaire de Passerini, soulignant à nouveau le grand potentiel de notre méthode pour la conjugaison régiosélective de protéines.

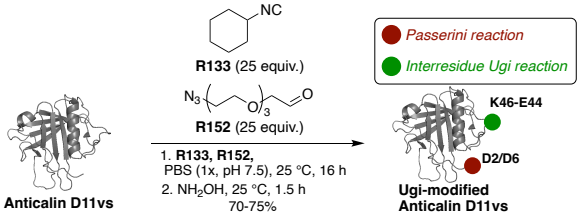

Figure 36. Réaction d'Ugi régiosélective sur le Anticalin D11vs.

En conclusion, nous avons prouvé que la réaction d'Ugi peut être un outil chimique puissant pour la conjugaison sélective d'anticorps et de petites protéines artificielles, et pour la production d'ADC homogènes.

Conclusion générale

Cette thèse s'est concentrée sur le développement et l'étude de nouvelles méthodes de bioconjugaison visant à la modification chimiosélective et régiosélective de protéines natives et artificielles. Deux de ces stratégies étaient axées sur le marquage chimiosélectif des résidus cystéine, tandis que l'autre était consacrée à l'incorporation d'un MCR Ugi pour la modification régiosélective des résidus lysine et aspartate/glutamage proches dans l'espace.

Un réactif multifonctionnel à base d'iode (III) hypervalent, et en particulier un analogue de l'éthynylbenziodazolone (EBZ), a ensuite été étudié pour déterminer s'il pouvait être utilisé comme réactif de pontage Cys-Cys. Après un travail méthodologique approfondi consistant à évaluer diverses combinaisons de conditions, nous avons réussi à l'ajuster de manière à obtenir un remaillage et une fonctionnalisation complets de Fabs et d'espèces entières d'AcM dérivées de diverses sources par le biais d'une réaction en trois étapes dans un seul et même pot. Cependant, le remaillage des Fabs était souvent accompagné de la formation de fragments Fd et LC en raison de la fragmentation du réactif mEBZ **R73**. Enfin, nous avons démontré l'excellente stabilité de nos conjugués rebridés dans le plasma humain à 37 °C et leur clivage contrôlé en présence d'espèces de cuivre(I) par réduction de l'iode(III).

Enfin, une réaction à plusieurs composants - la réaction d'Ugi à quatre composants et trois centres (U- 4C-3CR) - a été étudiée en tant que nouvelle stratégie de marquage régiosélectif. Après un autre travail méthodologique approfondi, soutenu par des études de cartographie peptidique, nous avons réussi à obtenir une conjugaison site-sélective de l'E1 *N*-terminal du Trastuzumab. En incorporant ces conditions de site sélectif, nous avons construit un ADC homogène avec un avDAR 1 qui a montré un excellent profil cytotoxique en comparaison avec l'ADC Kadcyla® avec un avDAR 3,5. Nous avons ensuite appliqué cette méthode à d'autres protéines natives, mais la conjugaison détectée était nulle ou faible. Cependant, lorsque nous avons appliqué la même méthode avec des conditions légèrement modifiées sur les anticalines, non seulement une conjugaison sélective de site a été détectée, mais aussi une conversion presque totale a été obtenue.

PUBLICATIONS AND PRESENTATIONS

PUBLICATIONS:

♦ PUBLISHED

1. **"Cysteine-Cysteine Cross-Conjugation of Both Peptides and Proteins with a Bifunctional Hypervalent Iodine-Electrophilic Reagent"**
   Koutsopetras, I.; Mishra, A. K.; Benazza, R.; Hernandez-Alba, O.; Cianférani, S.; Chaubet, G.; Nicolai, S.; Waser, J. *Chem. Eur. J.* **2023**, e202302689. https://doi.org/10.1002/chem.202302689.
2. **"Preparation of New Bicyclo[2.1.1]Hexane Compact Modules: An Opening towards Novel Sp^3-Rich Chemical Space"**
   Herter, L.; Koutsopetras, I.; Turelli, L.; Fessard, T.; Salomé, C. *Org. Biomol. Chem.* **2022**, *20* (46), 9108–9111. https://doi.org/10.1039/D2OB01669A.

♦ CURRENTLY UNDER REVIEW

1. **"Site-Selective Protein Conjugation by a Multicomponent Ugi Reaction"**
   Koutsopetras, I.; Vaur, V.; Benazza, R.; Diemer, H.; Sornay, C.; Ersoy, Y.; Rochet, L.; Longo, C.; Hernandez-Alba, O.; Erb, S.; Detappe, A.; Skerra, A., Wagner, A.; Cianferani, S.; Chaubet, G. Submitted to *Chem. Eur. J.* on **10/2023**
2. **"Use of Pyridazinediones for tunable and reversible covalent cysteine modifications applied to peptides, proteins and hydrogels"**
   Rochet, L.; Bahou, C.; Wojciechowski, J.; Koutsopetras, I.; Britton, P.; Spears, R.; Thanasi, I.; Shao, B.; Zhong, L.; Bucar, D.K.; Aliev, A.; Porter, M.; Stevens, M.; Baker, J.; Chudasama, V. S. Submitted to *Chem. Sc.* on **09/2023**
3. **"SEC-MS in Denaturing Conditions (dSEC-MS) for In-Depth Analysis of Rebridged Monoclonal Antibody-Based Formats"**
   Benazza R., Koutsopetras I., Vaur V., Chaubet G., Hernandez-Alba O., Cianférani S. Submitted to *Talanta* on **07/2023**. Available as pre-print at *ChemRxiv:* https://doi.org/10.26434/chemrxiv-2023-jmp5n.

POSTER PRESENTATION:

1. Multicomponent reaction for the site-selective conjugation of monoclonal antibodies. **May 2023**, PEGS – Boston, USA

Université de Strasbourg

Ilias KOUTSOPETRAS

Marie Skłodowska-Curie Actions

EDSC École Doctorale des Sciences Chimiques

Développement de nouvelles méthodes de conjugaison régiosélectives et chimiosélectives pour la modification de protéines natives

Résumé

Au cours des dernières décennies, la modification des protéines par le biais de stratégies chimiosélectives et site-sélectives a ouvert une nouvelle ère d'applications thérapeutiques, donnant lieu à des études intensives. L'ingénierie des protéines est une technique prometteuse pour fournir un marquage sélectif sur les protéines, mais elle est coûteuse ou conduit à l'agrégation en raison de changements dans la séquence des acides aminés. Ainsi, la fonctionnalisation contrôlée par modification chimique de diverses chaînes latérales d'acides aminés de protéines natives est apparue comme une stratégie alternative, à laquelle ce travail a été consacré. La première partie décrit l'étude des propriétés de déconjugaison des dérivés non-bromés de la pyridazinedione liés de manière covalente aux cystéines des protéines natives. La deuxième partie est consacrée au développement d'une méthode extensive afin d'affiner une molécule d'iode hypervalent (III) multifonctionnelle pour agir en tant qu'agent de pontage entre cystéines et cystéines. Enfin, dans la dernière partie de cette thèse, un autre projet de méthodologie est illustré pour la conjugaison sélective de l'extrémité N-terminale de protéines natives en utilisant une réaction multicomposants d'Ugi.

Mots-clés : Anticorps, anticalines, bioconjugaison, délivrance de médicaments, iodes hypervalents, pyridazinediones, réactions multicomposants, modifications de protéines.

Résumé en anglais

Over the past decades, protein modification *via* chemo- and site-selective strategies has emerged a new era on therapeutic applications giving breeding ground of intensive studies. Protein engineering is a promising technique to provide site-selective labelling on proteins, but with the expense of being costly, or lead to aggregation arising from changes in their amino acids sequence. Thus, the controlled functionalization *via* chemical modification of various amino acid side chains of native proteins has emerged as an alternative strategy, on which this work was devoted. The first part describes the investigation of deconjugation properties of non-brominated pyridazinedione derivatives covalently linked with cysteines of native proteins. The second part is dedicated to an extensive method development in order to fine tune a multifunctional hypervalent iodine (III) molecule to act as a cysteine-cysteine rebridging agent. Finally, at the last part of this thesis another methodology project is illustrated for the site-selective conjugation of native proteins' N-terminal by employing an Ugi multicomponent reaction.

Keywords: Antibodies, anticalins, bioconjugation, drug-delivery, hypervalent iodines, pyridazinediones, multicomponent reactions, protein modifications.